TECHNICAL REPORT STANDARD TITLE PAGE

1. Report No.	2. Government Accession No.	3. Recipient's Catalog No.
FHWA/TX-88+381-4F		

4. Title and Subtitle	5. Report Date
A STUDY OF PRETENSIONED HIGH STRENGTH CONCRETE GIRDERS IN COMPOSITE HIGHWAY BRIDGES—DESIGN CONSIDERATIONS	January 1988
	6. Performing Organization Code
7. Author(s)	8. Performing Organization Report No.
Reid W. Castrodale, M. E. Kreger, and Ned H. Burns	Research Report 381-4F
9. Performing Organization Name and Address	10. Work Unit No.
Center for Transportation Research The University of Texas at Austin Austin, Texas 78712-1075	11. Contract or Grant No. Research Study 3-5-84-381
	13. Type of Report and Period Covered
12. Sponsoring Agency Name and Address Texas State Department of Highways and Public Transportation; Transportation Planning Division P. O. Box 5051 Austin, Texas 78763-5051	Final
	14. Sponsoring Agency Code

15. Supplementary Notes

Study conducted in cooperation with the U. S. Department of Transportation, Federal Highway Administration. Research Study Title: "Optimum Design of Bridge Girders Made Using High Strength Concretes and Deflection of Long-Span Prestressed Concrete Beams"

16. Abstract

Recent developments have made concrete with strengths up to 12,000 psi commercially available for construction of pretensioned highway bridge girders. The implementation of this material has preceded the full understanding and documentation of its behavior and effect on the design of bridge structures. Therefore, a review of code, practice, and the literature is necessary for high strength concrete to be used safely and efficiently in pretensioned bridge girders.

Selected girder cross-sections are reviewed to determine their sensitivity to different design parameters and their effectiveness with the use of high strength concrete. A series of sections is proposed that make more efficient use of high strength concrete than some sections currently in use. Several factors are identified that limit the design potential of some sections.

AASHTO and ACI codes are reviewed for application to high strength concrete. Test data and analytical studies related to the use of high strength concrete are also reviewed.

Based on the review of codes, literature, test data, and additional analytical studies, proposals and recommendations are made regarding the design of pretensioned high strength concrete bridge girders.

17. Key Words	18. Distribution Statement
high strength concrete, bridge girders, behavior, design, structures, pretensioned, potential, application, analytical	No restrictions. This document is available to the public through the National Technical Information Service, Springfield, Virginia 22161.

19. Security Classif. (of this report)	20. Security Classif. (of this page)	21. No. of Pages	22. Price
Unclassified	Unclassified	306	

Form DOT F 1700.7 (8-69)

A STUDY OF PRETENSIONED HIGH STRENGTH CONCRETE GIRDERS IN COMPOSITE HIGHWAY BRIDGES - DESIGN CONSIDERATIONS

by

Reid W. Castrodale
M. E. Kreger
Ned H. Burns

PRELIMINARY REVIEW COPY

Research Report 3-5-84-381-4F

Research Project 3-5-84-381

"Optimum Design of Bridge Girders Made Using High Strength Concretes and Deflection of Long-Span Prestressed Concrete Beams"

Conducted for

Texas
State Department of Highways and Public Transportation

In Cooperation with the
U.S. Department of Transportation
Federal Highway Administration

by

CENTER FOR TRANSPORTATION RESEARCH
BUREAU OF ENGINEERING RESEARCH
THE UNIVERSITY OF TEXAS AT AUSTIN

January 1988

The contents of this report reflect the views of the authors, who are responsible for the facts and the accuracy of the data presented herein. The contents do not necessarily reflect the official views or policies of the Federal Highway Administration. This report does not constitute a standard, specification, or regulation.

There was no invention or discovery conceived or first actually reduced to practice in the course of or under this contract, including any art, method, process, machine, manufacture, design or composition of matter, or any new and useful improvement thereof, or any variety of plant which is or may be patentable under the patent laws of the United States of America or any foreign country.

PREFACE

This report is the fourth and final report in a series which summarizes an investigation of the feasibility of utilizing high strength concrete and low relaxation strands in pretensioned bridge girders. The first report summarized results of a field measurement program concerned primarily with the deflection history of long-span pretensioned girders. The second report summarized a laboratory investigation of the shear capacity of large-scale pretensioned girders fabricated with very high-strength concrete. The third report presented results of an experimental program that investigated the flexural behavior of long span, pretensioned high strength girders with a normal strength composite deck.

The work is part of research Project 3-5-84-381 entitled, "Optimum Design of Bridge Girders Made Using High-Strength Concrete and deflections of Long-Span Prestressed Concrete Beams." This report specifically addresses the appropriateness of current design provisions for use in the flexural analysis and design of long span, pretensioned high strength girders with a normal strength composite deck, and investigates the limitations of this type of construction. The research was conducted at the Phil M. Ferguson Structural Engineering Laboratory as part of the overall research program administrated by the Center for Transportation Research of The University of Texas at Austin. This work was sponsored jointly by the Texas State Department of Highways and Public Transportation and the Federal Highway Administration.

Liaison with the State Department of Highways and Public Transportation was maintained through contact representative, Mr. David P. Hohmann. Mr. R.E. Stanford was the contact representative for the Federal Highway Administration.

This portion of the overall study was co-directed by Michael E. Kreger, Assistant Professor of Civil engineering, and Ned H. Burns, Professor of Civil Engineering. Other portions of Project 381 were directed by John E. Breen, who holds the Nasser I. Al-Rashid Chair in Civil Engineering. The analysis presented in this report was carried out by Reid W. Castrodale, Research Engineer.

SUMMARY

Recent developments have made concrete with strengths up to 12,000 psi commercially available for construction of pretensioned highway bridge girders. The implementation of this material has preceded the full understanding and documentation of its behavior and effect on the design of bridge structures. Therefore, a review of code, practice, and the literature is necessary for high strength concrete to be used safely and efficiently in pretensioned bridge girders.

Selected girder cross-sections are reviewed to determine their sensitivity to different design parameters and their effectiveness with the use of high strength concrete. A series of sections is proposed that make more efficient use of high strength concrete than some sections currently in use. Several factors are identified that limit the design potential of some sections.

AASHTO and ACI Codes are reviewed for application to high strength concrete. Test data and analytical studies related to the use of high strength concrete are also reviewed.

Based on the review of codes, literature, test data, and additional analytical studies, proposals and recommendations are made regarding the design of pretensioned high strength concrete bridge girders.

IMPLEMENTATION

This report summarizes an investigation of the use of high strength concrete in design of long-span pretensioned girders with a normal strength composite deck. Selected girder cross-sections are reviewed to determine their sensitivity to different design parameters and their effectiveness with the use of high strength concrete. AASHTO and ACI Codes are reviewed for application to high strength concrete.

A series of sections that make more efficient use of high strength concrete than some sections currently in use is developed. Recommendations for changes in the ACI and AASHTO Codes are made to make the flexural design of prestressed concrete girders consistent with the design of reinforced concrete beams. Recommendations were also made for a simplified flexural analysis of high-strength pretensioned girders with a normal strength composite deck. Several factors are identified that limit some long-span girder designs. Of particular note in this group is stability considerations. Recommendations are made for reducing the effect of some of these limitations.

TABLE OF CONTENTS

TABLE OF CONTENTS

TABLE OF CONTENTS

L I S T O F F I G U R E S

L I S T O F T A B L E S

CHAPTER 1

INTRODUCTION

1.1 Background

The use of high strength concrete as a building material has been a topic of discussion for many years. In an article published in 1932, Thomas T. Towles [129] speculated on the benefits of using concrete with a design compressive strength of 7,000 psi compared with a 5,000 psi mix, which was considered to be near the maximum practical concrete strength at the time. It was clear to him that the use of higher strength concrete would lead to significant cost benefits, especially in long span construction and where many spans are required.

Since that time, it has become possible to produce concrete with a design strength much higher than even the expectations of Towles in 1932. Peterman and Carrasquillo [104] have demonstrated that concrete with a compressive strength between 9,000 and 12,000 psi can be readily obtained on a commercial basis by careful mix proportioning using standard portland cements, selected common aggregates, and chemical admixtures. The use of high range water reducers (HRWR), which are also referred to as "super-plasticizers", have made it possible to produce workable mixtures with the extremely low water/cement ratios that are required to attain high strengths.

The same observations that Towles made in 1932 are being made today, but with even greater expectations for cost benefits because of the higher strengths that are now possible. One way in which the use of high strength concrete has been demonstrated to provide greater efficiency is illustrated by the two bridge cross sections shown in Fig. 1.1, which illustrates the results of a study performed in Sec. 2.4.1. This figure shows that, for a span length of 115 ft and a bridge width of 36 ft, the required number of AASHTO-PCI Type IV girders can be reduced from nine using 6,000 psi concrete, which is the standard concrete strength for pretensioned girders in Texas, to four when 10,000 psi concrete is used. As indicated on the figure, the use of high strength concrete also results in a reduction in the total number of strands required for the bridge, which is a result of the reduced dead load. A normal strength concrete (4,000 psi) deck was used in both cases. The deck thickness was 1 in. greater for the design using high strength concrete girders because of the increased deck span. The use of fewer girders for a given span leads to savings in material, shipping, and erection costs and also reduces the time required for fabrication and erection.

Another benefit of the use of high strength concrete in highway bridge design is illustrated in Fig. 1.2, where an increase in girder concrete strength is shown to result in significantly greater maximum spans for a given

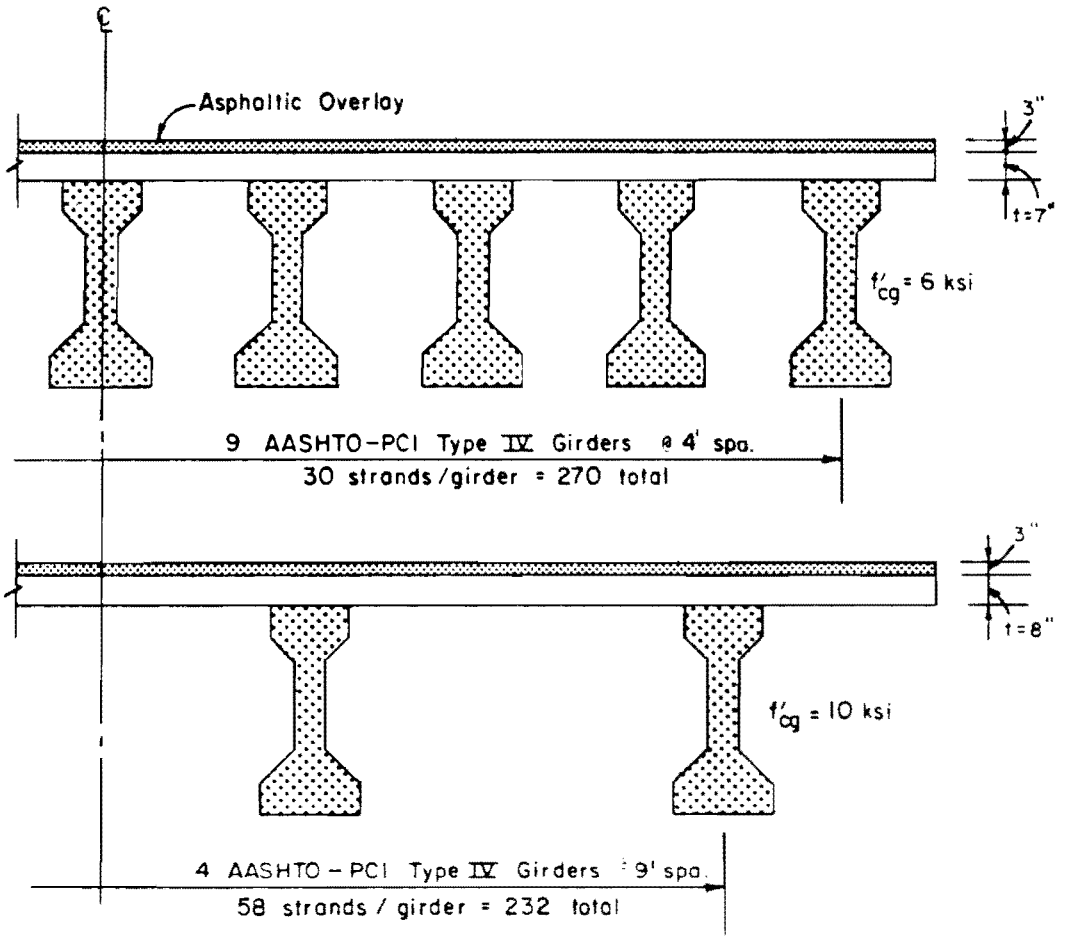

Fig. 1.1 Comparison of bridge designs for same span using normal and high strength concrete

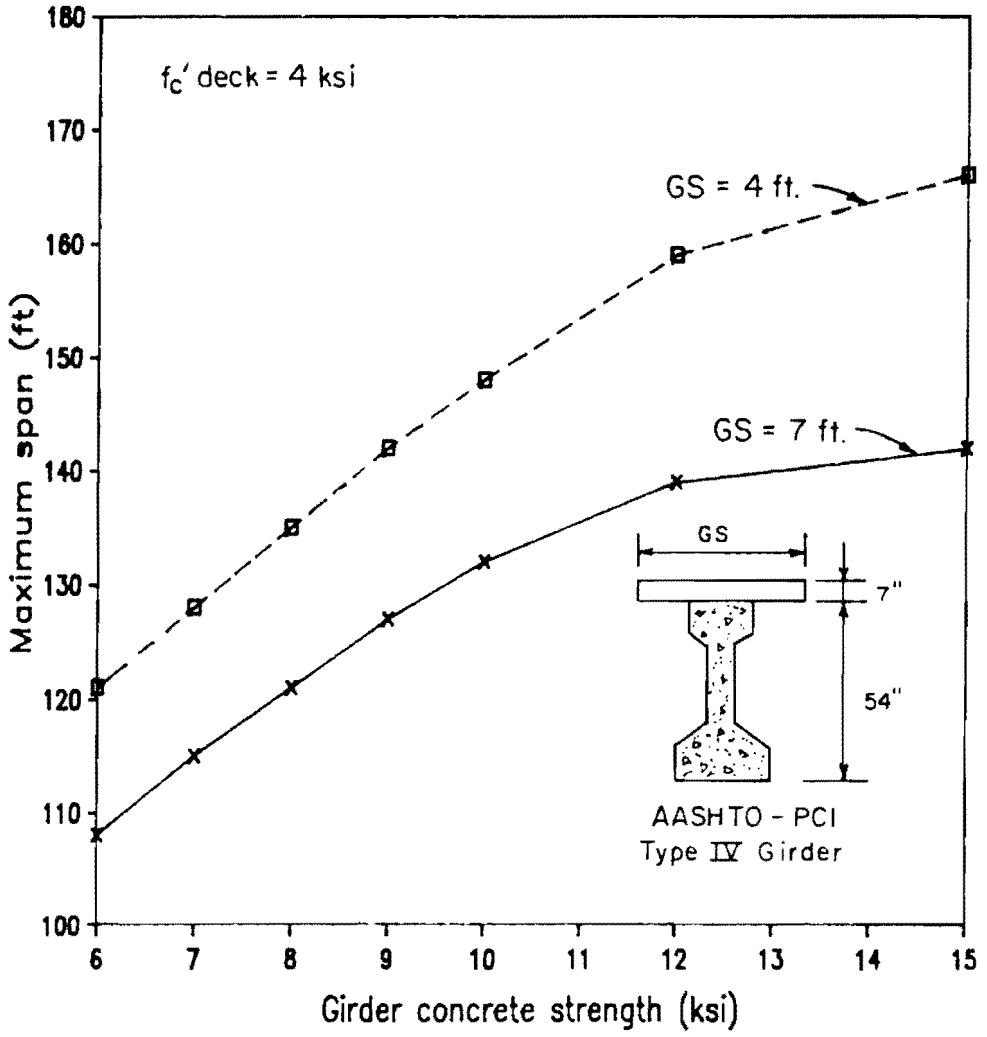

Fig. 1.2 Maximum span versus girder concrete strength

cross-section, girder spacing (GS), and deck thickness. The dashed line indicates spans which exceed a limiting span length based on stability considerations. While means are available to increase the limiting span for a section, the extent of the line emphasizes the importance of considering stability in the design of long-span girders.

Where multiple spans are required, an increase in possible span lengths leads to a reduced number of piers and lower shipping costs. Increased span lengths can also allow elimination of supports, which can improve traffic safety at highway crossings. Another possible benefit from increased maximum span lengths is the use of shallower members for the same span length, which would improve clearances or result in reduction of embankment costs.

There are uncertainties, however, regarding the adequacy of current design codes for high strength concrete. Research on material properties of high strength concrete has shown that some properties differ significantly from those of normal strength concrete. A major area of difference is in the stress-strain behavior as illustrated in Fig. 1.3 [81], where typical stress-strain curves are shown for a range of concrete strengths. High strength concrete has a greater stiffness (or modulus) than other concrete and is more brittle, which is demonstrated by the short and steep descending branch of the stress-strain curve. The more brittle nature of high strength concrete has led to concern regarding the ductility of members constructed using high strength concrete. It has also been speculated [22] that the brittle nature of high strength concrete will lead to smooth shear cracks which would reduce the contribution of aggregate interlock to the ultimate shear strength. Furthermore, many of the present code design provisions are based on test data for which the concrete strengths rarely exceed 6,000 psi. Since little data is available on the behavior of high strength concrete pretensioned bridge members, it is not possible to establish whether current codes are adequate for the design of such members.

The realization of the full potential of high strength concrete in pretensioned bridge girders may also be limited by traditional techniques and methods of design and construction which were developed for use with normal strength concrete. This may be especially true where standardization has taken place such as for pretensioned girders, where most cross sections in use today were developed in the late 1950's and early 1960's for use with normal strength concrete.

Because of these concerns regarding the use of high strength concrete and the applicability of current bridge codes to its use, it is essential that the material and structural behavior be clearly understood and incorporated into design codes before high strength concrete comes into general use. Current design and construction techniques should also be reviewed to determine where changes could be made for more efficient use of the material.

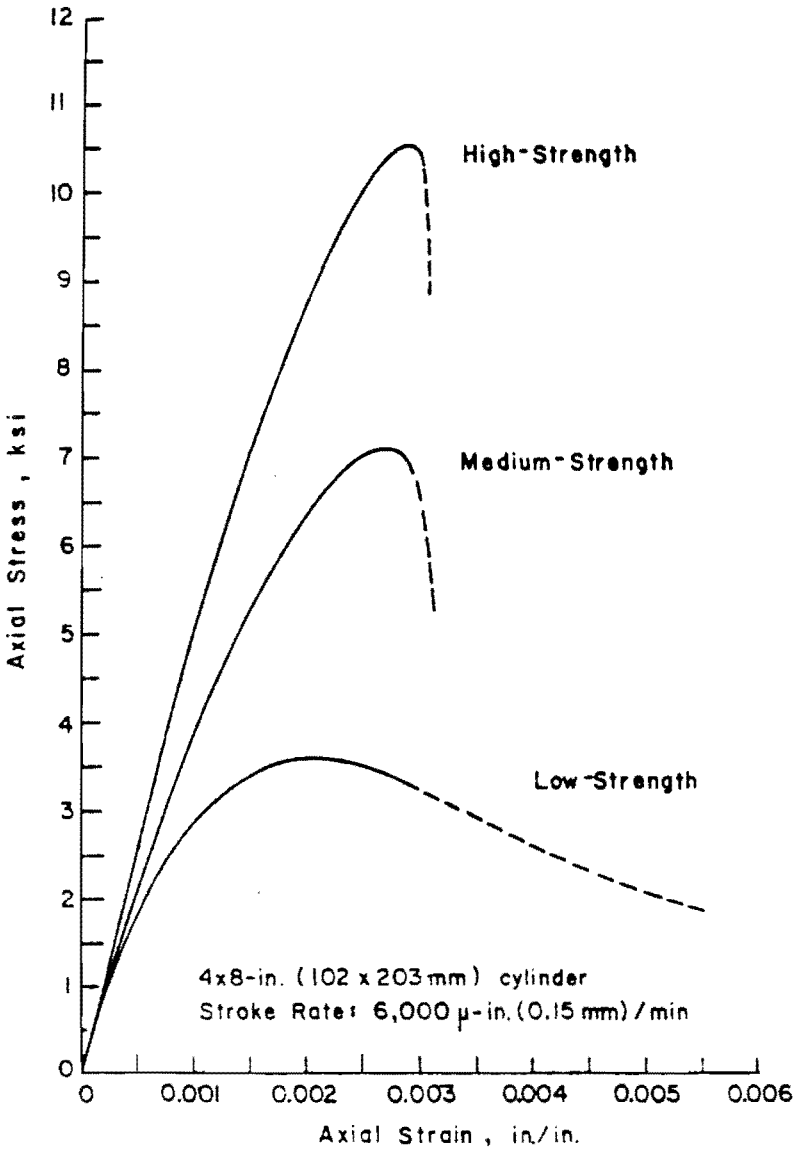

Fig. 1.3 Typical stress-strain curves

1.2 Objectives and Scope of the Study

1.2.1 General. This study was begun to investigate the feasibility and criteria for use of high strength concrete in the design of pretensioned highway bridge girders.

While the definition of high strength concrete varies for different regions of the country, for this study it is considered to be concrete with a design compressive strength between 6,000 and 12,000 psi. The lower limit corresponds to the standard concrete strength for pretensioned girders in Texas which is 6,000 psi and the upper limit represents a practical maximum strength that can be produced commercially. Since the upper limit is not intended to be restrictive, strengths higher than 12,000 psi are considered in some analyses that follow in order to better define trends. Only concrete made using common materials and admixtures will be considered.

The study is limited to the consideration of high strength concrete pretensioned bridge girders which become part of a highway bridge with a normal strength composite deck. Only simple span, non-skew bridges are considered. The deck is assumed to be applied with the girder unshored. Low relaxation strands are the only type considered in the study since this type of strand has virtually become the industry standard. Draping is used to control stresses at the ends of members.

The 13th edition of the American Association of State Highway and Transportation Officials (AASHTO) Standard Specifications for Highway Bridges [10] is used as the main source for design practice for the girders and bridge structures considered. Where helpful, the American Concrete Institute (ACI) Building Code Requirements for Reinforced Concrete (ACI 318-83) [15] and the Commentary on Building Code Requirements for Reinforced Concrete (ACI 318-83) [17] are also consulted for design practice.

1.2.2 Test Programs. Due to the lack of data in the literature on composite bridge construction with high strength concrete pretensioned girders, three test programs were developed to provide data that would allow evaluation of the use of high strength concrete in the design of pretensioned bridge girders. The three test programs included the investigation of transfer lengths, and flexural and shear behavior of reduced-scale high strength pretensioned girders. Results of the experimental programs are presented in Report No. 381-2 and 381-3 [138, 139].

1.3 Organization of this Study

Chapter Three consists of the comparison and evaluation of bridge designs using selected pretensioned girder cross-sections. Three proposed cross-sections, developed for use with high strength concrete, are included in the comparisons. Chapter Two contains a literature review of the topics of

interest in the report. Chapter Four combines the evaluation of current practice, as determined by the literature review of Chapter Two, and test data gathered in the experimental study [139] with representative bridge designs to develop recommendations for design of composite bridges using high strength concrete girders. The report concludes in Chapter Five with a summary of the investigation, and presentation of conclusions and recommendations.

Appendix D details the derivation of proposed maximum and minimum reinforcement limits.

CHAPTER 2

REVIEW OF LITERATURE AND CURRENT DESIGN PRACTICE

2.1 Introduction

Since some basic properties of high strength concrete differ from normal strength concrete in significant ways [22], it is imperative that current design practice be reviewed to identify and correct any problems in the use of high strength concrete with current design provisions. Material properties and design techniques that would allow the designer to make more efficient use of high strength concrete should also be identified. This, then, is the purpose of this chapter, with emphasis on the design and behavior of highway bridges with pretensioned girders.

The chapter begins with a review of overall design concepts that apply to pretensioned girder bridges. Material properties of high strength concrete are then presented. Topics are then considered where the different properties of high strength concrete may affect the design and performance of these bridge structures. As topics are considered, current code provisions are discussed, along with analytical studies and methods, proposals for code revisions, and the results of tests related to the topic. The background of code provisions will be considered when it is beneficial for understanding the intent of the code.

Production of high strength concrete is not considered in this chapter since it is outside the scope of this study. However, it should be noted that a study by Peterman and Carrasquillo [104] and ongoing research at the University of Texas at Austin have shown that high strength concrete as defined in this study can be commercially mixed and placed in pretensioning plants in Texas.

The AASHTO Standard Specifications for Highway Bridges [10] is the model code for the design of highway bridges in the United States and serves as a standard or guide for the preparation of State specifications. The AASHTO specifications will therefore be used as the primary reference to establish current or past practice in bridge design. Provisions of the specification related to the design of pretensioned girder bridges are similar to those for pretensioned and composite members found in the current ACI Building Code Requirements for Reinforced Concrete (ACI 318-83) [15]. While the ACI document is intended for use with buildings rather than bridges, it and its

Commentary [17] give an indication of the direction and intent of general design practice and will therefore be used as secondary code references.

Notation used in this chapter is generally consistent with the information source. In a number of cases, this leads to the use of different notation for the same quantity when discussing information from different sources. A proposal for a consistent set of notation is presented in Sec. 4.11.

2.2 Design Approach

The design of prestressed members by either AASHTO or ACI requirements is based on satisfaction of both ultimate and service load criteria. The service load criteria are satisfied when concrete and steel stresses, computed at all critical load stages during the life of the structure, do not exceed allowable values specified in the codes. Design for service conditions using these criteria is therefore referred to as "allowable stress design" [10]. Section 9.13.1.2 of the AASHTO Specification [10] implies that the intent of allowable stress design is to ensure satisfactory behavior of a member under service conditions throughout its life. The ACI Code Commentary [17] states that "permissible stresses are given to control serviceability." The design of an overwhelming majority of pretensioned girder bridges is controlled by allowable stress design and strength analysis is usually performed only as a check.

The allowable stresses that affect behavior most significantly are the concrete tensile stresses at service conditions which are intended to prevent or limit cracking. The AASHTO Specification allows three levels of tensile stress in the precompressed tensile zone of a member. The maximum tensile stress in this zone is $6\sqrt{f'_c}$ which may be used when bonded reinforcement is provided. One half that stress, or $3\sqrt{f'_c}$, is permitted where corrosive environments are encountered and bonded reinforcement is provided. No tensile stress is allowed if bonded reinforcement is not present. The basic limit of the ACI Code [15] permits a stress of $6\sqrt{f'_c}$ and allows a stress of up to $12\sqrt{f'_c}$ if deflections are within limits and concrete cover is increased. The stress limits may be waived entirely if tests or analysis demonstrate that performance will not be impaired. In this way the ACI Code recognizes that a low allowable tensile stress may not provide good servicability if, for example, the live load is large and transient, which could lead to large camber growth [17]. A method for determining allowable stresses appropriate for a given

structure is given in Ref. [105]. The ACI Code Commentary [17] also recognizes that the use of stressed or unstressed bonded tendons as well as reinforcing bars will serve to control cracking.

Major steps in the design of highway bridges using this approach are outlined in the top half of Fig. 2.1. Parameters given in the first step are largely determined by geometry of the structure and local construction practice. Girders are designed in the second step using trial designs to obtain a strand pattern which satisfies allowable stresses. After a pattern has been determined, the ultimate capacity of the structure is computed to demonstrate sufficient capacity to resist ultimate loads. Deflections should be checked, but AASHTO provides no limits.

A second approach to the design of bridge members has been suggested [95,105] in which the various aspects of the behavior of a structure are considered directly rather than indirectly as done in allowable stress design. This can be done by investigating the "limit states" appropriate for a highway bridge structure, as shown in the bottom half of Fig. 2.1. A limit state is some characteristic or aspect of behavior of a structure that must satisfy some standard in order for a structure to have acceptably fulfilled its intended purpose. Conversely, a limit state may be considered as a possible way in which the structure may fail to fulfill its intended purpose. All of the limit states shown must be addressed in some way if a code is to be complete, with the exception of the last three entries under serviceability which are outside the scope of a code. The 1983 Ontario Highway Bridge Design Code is an excellent example of a limit state design code.

Only a few of these limit states are directly addressed by the current code design approach for prestressed concrete, such as estimating the strength of a structure. Cracking is addressed by limiting tensile stresses and durability is ensured by specifying minimum concrete quality and cover over reinforcement, and by limiting cracking. The remaining limit states are treated indirectly by current codes, such as providing ductility by limiting reinforcement. Loads and effects are specified for computing instantaneous and long-term deflections, but no procedures or limits are given. Effects of fatigue are included by limiting concrete stresses.

It is not clear whether current design procedures, including allowable stress design, will be safe for high strength concrete, especially where code provisions are indirect as mentioned above. This question will be considered throughout the remainder of this

CURRENT DESIGN APPROACH

I. Set Certain Parameters

1. Bridge geometry
2. Girder cross section
3. Strand size and general pattern
4. Girder spacing and deck dimensions
5. Concrete strength of girder and deck

II. Determine number of strands to be used

1. Estimate prestressing losses
2. Check stresses at critical stages of construction
3. Adjust concrete strength of girder as required

III. Check other quantities

1. Ultimate flexural capacity
2. Ultimate shear capacity
3. Deflections

LIMIT STATES

I. Ultimate behavior

1. Capacity in flexure and shear
2. Ductility

II. Serviceability

1. Cracking
2. Deflections
3. Durability
4. Economy
5. Constructability
6. Esthetics

III. Effects of fatigue

Fig. 2.1 Current design approach and limit states

study to determine whether current provisions remain applicable and acceptable or need revision for use with high strength concrete.

2.3 Basic Properties of High Strength Concrete

2.3.1 Compressive Strength. Typically, concrete strength is determined using the 28-day compressive strength of 6 x 12-in. cylinders. A revision of these criteria for use with high strength concrete has been suggested.

The use of 4 x 8-in. cylinders has been proposed for high strength concrete to reduce the required crushing force. A number of investigators have determined relationships between 6 x 12-in. and 4 x 8-in. cylinder data for high strength concrete. Results conflict among investigators, with some suggesting that 4 x 8-in. cylinders are approximately 10 percent stronger than 6 x 12-in. cylinders [104,36], while others found that the smaller cylinders had strengths approximately seven percent less than the larger cylinders [35]. Malhotra [78], in a study of cylinders with strengths up to about 8,000 psi, found that the smaller cylinders were stronger and that the margin of difference increased with increasing concrete strength. He also found that the increased variability of compressive strength of the smaller cylinders resulted in the need to test more than twice as many 4 x 8-in. cylinders to obtain the same level of confidence.

Since high strength concrete often continues to gain strength after 28 days, a later age has been used for the standard test age in several cases [4,39,43]. Data on strength gain with age has been reported by several investigators [104,35,36] and summarized in the Committee 363 Report [22]. Data presented in Fig. 2.2 show that high strength concrete gains strength more rapidly at early ages, but after 28 days the gain is not significantly different from normal strength concrete.

High strength concrete is more sensitive to curing conditions than normal strength concrete [36,104], although strength reductions were not greater than 10 percent. This conclusion was based on comparisons of compressive strength tests at 28 days for moist cured cylinders and cylinders which were moist cured for 7 days, then allowed to dry until testing. Adequate curing is difficult due to self-dessication that is aggravated by the impermeability of high strength concrete which prevents externally applied water from participating in hydration [104].

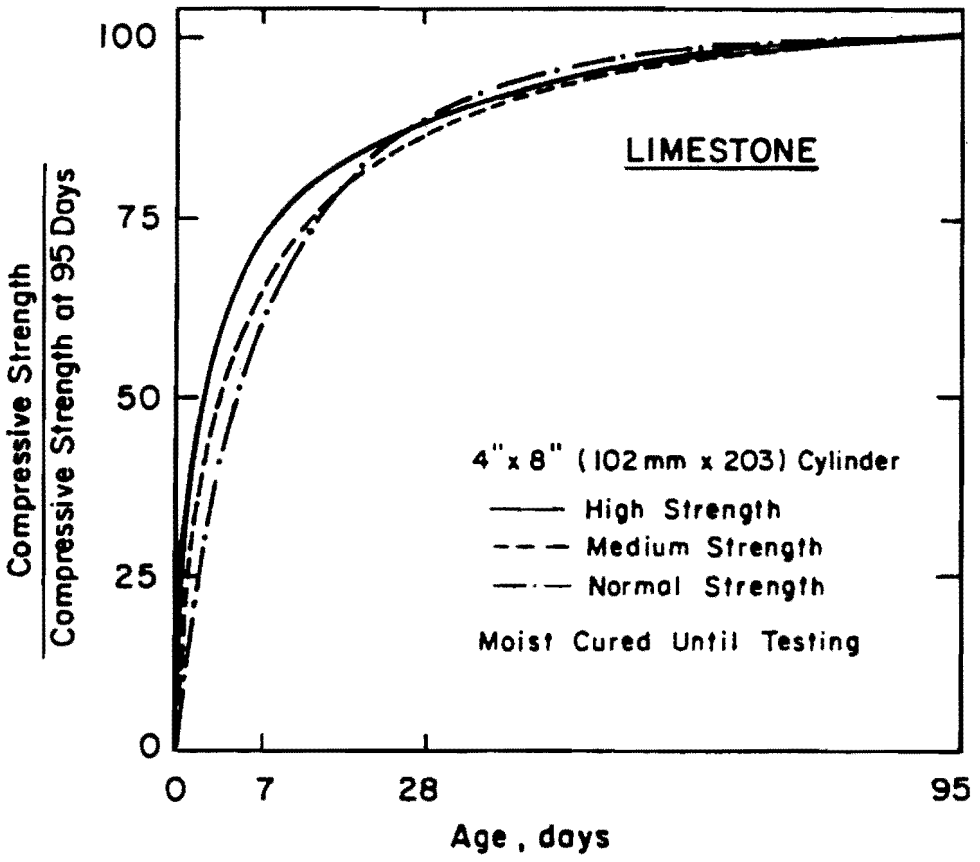

Fig. 2.2 Normalized strength gain with age [35]

2.3.2 Stress-Strain Curve and Modulus of Elasticity. It is widely recognized that high strength concrete behaves differently than normal strength concrete in compression [22,99,135]. The behavior is illustrated by the typical stress-strain curves in Fig. 2.3 [36]. Stress-strain curves for high strength concrete remain approximately linear to a higher fraction of the maximum stress, which occurs at slightly greater strains than for normal strength concrete, and the descending branch is much steeper. Behavior is sensitive to materials used, as evidenced by the two sets of curves in Fig. 2.3.

There is considerable discussion about the characteristics of the descending branch since results are highly dependent upon testing equipment and techniques. While special methods have been used to obtain strains as high as 0.01 in./in., the special test conditions required are seldom found in real structures [99]. Behavior for strengths above approximately 9,000 psi may be described as approximately linear elastic and brittle [99].

Much attention has been given to the determination of the modulus of elasticity of high strength concrete. Modulus data presented in Fig. 2.4 [81,124] show that wide scatter exists for high strength concrete. Because the expression currently used by both AASHTO and ACI to relate concrete strength to the modulus of elasticity is unconservative for much of the high strength data (Fig. 2.4), an alternate equation has been proposed by investigators at Cornell [82]. Modulus measurements are strongly affected by the type of aggregate used [36,126].

Measured strains at maximum stress for a range of concrete strengths are shown for flexure and axial compression tests separately in Fig. 2.5 and combined in Fig. 2.6. The strains tend to increase slightly with increasing strength. Data from flexure tests show good agreement with axial compression tests, with compression test data exhibiting slightly higher results.

Measured ultimate strains for a range of concrete strengths are shown for C-shaped specimens (flexure specimens, see Ref. [71, 103, 124]), beams, and cylinders in Fig. 2.7. All flexure data considered here are for rectangular sections, with the exception of the normal strength concrete test data reported by Mattock and Kriz [86], which had triangular compression zones. Data from all types of specimens, combined in Fig. 2.8, indicate that strains generally tend to decrease with increasing concrete strength and that cylinder data is noticably lower than flexure specimen data. This second fact is

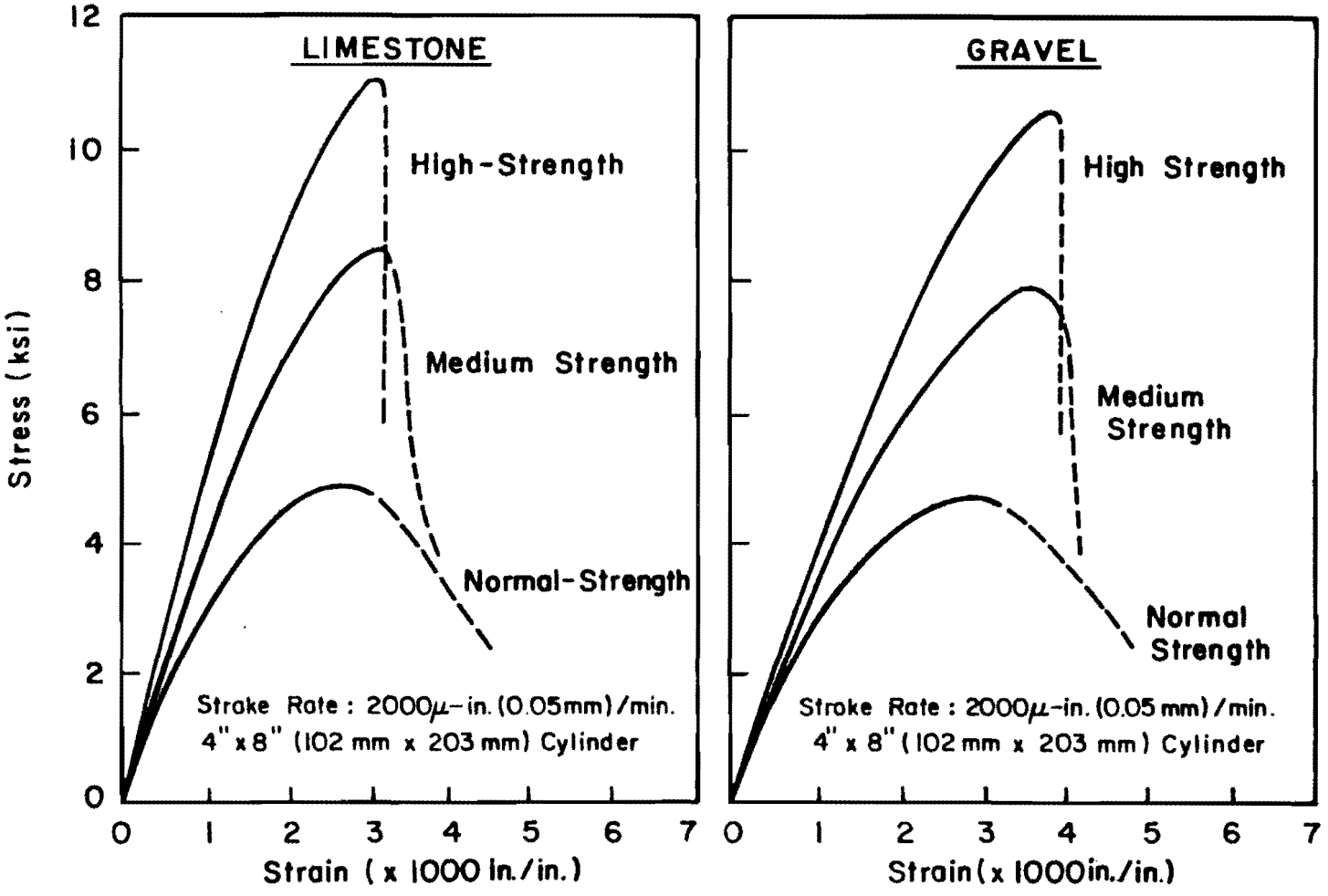

Fig. 2.3 Typical stress-strain curves for different concrete strength [36]

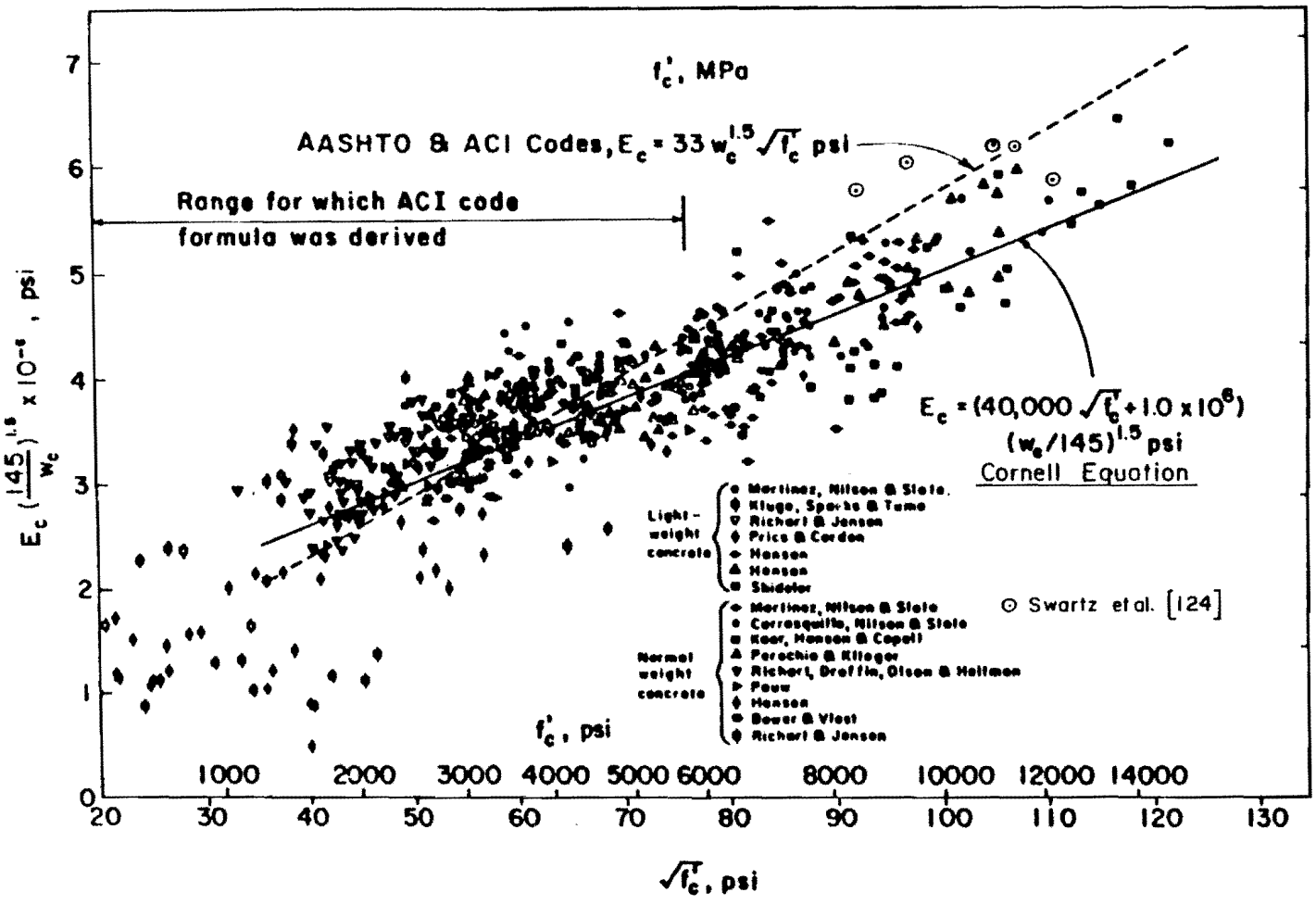

Fig. 2.4 Modulus of elasticity versus concrete strength [81, 124].

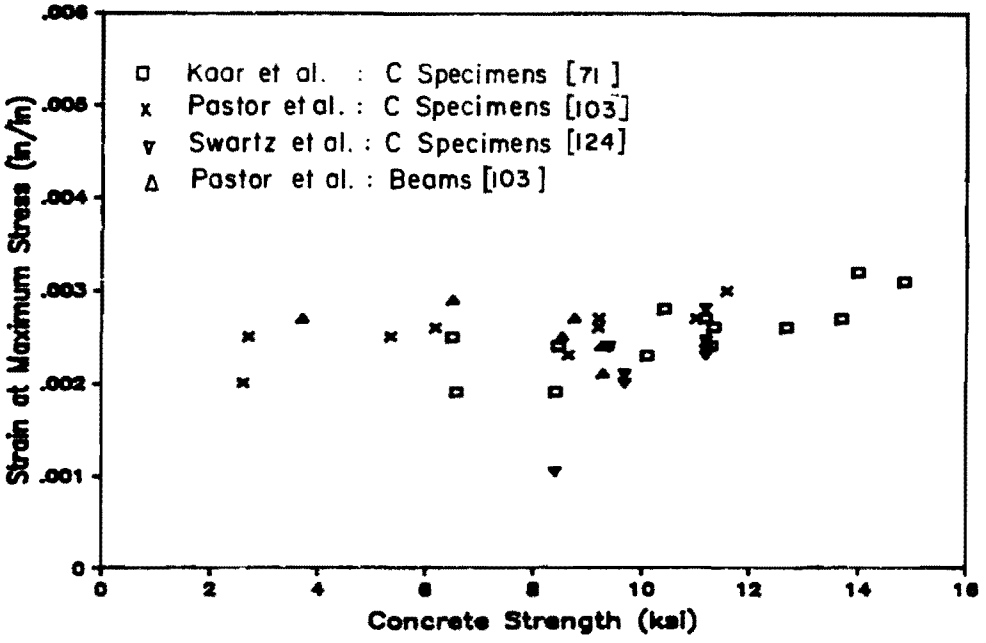

a) C Specimen and Beam Data

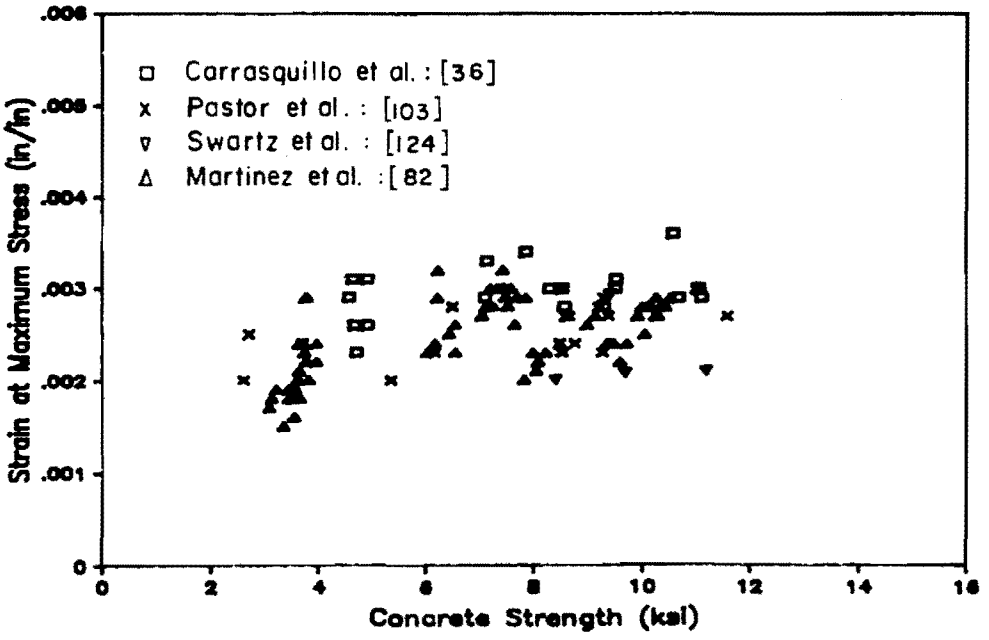

b) Cylinder Data

Fig. 2.5 Strains at maximum stress from flexure and axial tests.

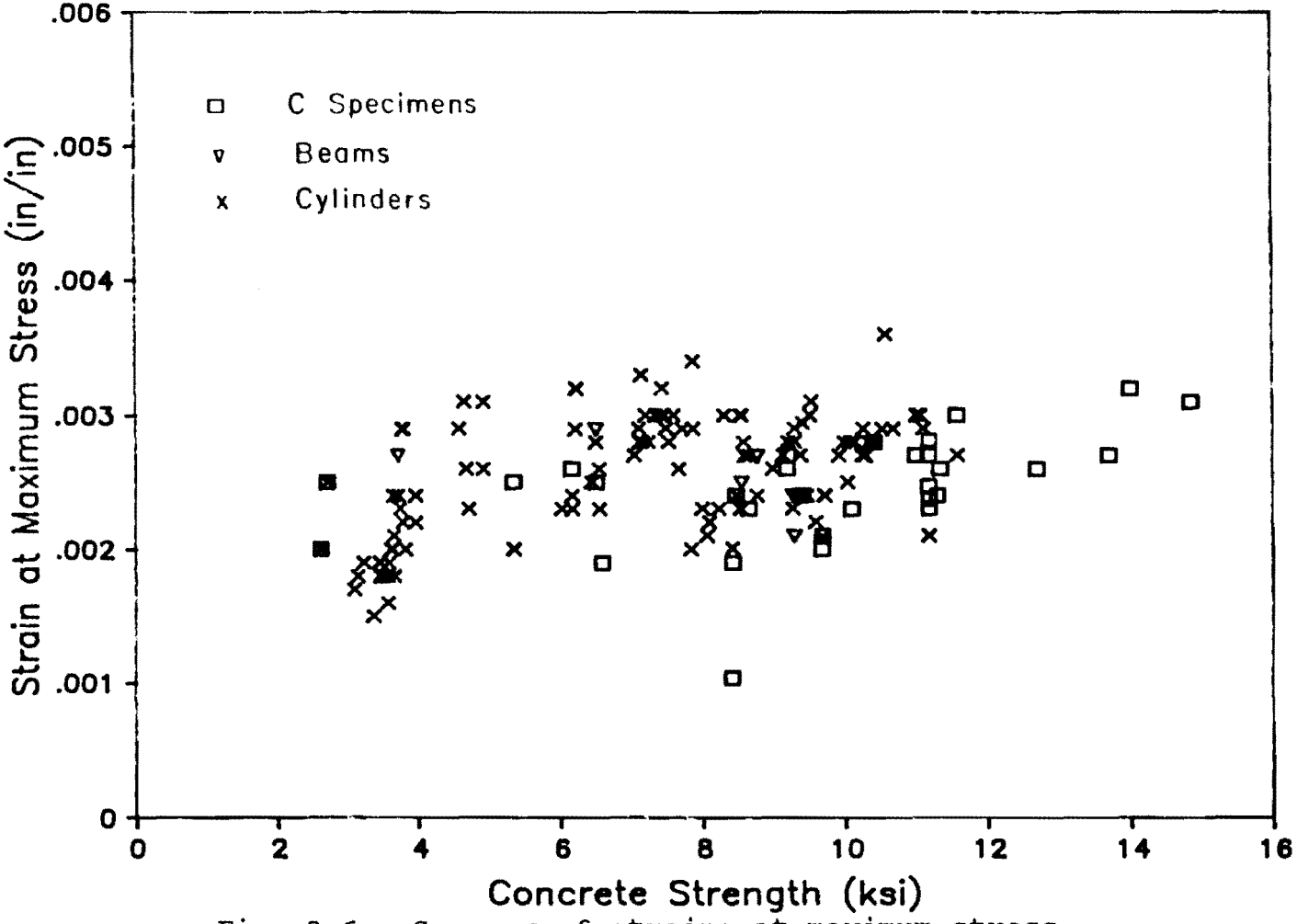

Fig. 2.6 Summary of strains at maximum stress

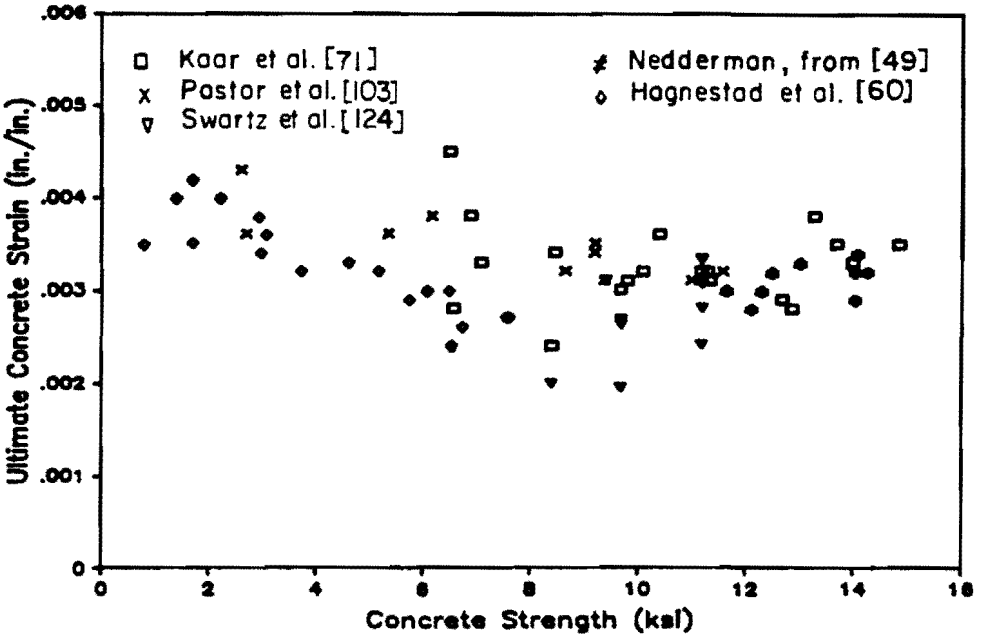

a) C Specimen Data

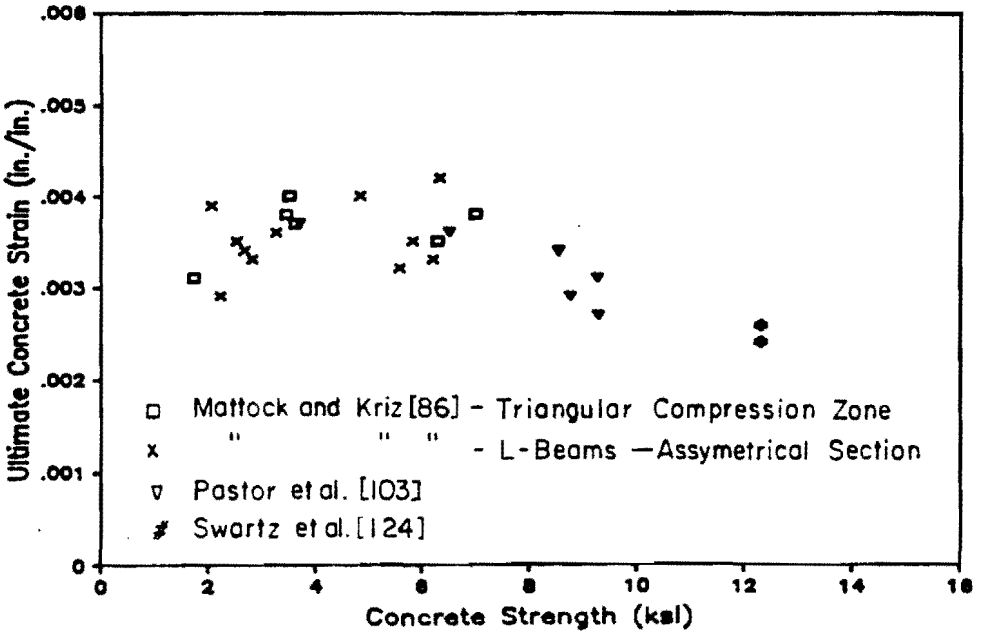

b) Beam Data

Fig. 2.7 Ultimate strains in concrete

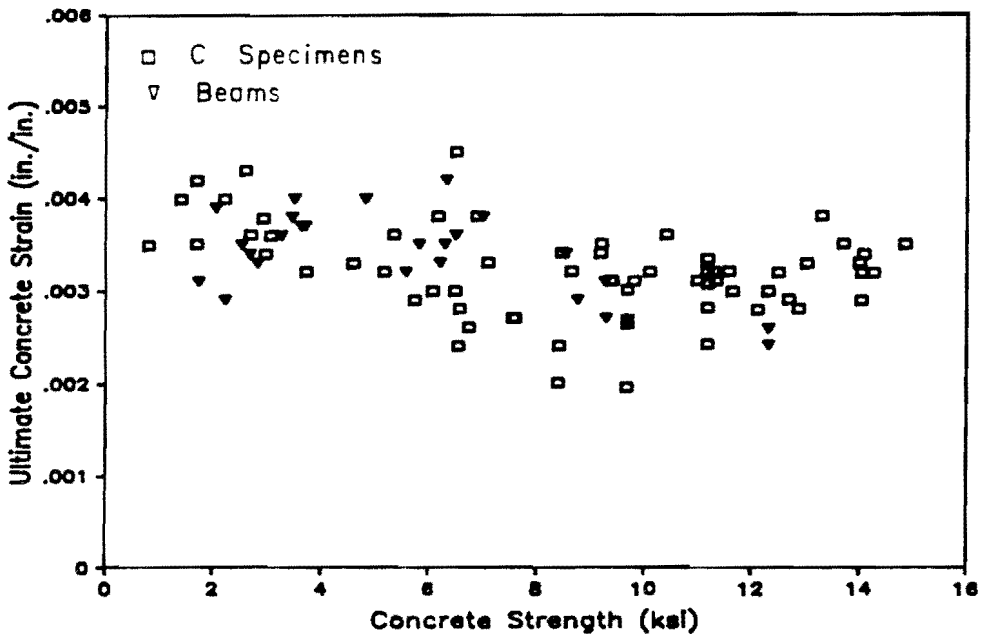

c) Combined C Specimen and Beam Data

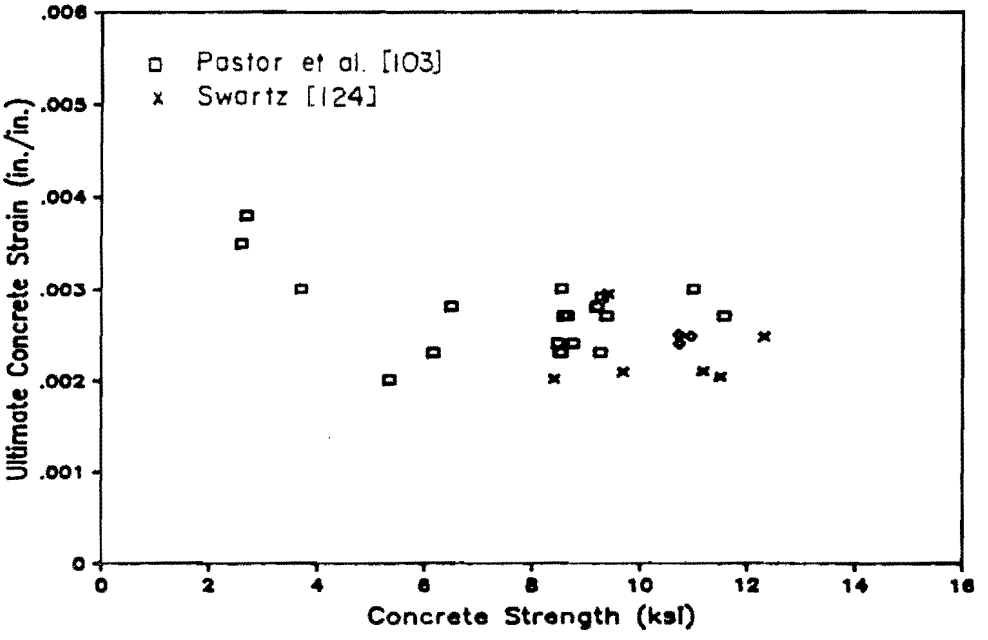

d) Cylinder Data

Fig. 2.7 Ultimate strains in concrete (continued)

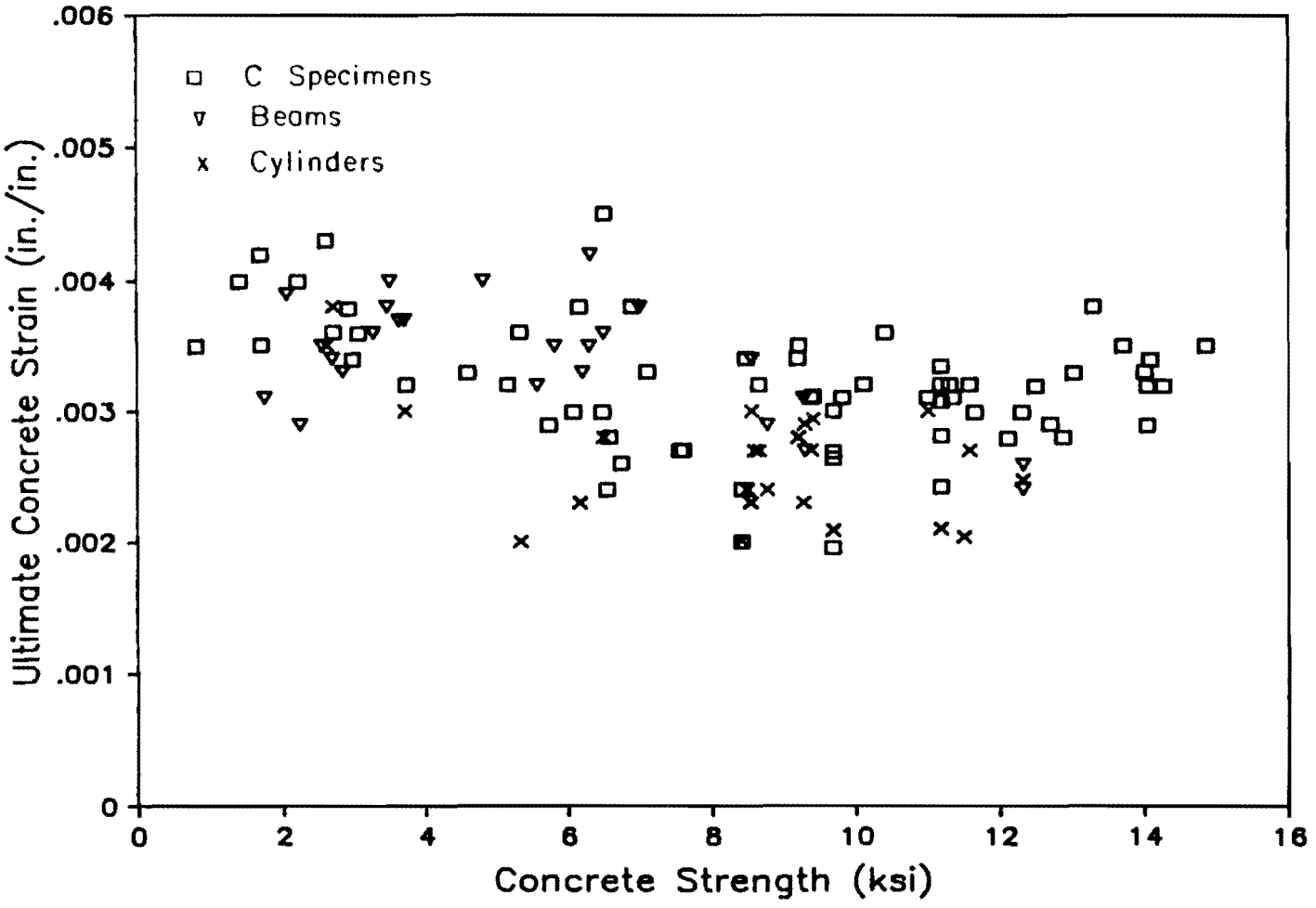

Fig. 2.8 Summary of ultimate strain data

illustrated by Fig. 2.9 which shows that the percentage of data falling below the code specified ultimate strain of 0.003 is much larger for cylinder data than for flexure specimen data. The data of Fig. 2.8 indicate that the current limit of 0.003 is not as conservative for high strength concrete as normal strength concrete (f'_c < 6000 psi) and also show that the use of a limiting strain of 0.004, as considered by some [31,135], would be unconservative. Data reported by Tognon et al. [128] for very high strength concrete (f'_c of about 19 ksi) indicate linear behavior to a strain of approximately 0.003 with failure occurring at a strain of about 0.004. Therefore, for very high strength concrete, the current limit may become overconservative.

Strains at maximum stress and ultimate are compared in Fig. 2.10 for flexure and cylinder data. For the cylinder data, no trend is evident as the two strains are nearly equal for the range of concrete strengths shown. For the flexure tests, the two strains tend to converge as concrete strength increases with the ultimate strains being greater than the strains at maximum stress. This indicates that the descending branch of the stress-strain curve is more readily detectable in flexure tests.

Strain and modulus data from flexure and compression tests of the same concrete are compared in Figs. 2.11 and 2.12. Values for the modulus and strain at maximum stress agree well between flexure and cylinder tests as indicated by the clustering of data about the line of equality. Kaar et al. [71] report that moduli from cylinder tests are higher than for flexure tests. For ultimate strains, cylinder test data underestimate strains obtained in flexure tests. Therefore, it appears that cylinder data can be used for predicting flexural behavior up to the peak stress but that the cylinder data tends to underestimate the extent of the descending branch of the stress-strain curve [103].

2.3.3 Tensile Strength. The tensile strength of concrete measured by split cylinder and modulus of rupture tests for high strength concrete tend to exceed values computed using ACI expressions [36,104]. New formulas have been proposed for predicting both types of tensile strength from compressive strength [36]. However, Nilson [99] suggests that because both measures of tensile strength are sensitive to curing conditions and because significant differences exist between curing conditions in the field and the laboratory, current expressions should remain unchanged. The modulus of rupture for high strength concrete under drying conditions was up to 26

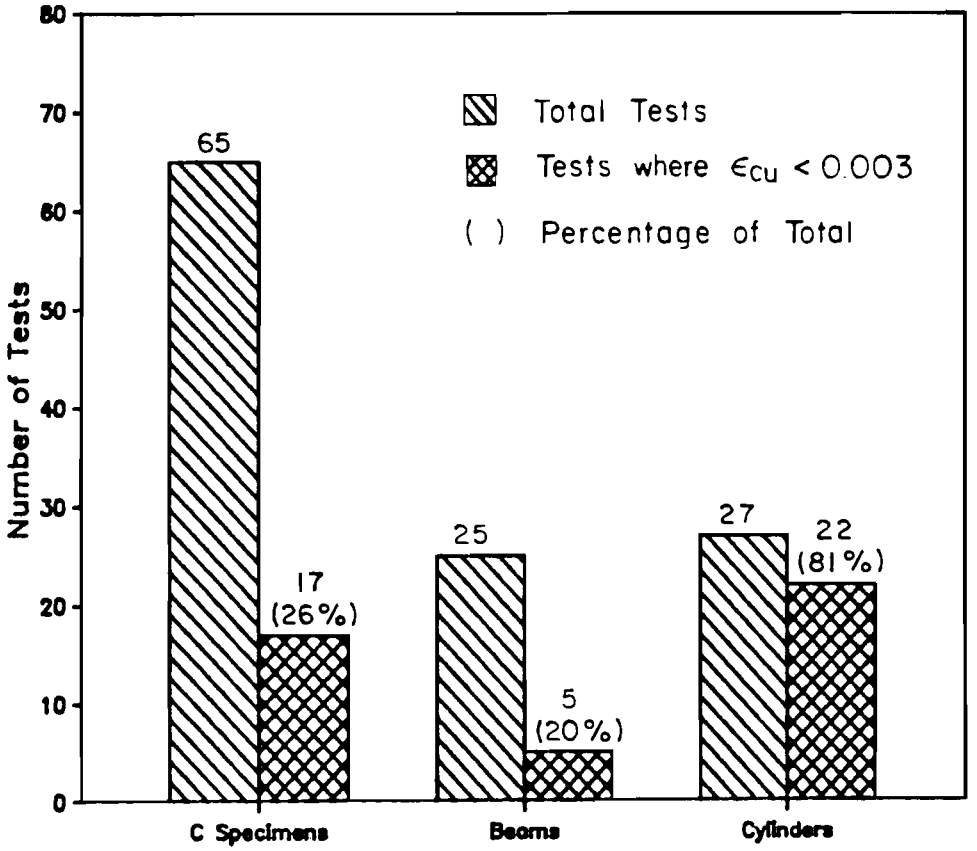

Fig. 2.9 Comparison of number of tests of different types of specimens for ultimate strain.

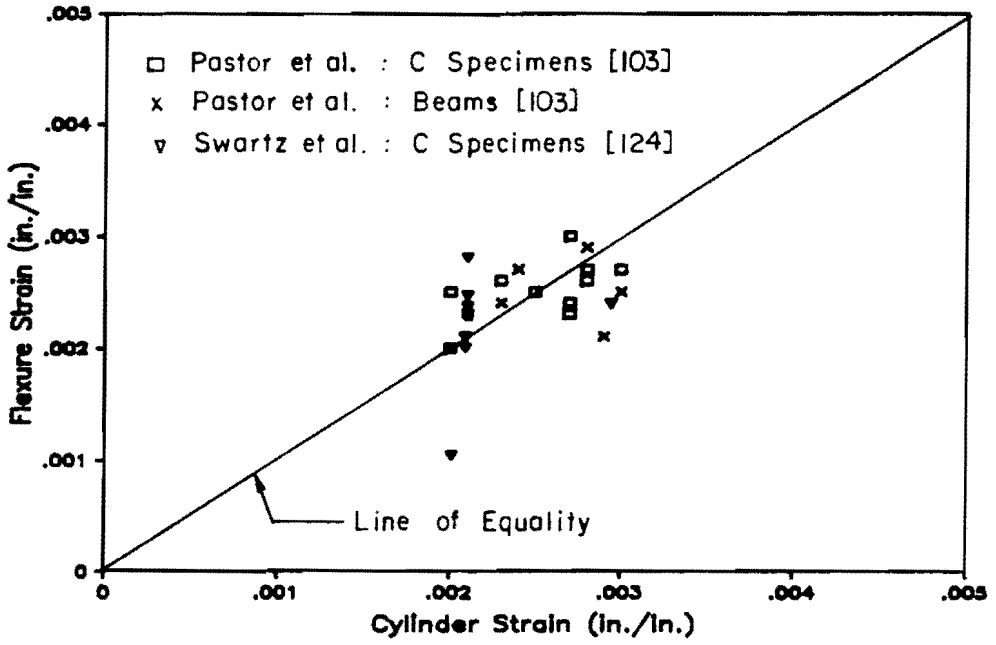

a) Strain at Maximum Stress

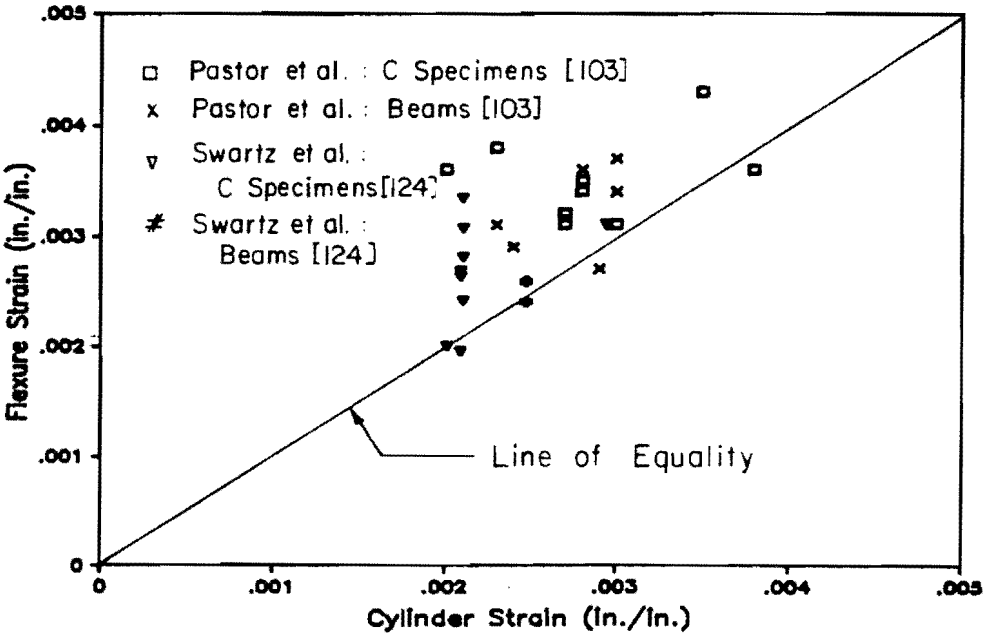

b) Ultimate Strain

Fig. 2.10 Comparison of ultimate strains and strains at maximum stress

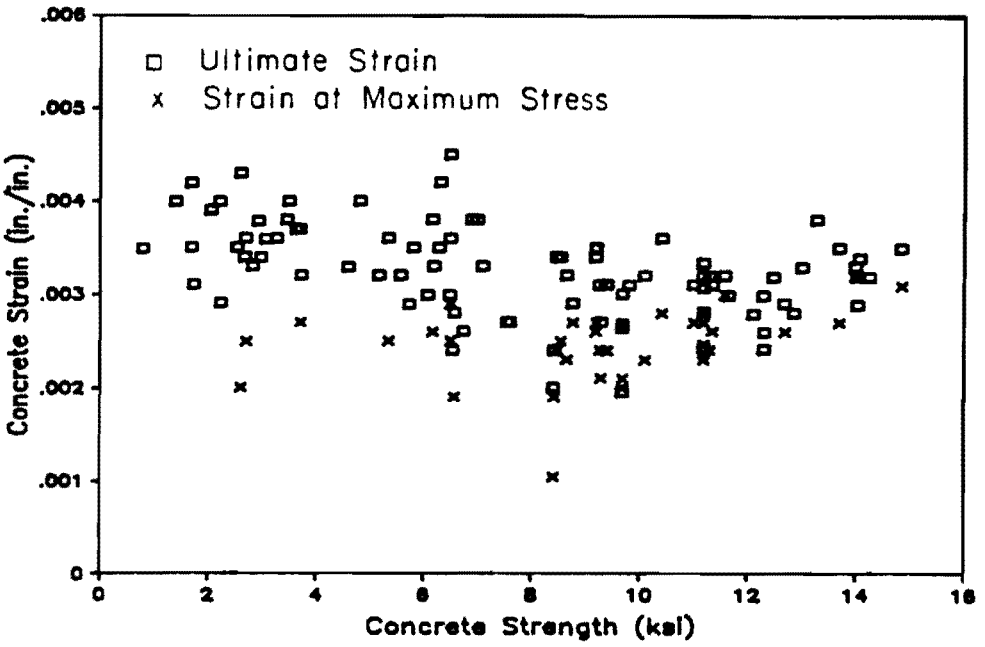

a) Combined C Specimen and Beam Data.

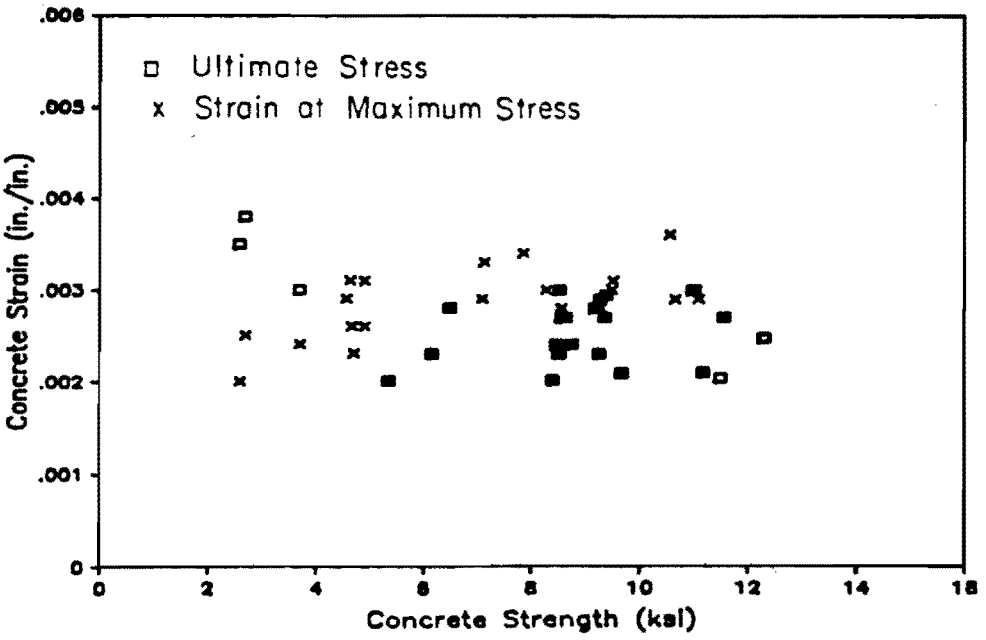

b) Cylinder Data

Fig. 2.11 Comparison of strains measured in flexure and cylinder tests

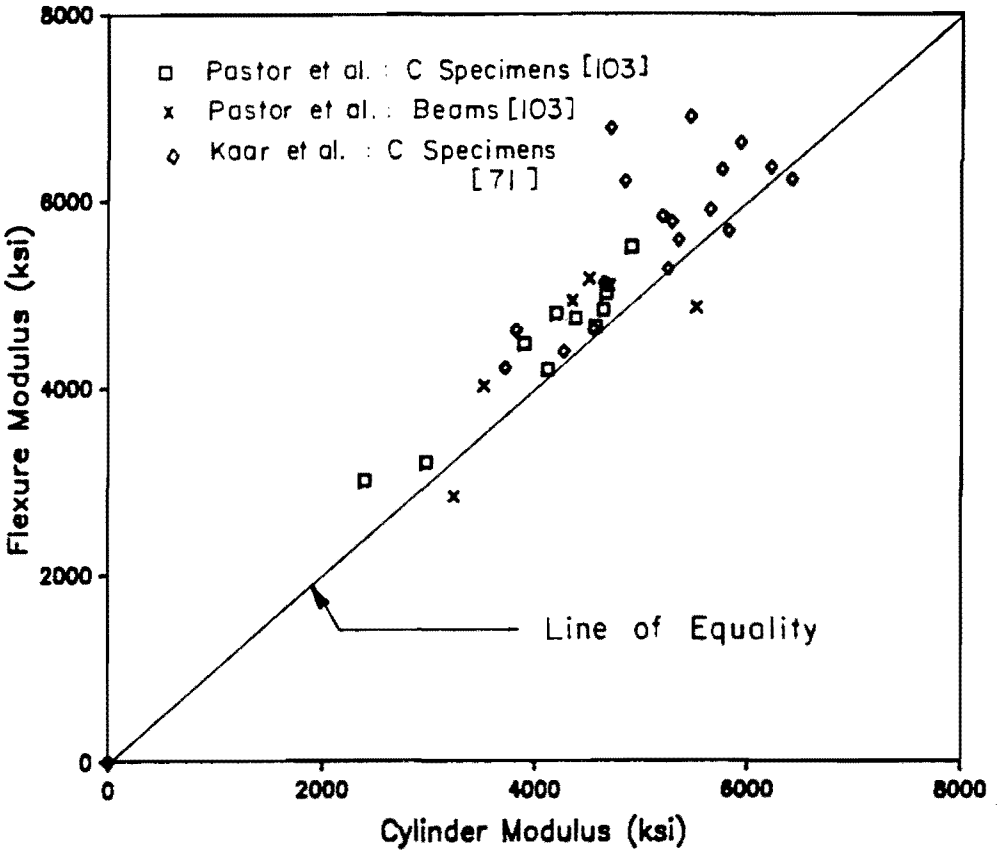

Fig. 2.12 Comparison of moduli measured in flexure and cylinder tests

percent less than values for moist cured concrete. This reduction is greater than observed for normal strength concrete [36].

It should be noted that as concrete strength increases aggregate fracture across the failure plane also increases, leading to a smoother failure surface [36].

Overman et al. [101] observed that, for full scale tests where beams are deep, cracking occurred at stresses less than the AASHTO specified $7.5\sqrt{f'_c}$. A value of 6.7 to $7.0\sqrt{f'_c}$ is recommended for bridge girders.

2.3.4 Creep, Shrinkage, and Thermal Effects. Studies at Cornell [99] have shown that creep coefficients for high strength concrete are lower than for normal and low strength concrete, as summarized in Table 2.1. However, because stresses applied to high strength concrete will generally be higher, total creep is expected to be similar to that of other concrete [22]. Ngab et al. [98] found the relation between applied stress and creep to be linear to about 70 percent of f'_c for high strength concrete rather than 30 to 50 percent for normal strength concrete. In the same study, the ratio of sustained-load strength to short-term strength for high strength concrete ranged from 0.85 to 0.95 while values for normal strength concrete varied from 0.70 to 0.75. Smadi et al. [117], after finding less variation in this ratio with concrete strength than reported by Ngab [98], suggest that 0.8 be used as the sustained strength ratio for all normal weight concrete. Ngab et al. [98] found that the sensitivity of creep to curing conditions often resulted in lower creep factors for dry cured concrete.

While available data is limited, total shrinkage for high strength concrete appears to be similar to normal strength concrete, although high strength concrete may shrink at a higher initial rate [4, 22]. Ngab et al. [98] indicate that total drying shrinkage of high strength concrete may be approximately 500 microstrains for concrete moist cured until 28 days, although there was much variation in the data.

Thermal properties of high strength concrete are similar to those for normal strength concrete [22].

2.3.5 Cover and Durability. To prevent corrosion, AASHTO [10] specifies a minimum cover of 1.5 in. for prestressing steel and principal reinforcement and 1 in. for stirrups and ties. Additional cover should be provided where direct exposure to salt water, salt

Table 2.1 Creep coefficients [99]

Material	f'_c (psi)	C_{cu}	$C_{cu}/C_{cu,LSC}$
Low strength concrete	3,000	3.1	1.00
Medium strength concrete	4,000	2.9	0.94
" " "	6,000	2.4	0.77
High strength concrete	8,000	2.0	0.65
" " "	10,000	1.6	0.52

LSC = Low strength concrete

= 3,000 psi

C_{cu} = Creep coefficient

= Creep strain / initial elastic strain

spray, or chemical vapor cannot be avoided. ACI Committee 343 [21] recommends that cover for reinforcement, where concrete is exposed to weather, should be 2 in. for principal reinforcement and 1.5 in. for stirrups and ties. If concrete is not exposed to weather, only 1.5 in. is required for principal reinforcement and 1 in. for stirrups and ties. If the environment is corrosive, increased cover and concrete quality should be considered. The ACI Code [15] requires cover of 1.5 in. for prestressed beam reinforcement whether exposed or not, but, when allowable tensile stresses are exceeded, the cover shall be increased by 50 percent. The ACI Commentary [17] recommends a cover of 2 in. where the environment is corrosive.

While ACI Committee 363 [22] recommends the use of entrained air where high strength concrete will be exposed to freezing while wet, the limited data available is not conclusive. Use of entrained air causes a significant reduction in strength and should be avoided if the highest possible strength is desired. A loss of from 2 to 5 percent of strength for each one percent void space in concrete has been reported [4,22].

2.3.6 Unit Weight. The unit weight of high strength concrete is slightly higher than for normal strength concrete. Carrasquillo et al. [36] found that average unit weights for normal strength (f'_c = 3,000 to 6,000 psi), medium strength (f'_c = 6,000 to 9,000 psi), and high strength (f'_c > 9,000 psi) mixes containing limestone aggregates were 144, 146 and 152 lb/cu ft, respectively.

2.4 Analysis and Ultimate Capacity in Flexure

This section begins with a review of the historical background and derivations of the basic AASHTO and ACI provisions which are based on simplifying assumptions regarding the concrete stress block and strand stress. Tests intended to verify the applicability of the simplified approaches for use with high strength concrete are reviewed. The more rigorous and general strain compatibility or moment-curvature approaches, which use either simplified or more realistic estimates for concrete and steel stress-strain relationships, will then be discussed. The strain compatibility approach may also be used to compute member behavior throughout its load history. The section concludes with a consideration of the application of the simplified and strain compatibility approaches to composite members.

Each analysis method provides an estimate of the stress in the reinforcement at ultimate, determines the location of the resultants of the resisting compression force in the concrete and compression reinforcement, and computes the moment capacity from these forces and locations using basic principles of analysis. The discussion in this section is limited to the consideration of the assumptions used in the analysis methods and the accuracy of ultimate capacity predictions using these methods.

2.4.1 Simplified Methods.

2.4.1.1 AASHO and AASHTO Specifications. Equations for computing flexural strength for prestressed members first appeared in the 1961 edition of the AASHO Specifications [9] after being a part of tentative specifications for two years. For rectangular or flanged sections where the neutral axis lies within the flange, the flexural strength was computed using

$$M_u = A^*_s f^*_{su} d(1-0.6p^* f^*_{su}/f'_c) \qquad (2.1)$$

and, for flanged sections in which the neutral axis falls outside the flange, which usually occurs if the flange thickness is less than $1.4dp^* f^*_{su}/f'_c$, the flexural strength, M_u, was computed using

$$M_u = A_{sr} f_{su} d(1-0.6A_{sr} f^*_{su}/b'df'_c) + 0.85f'_c(b-b')t(d-0.5t) \qquad (2.2)$$

where
- A^*_s = area of prestressing steel
- A_{sr} = $A^*_s - A_{sf}$
  = area of steel required to develop ultimate compressive strength of the web of a flanged section
- A_{sf} = $0.85f'_c(b-b')t/f^*_{su}$
  = the steel area required to develop the ultimate compressive strength of the overhanging portions of the flange
- d = effective depth of prestressing steel
- b = width of compression flange for flanged member or width of rectangular member
- b' = width of a web for a flanged member
- t = average thickness of the flange of a flanged member
- p^* = A^*_s/bd
  = reinforcing ratio for prestressing steel
- f^*_{su} = average stress in prestressing steel at ultimate load
- f'_c = compressive strength of concrete at 28 days.

These equations, which are shown using current notation, are unchanged from the 1961 Specifications.

The above equations are the only provisions given in the AASHTO Specifications for flexural strength design of prestressed members. In contrast, flexural strength design in the ACI Code is based on general assumptions, which can be applied to a wide variety of situations and section geometries. Equations similar to Eq. 2.1 and 2.2 are provided in the ACI Commentary. A set of general assumptions similar to those in the ACI Code appear in the chapter of the AASHTO Specifications on reinforced concrete design and are used for prestressed concrete design, although the Specifications state that provisions for reinforced and prestressed concrete are independent of each other.

These equations first appeared in the "Tentative Recommendations for Prestressed Concrete" [19] which were made in 1958 by ACI-ASCE Joint Committee 323 (now 423) on Prestressed Concrete. A report by Warwaruk, Sozen, and Siess in 1962 [133] summarized much of the testing and analysis from which the Committee recommendations were developed. The equations given above were developed by assuming the following: (1) a linear variation of strain across the section, (2) concrete resists no tension, (3) failure occurs when the strain in the extreme compression fiber reaches a useful limit, and (4) that the compression stress block may be characterized by factors k_2, k_u, and f_{cu} as shown in Fig. 2.13 (which also contains the equations and definitions of these quantities). Warwaruk et al. [133] reason that the factor k_2, which can vary from 0.5 for a rectangular stress distribution to 0.333 for a triangular distribution should be taken as 0.42 which is an average of the two extremes. The relation between f_{cu}, the effective concrete strength in the compression zone, and f'_c was determined experimentally for two ranges of concrete strength. These factors were combined, using the relation for f_{cu} for the lower strength range, to obtain the equation used in the AASHTO Specification for rectangular sections.

Warwaruk et al. [133] point out that the equation for flanged sections, which was developed by Committee 323, is inconsistent in that it assumes the flange to be stressed at $0.85f'_c$ while the web, treated as a rectangular section, is stressed to $0.72f'_c$. The equation is sufficiently accurate in spite of the discrepancy.

The current AASHTO Specifications provide an equation to estimate stress in bonded prestressed reinforcement at ultimate:

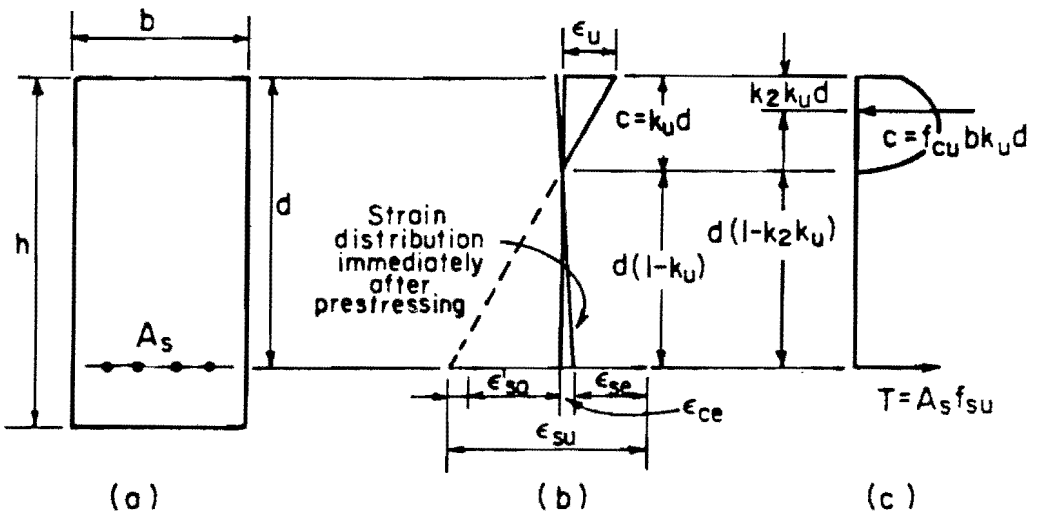

$$M_f = A_s f_{su} d(1-k_2 k_u)$$

where

- k_u = pf_{su}/f_{cu} = ratio of neutral axis depth at failure to effective depth
- k_2 = ratio of the depth of the compressive force to depth of the neutral axis
- f_{cu} = $0.7f'_c$ (from test data) = effective strength of the concrete in the compression zone at failure.
- ϵ_{su} = $\epsilon_{se} + \epsilon_{ce} + \epsilon'_{sa}$ = reinforcement strain at failure
- ϵ_{se} = effective prestrain corresponding to effective prestress
- ϵ_{ce} = concrete strain at the level of the reinforcement due to effective prestress.
- ϵ'_{sa} = increase in strain in the prestressed reinforcement between prestress and failure.
- ϵ_u = useful limit of strain in compressed concrete

Fig. 3.13 Stress and strain conditions at failure for prestressed beams reinforced in tension only - Warwaruk, et al. (Ref. [133]).

$$f^*_{su} = f'_s(1-0.5p^*f'_s/f'_c) \quad (2.3)$$

where f'_s = ultimate strength of prestressing steel.

This equation may be used when the stress-strain properties of the prestressing steel are similar to standard properties and the effective prestress after losses, f_{se}, is not less than $0.5f'_s$. The Specifications allow use of a detailed analysis to better determine f^*_{su}, but no guidance is given on how the analysis should be performed.

This equation also originated in Committee 323. Warwaruk et al. [133] discuss the expression and indicate that it is based on a comparison of the available test results with the parameter $p^*f'_s/f'_c$ which varies approximately in proportion to the depth of the neutral axis at ultimate for rectangular sections with prestressing steel only [84]. The report contains data for rectangular beams with compressive strengths of about 5000 psi prestressed with materials with ultimate strengths close to 250 ksi. According to Khachaturian and Gurfinkel [74], the equation is unconservative for flanged sections, giving steel stresses higher than actually exist. The equation may also underestimate the capacity of beams with high percentages of steel [17]. Warwaruk et al. [133] note the shortcomings of the equation but acknowledge that the simplicity of the equation more than offsets the small inaccuracies in its application.

Committee 323 [19] refers to the Warwaruk report [133] for detailed analyses that may be used in lieu of Eq. 2.3. Two alternate methods are given: the first is a series of equations that are used to develop a single equation which is very accurate for a given ratio of f_{sy}/f_{su}; and the second involves iterations or graphical solutions in which the stress-strain curve of the prestressing steel is used with equations developed from strain compatibility to determine the stress at ultimate.

2.4.1.2 ACI Building Code. The current ACI Code (318-83) [15] provisions for analysis of prestressed sections at ultimate consist of general assumptions regarding strain conditions at ultimate and parameters that define a simplified concrete stress block. Use of other ultimate stress blocks is allowed if they provide "predictions of strength in substantial agreement with results of comprehensive tests." No equations are given in the body of the Code, but equations are provided in the Commentary [17] as examples of the application of the assumptions. Design for prestressed flexural

members is the same as for conventionally reinforced concrete members with the substitution of strand stress at nominal strength, f_{ps}, for the yield stress of conventional reinforcement, f_y. The nominal moment capacity, M_n, for rectangular sections or flanged sections where the depth of the equivalent rectangular compression block, a, is equal to or less than the thickness of the compression flange, can be written for sections with only bonded prestressed tension reinforcement as:

$$\phi M_n = \phi[a_{ps} f_{ps} d_p (a - 0.5\rho_p F_{ps}/f'_c)] \quad (2.4a)$$

$$= \phi[A_{ps} f_{ps} 9 d_p - a/2)] \quad (2.4b)$$

where $a = A_{ps} f_{ps}/(0.85 f'_c b)$ (2.5)

$= $ depth of equivalent rectangular stress block

$A_{ps} = $ area of prestressed reinforcement in tension zone

$f_{ps} = $ stress in prestressed reinforcement at nominal strength (see Eq. 2.12)

$d_p = $ distance from extreme compression fiber to centroid of prestressed reinforcement

$\rho_p = $ reinforcement ratio for prestressed reinforcement $= A_{ps}/bd_p$

$\phi = $ strength reduction factor.

Where the compression flange thickness is less than a, the design moment strength for members with only prestressed tension reinforcement can be computed using:

$$\phi M_n = \phi[A_{pw} f_{ps} (d_p - a/2) + 0.85 f'_c (b - b_w) h_f (d_p - h_f/2)] \quad (2.6)$$

where $A_{pw} f_{ps} = A_{ps} f_{ps} - 0.85 f'_c (b - b_w) h_f$ (2.7)

$a = A_{pw} f_{ps}/(0.85 f'_c b)$ (2.8)

$A_{pw} = $ that part of the tension reinforcement required to develop the web

$b_w = $ web width

$h_f = $ overall thickness of flange.

The strength design provisions from which these equations were developed are based on stress-strain relationships for flexural strength design proposed by Whitney [134], Jensen [68], and others [58]. A modified form of the Stussi stress block and Whitney's

equivalent rectangular stress block (ERSB), shown in Fig. 2.14 for reinforced concrete members reinforced in tension only, were used to model the compression stress block at failure [61,87]. The Stussi parameters k_1, k_2, and k_3 define the magnitude and location of internal compressive force in the concrete at failure. Using these factors and assuming linear distribution of strain across the section, the ultimate moment capacity and depth of compression zone, $k_u d$, for failure initiated by yielding of the tension steel was shown to be:

$$M_u/(bd^2f'_c) = q(1-(k_2/(k_1k_3))q) \tag{2.9}$$

$$k_u = \epsilon_u/(\epsilon_{su} = \epsilon_u) \tag{2.10}$$

where M_u = factored moment at a section
$\leq \phi M_n$
q = reinforcement index
$= A_s f_y/(bdf'_c) = pf_y/f'_c$
ϵ_u = strain in extreme fiber of concrete in compression at ultimate load
ϵ_{su} = strain in reinforcement at ultimate load
f_y = yield point of reinforcement
c = distance from neutral axis to compression edge of member.

Data from tests of special unreinforced C-shaped specimens were used to establish the range of values for the Stussi parameters [61].

The ACI-ASCE Joint Committee 327 on Ultimate Strength Design [20] recommended use of a form of Eq. 2.9 for reinforced members in which the tension steel yields at failure:

$$M_u = A_s f_y d(1-0.59pf_y/f'_c) \tag{2.11}$$

which assumes the Stussi parameters to be

$$k_3 = 0.85$$
$$k_2/k_1 = 0.5.$$

Similar equations are provided for use with other types of reinforced concrete sections. An abstract of the Committee report appeared as an appendix to the 1956 edition of the ACI Code [11] to introduce ultimate strength design. Prestressed concrete was not addressed in this edition.

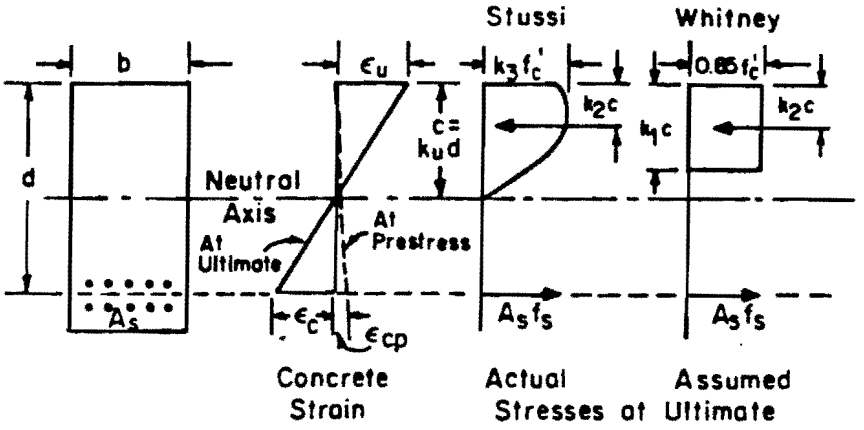

$$M_{ult} = A_s f_s (d - k_2 c) = 0.85 k_1 f'_c bc(d - k_2 c)$$

where

f_s = stress in tensile reinforcement at ultimate strength

k_u = c/d
= $\epsilon_u/(\epsilon_c + \epsilon_u)$

k_1 = ratio of average stress to maximum stress

k_2 = $k_1/2$
= ratio of depth to resultant of concrete compressive force, to depth of neutral axis

k_3 = 0.85
= ratio of maximum stress to 6 x 12-in. cylinder strength, f'_c

ϵ_s = $\epsilon_u[0.85 k_1 f'_c/(pf_s)-1] + \epsilon_{cp} + \epsilon_{se}$
= tensile steel strain at ultimate beam strength

ϵ_{se} = effective steel prestrain

ϵ_{cp} = concrete precompression strain at level of steel in a prestressed beam

ϵ_c = concrete tensile strain at ultimate at level of steel in prestressed beam

ϵ_u = maximum concrete compression strain at ultimate beam strength

Fig. 2.14 Stress and strain conditions at failure for prestressed beams reinforced in tension only - Matlock, et al. (Ref. [87]).

In 1957, Hognestad [59] presented further analyses of test data to verify the validity of the 0.59 coefficient in Eq. 2.11 and demonstrated this coefficient could be obtained using the assumptions of Whitney's ERSB. Although the assumptions used to develop these equations are not accurate for non-rectangular sections and rectangular sections subjected to assymetrical bending, the error is small if failure is initiated by yielding of the reinforcement. Later tests and analysis confirmed this [86]. Ultimate design methods were also shown to be sufficiently accurate for prestressed members [66].

Mattock, Kriz, and Hognestad [87] proposed the general statement of the ultimate design assumptions including the ERSB in 1961. Prestressed members were discussed and an iterative approach was suggested to determine the steel stress at ultimate.

The ACI Building Code (318-63) [12] adopted this general statement of ultimate strength design with only a few revisions and extensions for both reinforced and prestressed concrete. Capacity reduction factors were also introduced. Strand stress at ultimate was estimated using the same equation and limitations as appear in the AASHTO Specifications.

Other than changes in notation, only a few substantial changes in the Code provisions have occurred since 1963. In 1971 [13], equations for computing flexural strength were removed from the body of the Code. In the 1983 edition of the ACI Code, the equation used to provide an estimate of strand stress at ultimate was revised to better reflect current practice, including use of low relaxation strand, high strength concrete, compression steel, and nonprestressed reinforcement [84]. The equation now appears as

$$f_{ps} = F_{pu}\left(1 - \frac{\gamma p}{\beta_1}\left[\rho_p \frac{f_{pu}}{f'_c} + \frac{d}{d_p}(\omega - \omega')\right]\right) \qquad (2.12)$$

where f_{pu} = specified tensile strength of prestressed reinforcement

γ_p = factor for type of prestressing tendon

= 0.40 for f_{py}/f_{pu} not less than 0.85 (stress-relieved strand)

= 0.28 for f_{py}/f_{pu} not less than 0.90 (low relaxation strand)

β_1 = a factor used in the definition of the ERSB which relates the depth of the compression block, a, to the depth to the neutral axis, c. For $f'_c \leq 4{,}000$ psi, $\beta_1 = 0.85$. For

$f'_c \geq 4{,}000$ psi, β_1 is reduced continuously at a rate of 0.05 for each 1,000 psi of strength in excess of 4,000 psi, but β_1 shall not be less than 0.65.

ω = reinforcement index for nonprestressed tension reinforcement
= $A_s f_y / bdf'_c$

ω' = reinforcement index for nonprestressed compression reinforcement
= $A'_s f_y / bd' f'_c$

d = distance from extreme compression fiber to centroid of nonprestressed tension reinforcement, in.

d' = distance from extreme compression fiber to centroid of nonprestressed compression reinforcement, in.

2.4.1.3 Results of Tests. The first research on high strength concrete in flexure was conducted by Nedderman in 1973 at the University of Texas at Arlington (see [76,49]). Concrete strengths in the range of approximately 11.6 to 14.25 ksi were used in the study. Kaar, Hanson, and Capell reported additional work in 1978 [71] in which concrete strengths up to 14.85 ksi were used. Both investigations used C-shaped specimens similar to those used in the tests by Hognestad et al. [60] to determine the validity of the ERSB for high strength concrete. On the basis of their findings, a lower limit was placed on the factor β_1 (formerly k_1) in the 1977 edition of the ACI Code [14], but otherwise, the ERSB was found to be appropriate for use with high strength concrete.

Leslie, Rajagopalan, and Everard [76] published results from tests of high strength concrete beams in 1976 and recommended a smaller value for the ultimate strain and a triangular stress block instead of the ERSB. However, in the discussion of this paper, Ghosh and Chandrasekhar [49] and Wang, Shah, and Naaman [130] demonstrate that a triangular stress block would produce a negligible improvement over the current ERSB, and question the need for a reduced ultimate strain.

An analytical study by Wang, Shah and Naaman [131] in 1978 gave further indication that the current ERSB could be used with high strength concrete to provide reasonable estimates of ultimate capacity in flexure. They maintain that ultimate strains in excess of the current limit of 0.003 could be attained even for high strength

concrete. This assertion was supported by a later paper by the same authors [132] which reported data for concrete cylinders tested in parallel with a hardened steel tube where strains of 0.006 were consistently obtained for concrete strengths up to 11,000 psi.

Tests of C-shaped specimens and reinforced beams made with high strength concrete conducted at Cornell University by Pastor, Nilson and Slate [103] were reported in 1984. Again, the data show that current ERSB parameters give a reasonable and conservative representation of high strength concrete at ultimate. The use of more sophisticated stress blocks was recommended only if very accurate results were desired. Nilson [99] commented later that, on the basis of test data, existing flexural strength design provisions were satisfactory for all concrete strengths if the tensile steel yielded.

The State-of-the-Art Report on the use of high strength concrete presented by ACI Committee 363 in 1984 [22] echoed the above findings by stating that present ACI provisions could be used without change for under-reinforced members with concrete strengths up to 12,000 psi.

A recent report on additional tests of C-shaped specimens and reinforced beams by Swartz et al. [124] showed the factor $k_2/(k_1k_3)$ was close to the ACI value, but β_1 was closer to 0.83 which is higher than the 0.65 given by the Code. fficient accuracy.

2.4.2 Strain Compatibility Methods. The compatibility or moment-curvature analysis method for determining the ultimate moment capacity of prestressed members is a more general form of the basic approaches that have been discussed above. The method can be used with the assumptions of the ERSB to obtain ultimate moment capacities without the use of an equation to estimate the strand stress. It can also be used to predict the complete load-deformation behavior of a member if a complete representation of the stress-strain relationship for the concrete is used.

The basic requirement of the method is the establishment of strain compatibility and force equilibrium across the section. A top fiber strain (or some other quantity) is assumed and height of the neutral axis is adjusted until a strand strain is obtained that

produces a force equal to the compression force in the concrete. The ultimate moment can be either the moment when the top fiber strain is a certain value, such as 0.003 for ACI, or, more accurately, the maximum moment resisted by the section as top fiber strain is increased. Compression reinforcement or nonprestressed tension reinforcement can be accomodated in the analysis, the details of which can be found elsewhere [34,93,133].

While many analytical expressions have been proposed for the concrete stress-strain curve, only a sampling of those which are simple and do not require stress-strain data for calibration of coefficients are presented here. Equations and parameters for five stress-strain relationships are presented in Fig. 2.15 and the curves are compared for 5,000 and 10,000 psi concrete in Fig. 2.16.

Naaman [95], after reviewing a number of expressions for the stress-strain characteristics of prestressing strand, recommended the expression by Menegotto and Pinto as most suitable. Figure 2.17 illustrates the relationship and Table 2.2 gives coefficients derived for use in the relationship.

The stress-strain behavior of nonprestressed steel can be approximated by assuming elastic-plastic behavior, which is conservative. If strain hardening is to be considered, Wang, Shah, and Naaman [131] present a method for describing the complete stress-strain curve for nonprestressed steel.

2.4.3 Composite Design. Both the AASHTO Specifications [10] and the ACI Code [15] give little guidance in the application of the flexural strength equations and concepts to composite structures. The only specific comment of help is found in the ACI Code which indicates that, where properties of the elements of a composite structure differ, "...the properties of the individual elements or the most critical values, shall be used in design."

When a strain-compatibility analysis is used, actual properties for girder and flange concrete can be used unless the ERSB is used. If the ERSB is used, the section must be assumed to be composed of a single strength of concrete or the assumptions of the ERSB can be applied to the girder and deck concrete individually. When the girder and deck concrete strengths are considered individually, the top fiber strain of both the girder and deck must be assumed incorrectly to be 0.003 in order to satisfy the assumptions of the ERSB approximation.

Investigator			Equations and Parameters	
Jensen [68]	f_c	=	$\epsilon_c E_c$	for $\epsilon \leq \epsilon_0$
	f_c	=	f'_c	for $\epsilon > \epsilon_0$
	ϵ_0	=	f'_c/E_c	
	ϵ_{cu}	=	$f'_c/E_c/(1-\beta)$	
	β	=	$1/(1+(f'_c/4000)^2)$	

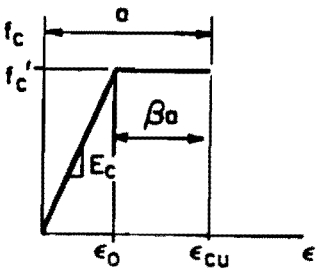

Hognestad [58]	f_c	=	$f''_c(2\epsilon/\epsilon_0-(\epsilon/\epsilon_0)^2)$
	ϵ_0	=	$2f''_c/E_c$
	f''_c	=	$0.85f'_c$
	ϵ_{cu}	=	0.0038

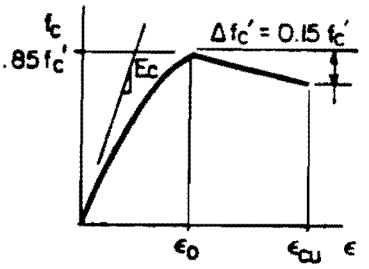

Burns [34]	f_c	=	$f'_c(2\epsilon/\epsilon_0-(\epsilon/\epsilon_0)^2)$
	ϵ_0	=	$2f'_c/E_c$
	ϵ_{cu}	=	0.0035

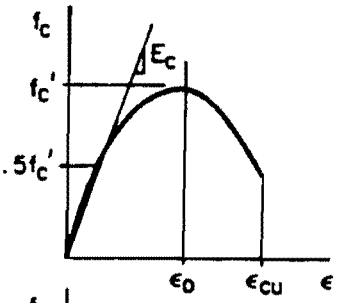

Kent and Park [73]	f_c	=	$f'_c(2\epsilon/\epsilon_0-(\epsilon/\epsilon_0)^2)$
	ϵ_0	=	0.002
	ϵ_{50u}	=	$\dfrac{3 + 0.002f'_c}{f'_c - 1000}$

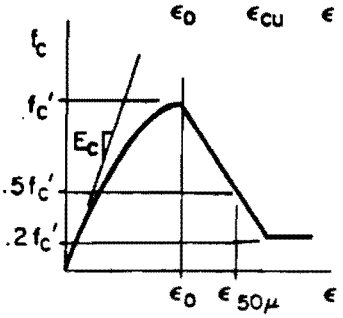

Carreira and Chu [37]	f_c	=	$f'_c(\beta(\epsilon/\epsilon_0)/(\beta-1+(\epsilon/\epsilon_0)^\beta))$
	ϵ_0	=	$(4.88f'_c+168)\times10^{-5}$
		=	0.002 (approx.)
	β	=	$1/(1-(f'_c/E_{it}\epsilon_0))$
	E_{it}	=	E_c (approx.)

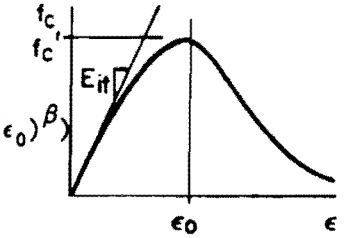

Fig. 2.15 Analytical stress-strain curves for concrete

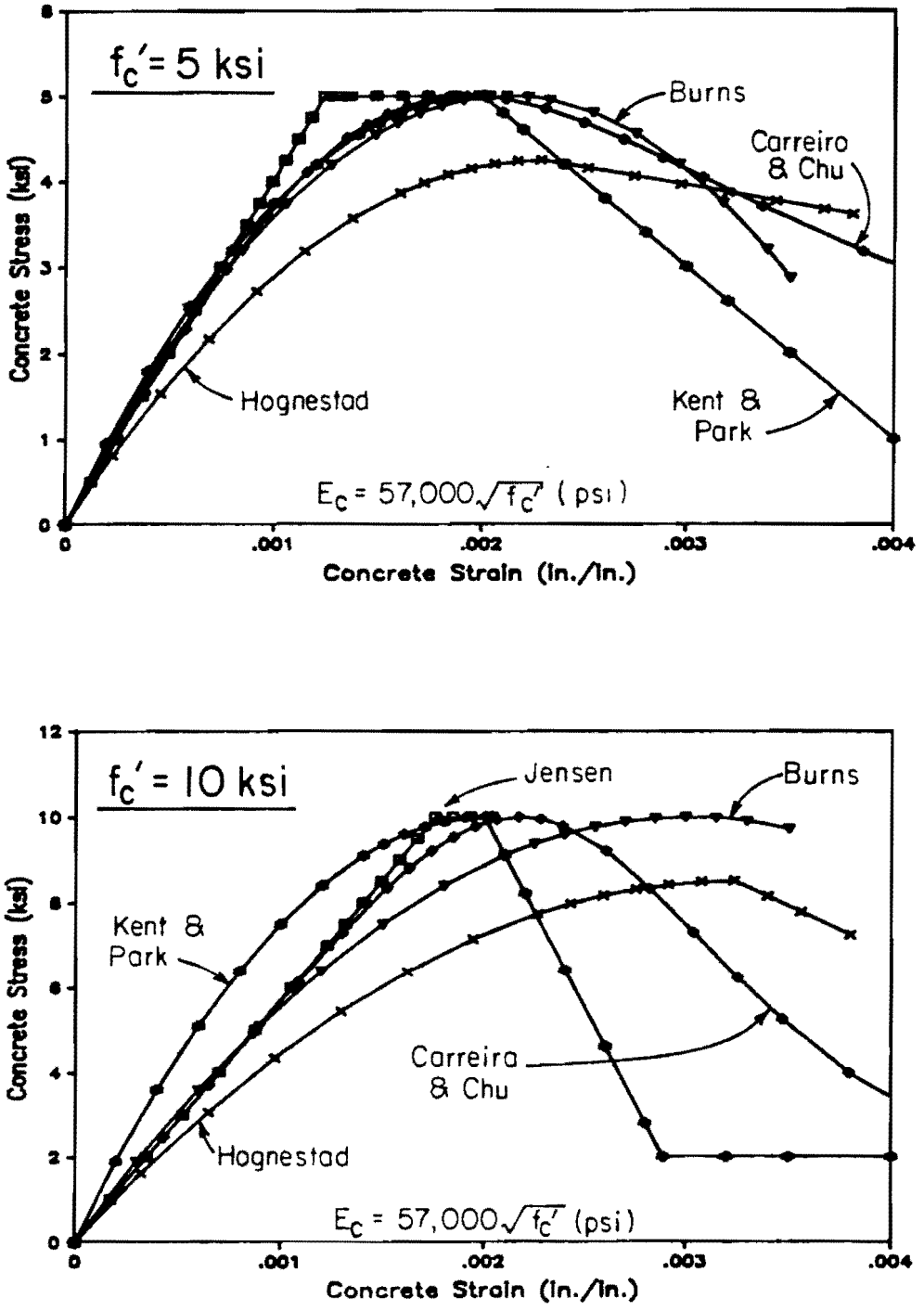

Fig. 2.16 Comparison of analytical stress-strain curves for concrete.

$$f = E\epsilon \left[Q + \frac{1 - Q}{\left[1 + \left(\frac{E\epsilon}{Kf_y} \right)^N \right]^{1/N}} \right]$$

$$Q = \frac{f_u - Kf_y}{E\epsilon_u - Kf_y}$$

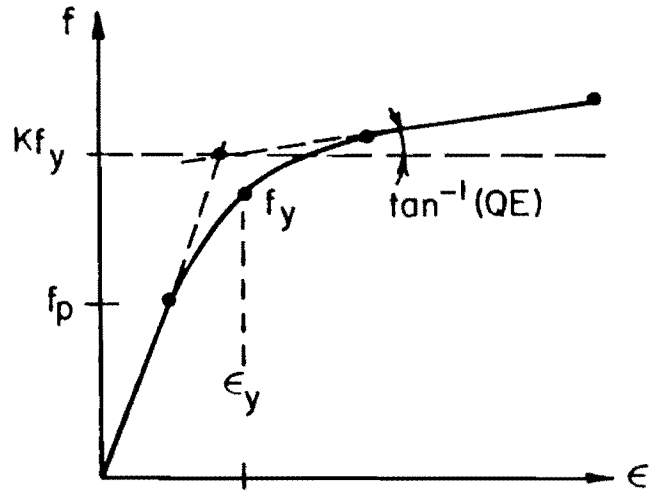

Menegotto and Pinto (1973)

Notation applies to reinforcing or prestressing steel:

Subscript y for yield, u for ultimate,
p for proportional limit, E for elastic modulus.

Fig. 2.17 Analytical stress-strain curve for prestressing steel [95]

Table 2.2 Coefficients for the stress-strain relationships of typical prestressing steels [95]

Fitting Constraints	Stress-Strain Relationship	Bars 160 ksi (1104 N/mm^2)	Wires 235 ksi (1620 N/mm^2)	Strands 270 ksi (1863 N/mm^2)
To satisfy Minimum Specified ASTM Standards*	Goldberg and Richard	N = 2.773	N = 2.743	N = 4.265
	Menegotto and Pinto	N = 4.24 K = 1.04728 Q = 0.01797	N = 2.91 K = 1.1470 Q = 0.00625	N = 4.77 K = 1.1341 Q = 0.01185
Typical Actual Behavior	Menegotto and Pinto	N = 7.1 K = 1.0041 Q = 0.0175 for E_{ps} = 28790 f_{pv} = 141.8 f_{pu} = 160 $_{pu}$ = 0.041	N = 6.06 K = 1.0325 Q = 0.00625 for E_{ps} = 29300 f_{pv} = 222.4 f_{pu} = 244 $_{pu}$ = 0.087	N = 7.344 K = 1.0618 Q = 0.01174 for E_{ps} = 27890 f_{pv} = 243.5 f_{pu} = 278 $_{pu}$ = 0.069

*f_{py} = 0.85 f_{pu}; $_{pu}$ = 0.010 for wire and strands and 0.007 for bars, $_{pv}$ = 0.040; elastic modulus = 27000 ksi for strands, 28000 ksi for bars and 29000 ksi for wires; 1 ksi = 6.9 N/mm^2.

2.5 Ductility and Reinforcement Limits

Naaman [95] defines ductility as "a measure of the ability of a material, section, structural element or structural system to sustain inelastic deformation prior to collapse, without substantial loss in resistance." This ability is essential for structures if sufficient warning of impending collapse is to be given to permit evacuation, removal of load, repair, or other action before collapse of the structure. Another general way of expressing this concept is that brittle failures are to be avoided [102]. In practice, limits are placed on the quantity of reinforcement to ensure ductility [77].

In this section, the ductility of pretensioned sections or members and related reinforcement limits will be considered.

2.5.1 Development of Code Provisions. The development of code provisions began with the ACI-ASCE Joint Committee 327 Report on Ultimate Strength Design [20] that appeared in 1955 and 1956. This Report contained the following limit on the reinforcement ratio, p, for reinforced concrete:

$$p \leq 0.40f'_c/f_y \tag{2.13}$$

where the coefficient 0.40 was to be reduced by 0.025 for each 1,000 psi in excess of 5,000 psi. This limited the reinforcement ratio to about "...0.9 of that required to develop the full compressive strength of the section." A different method was used for columns in which behavior was categorized with respect to the load producing balanced failure, i.e., the load at which concrete reaches the ultimate strain and the tension steel yields. No provision for minimum reinforcement was given. The report was intended to apply to reinforced concrete members.

The Appendix to the 1956 ACI Code [11], which dealt with the ultimate strength design of reinforced concrete members, contained Eq. 2.13 with the related variation in the coefficient for different concrete strengths. No minimum reinforcement limit or provisions for prestressed concrete were given.

The "Tentative Recommendations for Prestressed Concrete" prepared by ACI-ASCE Joint Committee 323 [19] in 1958 included the following maximum reinforcement limits:

$$pf_{su}/f'_c \leq 0.30 \quad \text{(rectangular)} \tag{2.14}$$

$$A_{sr}f_{su}/b'df'_c \leq 0.30 \qquad \text{(flanged)} \tag{2.15}$$

These limits on prestressed reinforcement were intended to "avoid approaching the condition of over-reinforced beams for which the ultimate flexural strength becomes dependent on the concrete strength...." Members with reinforcement ratios which exceeded these limits were permitted, although the ultimate capacity was limited. A mix of prestressed and nonprestressed steel was permitted and the maximum reinforcement limit for this case was

$$pf_{su}/f'_c + p'f'_y/f'_c \leq 0.30 \tag{2.16}$$

where p'and f'_y are the reinforcement ratio and yield stress, respectively, for the nonprestressed reinforcement. No requirements for mimimum reinforcement were given.

The requirements of the 1961 edition of the AASHTO Specifications [9] were the same as those of the Committee 323 Report [19] with an additional expression similar to Eq. 2.16 given that applied to flanged sections with nonprestressed reinforcement. Minimum steel percentage was mentioned in the heading of a section, but no limit was provided.

Mattock, Kriz, and Hognestad [87] suggested that "if it is considered desirable for design purposes to establish a limiting value of q, the reinforcement index, less than q_b..., then ... this limiting value [should] be expressed as a fraction of q_b and not in the form in current use." The tension reinforcement index for the balanced condition, q_b, was given for reinforced concrete as

$$q_b = p_b f_y/f_c' = 0.85k_1\epsilon_u/(\epsilon_y + \epsilon_u) \tag{2.17}$$

where p_b = the reinforcement ratio corresponding to the balanced condition

ϵ_u = maximum concrete compression strain in flexure

ϵ_y = yield strain in the conventional reinforcement.

A simple, approximate formula was given to determine an alternative limit, q_{lim}, for the reinforcement index, q:

$$q_{lim} = 80/\sqrt{f_y}, \qquad (f_c' < 4{,}000 \text{ psi}) \tag{2.18}$$

where, for concrete strengths in excess of 4,000 psi, q_{lim} is reduced by 0.02 for each 1,000 psi. This formula ensures that q would be from 70 to 80 percent of q_b for a wide range of concrete and steel strengths.

An examination of the report on prestressed concrete by Warwaruk, Sozen, and Siess [133] of 1962 is very instructive. The introduction to the section "Limits on Longitudinal Reinforcement" is extracted below:

> Ideally, there need be no limits on the amount of longitudinal reinforcement that is provided in a prestressed concrete beam. Whatever the amount of reinforcement, the flexural strength can be calculated.... However,... in certain ranges the flexural strength is very sensitive to variations in the beam properties and it would be undesirable to proportion a beam in such a range, not only because the theory may not be accurate, but also because errors made in the field may prove catastrophic. Consequently, limits must be placed on amount of longitudinal reinforcement in relation to the concrete strength, the properties of the reinforcement, and the dimensions of the section. To insure that the strength of the beam is insensitive to possible variations in the material and geometrical variables, the reinforcement strain at ultimate must be well in the inelastic range of the stress-strain curve.... Thus, a reasonable lower limit to the computed reinforcement strain at ultimate ϵ_{su} is 0.01.

For prestressing steel in use at the time, a strain of 0.01, which is used in ASTM A416 [25] to define yield, was near the end of the knee in the stress-strain curve. Therefore, variations in the steel strain caused by variations in other properties of the section would produce only minor changes in the stress in the steel, and the effect on the ultimate capacity would be minimal. This is illustrated graphically in Fig. 2.18 where a slight variation in pf_c' for Case 2 will lead to a large variation in stress in the prestressing steel, resulting in a significant fluctuation in moment capacity.

Warwaruk et al. [133] used the strain compatibility relationship

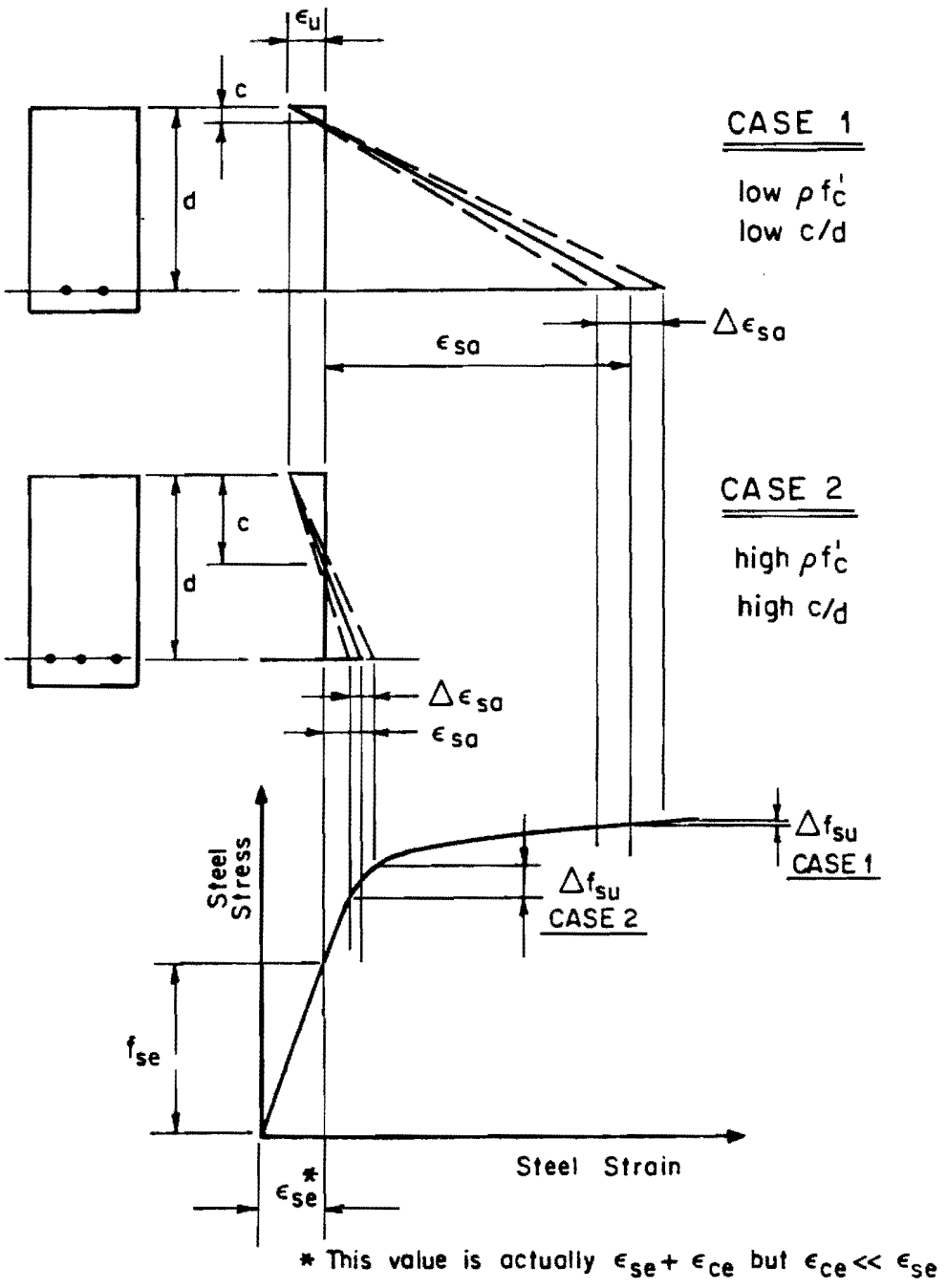

Fig. 2.18 Effects of variation in ρ and f'_c on f_{su}

$$k_u = F\epsilon_u/(F\epsilon_u + \epsilon_{su} - \epsilon_{se} - \epsilon_{ce}) \quad (2.19)$$

(see Appendix A for explanation of terms) to derive the maximum limit on the reinforcement index. It was assumed that $F\epsilon_u = 0.003$ for bonded beams, $\epsilon_{se} = 0.0045$ which is an average for the typical range of 0.004 to 0.005, and $\epsilon_{ce} \approx 0$ since it is small compared with other strains. The minimum value of ϵ_{su}, which corresponded to the maximum value of k_u, was set at 0.01. The resulting equation was:

$$k_u = pf_{su}/f_{cu} \leq 0.35 \quad (2.20)$$

where f_{cu} = average compressive stress in concrete.

Using the relationship $f_{cu} = 0.7f_c'$, Eq. 2.18 becomes

$$pf_{su}/f_c' \leq 0.25 \quad (2.21)$$

The limit in Eq. 2.21 differs from the limit of 0.30 used in the Committee 323 Report [19] because there, $F\epsilon_u$ was assumed to be 0.004. These equations apply to rectangular beams with no supplementary reinforcement. Warwaruk et al. [133] indicated that the use of beams with values of k_u near the limit was not advisable except "under controlled conditions of manufacture" and that lower values of k_u indicate increased ductility.

Warwaruk et al. [133] introduced a minimum reinforcement limit by requiring the moment capacity, M_u, to exceed the moment causing cracking, M_{cr}, i.e.,

$$M_u \geq M_{cr} \quad (2.22)$$

to prevent sudden failure immediately after cracking.

The 1963 edition of the ACI Code [12] contained the maximum reinforcing limit given by Committee 323 [19] for prestressed members and also introduced a minimum requirement of

$$M_u \geq 1.2M_{cr} \quad (2.23)$$

The maximum reinforcement limit for non-prestressed reinforced concrete members was changed to

$$p \leq 0.75p_{bal} \quad (2.24)$$

as suggested by Mattock, Kriz, and Hognestad [87].

In the Bureau of Public Roads document [33] of 1966 on flexural strength design of conventionally reinforced concrete bridge structures, the maximum reinforcement concept of Eq. 2.24 was used but the coefficient was reduced to 0.5.

The Codes have changed little in the intervening years. ACI Committee 343 [21] has endorsed use of ACI and AASHTO limits without change. The current AASHTO Specifications [10] indicate that the maximum reinforcement limit is intended to ensure yielding of the steel as ultimate capacity is approached. In the 1983 edition of the ACI Code [15], the value of the maximum reinforcement limit was changed from 0.30 to $0.36\beta_1$ in order to account for the use of high strength concrete.

2.5.2 Analytical Studies and Recent Proposals. Since the approaches to limiting the maximum reinforcement of non-prestressed and prestressed members differ and neither directly address the ductility of members, much analytical work has been done to (1) try to relate the different limits to ductility indices and to determine the usefulness and accuracy of current methods, or (2) propose alternate methods. Recent analytical studies are summarized below. Ductility is most often defined in terms of the ratio of deformation at ultimate to the deformation at yield. The deformation considered can be curvature, which is related to the ductility of the section, or deflection, which gives an indication of the ductility of the member. The current limits provide curvature ductilities of at least 2 for reinforced sections [77] and from 1.5 to 3 for prestressed sections [57]. MacGregor [77], after reviewing levels of ductility suggested by others, recommends a minimum curvature ductility of 3 for structures requiring limited ductility and 4 for structures in seismic regions. The use of the definition of ductility as a ratio of deformations is complicated for prestressed members by the stress-strain response of prestressing strand which lacks a well defined yield point. This results in poorly defined yield curvatures or deflections that must be arbitrarily determined [55,57].

The effect of the use of high strength concrete on the applicability of code provisions has been studied for reinforced members [2,131] and for prestressed members [57,94]. Studies of reinforced members indicate that sections or members made from high strength concrete have ductilities comparable to normal strength concrete and that the method of computing the balanced reinforcement ratio is conservative when compared with results of analytical studies

[135,131]. Harajli et al. [57] found that a significant reduction in ductility could occur for both prestressed and reinforced members at low levels of the reinforcement index ω. The evaluation and comparison of results of the studies is complicated by the use of different parameters as the basis for comparisons.

A number of changes to the current provisions have been proposed as simplifications or clarifications. Naaman [94] recommends that the current maximum reinforcement limit (ω) for prestressed members remain at 0.30 but that the definition of the effective depth be changed slightly. Naaman, Harajli, and Wight [57] show that

$$\omega = 0.85\beta_1 c/d \tag{2.25}$$

which could apply to both prestressed and partially prestressed members with a slight modification of current definitions. Using this concept, Naaman [95] proposes a new form of the maximum reinforcement limit that applies to all sections and combinations of types of reinforcement

$$c/d \leq 0.42 \tag{2.26}$$

which is equivalent to the current limit. A similar proposal was made by Thompson and Park [127]

$$a/h \leq 0.2 \tag{2.27}$$

as a result of a series of analytical studies related to seismic design. A second recommendation was to reduce the current maximum reinforcement ratio limit (ω) to 0.2.

Tadros and Peterson [125] report a proposal by Dilger to replace ϵ_y in the balanced reinforcement equations for reinforced concrete in the ACI Code [15] by $(f_{py} - f_{se})/E_{ps}$ for use with prestressed members. However, they find a number of difficulties with this approach.

Khachaturian and Gurfinkel [74] recognize the intent of Code requirements and recommend use of a limiting strain in the prestressing steel, i.e.,

$$\epsilon_{su} \geq \epsilon_{sl} \tag{2.28}$$

where ϵ_{s1} = strain in prestressing steel at ultimate
ϵ_{s1} = limiting strain in prestressing steel
= 0.01 for low (minimum) ductility
= 0.02 for high ductility.

The lower limit corresponds to current Code limits.

2.5.3 Results of Tests. Data from flexural tests of prestressed beams with high strength concrete appear to be nonexistant. However, high strength concrete beams with conventional reinforcement have been tested. These test programs are summarized below and results are compared later in the section.

Leslie, Rajagopalan, and Everard [76] reported tests of 12 singly reinforced beams with four reinforcement ratios and three cement contents. Concrete strengths ranged from 9,300 to 11,800 psi. The beams were loaded monotonically to failure at third points with a shear span-to-effective depth ratio of 2.67. Deflection data from the tests were used to determine the ductility index for each beam.

Tognon, Ursella, and Coppetti [128] tested four beams with a concrete strength of approximately 18,800 psi and three beams with a concrete strength of about 4,600 psi. Concrete strengths were converted from cube strengths using a multiplier of 0.8 [41]. Pairs of high and normal strength beams with equal reinforcement ratios were tested. Beams were singly reinforced and loaded approximately at third points with shear span-to-effective depth ratios of approximately 2.8 to 4. Deflection was measured and plotted for each test.

Swartz, Nikaeen, Narayan Babu, Periyakaruppan, and Refai [124] tested four high strength concrete beams with different reinforcement ratios and stirrup spacings in the shear spans. The beams were singly reinforced and loaded at third points with shear span to effective depth ratios of 2.6 and 3 for the two beams that failed in flexure. The other beams failed in shear. Deflection at midspan was measured and plotted for all four beams.

Pastor, Nilson, and Slate [103] tested a series of four high strength concrete rectangular beams with various tension reinforcement ratios and two beams with lower strengths for comparison. A second series of six high strength concrete beams were tested to study the effect of compression steel and transverse reinforcement on member and section ductility. Beams were loaded at third points to failure with

a shear span-to-effective depth ratio varying between 4.4 and 4.9. Deflections and curvatures were determined throughout the test, and ductility indices were computed for each beam. Beams B-4, B-5, and B-6 failed prematurely due to rupture of longitudinal steel at locations where stirrups were welded to the bars.

The curvature and deflection ductility data from the above tests are plotted versus the reinforcement ratio, the fraction of the balanced reinforcement ratio (computed by ACI), and the reinforcement index in Fig. 2.19, 2.20, and 2.21. Where ductility ratios were not given, an estimate was made from available data. There is considerable scatter in the data, but Fig. 2.20 shows a rather clear trend in the plot of the ratio of the reinforcement ratio to the balanced reinforcement ratio and the curvature ductility. The high strength concrete data from Tognon et al. [128] include one point which fell below most of the other data in the figure. For this beam a brittle failure occurred (i.e., the ductility ratio was approximately 1) at a reinforcement ratio of about two thirds of balanced. This indicates that current practice, which assumes that a brittle failure occurs when the reinforcement ratio equals the balanced ratio and limits the reinforcement ratio to 75 percent of the balanced ratio, would have allowed this design which resulted in a brittle failure. A similar figure was not possible for the reinforcment index because values at balanced conditions were not available for the data.

Figure 2.22 shows the relation between curvature and deflection ductilities measured for the same test specimens. Agreement is not good which demonstrates that the two measures of ductility are not uniquely related and therefore cannot be used interchangeably.

Results of analytical studies by Ahmad and Shah [2] for deflection ductility of singly reinforced beams (Fig. 2.23) and by Wang et al. [131] for curvature ductility of singly and doubly reinforced beams (Fig. 2.24) show that both ductility ratios are nearly independent of concrete strength for a given fraction of the balanced reinforcement ratio. The second study also shows that ductility increases with increasing concrete strength for a constant reinforcement ratio.

Pastor et al. [103] conducted a series of tests studying the effect of compression reinforcement and ties. Compression steel was found to be more effective in increasing ductility than ties. It was proposed that an area of compression steel equal to at least one half

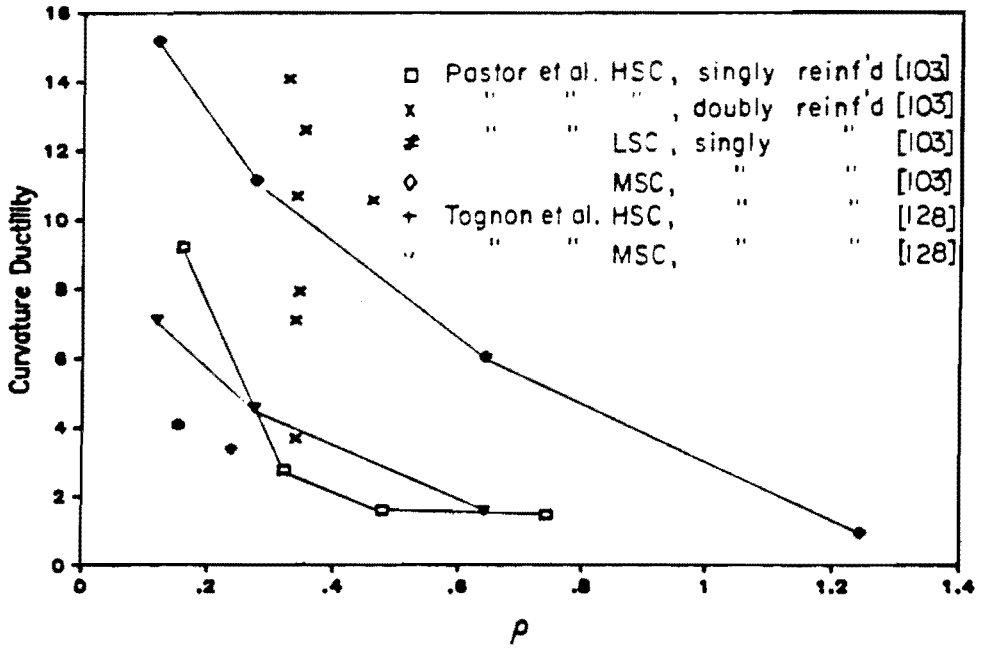

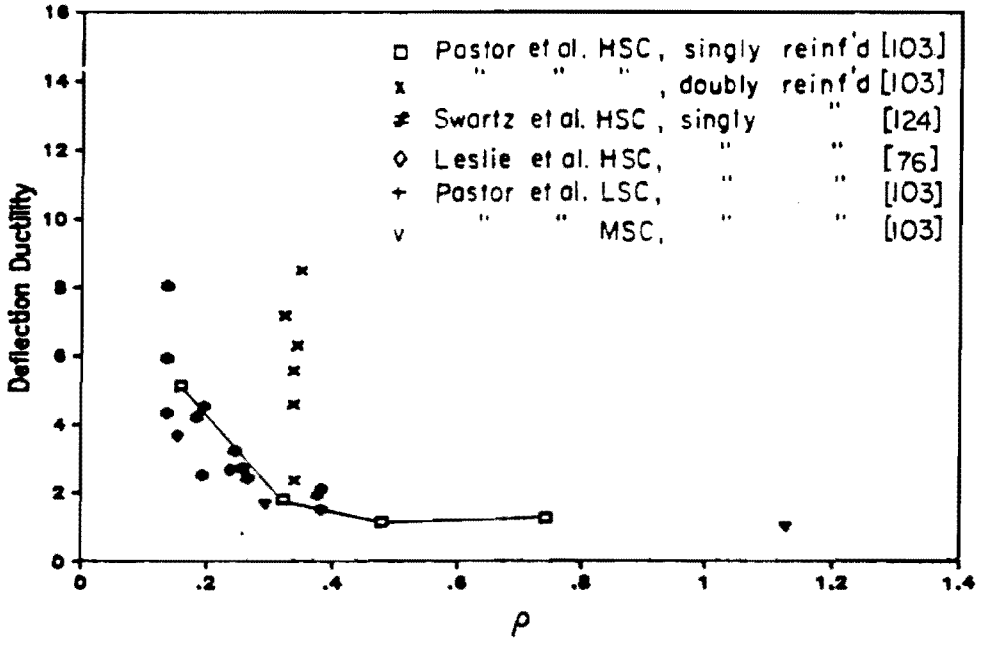

Fig. 2.19 Ductility indices versus reinforcement ratio

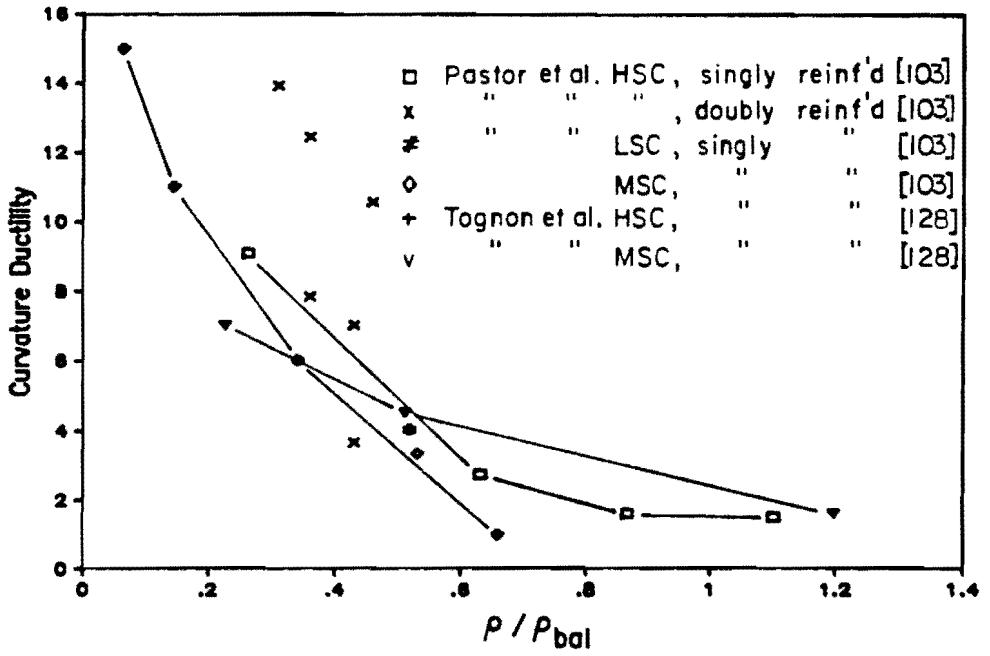

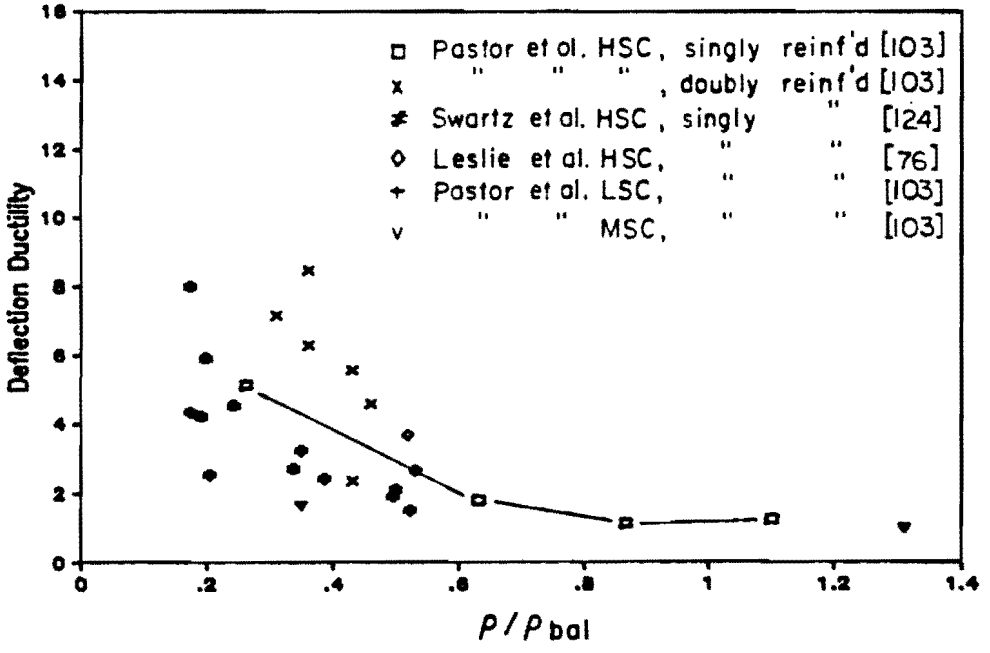

Fig. 2.20 Ductility indices versus fraction of balanced reinforcement ratio

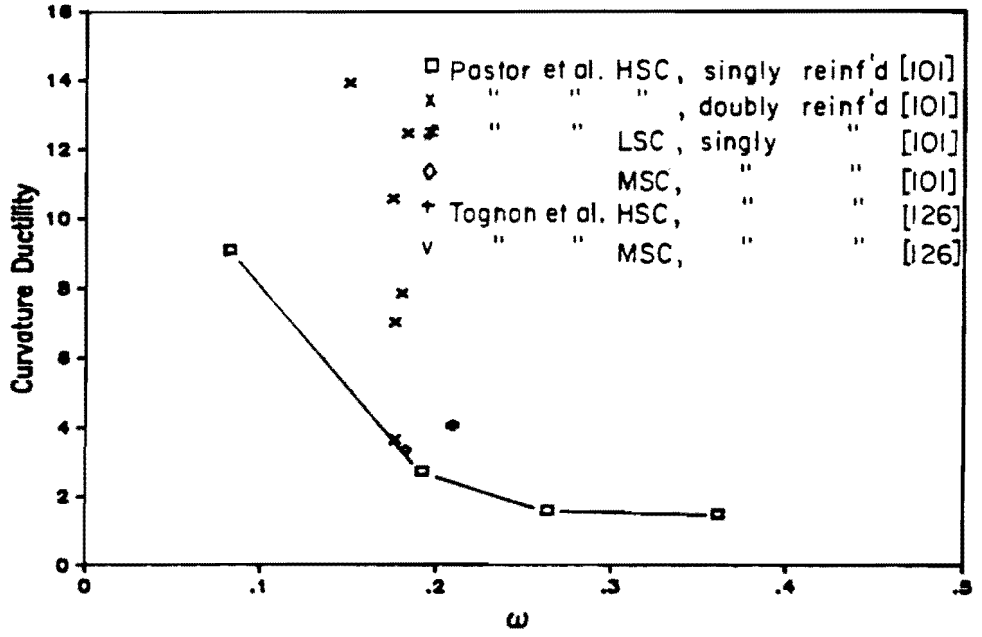

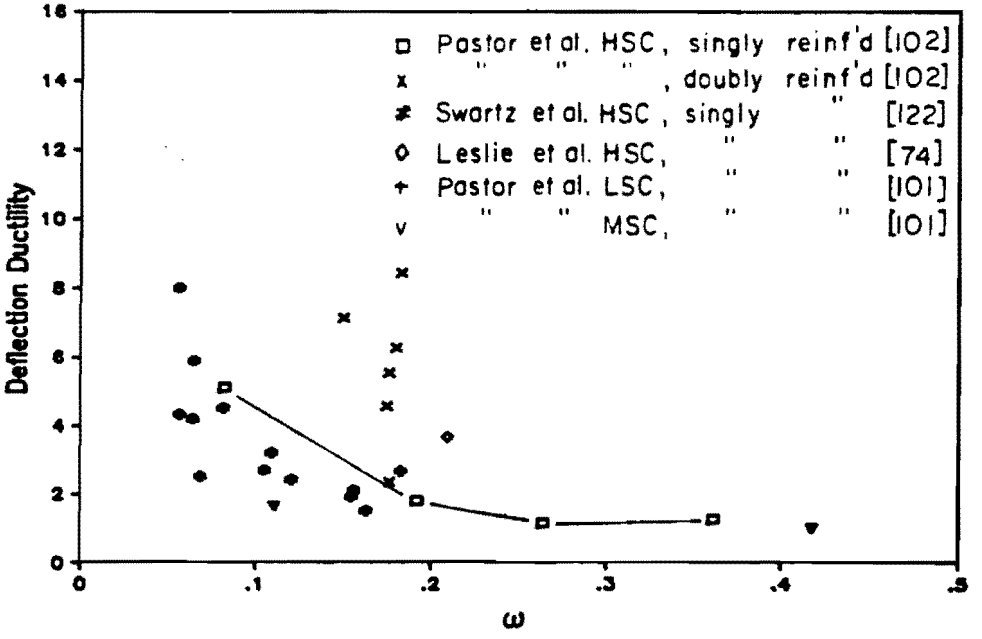

Fig. 2.21 Ductility indices versus reinforcement index

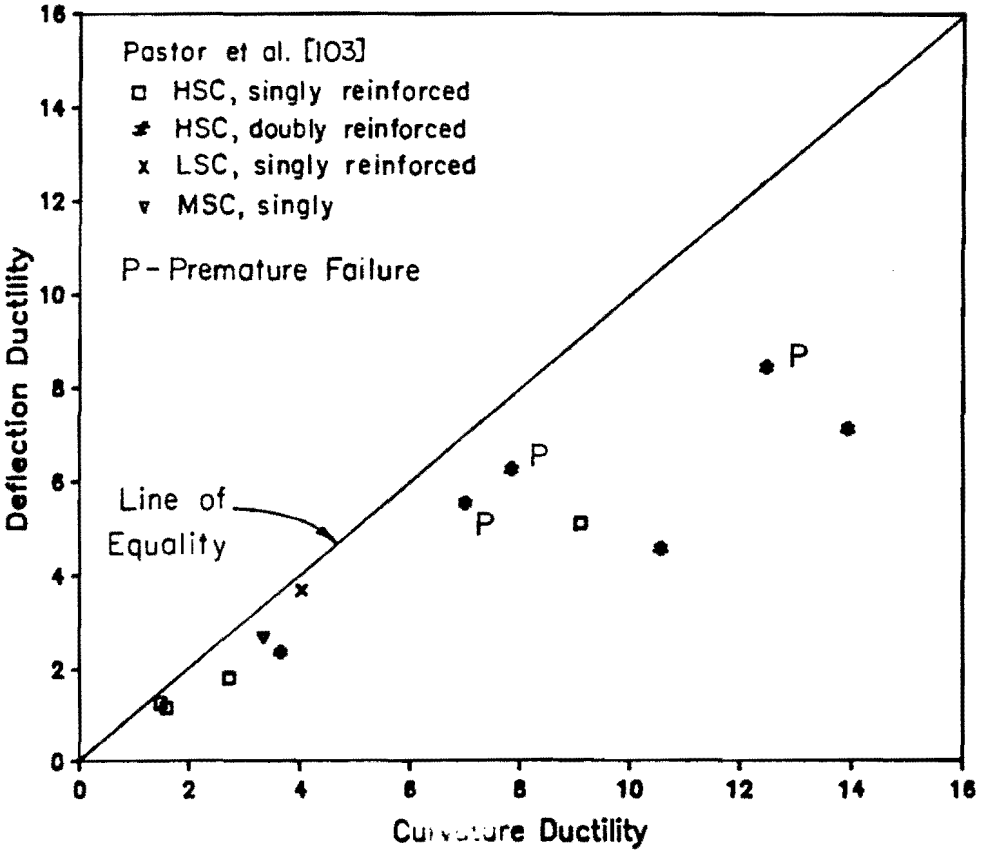

Fig. 2.22 Comparison of curvature and deflection ductility for same specimens

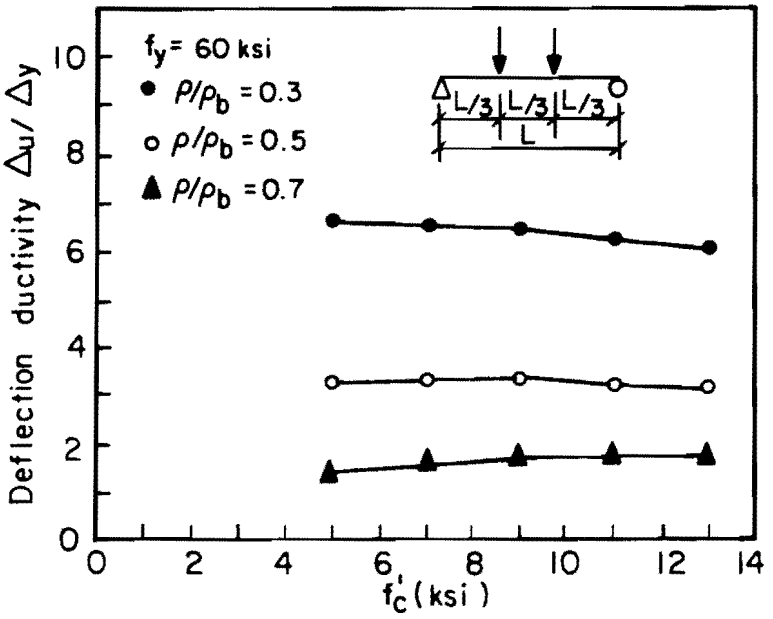

Fig. 2.23 Effect of concrete strength on the deflection ductility of a singly reinforced beam [2]

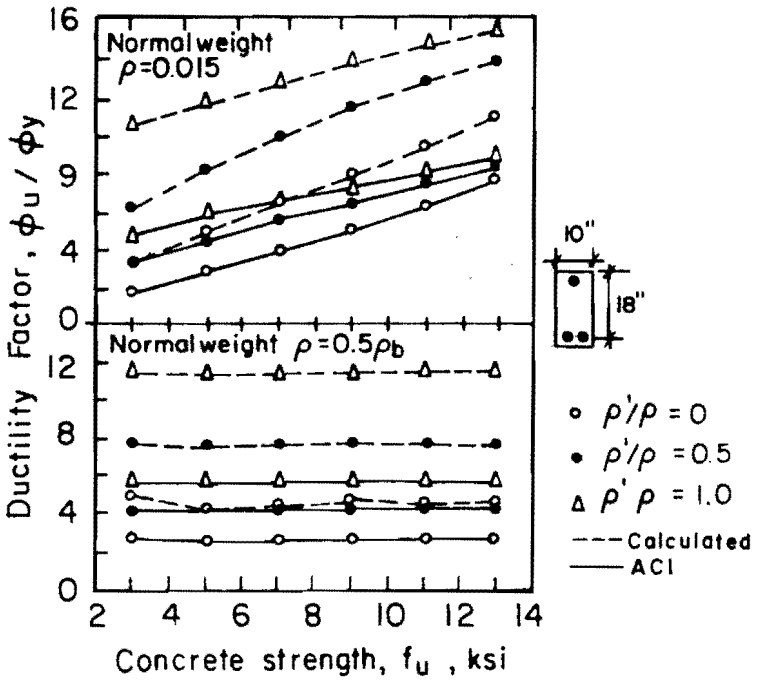

Fig. 2.24 Comparison of ductility ratios for beams (Ref. [131])

the tension steel area be used to improve ductility. Ties should be provided to restrain buckling of the compression steel.

Tests and analytical studies by Martinez et al. [82] and Ahmad and Shah [1] on columns indicate that confinement of high strength concrete was effective in increasing the ultimate strain and stress. However, as noted by Pastor et al. [103], confinement is not as effective in beams because of the presence of a strain gradient that leads to non-uniform expansion of the concrete.

Harajli and Naaman [55,56] observed some loss of ductility in normal-strength-concrete partially and fully prestressed beams that survived 5 million cycles of fatigue loads.

2.6 Deflections

2.6.1 Code Provisions and Limits. The AASHTO Specification [10] and ACI Code [15] do not provide specific methods for computation of short or long-term deflections of prestressed members. The AASHTO Specifications only mention that all effects must be considered in the calculation of deflections. The ACI Code states that computation of immediate deflections shall be based on elastic analysis and that the gross section modulus may be used for uncracked sections. For long-term deflections, all effects must be considered. The Commentary to the ACI Code [17] provides a list of references that give specific recommendations regarding the computation of deflections.

AASHTO gives a table of recommended minimum depths for reinforced sections unless computed deflections show that shallower depths can be used with no adverse effects. No such table is given for prestressed members. The same table appears in the ACI Committee 343 Report [21] for general use. The fact that the values in the table are intended for continuous members and should be increased for simple spans is not acknowledged. In the ACI Code, immediate and long-term live load deflections of prestressed members must meet limits intended for buildings. The Bureau of Public Roads booklet [33] provides limits on live load deflections for reinforced concrete bridges with simple spans less than 70 ft. These limits are based on the ratio of live load to full service load. The 1983 Ontario Highway Bridge Design Code contains a deflection limit based on the maximum deflection due to a factored highway live load and the fundamental flexural frequency of the bridge.

In the chapter related to design of steel structures, the AASHTO Specification limits the live load deflection to the span length divided by 800 for bridges without pedestrian traffic, and the span length divided by 1000 for bridges with pedestrian traffic. These limits, which have apparently been suitable when applied to steel structures, have often been used in the absence of other limits for prestressed concrete bridges.

2.6.2 Analytical Methods. Estimating deflection for prestressed members under short-term service loads is straight-forward because the section is generally uncracked, and elastic analysis with gross section properties can be used as recognized by the codes [10, 15]. If a member is cracked and the concrete is still behaving elastically, a cracked section analysis must be used. The ACI Commentary [17] suggests other references. Moment-curvature techniques also provide a general approach to estimating deflections at any level of load. Warwaruk et al. describe this procedure and demonstrate its accuracy by comparing calculated deflections with test results for normal-strength concrete beams.

The determination of long-term deflections is much more complex and has been the subject of much investigation. As mentioned previously, the Commentary to the ACI Code [17] provides a list of references that include methods for computing long-term deflections. Martin [80] proposed a simplified method which extends the long-term deflection multiplier approach used for reinforced concrete in the ACI Code by making many assumptions about time effects. Naaman [95] reviews several methods of computing both long and short-term deflections. Suttikan [119] developed a computer program PBEAM that included time effects in the analysis of prestressed members and showed good agreement with test data. Kelly [72] reviewed a number of methods including those by Martin [80] and Suttikan [119], and proposed an approach similar to Martin's but with more detail in the analysis. The method was programmed for use on a microcomputer and gave excellent results for a set of full-scale bridge girders.

2.6.3 Expected Effect of High Strength Concrete. Little work has been done on measuring the long-term deflection behavior of high strength members. The ACI Committee 363 Report [22] mentions that some work is underway at Cornell University and that preliminary results indicate deflections of high strength concrete members are significantly lower than those for similar normal strength members. This leads the investigators to believe that concrete strength should be included in formulas used to determine long-term deflection multipliers. However, the Committee feels that the expected long-term

behavior of prestressed high strength concrete members may not be much different from normal strength concrete members because, while creep would be lower, stresses would be higher.

The members studied in Kelly's work [72] and related work by Bradberry [32], while designed as normal strength members, were actually high strength members with low stresses. Deflections of the girders were measured from fabrication to completion of the bridge structure. Kelly conducted a sensitivity study comparing the long-term behavior of low, typical, and high strength concrete and found that, for the single bridge studied and a typical construction schedule, the girders and bridge using high strength concrete exhibited the least camber at erection, the smallest time dependent response, and the greatest final camber. The differences in behavior were attributed to the increased modulus of elasticity for high strength concrete.

2.7 Girder Stability

In this section, the analysis used to examine the lateral stability of girders is discussed.

2.7.1 Analytical Methods. A number of papers have been written regarding the analysis of the lateral stability of slender concrete members when lifted. Papers by Swann and Godden [123] and Muller [92] consider the problem in detail with the former study also reporting data from tests of model girders. However, the approach presented by Anderson in Ref. [6] is simple and clear. This approach was corroborated and amplified by Swann [122], the coauthor of Ref. [123], and also by Anderson [7] in response to the comments by Swann. The fact that Swann supports use of this simple analysis is significant since he had earlier published the more detailed analytical and experimental investigation of the problem. The modified form of Anderson's analysis is presented below.

In the analysis, the factor of safety against lateral buckling, FS, is expressed as

$$FS = y_T/0.64\Delta_y \tag{2.29}$$

where y_T = distance from the center of rotation to the centroid of the member and is generally taken as the distance from the top face of the beam to the centroid of the section

Δ_y= midspan deflection of the beam under its own weight with the beam simply supported so that bending occurs about the y axis.

For a beam with constant section properties along its length, the deflection Δ_y can be computed using the equation

$$\Delta_y = \frac{5\ \omega_g l^4}{384\ E_c I_y} \tag{2.30}$$

where ω_g = self weight of the beam
l = span length
E_c = modulus of elasticity for concrete
I_y = weak axis moment of inertia for section.

A factor of safety aganist buckling of at least 2 is recommended which means that y_T should be greater than $1.28\Delta_y$. Swann [122] recommends that y_T be taken as the vertical distance between a line through the lifting points and the center of gravity of the whole beam, since camber of the beam may significantly reduce this quantity in some cases.

Anderson [6] suggests that resistance to lateral buckling can be improved in a number of ways. One method is to move the lifting points further from the ends of the girder. This is effective, but stresses must be checked at the lifting points and at critical points near midspan. Calculation of Δ_y would then be based on the beam supported on its side at the lifting points, which can be computed as the difference between the deflection computed using Eq. 2.30 with l equal to the distance between lifting points and the deflection caused by the moment at the lifting point due to the overhanging portion of the member, ΔO, which can be computed using the equation

$$\Delta_0 = \frac{M_0(1-2a)^2}{8E_c I_y}$$

where M_0 = moment at lifting point due to overhang
= $\omega_g a^2/2$
l = full length of beam
a = distance from lifting point to end of beam

Other methods for improving resistance to lateral buckling are to use or develop sections with greater weak axis moment of inertia, to use high strength concrete which increases E_c, to keep the self weight of the beam low, and to attach temporary bracing to the member during handling.

Swann [122] introduced an additional analysis in which the lateral bending moment, M_y, which is the potential cause of failure, can be determined using the equation

$$M_y = M_x\theta$$
$$= M_x\theta_o(1/1(1-1/FS)) \qquad (2.31)$$

where M_x = bending moment about the x-axis due to self weight
θ = angle of tilt (in radians) of the member about a line through the lifting points
θ_o = angle of tilt (in radians) due to imperfections if the beam was completely stiff

This analysis reveals that use of a reasonable factor of safety against buckling may not prevent failure if imperfections are large. The value of θ_o can be estimated using the equation

$$\theta_o = (d_o + 0.67b_o)/y_T$$

where d_o = transverse distance from the minor axis of the section to where the lifting points have been inadvertently fixed
b_o = lateral bow or sweep of the beam at midspan

Swann adds that the factor of safety can be increased by use of a lifting yoke which is rigidly attached to the beam. Such a device places the center of rotation above the top of the beam which increases y_T and therefore reduces θ_o. This method of improving lateral buckling behavior may be more economical than the use of external bracing.

2.7.2 Practice and Experience in Texas. This section contains information obtained from the Texas State Department of Highways and Public Transportation (TSDHPT) related to the lateral stability of bridge members during fabrication, transportation and erection.

The section that has experienced the most problems in use is the Texas Type 54 (see Fig. 3.1). In a number of cases, members have been damaged prior to placement in bridges. As a result, spans for this section have been limited to 96 ft. Limits have also been set for other Texas sections including the Type 72, which is restricted to spans less than 122 ft. "Hog-rods" are specified for use as temporary lateral bracing where spans exceed these limits. No such limit is

imposed on the AASHTO-PCI Type IV, which is the only AASHTO-PCI section in use in Texas. Type 72 girders have been used for spans up to 136 ft and AASHTO-PCI Type IV girders have been used for spans of 130 to 135 ft.

State standards recommend that lifting loops be placed at the maximum practical distance from ends of girders and that vertical lines be used for lifting. The State, however, exercises no control over the location of lifting loops or the means of handling or transport. It is estimated that lifting loops could be placed as far as 1 in. away from the minor axis. Sweep of beams may be as much as 4 in. and may be aggravated by transportation and exposure to unbalanced solar heating. Pairs of lifting loops, which are often used for long beams, were estimated to be located 3 and 14 ft from ends of girders for a specific case. Rigidly attached lifting yokes have been used in some cases to improve lateral stability of girders during handling.

2.8 Fatigue

The AASHTO and ACI code documents treat the issue of fatigue in pretensioned members by setting allowable stresses. A thorough review of previous tests and the development of fatigue related provisions in the AASHTO Specifications, ACI Code, and other pertinent documents are given by Overman, Breen, and Frank [101]. On the basis of this review and results of tests of full-scale pretensioned girders, the use of strand stress range as the basis for design of pretensioned bridges for fatigue is recommended and a proposed procedure and limits are given. No special consideration is given to high strength concrete in this report.

ACI Committee 363 [22] reports that very little data is available on the behavior of high strength concrete subjected to repeated loads, but expects that "the fatigue strength of high strength concrete is the same as that for concretes of lower strengths."

No known studies have been conducted on how the stress range in strands will be affected by the use of high strength concrete in pretensioned bridge girders.

2.9 Loss of Prestress

The AASHTO Specification [10] provides a basic method for estimating prestress losses that accounts for the factors involved. A lump sum estimate for losses is also given, but the concrete strengths considered are 4,000 and 5,000 psi.

The 1983 edition of the ACI Code [15] gives no procedure for computing losses. The Commentary [17] recommends references [19, 23, 106, 137] for use in computing losses. Lump sum losses that appeared in earlier editions of the Commentary were considered obsolete and were therefore omitted.

The references mentioned above may not be sufficient if a very detailed analysis is required because the total loss occurs at an unspecified time [63]. Many of the detailed analytical methods for determining long-term deflections compute prestress losses as part of the analysis and may therefore be used if necessary. The procedure by Suttikan [119] is an example of such a procedure.

Kelly [72] compares several procedures for computing prestress losses, including those found in AASHTO [10] and the Texas SDHPT computer program PSTRS10. He concludes that the AASHTO approach is the best, although some modifications were recommended.

There are no known detailed studies of the effect of high strength concrete on losses in pretensioned members.

2.10 Bond and Development of Reinforcement

2.10.1 Prestressing Steel. Bond and development of prestressing strand in pretensioned members must be examined for two conditions. The first is the transfer or transmission length which is the distance required to transfer the force in the tendon to the concrete through bond, usually at release. The second is the anchorage or development length which is the bonded length of strand required to develop the ultimate stress in the tendon. The same equation is given in AASHTO and ACI for computing the development length, L_d, and included in it is the equation for transfer length, L_t:

$$L_t = (f_{se}/3)D \tag{2.32}$$

$$L_d = (f_{se}/3)D + (f_{su}^* - f_{se})D$$

$$= (f_{su}^* - 2/3\ f_{se})D \tag{2.33}$$

where D = nominal diameter of bar, wire, or prestressing strand, in.
f_{se} = effective stress in prestressed reinforcement after allowance for all prestress losses, ksi
f_{su} * = average stress in prestressing steel at ultimate load, ksi

Figure 2.25 shows how the development length is composed of the transfer length and an additional length. The derivation of these equations cannot be found in the literature but is based on data from a series of tests conducted at PCA in the late 50's and early 60's [54,70]. These equations have not changed since their introduction in the codes of the early 60's. Committee 343 [21] includes the same provisions in its report.

There is little data available for transfer length determination and less for development length. Kaar, LaFraugh, and Mass [70] studied the effect of the variation of concrete strength at release on the transfer length. A total of 43 test prisms were constructed to study the behavior of five sizes of strand, as many as five concrete strengths, and the effect of gradual or sudden release. The authors concluded that concrete strength had little effect on the transfer length for strand diameters up to 0.5 in. They also found that the transfer length changed very little with time, increasing generally less than 10 percent over a year.

Average transfer length data from the study by Kaar et al. [70] are presented in Fig. 2.26 for the larger sizes of strand. This figure presents data from pairs of specimens where each increment on the horizontal scale represents a different concrete strength within the range shown on the figure. Mean data for the cut end and dead end are connected by a vertical line for each pair of specimens. A value for the transfer length for each pair of specimens was computed using Eq. 2.32 and is also shown on the figure. A comparison of the computed values with the test data indicate that Eq. 2.32 generally predicts a shorter transfer length than was measured and is therefore unconservative for much of this data.

Hanson and Kaar [54] studied the development length of three sizes of strand using 47 beam specimens, 34 of which failed in bond or had bond failure simultaneously with flexural failure. The condition of the strand was a minor variable and an external anchor was provided on three specimens. Seventeen of the specimens were constructed using 0.5-in. diameter strand. An analytical method for determining the development length of strand was presented which

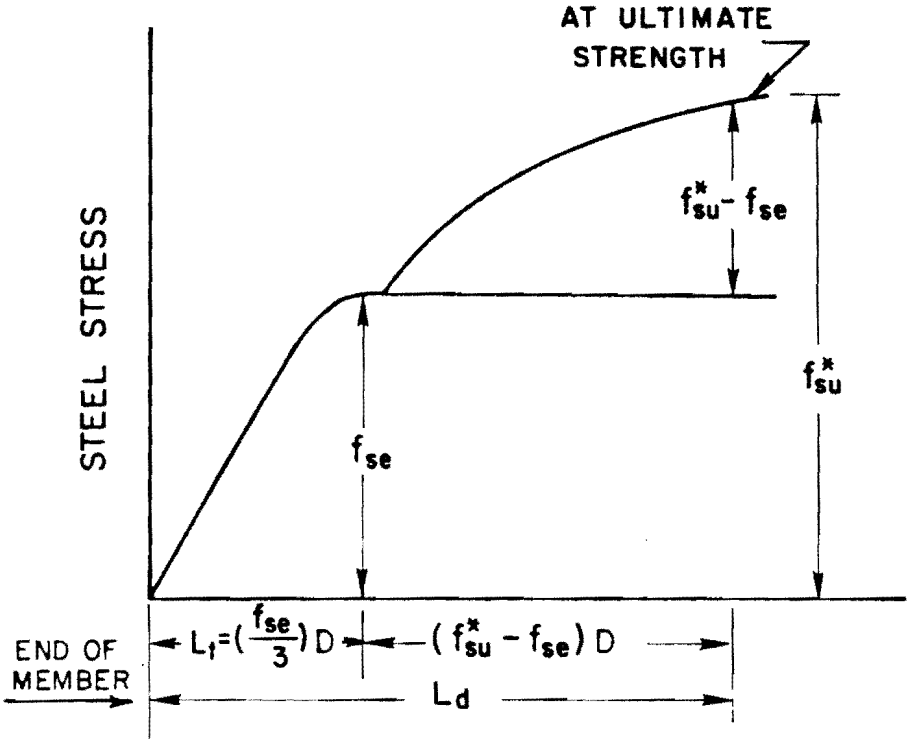

Fig. 2.25 Variation of steel stress with distance from free end of strand (Ref. [17])

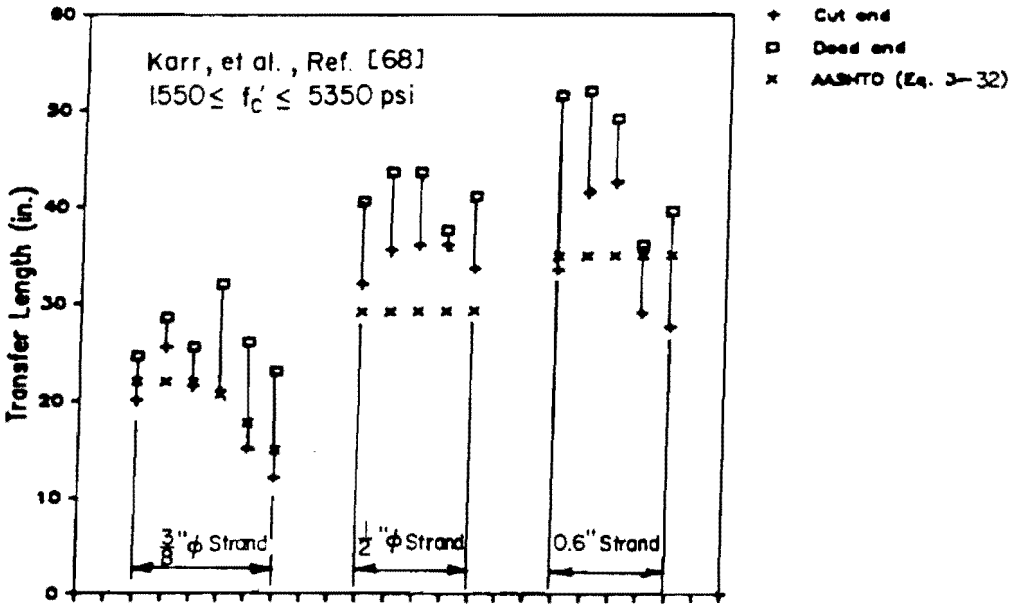

Fig. 2.26 Transfer lenths for different sizes of strand and concrete strengths [68]

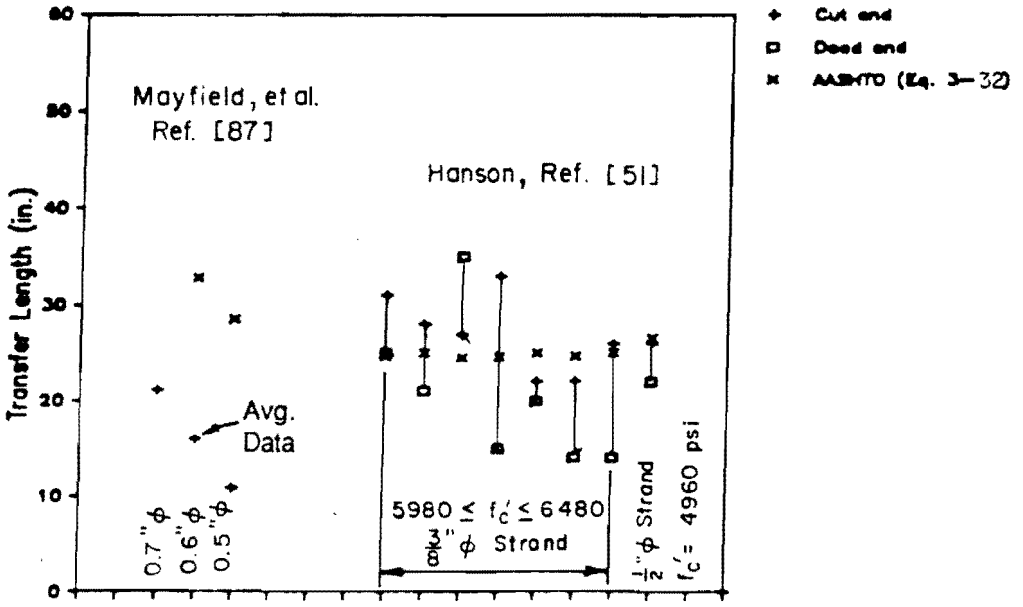

Fig. 2.27 Transfer lengths for different sizes of strand and concrete strengths [51, 87]

demonstrated reasonable agreement with the data. On the basis of the analytical model, minimum embedment lengths for the sizes of strand tested were given: 70 in. for 1/4-in. strand; 106 in. for 3/8-in. strand; and 134 in. for 1/2-in. strand. It was also found that the strand size and length of embedment had a significant effect on the average bond stress that led to general bond slip. It was noted that an appreciable capacity existed in the strand after initial slip had been observed.

Other data on transfer and development length have been reported [27,28,29,53,65,89,100,121]. It is difficult to make direct comparisons due to differences in testing procedure or reporting and the use of different materials, such as Dyform strand and plain wire. However, a number of investigators [53,62,79,136] have used this and other data to attempt to develop a better expression for both transfer and development lengths. From their work a number of expressions have been proposed, but none has achieved widespread acceptance.

Committee 363 [22] states that there is insufficient data on bond of strand in high strength concrete to make any recommendations. No references are given. Transfer data from Mayfield et al. [89] and Hanson [53], and corresponding transfer lengths computed using Eq. 2.32 are presented in Fig. 2.27 using the same format as Fig. 2.26. Only data on standard strands and moderate to high strength concrete are shown. The AASHTO equation is quite conservative for Mayfield's data but appears to be more of an average for the data reported by Hanson. Other data is available for high strength concrete transfer and development lengths [120,121], but the information regarding the tests is incomplete.

2.10.2 Nonprestressed Steel. The Committee 363 [22] statement regarding lack of data for making recommendations holds for nonprestressed reinforcement as well.

2.11 Summary

This literature review indicates that numerous aspects of behavior and design using high strength concrete remain to be investigated. Material properties of high strength concrete have been studied extensively and general trends have been identified but general expressions which include behavior of high strength concrete must still be developed. A limited number of tests have demonstrated that the simplified strength design methods used in current codes are satisfactory for predicting the capacity of high strength concrete

members. However, no test data exist for composite, pretensioned members that use high strength concrete. It was noted that no procedures are given in current codes for designing composite members composed of different concrete strengths.

Current code provisions concerning ductility were found to be based on assumptions inconsistent with certain aspects of current practice and codes. A simple, understandable, meaningful, and general approach for determining the relative ductility of prestressed structures does not appear to be available. Good methods have been developed for estimating both long and short-term deflections of members, although they have not been confirmed for members designed with high strength concrete. No limits on deflections of prestressed members are given in the AASHTO Specifications. An approach was presented for the analysis of the lateral stability of members and the experience and practice of the TSDHPT regarding the handling of girders was given. No studies of prestress losses, fatigue, or bond of conventional reinforcement are available for high strength concrete. However, a limited amount of data is available for the transfer length of prestressing strand in concrete, although the concrete strengths are in the middle and lower part of the range considered in this study.

The test programs reported in Ref. [139] are intended to provide data in a number of the areas identified above where additional work is needed. The topics of strand bond (transfer length) and member behavior were isolated as areas in which tests would be conducted. Tests of composite members were specifically directed toward the study of capacity and ductility of such members. The tests also allowed study of the behavior of composite structures at levels of load near service conditions. While properties were determined for materials used in the tests, providing additional high-strength material data for analysis of material properties was not intended.

The current state of knowledge and design practice regarding high strength concrete will be considered again in Chapter 4, where the findings of this literature review and the results of the test programs described in Ref. [139] are combined to form the basis for further evaluation, analysis and development of design procedures for use with high strength concrete. The additional studies will include development of a strength design approach for composite members, revision of current ductility provisions (maximum and minimum reinforcement limits), and analytical examinations of other aspects of

design including lateral stability, strand stress ranges with respect to fatigue, prestress losses, and deflections.

CHAPTER 3

STUDY OF BASIC PARAMETERS AFFECTING DESIGN

3.1 Introduction

The preceding chapter presented a brief outline of potential benefits of using high strength concrete in pretensioned bridge girders. In this chapter, designs using a range of concrete strengths are compared to provide a more complete understanding of the benefits and trends that accompany the use of high strength concrete. Different girder cross section shapes are considered in the study to determine which are better suited for use with high strength concrete. Conditions which may limit span lengths in some cases are also identified.

The design procedure used in this chapter conforms to the current AASHTO Specifications [10], using both allowable stress and ultimate strength design criteria and specified highway bridge loadings. The computer program BRIDGE, which is described in Appendix C of Ref. [140], was used to perform design calculations.

The chapter begins by presenting a sample of girder cross sections which are either in current use or have been proposed for use, including a series of girder sections developed as a part of this study. A comparison of designs for the selected cross sections is made with specific interest in the ability of sections to utilize high strength concrete. The final section of the chapter contains conclusions regarding the cross sections studied, their use with high strength concrete, and general comments on the use of high strength concrete.

3.2 Girder Cross Sections

In a recent study performed at the Portland Cement Association (PCA), Rabbat et al. [109] reviewed many girder cross sections in use in the United States at the time and proposed a series of bulb-tee sections as the national standard. However, that study did not consider concrete strengths greater than 7,000 psi. Therefore, it is desirable to study the use of different girder cross sections with high strength concrete. This section presents a selected set of girder cross sections that will be used in comparisons to determine

the effect of high strength concrete on bridge designs. A set of cross sections will also be proposed.

3.2.1 Girder Cross Sections Considered. While many girder cross sections are in use today across the country, only a representative sampling of sections will be considered in this study. Three section depths were chosen to provide a range of span capabilities: 40 in., 54 in., and 72 in. The 40 and 54-in. depths are the most commonly used in the state of Texas and the 72-in. depth has been commonly used and proposed elsewhere. The sections selected for consideration in this study are shown in Fig. 3.1, grouped by depth. Section dimensions are given in Table 3.1. The notation used for section dimensions is illustrated in Fig. 3.2. Where two numbers separated by a slash are part of the section designation, the first number specifies the section depth and the second number represents the web width. Of the sections shown, the Type C, Type 54, Type 72, and AASHTO-PCI Type IV girders are currently used in Texas.

To provide a comparison of different cross section shapes free from the effects of depth, 54-in. sections were created based on the PCA bulb-tee (PCA BT) [109] and the Ministry of Transport/Cement and Concrete Association (MOT/C&CA) inverted-tee sections [113]. The MOT/C&CA sections, which are referred to as "M-sections", have been used in shallower depths for bridges in the UK. Both sections were created by using standard dimensions for the top and bottom flanges and adjusting the height of the web to produce the desired depth. A modified AASHTO-Prestressed Concrete Institute (PCI) Type IV section, which was also proposed and studied in Ref. [109], will also be included in the studies of this chapter. This cross section was used as the prototype for the scale-model girder tests described in Research Report 381-3 [139].

3.2.2 Proposed Girder Cross Sections. New proposals for girder cross sections, which are designated using a "UT" prefix, are shown in Fig. 3.1 for three depths considered. Dimensions for these sections are included in Table 3.1.

The following objectives were used in the development of the proposed sections:

1. to provide span capabilities similar to those for sections in current use, but with reduced area,

2. to provide extended span capabilities with the use of high strength concrete

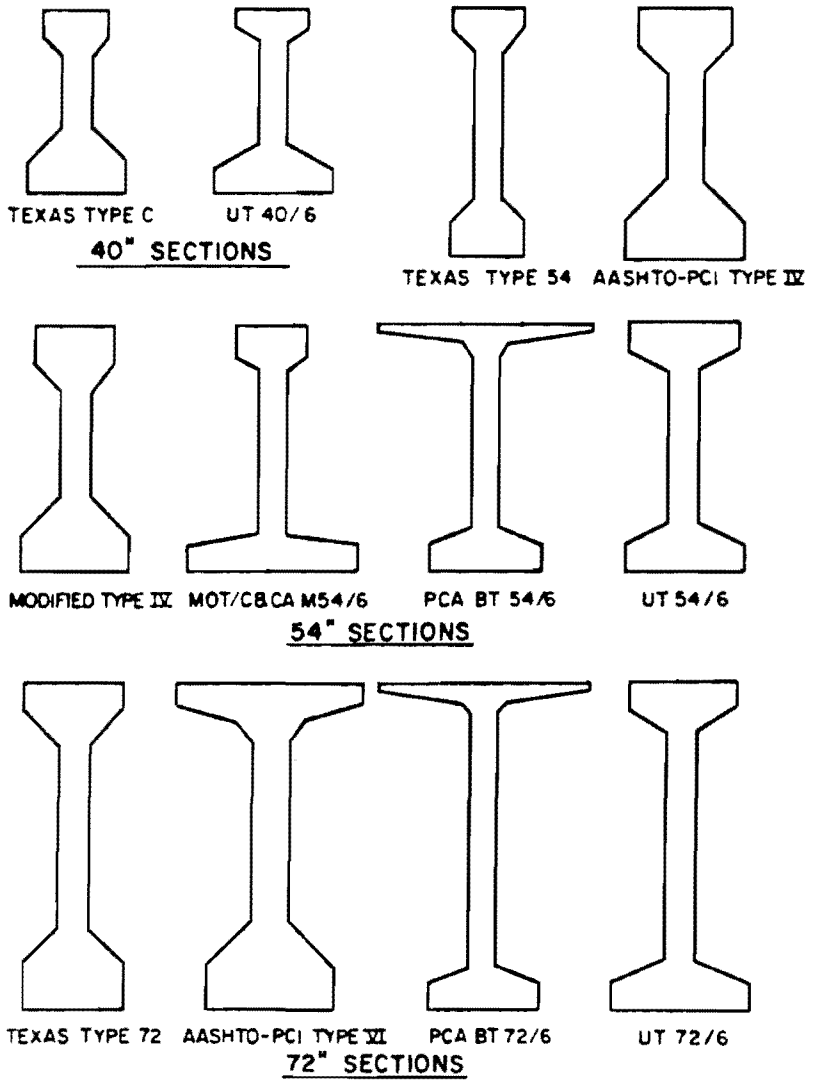

Fig. 3.1 Girder cross sections considered in this study

Table 3.1 Sections dimensions

	Horizontal dimensions				Vertical dimensions					
	b1	b2	b3	b4	h1	h2	h3	h4	h5	h6
40-in. sections										
Texas Type C	14	7	7	22	6	3.5	0	16	7.5	7
UT 40/6	16	6	6	26	4.5	2.5	0	22.5	5	5.5
54-in. sections										
Texas Type 54	16	6	6	16	4	5	0	32	5	8
AASHTO-PCI Type IV	20	8	8	26	8	6	0	23	9	8
Modified Type IV	18	6	6	24	8	6	0	23	9	8
MOT/C&CA M 54/6	16	6	6	38	7	2	0	37	2	6
PCA BT 54/6	48	10	6	24	2	2	2	39	3	6
UT 54/6	24	6	6	26	5.5	4.5	0	33.5	5	5.5
72-in. sections										
Texas Type 72	22	7	7	22	5.5	7.5	0	40.5	7.5	11
AASHTO-PCI Type VI	42	16	8	28	5	3	4	42	10	8
PCA BT 72/6	48	10	6	24	2	2	2	57	3	6
UT 72/6	24	6	6	30	5.5	4.5	0	50.5	6	5.5

Dimensions in inches; See Fig. 2.2 for key to dimensions.

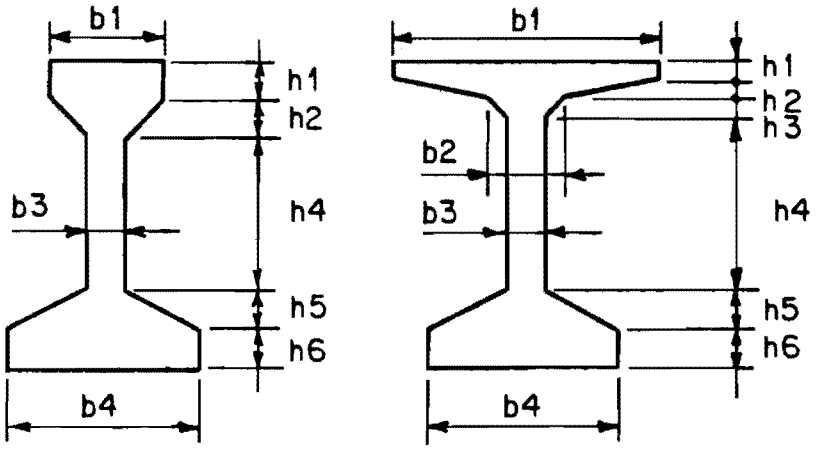

Fig. 3.2 Key to cross section dimensions in Table 3.1

3. to provide a range of span capabilities that gives flexibility of section use to the designer.

Dimensions for the proposed sections were selected using the following criteria:

1. use a 6-in. web to facilitate concrete placement and to provide sufficient shear capacity,

2. use a 2:1 slope on the taper of the flanges to provide a good concrete finish and permit easy form removal,

3. provide sufficient thickness of top and bottom flanges to minimize damage during handling,

4. provide sufficient bottom flange width for stability during erection,

5. size bottom flange to minimize excess concrete using a 2 x 2-in. strand grid with 2 in. from girder surface to center of strand (cover was increased by 0.25 in. on the top surface of the bottom flange),

6. provide sufficient thickness in the top flange to minimize the need for reinforcement, yet allow room for standard ties to be placed,

7. provide sufficient top-flange width to allow use of precast deck panels.

Although not included in the designs on which the proposed sections were based, the bottom flange should be of sufficient size to permit use with continuous construction [42].

A series of designs were performed for each trial section shape to determine the maximum span capabilities for different concrete strengths and girder spacings. The maximum span lengths were then compared with maximum spans for other sections of the same depth. Dimensions were then adjusted in an attempt to increase the maximum span or reduce the area. In evaluating the trial designs, practical upper limits were recognized for span length (150 ft), which was due to transportation and lifting constraints, and number of strands (74 0.5-in. diameter strands), which corresponds to the current maximum stressing capacity of a typical prestressing plant in Texas. The

final dimensions represent the best compromise between maximum span capability, cross-sectional area, and use of desired dimensions.

3.3 Comparisons of Section Properties

3.3.1 Basic Properties. Section properties are given for the selected and proposed cross sections in Table 3.2. From the data in this table, it can be seen that the proposed sections have smaller cross section areas and lower weights than comparable Texas and AASHTO-PCI sections. Such comparisons are incomplete unless accompanied by results of actual designs, which will be presented in the sections which follow.

3.3.2 Strand Pattern. The number and location of strands that can be contained within a section are significant factors in determining the span capacity of the section. Characteristics of strand patterns for sections considered in this study are summarized in Table 3.3. Strands are placed on a 2 by 2-in. grid with two columns of strands centered in the web and a minimum of 2 in. from the center of a strand to the surface of the concrete as shown in Fig. 3.3. Strands are added in pairs to the lowest unfilled row.

Columns 1 through 3 are related to the number of strands that can be placed in the bottom flange (see Fig. 3.3). A greater number of strands in the bottom flange generally corresponds to the possibility of longer spans, especially with higher concrete strengths. However, it was found while developing the proposed sections, that an additional row of strands in the bottom flange made little difference in the maximum span until very high concrete strengths were used. Therefore, the large number of strands in the bottom flanges of some Texas sections and the AASHTO sections may not be efficient for practical designs.

The remaining columns of the table concern an effective limit on the number of strands that can be used in design. This limit is encountered if strands must be added above the centroid of the section in an attempt to satisfy allowable stresses. Once the strand pattern is filled to the centroid of the concrete section, the addition of more strands reduces the prestress moment and increases the compression acting on the section.

This effect is illustrated in Fig. 3.4 where the product of the eccentricity and the number of strands, which is an index of the prestress moment available in the section, is plotted versus the

Table 3.2 Section properties

	Area (in^2)	I_x (in^4)	y_b (in)	y_t (in)	S_b (in^3)	S_t * (in^3)	Weight ** (lb/ft)
40-in. sections							
Texas Type C	495	82602	17.09	22.91	4833	3606	516
UT 40/6	458	84961	16.60	23.40	5118	3631	477
54-in. sections							
Texas Type 54	493	164022	25.53	28.47	6425	5761	514
AASHTO-PCI Type IV	789	260741	24.73	29.27	10544	8908	822
Modified Type IV	681	233854	24.37	29.63	9596	7892	709
MOT/C&CA M 54/6	628	227192	21.55	32.45	10543	7001	654
PCA BT 54/6	593	237893	27.44	26.56	8670	8957	617
UT 54/6	624	237824	26.28	27.72	9050	8580	649
72-in. sections							
Texas Type 72	863	532060	33.73	38.27	15773	13902	899
AASHTO-PCI Type VI	1085	733320	36.38	35.62	20157	20587	1130
PCA BT 72/6	701	484993	36.36	35.64	13339	13608	730
UT 72/6	776	530295	33.45	38.55	15853	13756	808

* - Section modulus for top fiber of section.

** - Computed using concrete unit weight of 150 pcf.

Table 3.3 Strand pattern characteristics

Column number:	1	2	3	4	5	6	7
40-in. sections							
Texas Type C	10	6	48	17.09	8	52	74
UT 40/6	12	4	36	16.60	8	44	66
54-in. sections							
Texas Type 54	6	5	28	25.53	12	42	70
AASHTO-PCI Type IV	12	7	64	24.73	12	74	102
Modified Type IV	10	7	58	24.37	12	68	96
MOT/C&CA M 54/6	18	2	36	21.55	10	52	84
PCA BT 54/6	10	3	26	27.44	13	46	72
UT 54/6	12	4	36	26.28	13	54	80
72-in. sections							
Texas Type 72	10	8	68	33.73	16	84	112
AASHTO-PCI Type VI	12	8	76	36.38	18	96	120
PCA BT 72/6	10	3	26	36.36	18	56	80
UT 72/6	14	4	44	33.45	16	68	96

Column headings:

1. Number of strands in bottom row
2. Number of rows in bottom flange, i.e., with more than 2 strands in row
3. Number of strands in bottom flange
4. Distance from bottom of girder to centroids of strands, y_b
5. Number of rows below centroid of section
6. Maximum number of strands below centroid of section
7. Maximum number of strands possible in section

Assumptions:

- 2 x 2-in. grid
- 2 in. minimum from center of strands to surface of girder

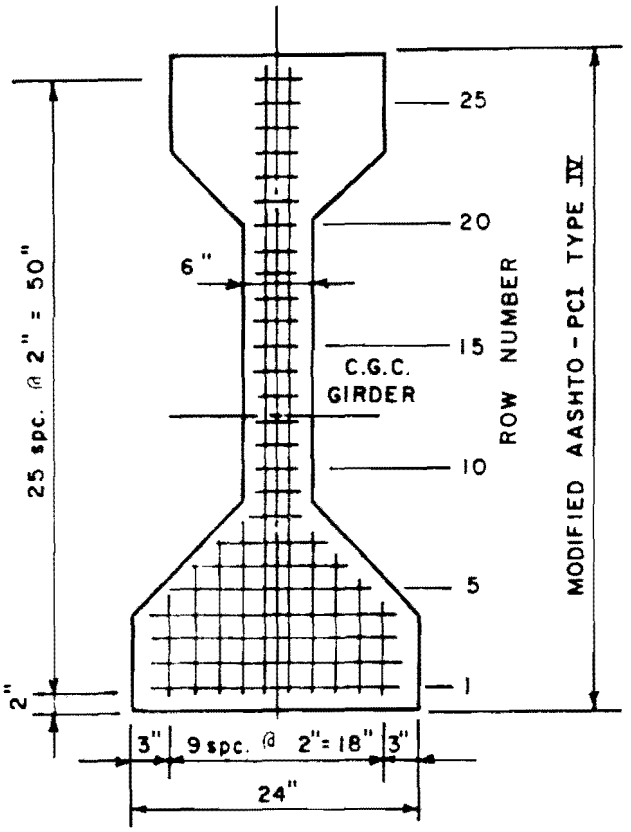

Fig. 3.3 Typical strand pattern

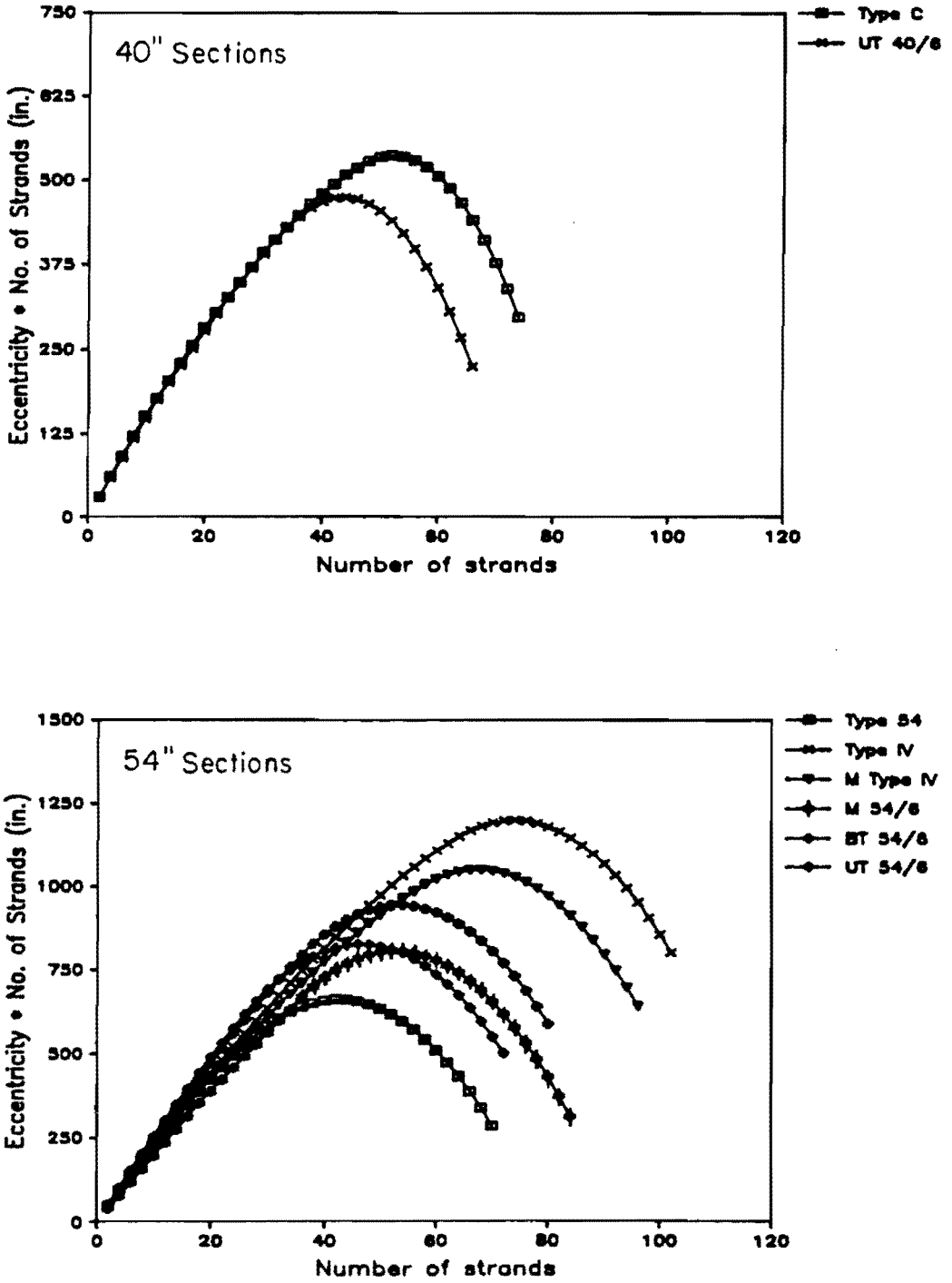

Fig. 3.4 Product of eccentricity and number of strands versus number of strands.

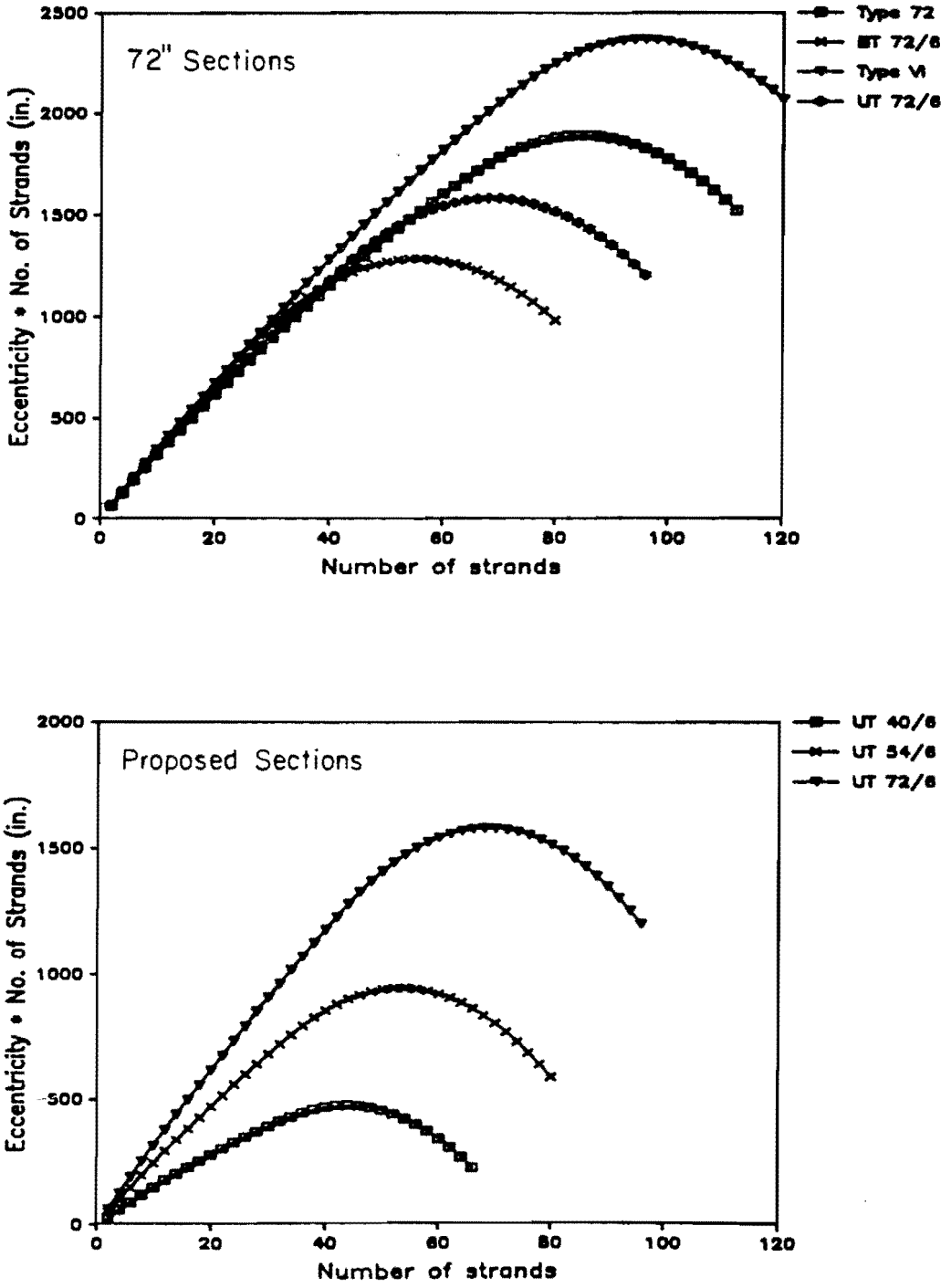

Fig. 3.4 Product of eccentricity and number of strands versus number of strands (continued).

number of strands for the three section depths. Adding strands above the centroid results in the descending branch of each curve. The point of zero slope corresponds to the number of strands given in column 6 in Table 3.3. The cause for this effect is illustrated by the plots of eccentricity versus number of strands presented in Fig. 3.5. Here the slope of the plots, which begins by descending only slightly, increases as the limiting number of strands is approached and exceeded. The product of the decreasing function (Fig. 3.5) and the linearly increasing number of strands leads to the curves found in Fig. 3.4.

There are few situations in which the addition of strands above the centroid will be beneficial or desirable in design. Therefore, the numbers in column 6 of Table 3.3 provide a practical estimate of the maximum number of strands that can be effectively used in a section.

A further consideration in determining the maximum number of strands that can be used for a design is the stressing capacity of available prestress plants. According to information obtained from the Texas State Department of Highways and Public Transportation (TSDHPT), a single 2.5 million lb stressing bed exists in the state, while other large beds have a capacity of 2 million lb. Using 0.5-in. diameter strands stressed to the maximum stress limit allowed by AASHTO ($0.8f_{pu}$, where f_{pu} is the specified ultimate stress of the strand), these beds would be limited to sections with no more than 74 and 60 strands, respectively. Using 74 strands as the limit for prestress bed capacity and the number of strands below the centroid from Table 3.3 as a general indication of the maximum number of strands used in a section, all designs with 40 and 54-in. sections could be constructed in Texas. Using the same basis for 72-in. sections, all designs utilizing the PCA BT and UT sections could be constructed, but some designs could not be built for the Texas and AASHTO sections due to the excessive number of strands. However, larger capacity beds could be constructed or a combination of pretensioned and post-tensioned construction could be used to utilize designs with a large number of strands.

3.3.3 Girder Stability. Two aspects of girder stability will be considered here: the width of the bottom flange with respect to overturning, and the lateral stability of the girder. Both conditions are critical during handling and erection of the girder when it is unbraced and subjected to lifting loads. Section properties related to both conditions are given in Table 3.4 and are discussed below.

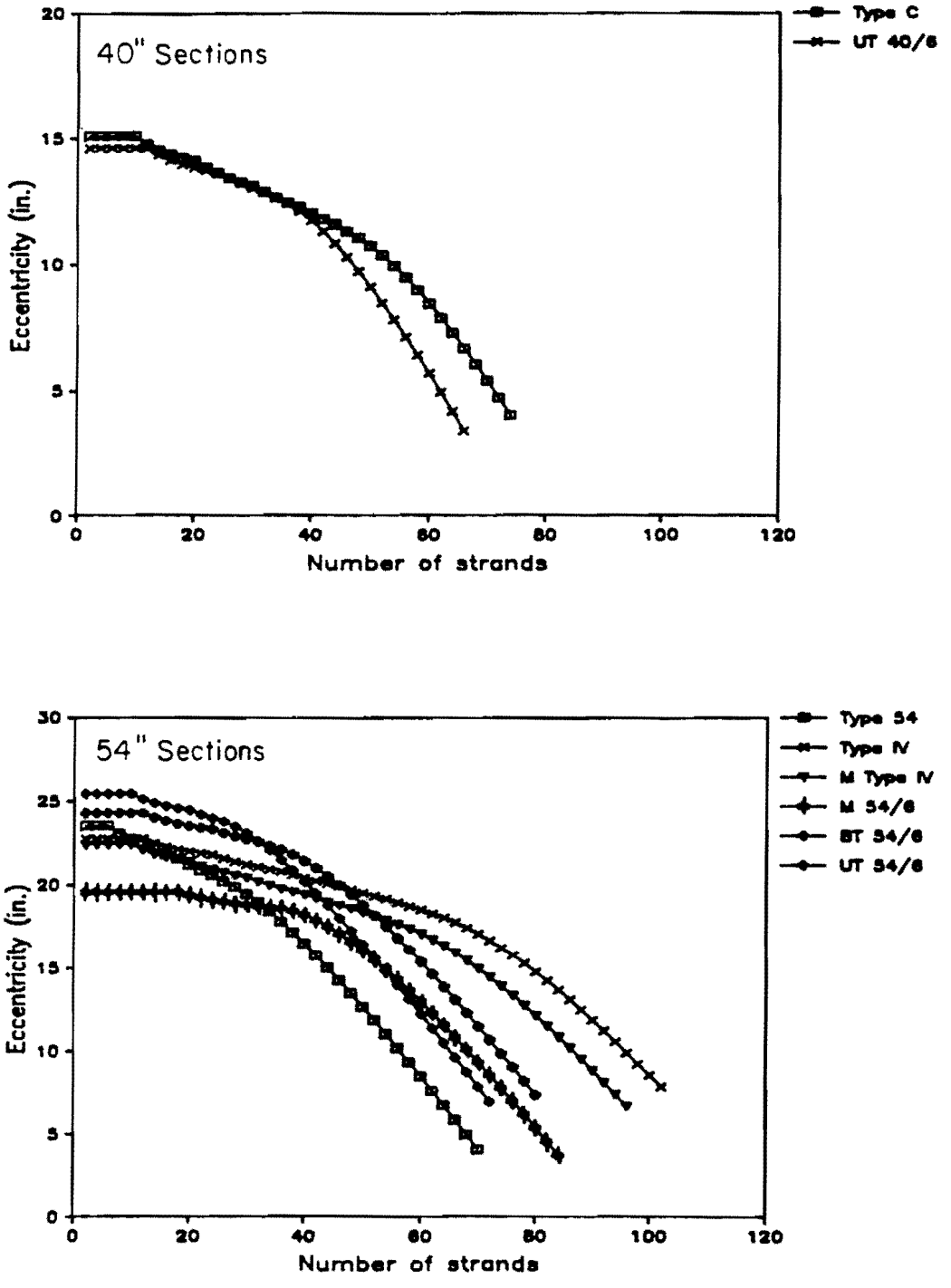

Fig. 3.5 Eccentricity versus number of strands.

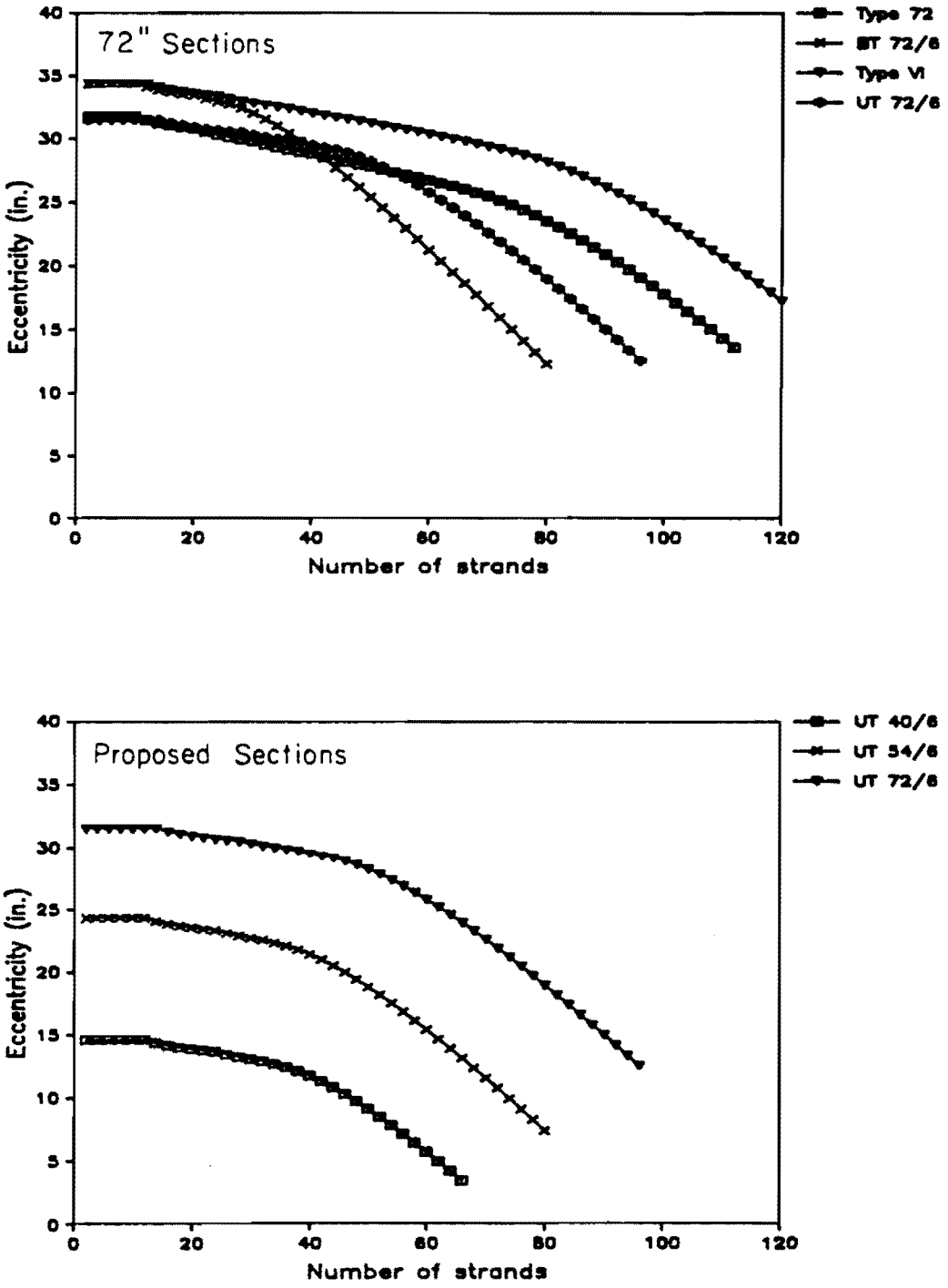

Fig. 3.5 Eccentricity versus number of strands (continued).

Table 3.4 Lateral stability factors for sections.

	I_y (in.^{4})	Maximum lifting span * (ft)	Tilt angle ** (deg)	Tilt ratio **
40-in. sections				
Texas Type C	13,020	106	32.8	1.55
UT 40/6	18,486	118	35.6	1.40
54-in. sections				
Texas Type 54	6,927	95	17.4	3.19
AASHTO-PCI Type IV	29,513	123	27.7	1.90
Modified Type IV	22,550	119	26.2	2.03
MOT/C&CA M 54/6	37,410	141	41.4	1.13
PCA BT 54/6	41,310	140	23.6	2.29
UT 54/6	23,578	121	26.3	2.02
72-in. sections				
Texas Type 72	24,707	123	18.1	3.07
AASHTO-PCI Type VI	72,776	149	21.1	2.60
PCA BT 72/6	41,634	145	18.3	3.03
UT 72/6	32,560	135	24.2	2.23

* - Spans were computed using the approach given in Ref. [6] and modified in Ref. [7,122], assuming:

Lifting points located at 5 percent of the span from ends of the girder, factor of safety against buckling (FS) = 2.0, E_c = 4,000 ksi, and $y_T = y_t$.

** - These values represent the angle or slope from the bottom corner of the bottom flange to the centroid of the girder (see Fig. 3.6).

From a conversation with a manufacturer of girders, it was learned that the Texas Type 72 girders tend to be unstable and may blow over in the wind if not adequately braced. The problem also exists with the Texas Type 54 girders, but to a lesser degree. This problem of overturning is related to the width of the base relative to the height of the member, and can be considered mathematically by computing a "tilt ratio" or "tilt angle" which is the slope or angle of the line connecting the outer edge of the bottom flange and the centroid of the section (see Fig. 3.6). This gives a quantitative indication of whether the section is top heavy with a tendency to turn over. As shown in Table 3.4, the two Texas sections mentioned above have the highest tilt ratios which appears to confirm the applicability of this measure for predicting overturning problems. The 72-in. PCA bulb-tee has a ratio very near those of the Texas sections, which indicates that overturning may be a problem for this section as well. The lower tilt ratios computed for other sections agree with experience in the field for these sections. The UT sections have ratios comparable or less than those associated with sections which generally exhibit no overturning problems. Therefore, it is unlikely that the proposed sections will experience problems associated with overturning.

An important factor in assessing the lateral stability of a section is the weak axis moment of inertia, I_{yy}, which is given for each section in Table 3.4. There is considerable variation, especially for the 54-in. sections. The UT sections have lower weak axis moments of inertia than bulb-tee and AASHTO sections but have greater values than the Texas sections.

Lateral stability of a member is generally most critical during lifting. This problem has been addressed in a number of papers [6,7,92,122,123]. Using a modified form [7,122] of a method given by Anderson [6], the maximum span permitted for lifting a girder can be determined, as shown in Table 3.4. The analysis is based on a factor of safety against buckling of 2. For the values in the table, the concrete modulus of elasticity, E_c, was assumed to be 4,000 ksi and lifting loops were assumed to be positioned at a distance equal to 5 percent of the span from each end of the girder. The dimension, y_T, was assumed to be the distance from the top face to the centroid of the girder. The analyses are presented and discussed in greater detail in Sec. 2.7 and 4.7.

The UT sections compare favorably with the Texas standard sections and the two forms of the AASHTO-PCI Type IV girder. However, sections with wide top or bottom flanges showed marked

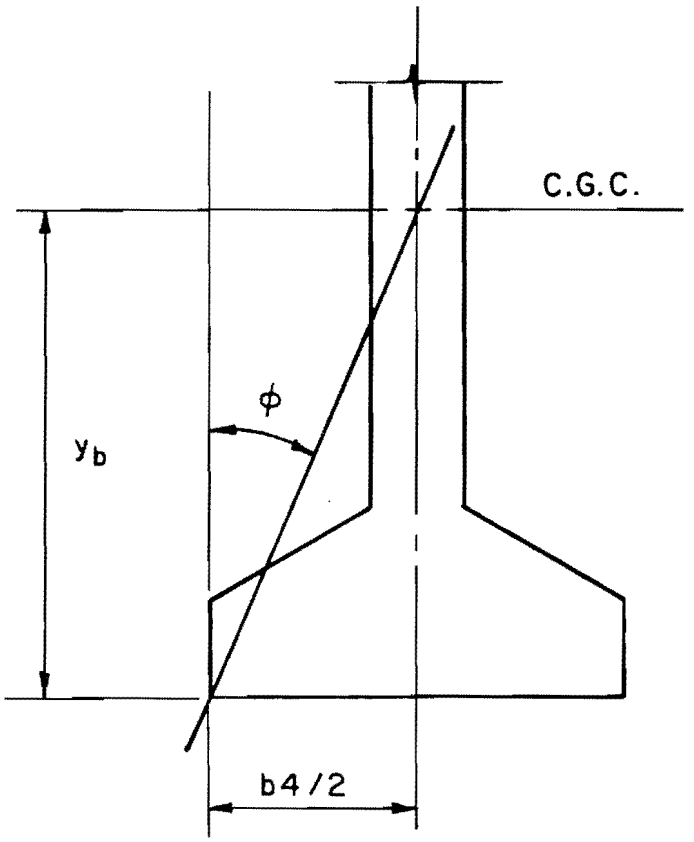

$$\text{TILT RATIO} = \frac{y_b}{b4/2}$$

$$\text{TILT ANGLE} = \phi$$

$$= \tan^{-1}\left(1/\text{TILT RATIO}\right)$$

Fig. 3.6 Definition of tilt ratio and tilt angles

increases in maximum span length. This trend was quite evident for the 54-in. sections but less pronounced for the 72-in. sections. This analysis shows that UT sections have maximum spans as long or longer than other I-shaped sections but shorter than sections with very wide top or bottom flanges.

It should be noted that the maximum lifting spans which appear in Table 3.4 are not absolute limits and that spans exceeding these limits can be used if appropriate measures are taken. Spans may be increased by moving lifting loops farther into the span, although stresses must be checked at critical locations. Moving the lifting loops to a distance of 10 percent of the span from the ends results in a 12.5 percent increase in the span lengths given in Table 3.4 for all sections. The use of rigidly attached lifting yokes at the ends of the girder will also improve the maximum lifting span by increasing y_T. Raising the lifting point 12 in. above the top of the girder increases the maximum spans given in Table 3.4 by 7 to 11 percent. Changing the modulus of elasticity of concrete from 4,000 to 5,400 ksi, which corresponds to an increase in concrete strength from 4 to 9 ksi, results in an increase in the maximum span of 7.8 percent for all sections.

Because the maximum span capability of many sections is limited by the maximum lifting span, spans in excess of the lifting limit will be indicated, where appropriate, by a broken line on the figures that follow. The maximum lifting span, however, does not remain constant in these figures, but increases with increasing concrete strength. The modulus corresponding to the concrete strength at release, which is defined below for these designs, is used to determine the maximum lifting span.

The maximum lifting span limit was compared with field experience in Texas in Sec. 2.7.2 and will be compared with behavior, observed during fabrication and testing of long-span scale-model girder specimens, in Sec. 4.7.2.

3.4 Comparison of Designs

A series of designs was performed using the sections presented earlier in this chapter. Girder spacings (GS) of 4, 7 and 10 ft were used with concrete design strengths varying from 6 to 15 ksi. Unless indicated otherwise, the concrete at release was 75 percent of the design strength, except for 6 ksi designs where the release strength was 5 ksi (83 percent). All designs used low relaxation seven wire

strand of 0.5-in. diameter except for a limited series which used 0.6-in. diameter low relaxation strands and is noted as such. Strand patterns described in the preceding sections were used.

Designs conformed to the AASHTO Specifications [10], using allowable stress and ultimate strength design criteria and specified highway bridge loadings including impact. The criteria used in these designs were found, in Chapter 4, to be acceptable for use with high strength concrete. These design computations were performed using the computer program BRIDGE which is described in Appendix C of Ref. [140].

3.4.1 Maximum Spans. The maximum span for which the allowable stress and ultimate strength design criteria could be satisfied was determined for combinations of girder spacing and concrete strength for each section. The results of these maximum span designs are summarized in the plots of Fig. 3.7 through 3.10. The figures show the increase in maximum span with increasing concrete strength for the sections and girder spacings considered. In order to more clearly show the increase in maximum span length with increasing concrete strength, ratios of the maximum span length to the maximum span for the 6 ksi design are plotted versus concrete strength in Fig. 3.11 through 3.14. For both series of figures, a separate figure is provided for each section depth, and the final figure shows the plots for the three proposed sections. Sub-figures are used, as required for clarity, to show the plots for the three girder spacings. Where spans exceed the maximum lifting spans computed using the modulus corresponding to the concrete strength at release, broken lines are used to define the curves. Maximum lifting spans for designs with a design strength of 15 ksi are 10.7 percent greater than those for 6 ksi designs. The values found in Table 3.4 are very close to the maximum lifting spans actually used for some 6 ksi designs. Results for each section depth will be reviewed, then overall trends observed in these figures will be discussed.

Maximum spans for the two 40-in. sections were similar for all concrete strengths and girder spacings, with the difference in spans never exceeding 3 ft. The figures indicate that spans in excess of 110 ft can be obtained using these sections with high strength concrete. The increase in span from normal strength (6 ksi) concrete to 12 ksi concrete ranged from approximately 30 to 40 percent with an increase of approximately 15 to 20 percent for 9 ksi concrete. The plots indicate that spans continue to increase even with very high strength concrete. Designs for the Type C section with GS = 4 ft and fc' greater than 11 ksi are the only designs to exceed maximum

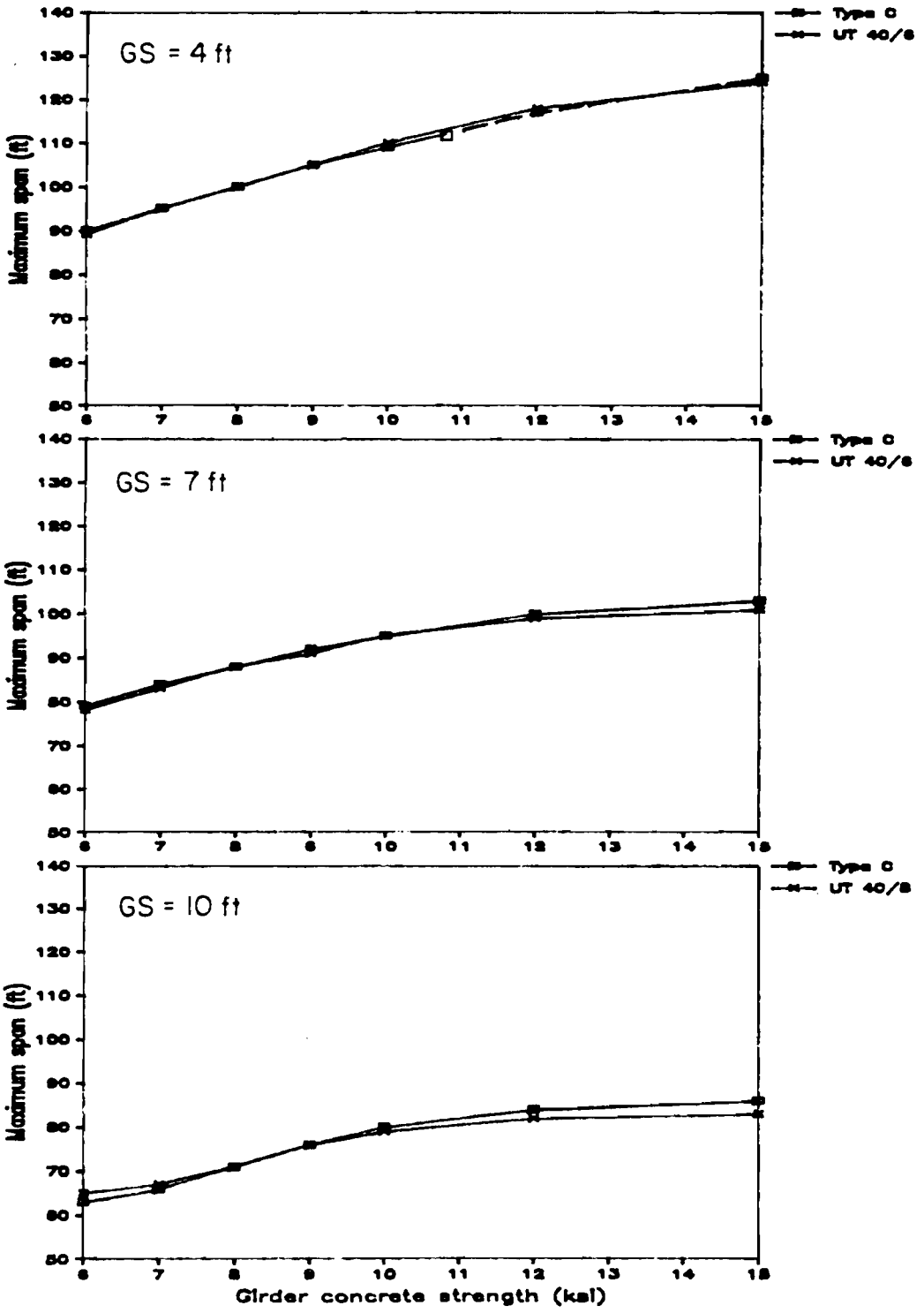

Fig. 3.7 Maximum span versus concrete strength - 40" sections.

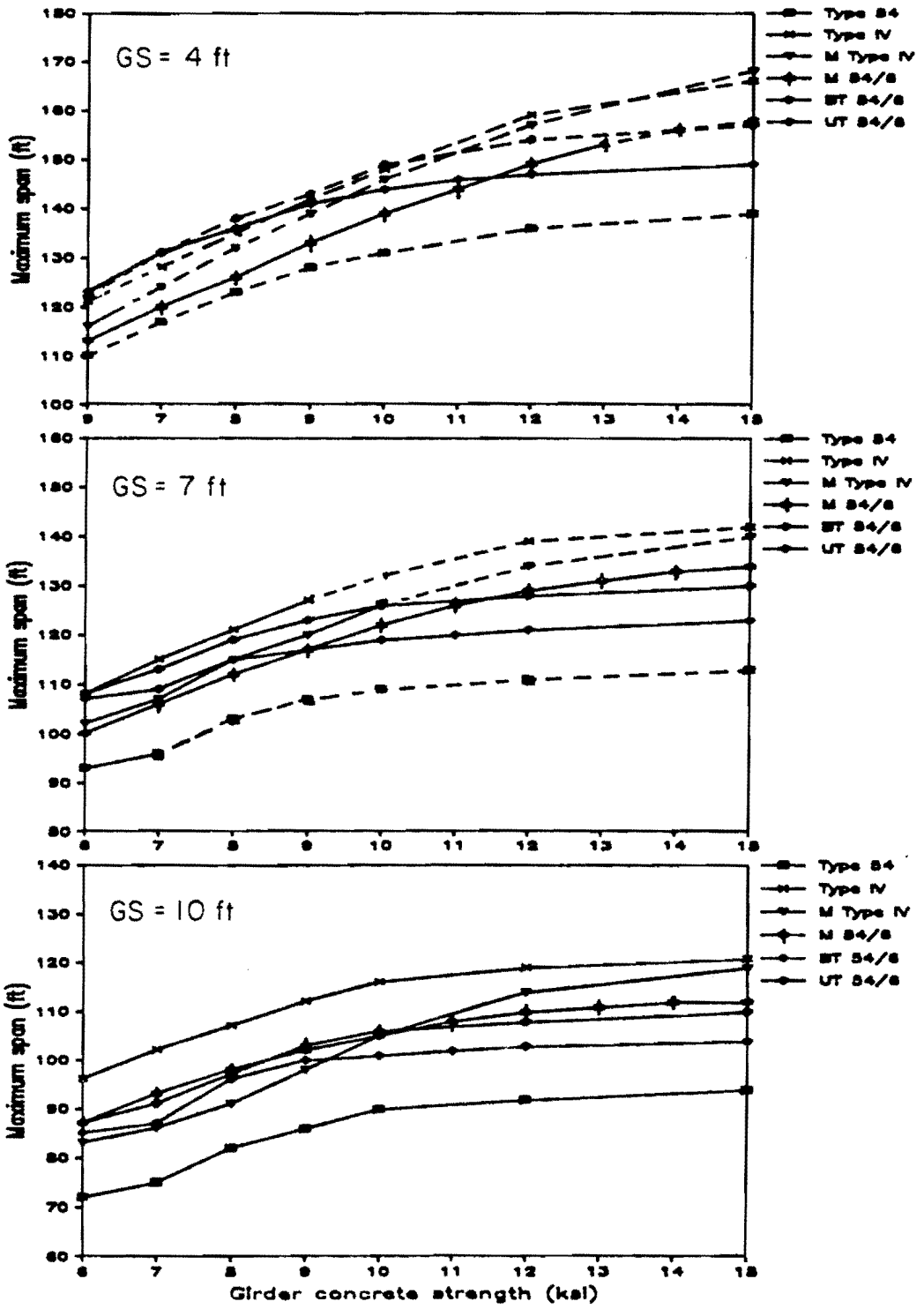

Fig. 3.8 Maximum span versus concrete strength - 54" sections.

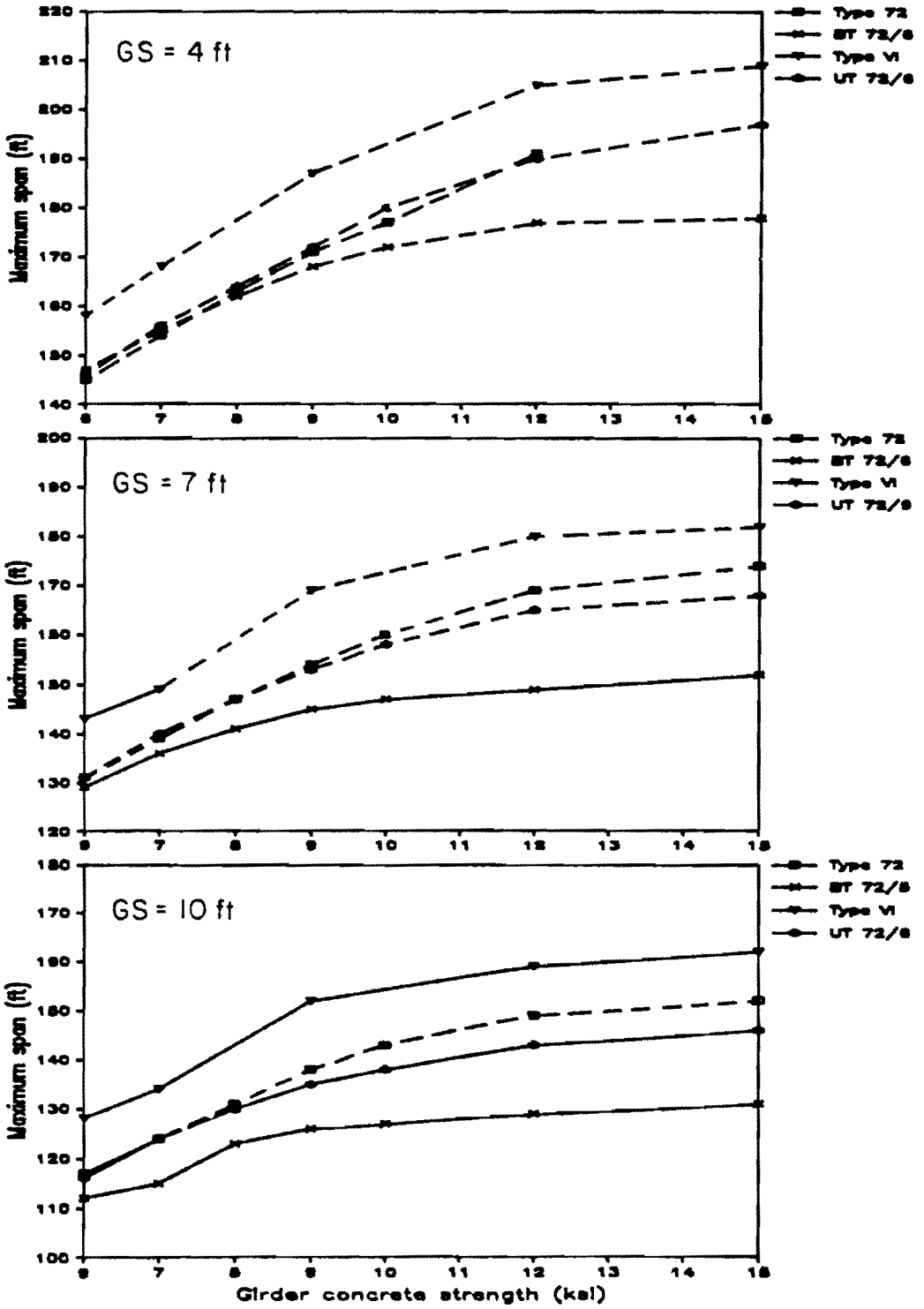

Fig. 3.9 Maximum span versus concrete strength - 72" sections.

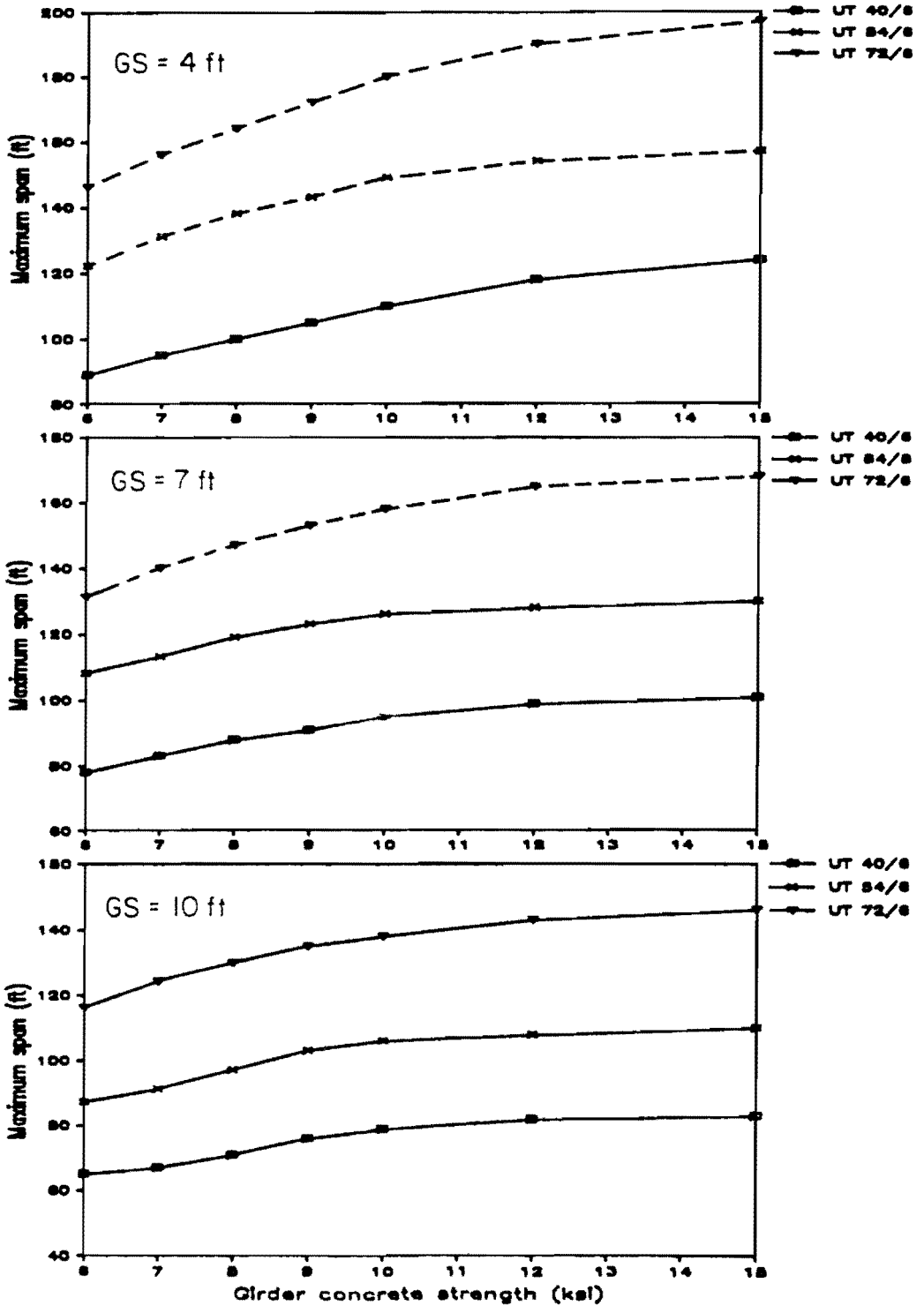

Fig. 3.10 Maximum spans versus concrete strength - proposed sections.

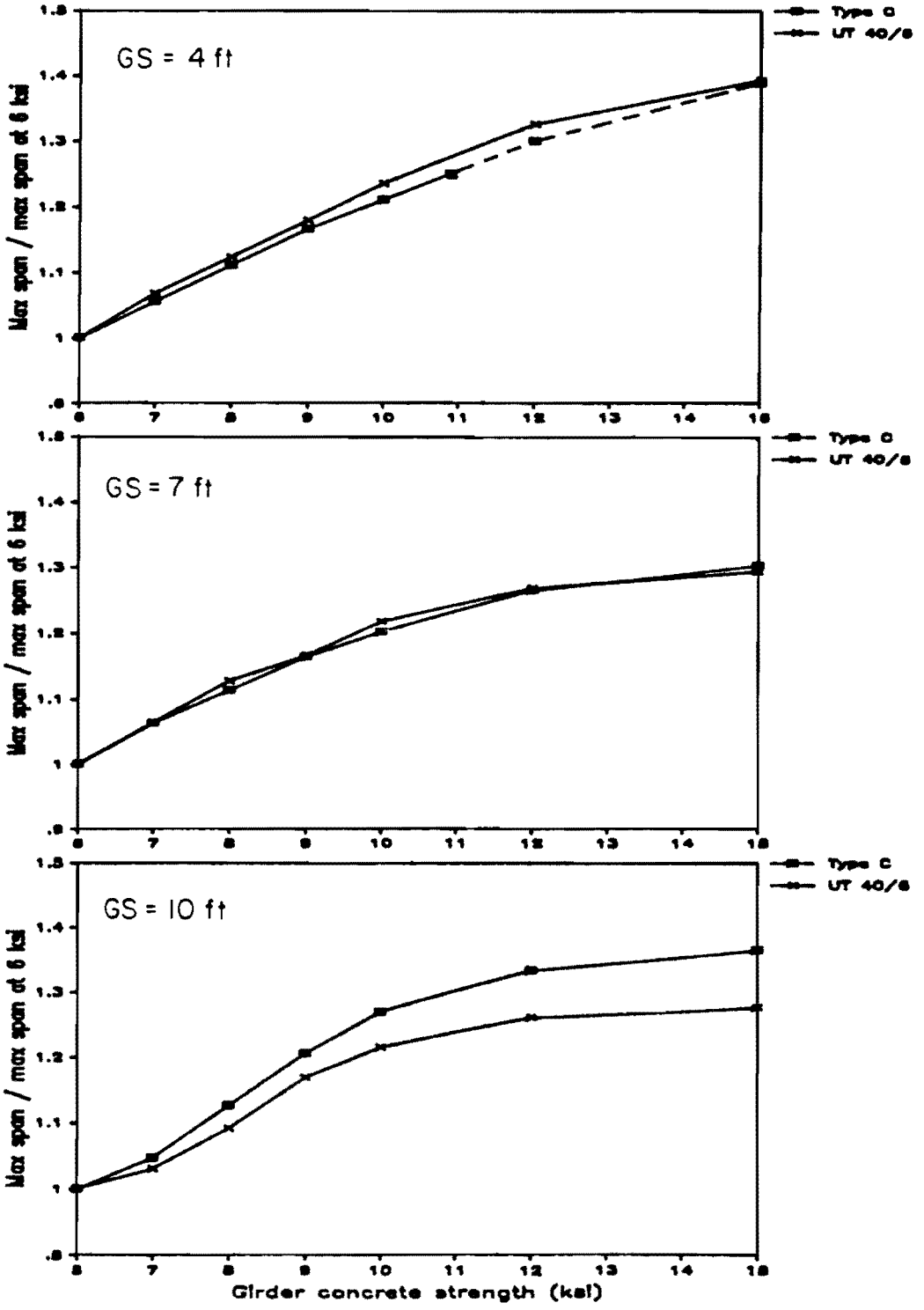

Fig. 3.11 Ratio of increase in maximum span versus concrete strength for 40" sections.

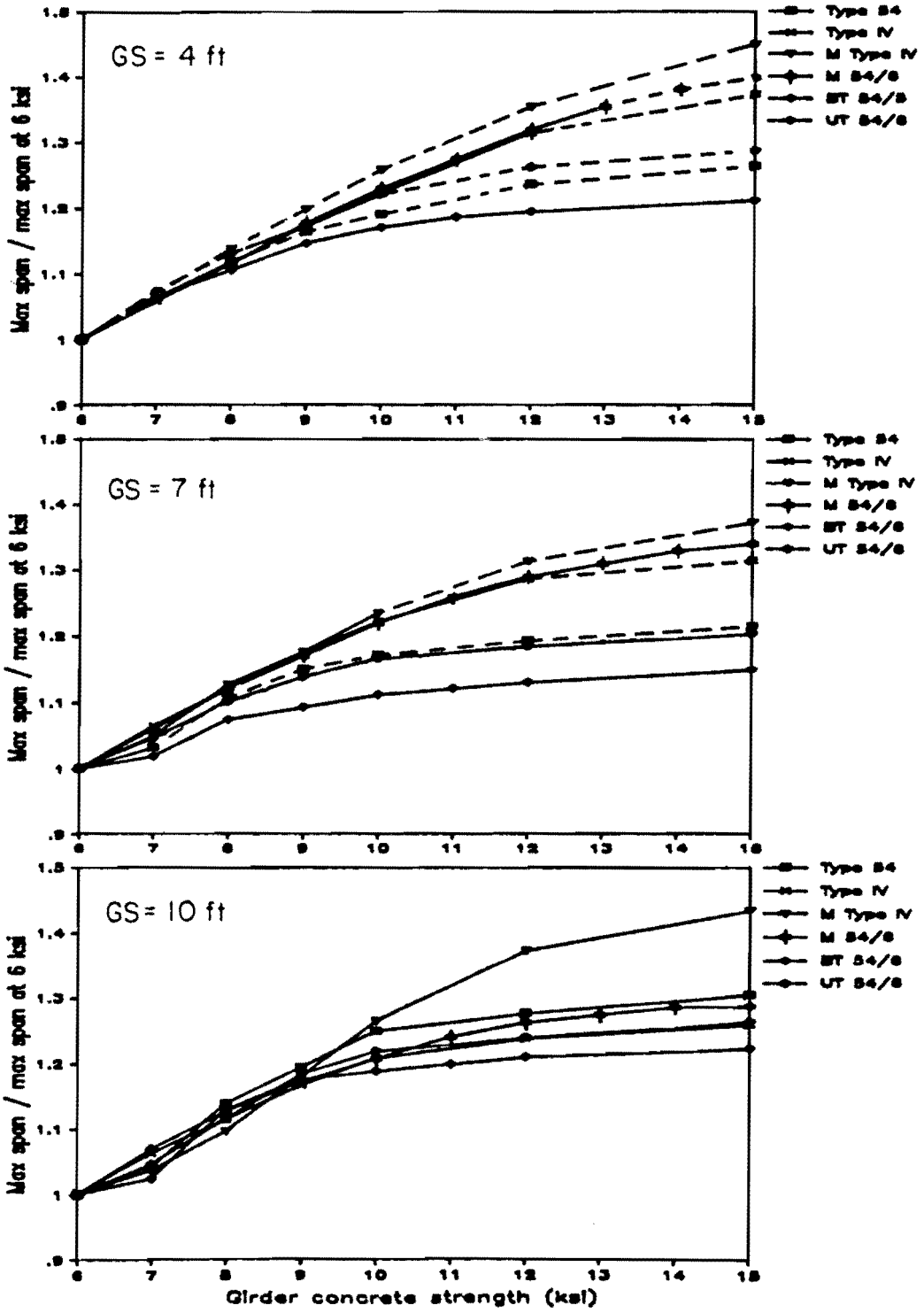

Fig. 3.12 Ratio of increase in maximum span versus concrete strength for 54" sections.

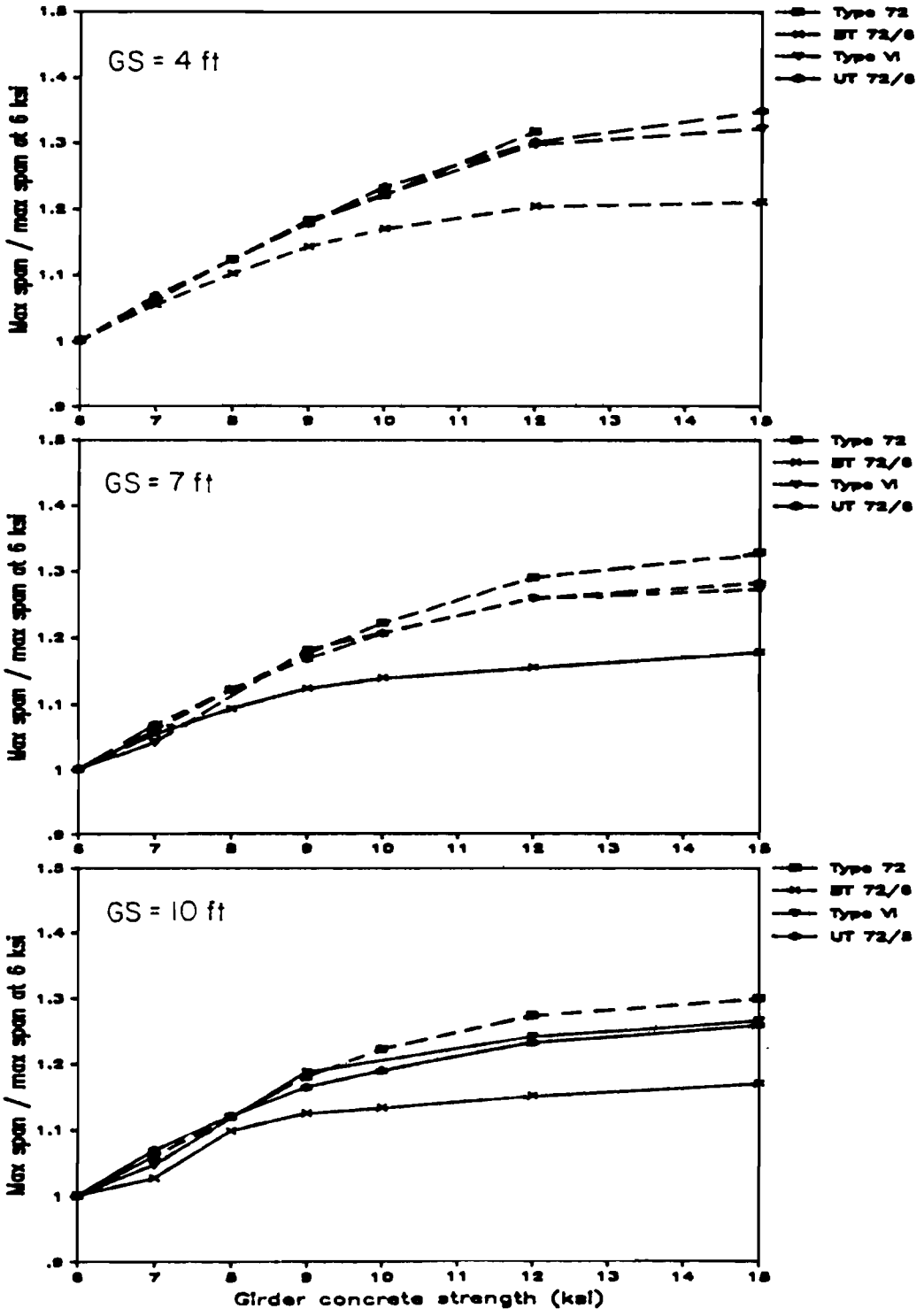

Fig. 3.13 Ratio of increase in maximum span versus concrete strength for 72" sections.

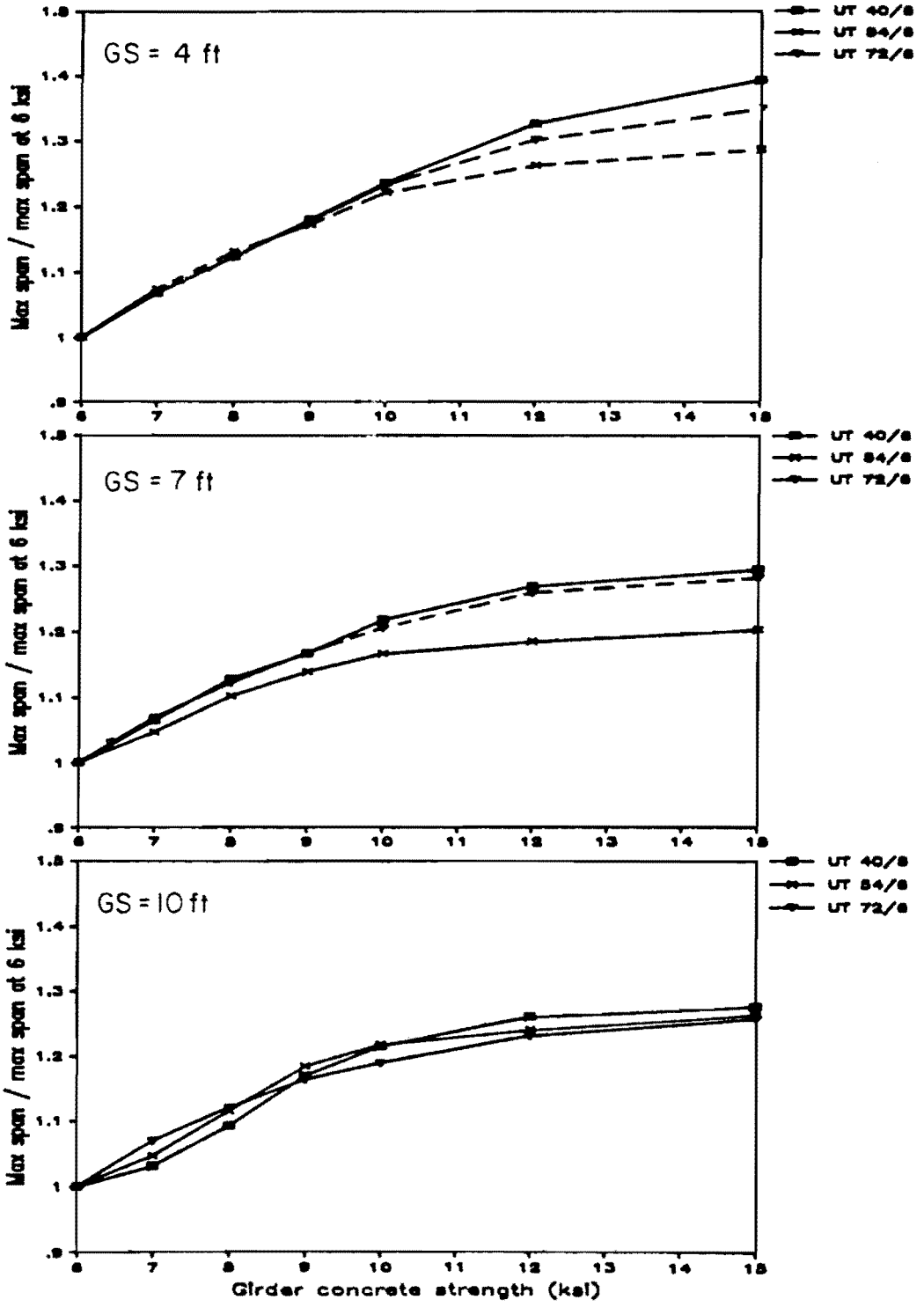

Fig. 3.14 Ratio of increase in maximum span versus concrete strength for proposed sections.

lifting spans. Therefore, stability does not appear to be a large concern for maximum span designs using 40-in. sections.

The maximum spans for the 54-in. sections show great variability due to the variety of sections examined. The very light Texas Type 54 produced the shortest spans and the heaviest section, the AASHTO-PCI Type IV, gave the longest spans for all but a few cases. All sections except the Texas Type 54 and the bulb-tee reached spans in excess of 150 ft for GS = 4 ft. The proposed section had spans that were very close to the spans for the Type IV section for lower concrete strengths at GS = 4 and 7 ft while, for GS = 10 ft and concrete strengths in excess of 9 ksi, the proposed section gave spans of approximately 10 ft less than the Type IV. Some sections showed continuing increases in span with increasing concrete strength while the increase in maximum span length for most sections decreased or stopped for concrete strengths greater than 10 ksi. The Type IV, modified Type IV, and M54/6 (or inverted-tee) girders showed the most consistent span gain with increasing concrete strength, especially for girder spacings of 4 and 7 ft. Span lengths for the bulb-tee increased only 15 to 20 percent for high strength concretes. The proposed section provides an increase in maximum span length of about 5 percent over the bulb-tee for high strength concrete, but this increase is less than most other sections provide.

The lateral stability of 54-in. sections at maximum spans is a significant concern for the closer girder spacings. Only the bulb-tee and inverted-tee (M 54/6) sections had maximum span designs less than the maximum lifting span for concrete strengths of 7 ksi or greater for GS = 4 ft. This means that the increase in span length with higher strength concrete cannot be realized for most sections due to stability considerations. For GS = 7 ft, maximum span designs for bulb- and inverted-tee sections and the proposed (UT) section were unaffected by maximum lifting span limitations. A significant increase in maximum spans for the Type IV and Modified Type IV sections occurred before the maximum lifting span was exceeded at concrete strengths of 9 and 10 ksi, respectively. The Type 54 was still severely limited by stability considerations at this girder spacing. For GS = 10 ft, maximum span designs remained below the maximum lifting spans for all sections. Therefore, stability is a major concern where high strength concrete is used to obtain longer spans for closely spaced 54-in. girders and may restrict the use of span lengths that would otherwise be acceptable. In general, sections with the largest weak axis moment of inertia are affected least by stability limitations.

The maximum spans were similar for the proposed 72-in. section and Texas Type 72 section for all concrete strengths and girder spacings. The AASHTO Type VI had significantly greater spans and the bulb-tee had shorter spans. The Type VI could be used to reach spans of over 200 ft with high strength concrete, while the proposed and Texas Type 72 sections reached spans in excess of 180 ft. These spans are too long to be practical for general use and therefore are not of great significance. For the proposed section, the increase in span from normal strength concrete to 12 ksi concrete ranged from about 25 to 30 percent with an increase of approximately 15 to 20 percent for 9 ksi concrete. Spans did not increase significantly for concrete strengths greater than 12 ksi.

These plots indicate that maximum span designs for the 72-in. sections are limited even more severely by stability considerations than the 54-in. sections. For GS = 4 ft, all designs shown exceed the maximum lifting spans. For GS = 7 ft, only small increases in the maximum spans are possible before the maximum lifting span is exceeded, except for the bulb-tee designs which did not exceed the maximum lifting span limit. At GS = 10 ft, designs for the Texas Type 72 were still severely limited while designs for all other sections were unaffected by the lifting span limit. As for the 54-in. sections, stability considerations are very significant in the design of long spans using 72-in. sections and will restrict, in many cases, the possible span lengths resulting from increased concrete strength.

The plots for the proposed sections (Fig. 3.10) indicate that a wide range of spans can be obtained using the three sections. The sections also exhibit similar behavior in that increasing concrete strengths result in increased maximum spans for concrete strengths up to at least 10 ksi. This is also evident in Fig. 3.14, where spans for the 40 and 72 in. sections increase approximately 25 to 40 percent with increasing concrete strength, while the 54-in. section gives roughly a 20 to 25 percent increase and exhibits a reduction in the rate of span increase at a lower concrete strength.

Figure 3.10 also indicates that for these sections stability limitations are more restrictive as the section depth increases. Maximum span designs for the 72-in. section are significantly restricted for GS = 4 and 7 ft while maximum span designs for the 40-in. section are unaffected by the lifting span limit. Maximum span designs for the UT 54/6 are limited by stability only for GS = 4 ft.

All of these figures indicate a general trend that, as girder spacing increases, the benefit from use of the higher concrete strengths is reduced. This means that for GS = 10 ft, the maximum useful concrete strength is about 9 ksi, but for GS = 4 ft, the use of concrete with strengths in excess of 12 ksi continues to provide noticeable increases in span length. Sections with greater area also appear to provide greater spans which is most evident for the AASHTO-PCI Type IV and VI sections.

A plateau is apparent in a number of the curves at lower concrete strengths. This is attributed to the use of a 5 ksi release strength for 6 ksi designs which is a higher proportion of the design strength than was used for other designs.

Maximum span data can also be presented as a plot showing the maximum girder spacing permitted for a given span and concrete strength. This type of plot is shown for the AASHTO-PCI Type IV section in Fig. 3.15 for spans of 100, 120, and 140 ft. As noted the figure, the 140 ft span exceeds the maximum lifting spans for the section for all concrete strengths considered.

These data indicate that a significant increase in girder spacing is possible when increased concrete strengths are used. However, strengths in excess of about 11 ksi provide little additional benefit. This plot shows that for a 120-ft span, half the number of girders will be required if a concrete strength of approximately 8.5 ksi is used instead of 6 ksi, which is the normal concrete strength for pretensioned girders in Texas. This is a significant reduction for only a moderate increase in concrete strength. It should be noted that this benefit only occurs for longer spans and that for shorter spans, the effect of increasing concrete strength is limited by maximum allowable spacing requirements.

3.4.2 Strand Usage. Strand usage for two types of designs will be discussed in this section. The number of strands required to produce the maximum spans examined above will be considered first. Then, the effect of concrete strength on the number of strands required for a given span will be investigated. The minimum number of strands required for the maximum spans are plotted versus the concrete strength in Fig. 3.16 through 3.19, for each section depth and for the proposed sections, respectively. In most cases, strand usage parallels the maximum span plots with sections demonstrating the greater maximum spans requiring more strands to achieve the greater span. This is an expected observation and reveals little about section efficiency. Some designs using the AASHTO-PCI Type IV and

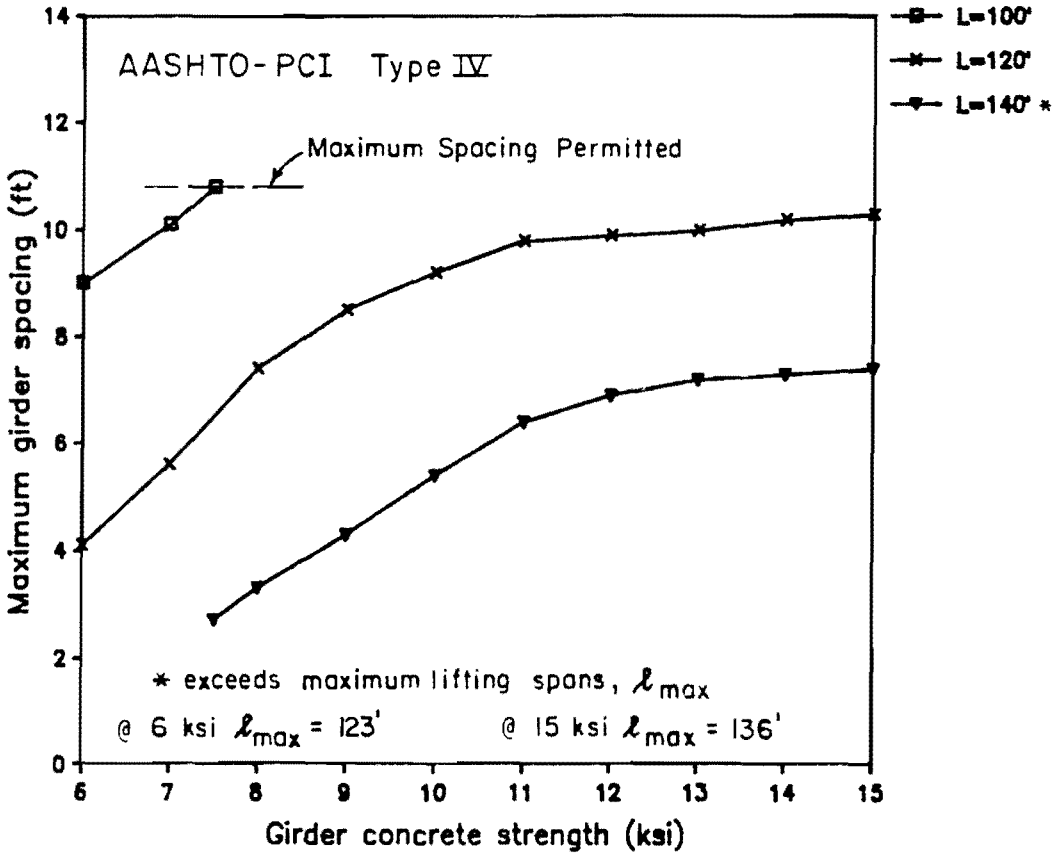

Fig. 3.15 Variation in girder spacing with concrete strength.

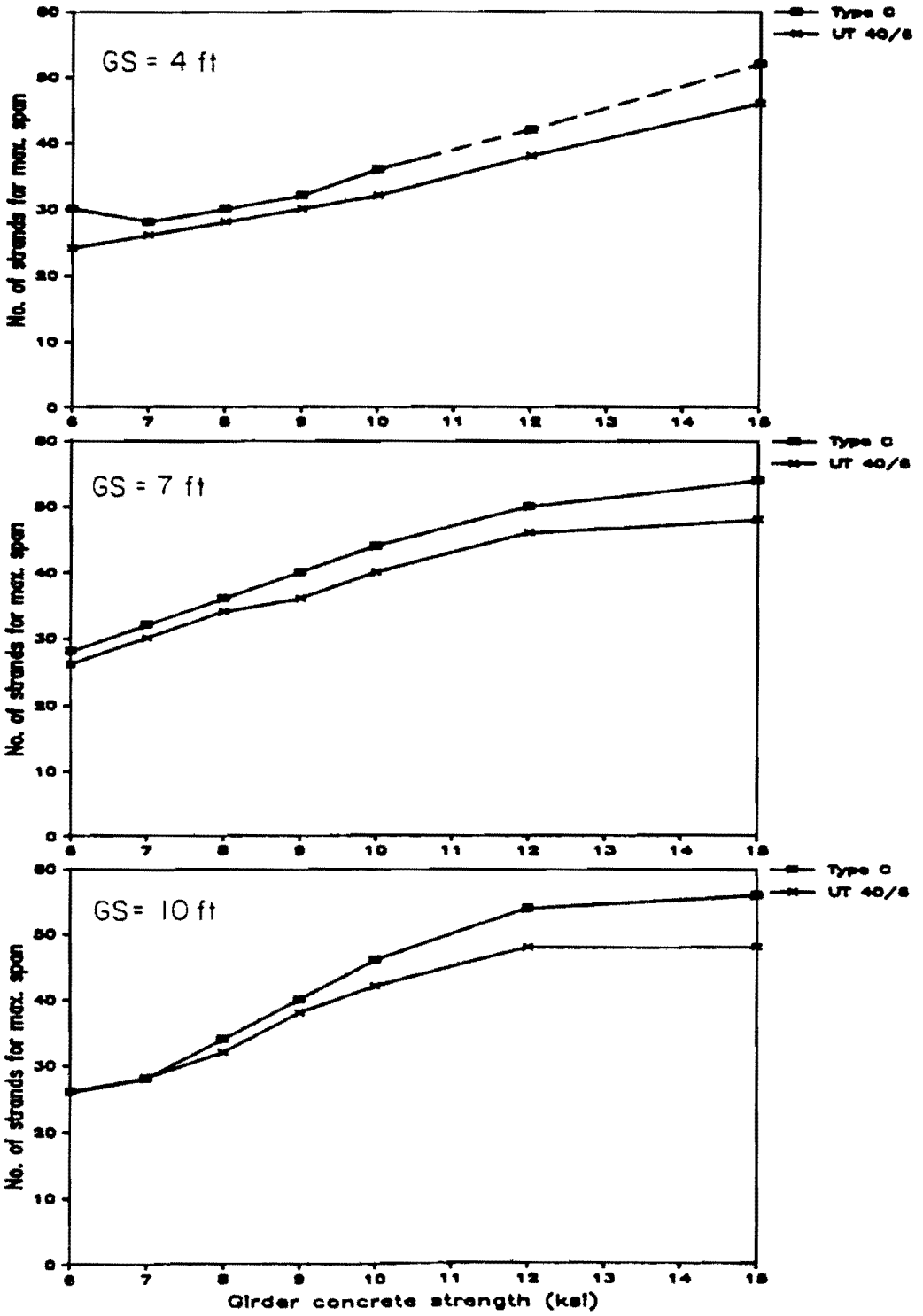

Fig. 3.16 Numbers of strands for maximum span versus concrete strength - 40" sections.

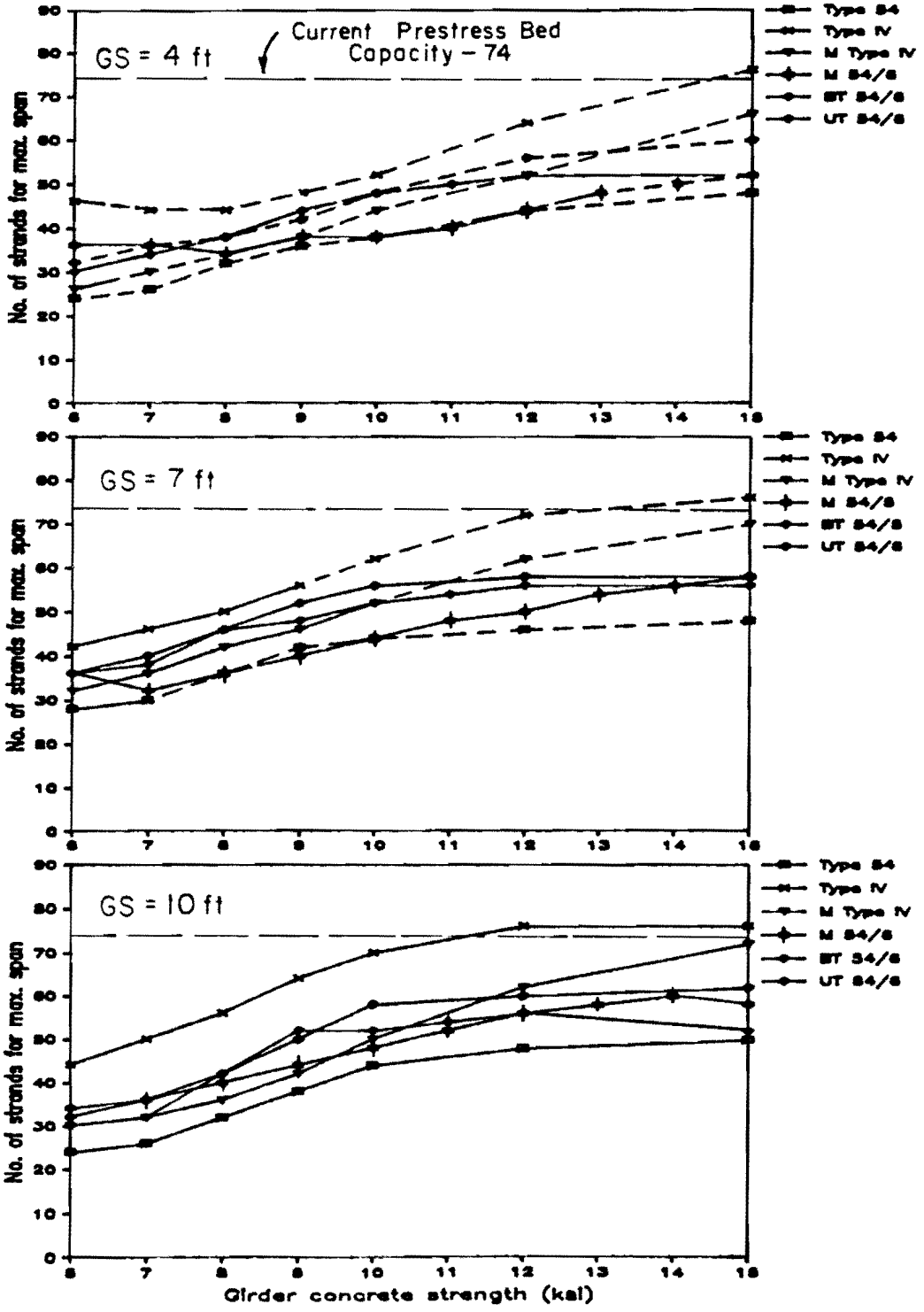

Fig. 3.17 Numbers of strands for maximum span versus concrete strength - 54" sections

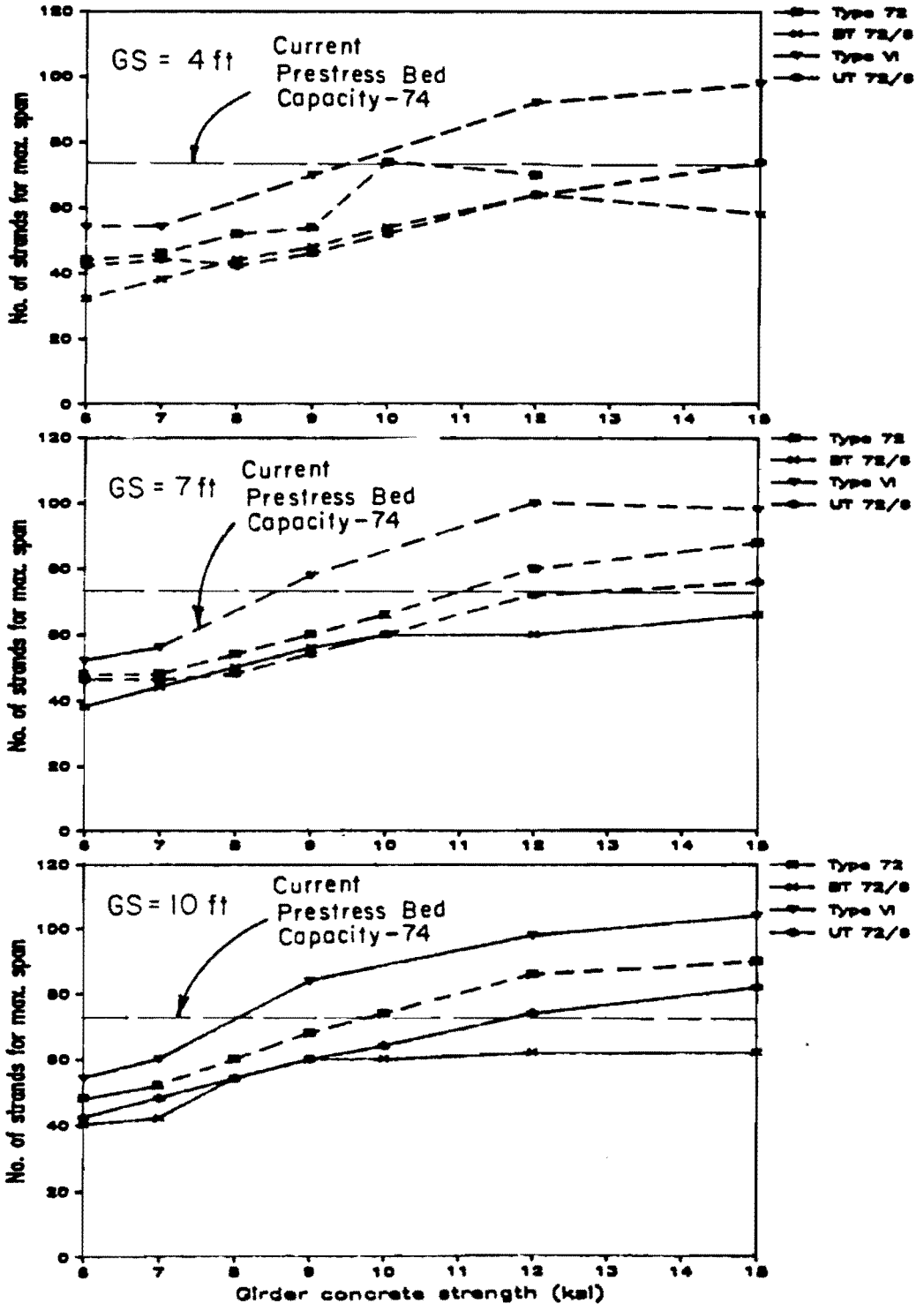

Fig. 3.18 Numbers of strands for maximum span versus concrete strength - 72" sections

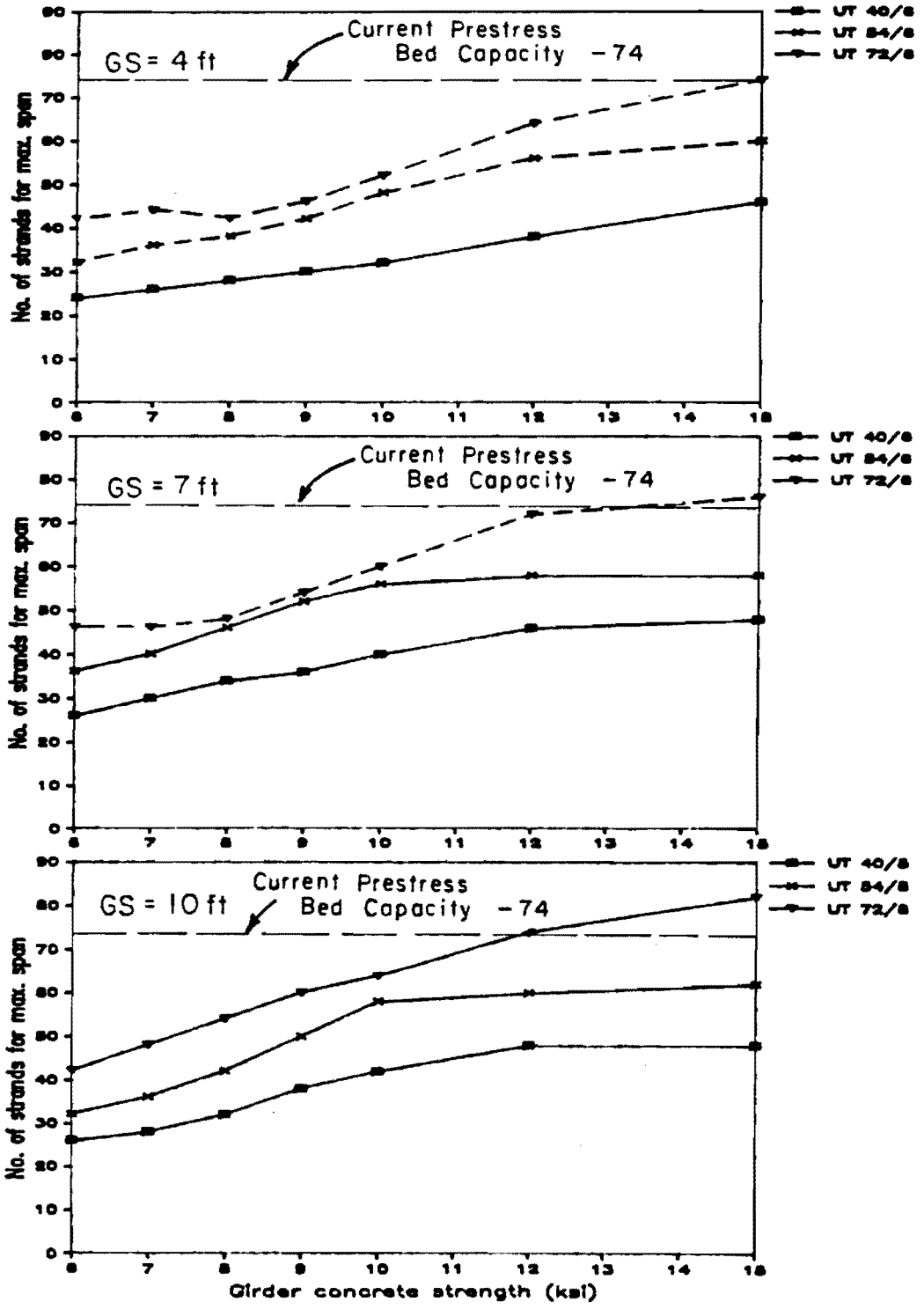

Fig. 3.19 Number of strands for maximum span versus concrete strength - proposed sections

Type VI sections and the Texas Type 72 section may require a number of strands greater than the capacity of current prestress beds in Texas, which is indicated on the figures. This indicates that the large maximum spans shown in preceding plots may not only be impractical from the perspective of handling and transportation, but also with respect to construction, since such large prestress forces are required. The proposed 72 in. UT section requires up to 80 strands, but only for very high concrete strengths.

For maximum span designs, the number of strands indicated on the figures generally represents both the minimum and maximum number of strands that can be used for the maximum span. This is because a maximum span is usually defined by the convergence of more than one limiting stress as illustrated in Fig. 3.20 for an AASHTO-PCI Type IV girder. For different combinations of section, girder spacing, span, and concrete strength, different combinations of stress limits define the maximum span. In some cases, a single condition may control the design in cases where strands are being added above the centroid of the section (Fig. 3.20, GS = 4 ft). Designs may also be controlled because draping strands at the ends of the girder is not sufficient to keep stresses within allowable limits at release.

The minimum number of strands required for spans up to the maximum span are shown in Fig. 3.21 for AASHTO-PCI Type IV and 54 in. bulb-tee sections. Data are presented for two girder spacings and the figure for both sections. The data indicate that the number of strands required for the maximum span increases rapidly for longer spans, which are possible through the use of higher concrete strengths. Approximately the same number of strands is required for a maximum span design at the two girder spacings. The range of maximum lifting spans for the concrete strengths considered is indicated on the figure for both sections.

The minimum number of strands required to obtain a given span versus concrete strength is shown in Fig. 3.22 for an AASHTO-PCI Type IV section. The data show that the number of strands used in spans less than the maximum span are not significantly affected by the concrete strength. Therefore, there is no significant benefit with respect to strand usage when replacing normal strength concrete with high strength concrete in an otherwise identical bridge design. The ultimate capacity of the section is found to control the designs of many of the short span girders.

3.4.3 Section Efficiency. An indication of the efficiency of the different sections was obtained by dividing maximum spans

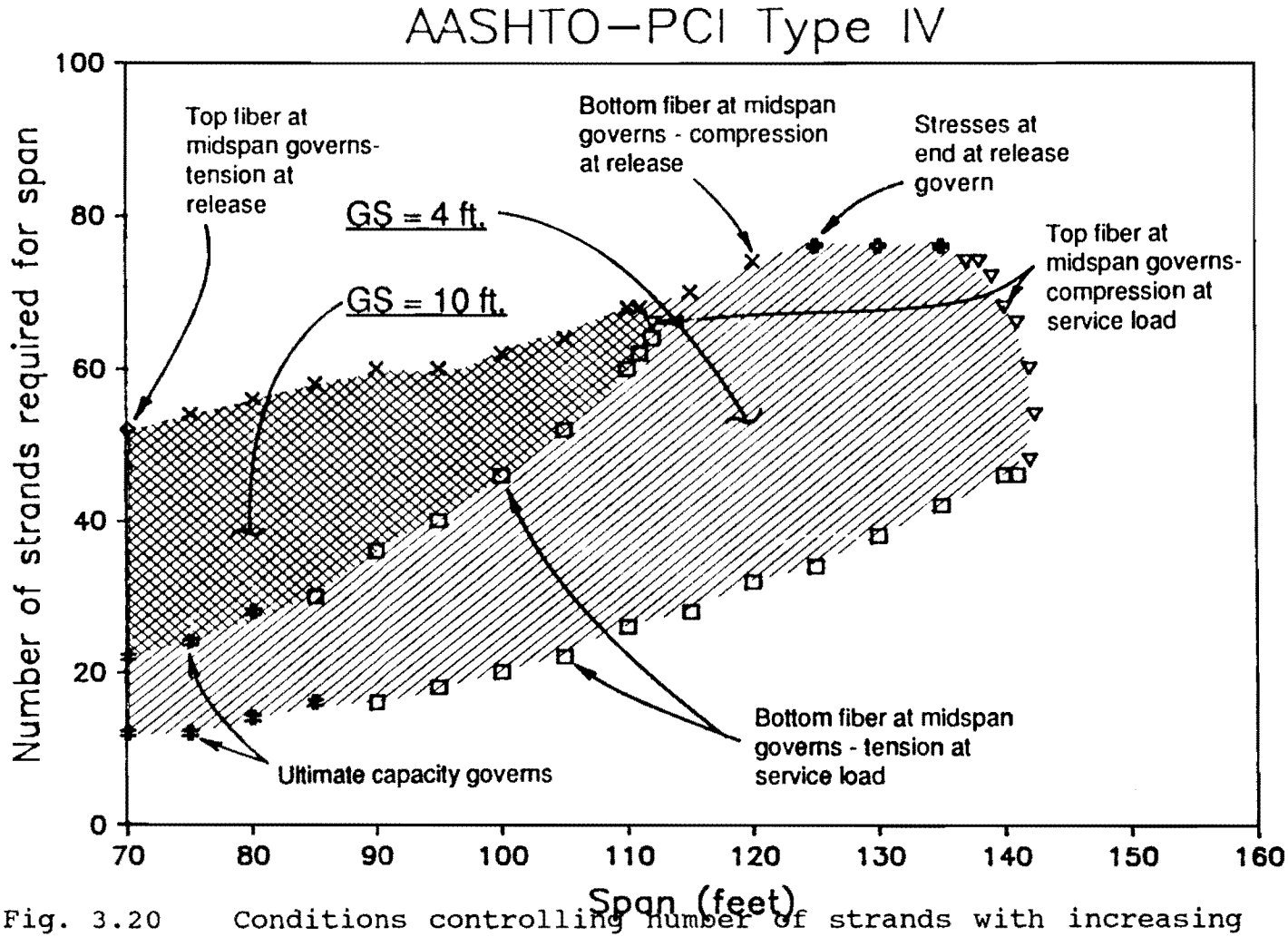

Fig. 3.20 Conditions controlling number of strands with increasing spans

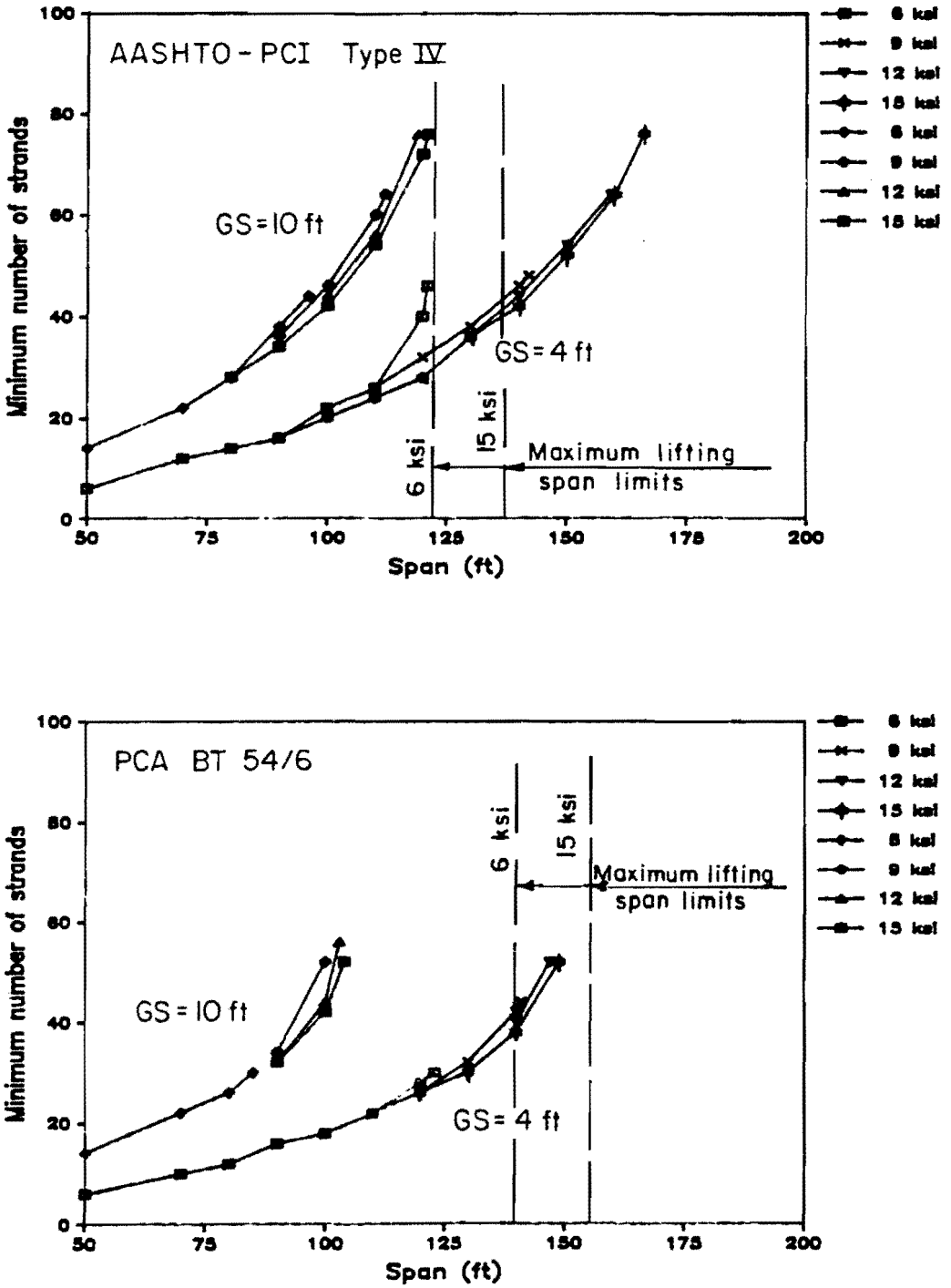

Fig. 3.21 Variation in number of strands required for maximum spans.

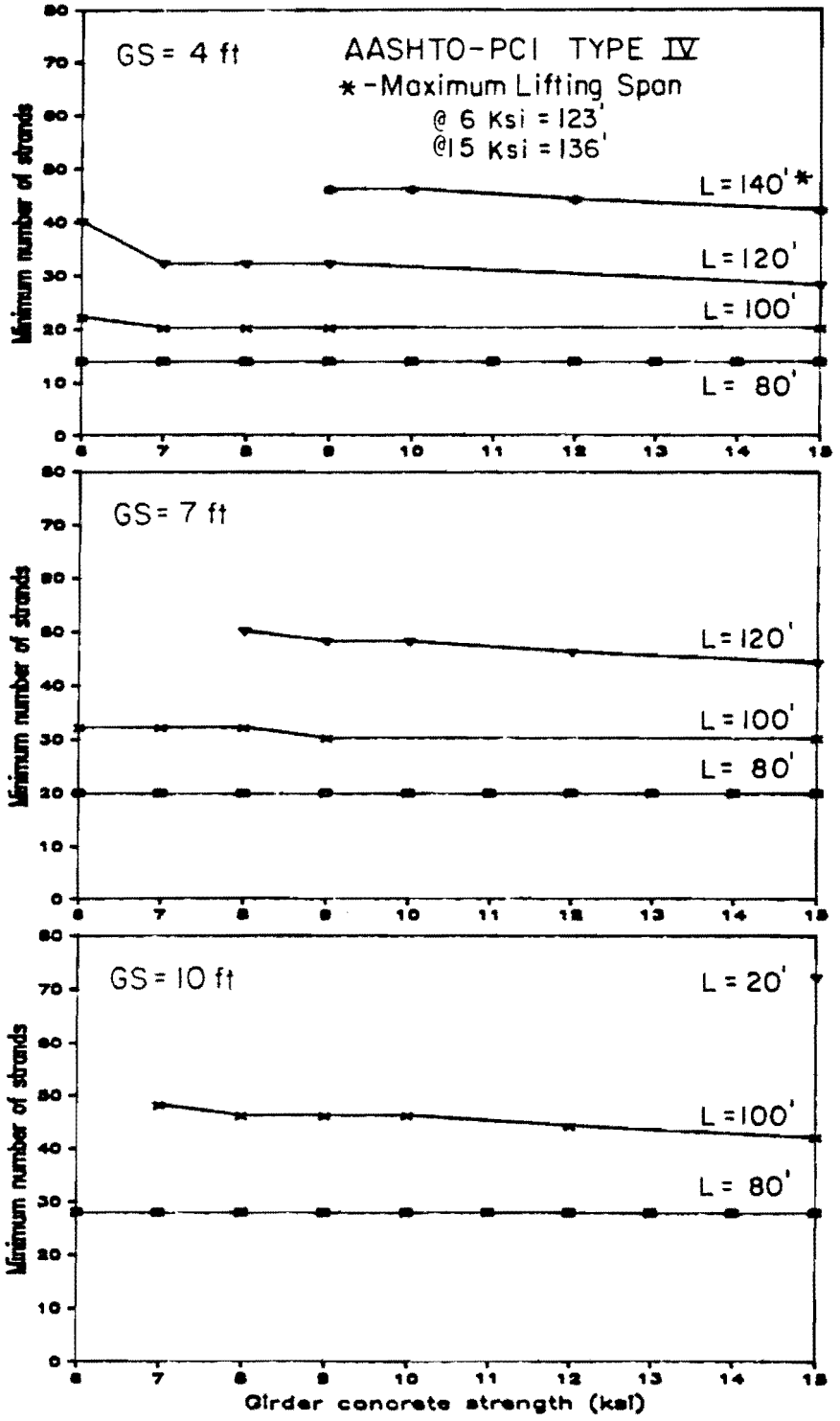

Fig. 3.22 Variation in minimum number of strands with girder concrete strengths.

(determined by allowable stress and ultimate strength criteria) by the girder area or by the number of strands required for the span. The resulting values represent the span per unit of cross-sectional area and the span per strand and therefore, larger values indicate a more efficient use of girder area or strands. The maximum span-to- area ratios are plotted in Fig. 3.23 through 3.26 and the maximum span-to-number of strand ratios are plotted in Fig. 3.27 through 3.30. For each ratio, a figure is provided for each section depth and the proposed sections. Spans exceeding maximum lifting spans are indicated by dashed lines on the plots. Designs where the current maximum prestress bed capacity is exceeded are indicated by placing a circle around the point.

For the 40-in. sections, the proposed section proves to be more efficient in both comparisons. For both comparisons with 54-in. sections, the proposed section is very close to the bulb-tee and is a significant improvement over the Type IV girder. For the comparison with respect to area, the proposed section and the bulb-tee are exceeded by only the Type 54 girder which is limited in span. However, for the strand comparison, other sections proved to be more efficient in most cases, although trends are difficult to identify due to the erratic nature of the plots. The situation is similar for the 72-in. sections where in the area comparisons the bulb-tee is best, with the proposed section slightly less or equally efficient. In the comparison involving number of strands, the proposed section proved superior in some cases to the other sections. An examination of the figures showing plots for the proposed sections reveals that the efficiency of the sections is similar.

While these comparisons give an indication of the relative efficiency of the sections, the results of the comparisons are not conclusive and do not consider all aspects of design. However, they do indicate that the proposed sections have efficiencies similar to the bulb-tees, and are generally superior to the AASHTO-PCI and Texas standard sections.

3.4.4 Sensitivity to Strength at Release. Sensitivity of the maximum span designs to concrete strength at release is indicated in Fig. 3.31 through 3.34 by the ratio of maximum span computed using a release strength of 50 percent of the design strength to the span computed using a release strength of 75 percent of the design strength, except for 6 ksi, where 83 percent is used. The data shown indicate that the effect of the reduction in release strength is lessened as the concrete strength is increased and as the girder spacing is decreased. The proposed sections tended to be about

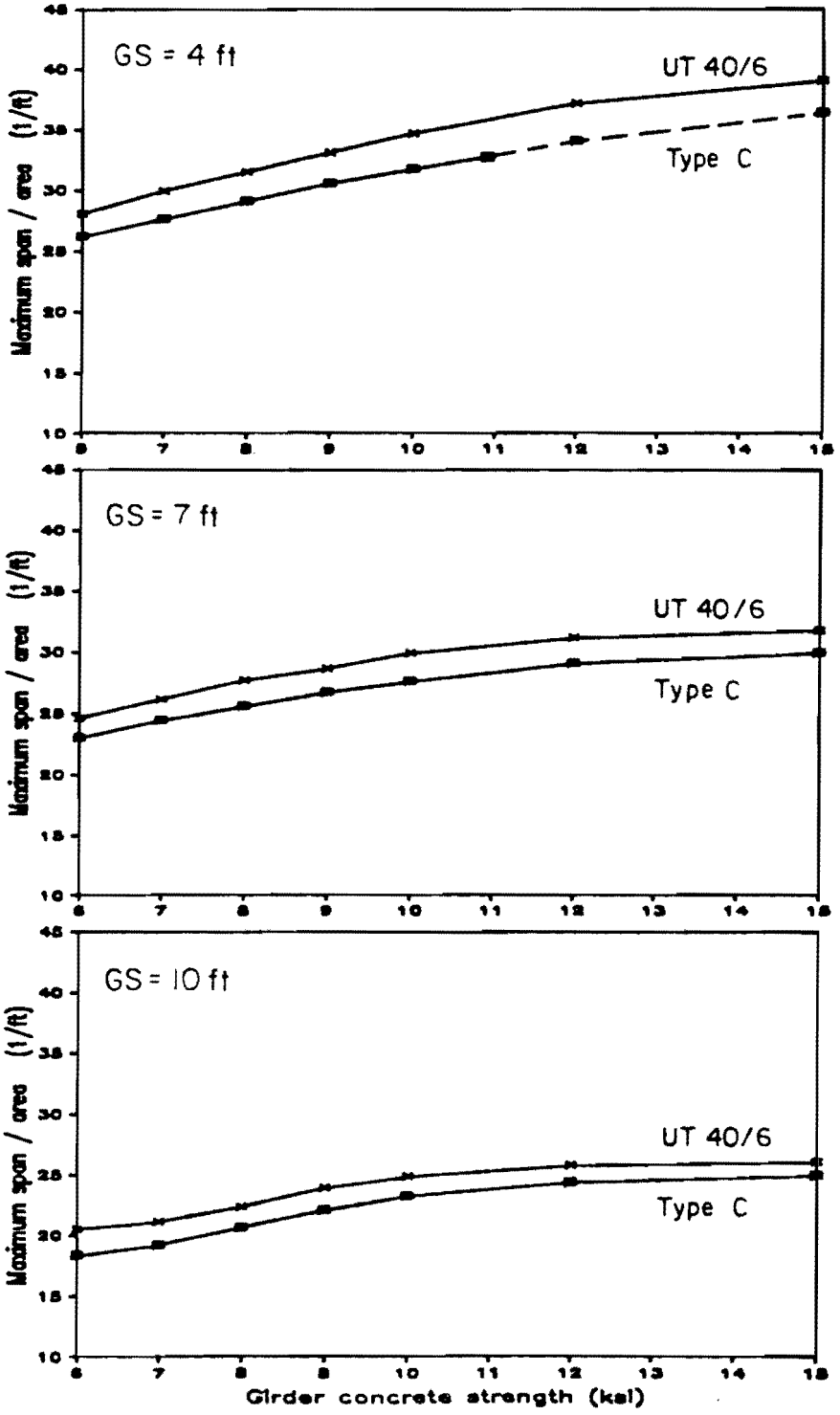

Fig. 3.23 Ratio of maximum span to area of girder versus concrete strength - 40" sections.

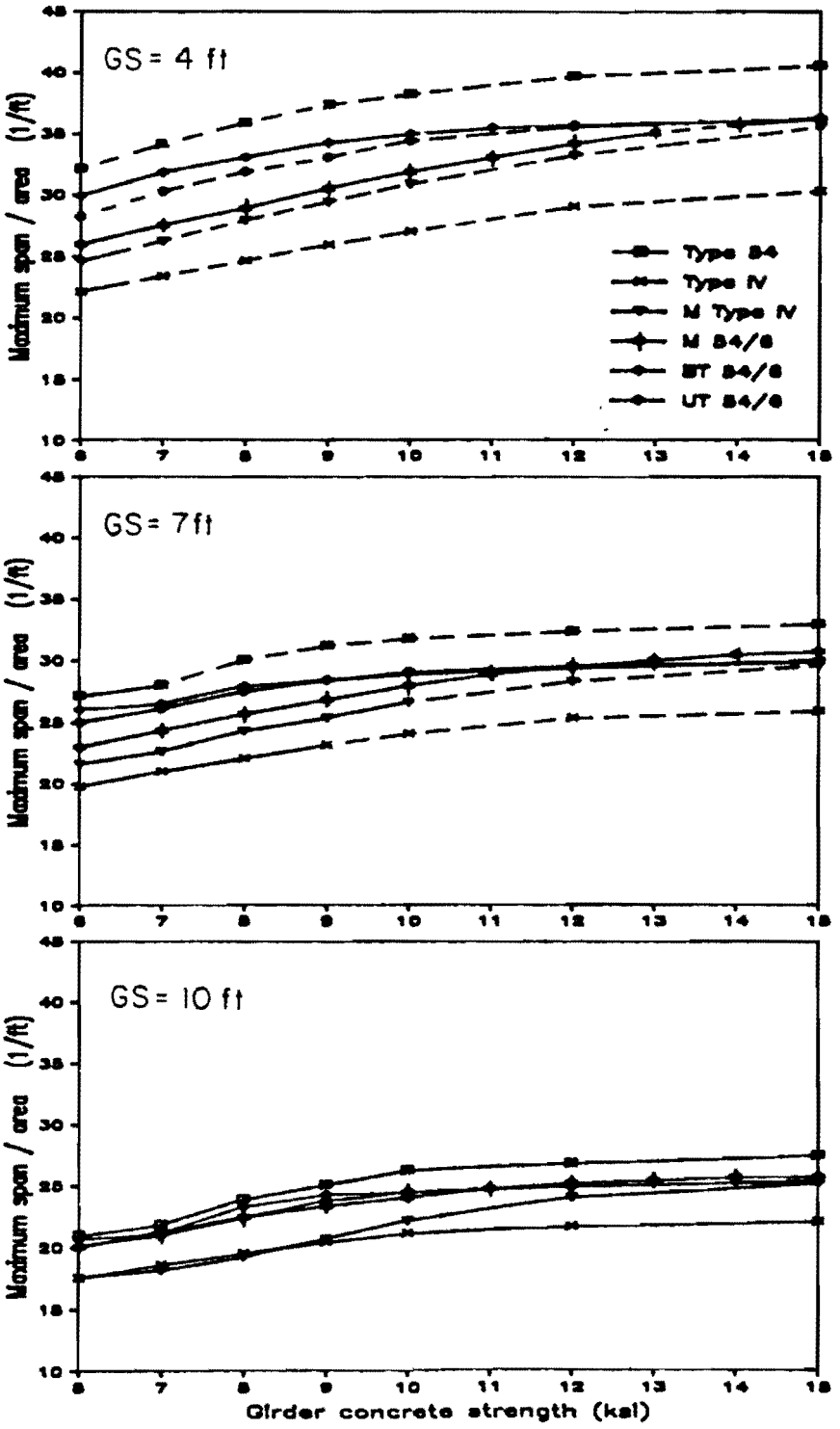

Fig. 3.24 Ratio of maximum span to area of girder versus concrete strength - 54" sections.

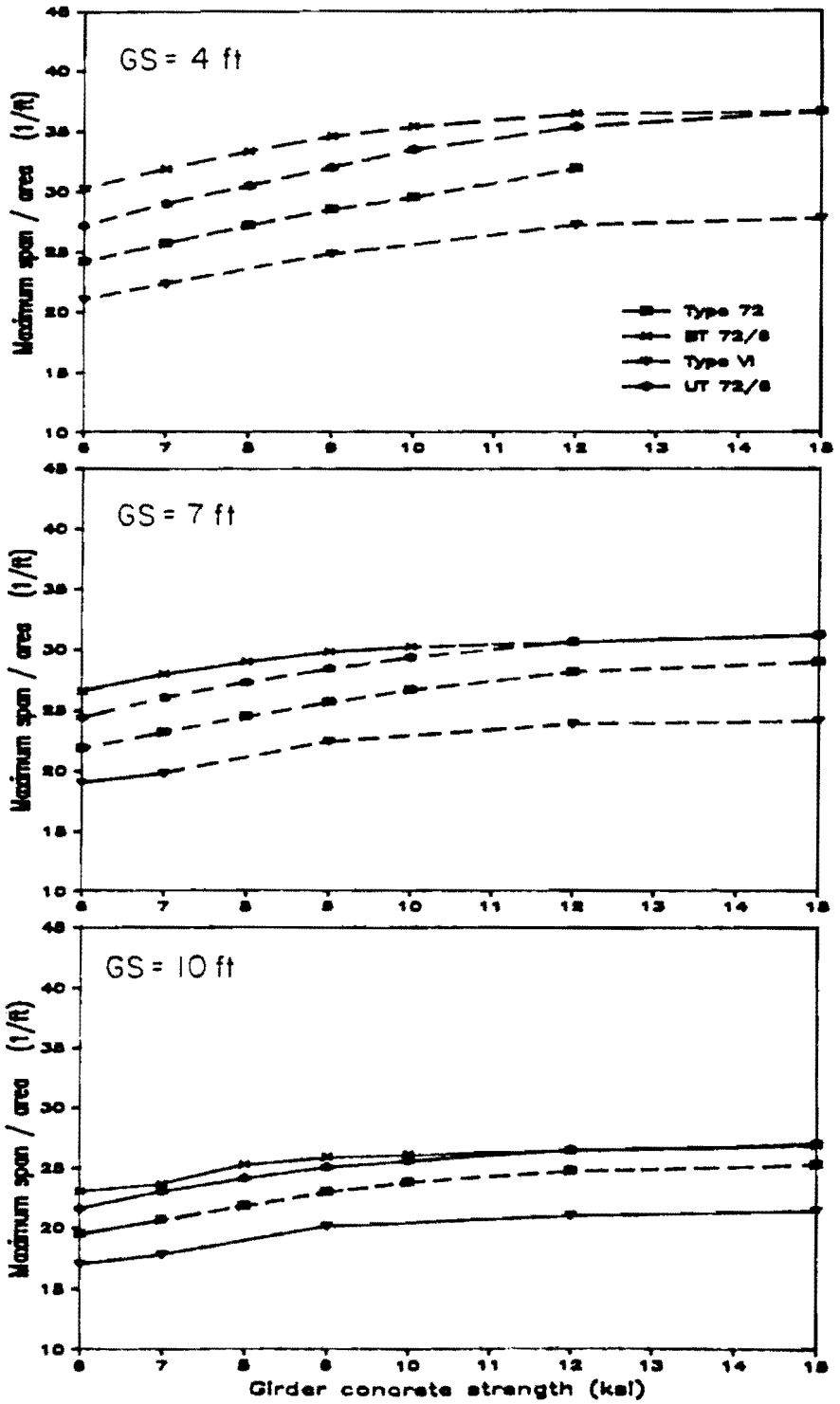

Fig. 3.25 Ratio of maximum span to area of girder versus concrete strength - 72" sections

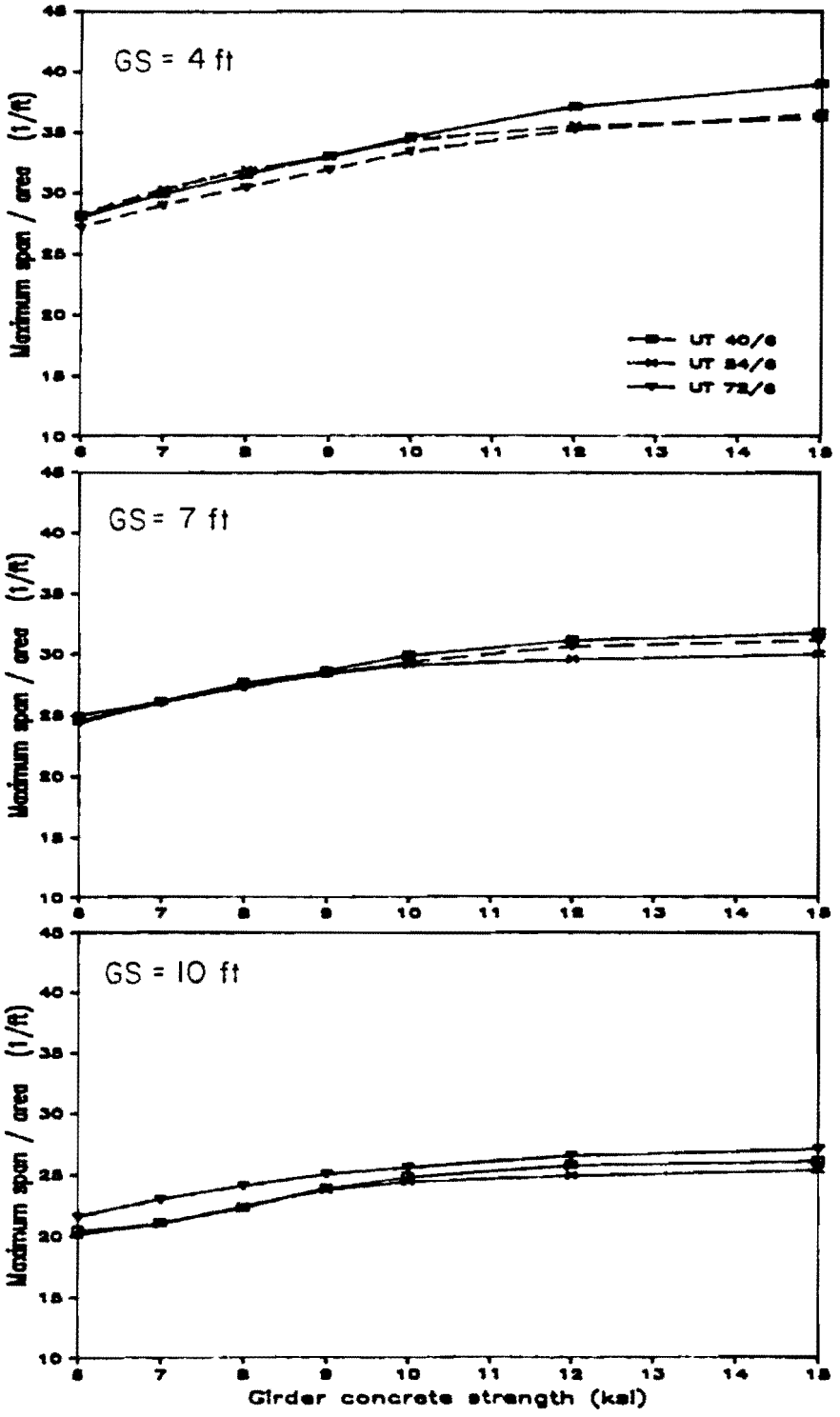

Fig. 3.26 Ratio of maximum span to area of girder versus concrete strength - proposed sections.

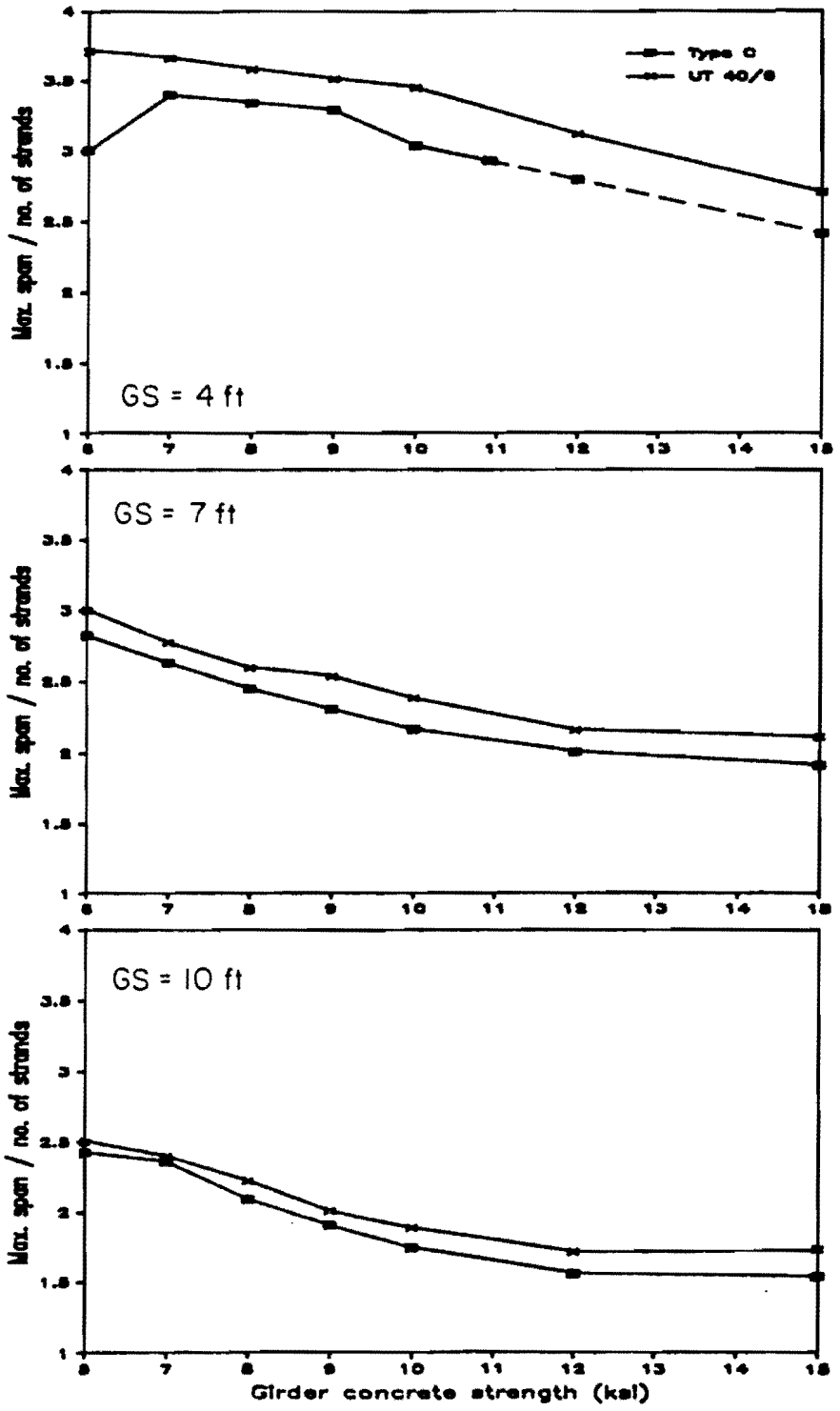

Fig. 3.27 Ratio of maximum span to number of strands versus concrete strength - 40" sections.

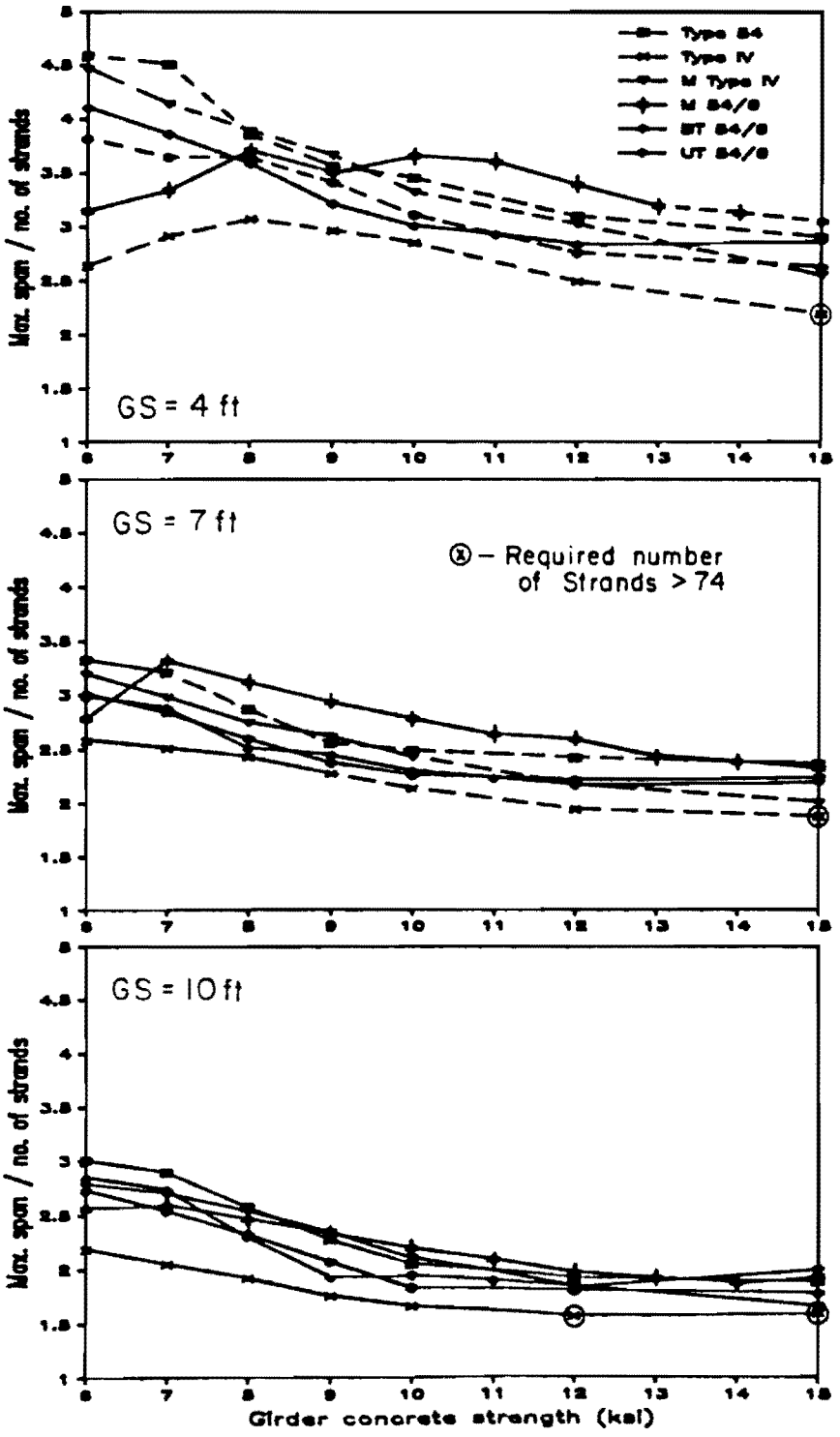

Fig. 3.28 Ratio of span to number of strands versus concrete strength - 54" sections.

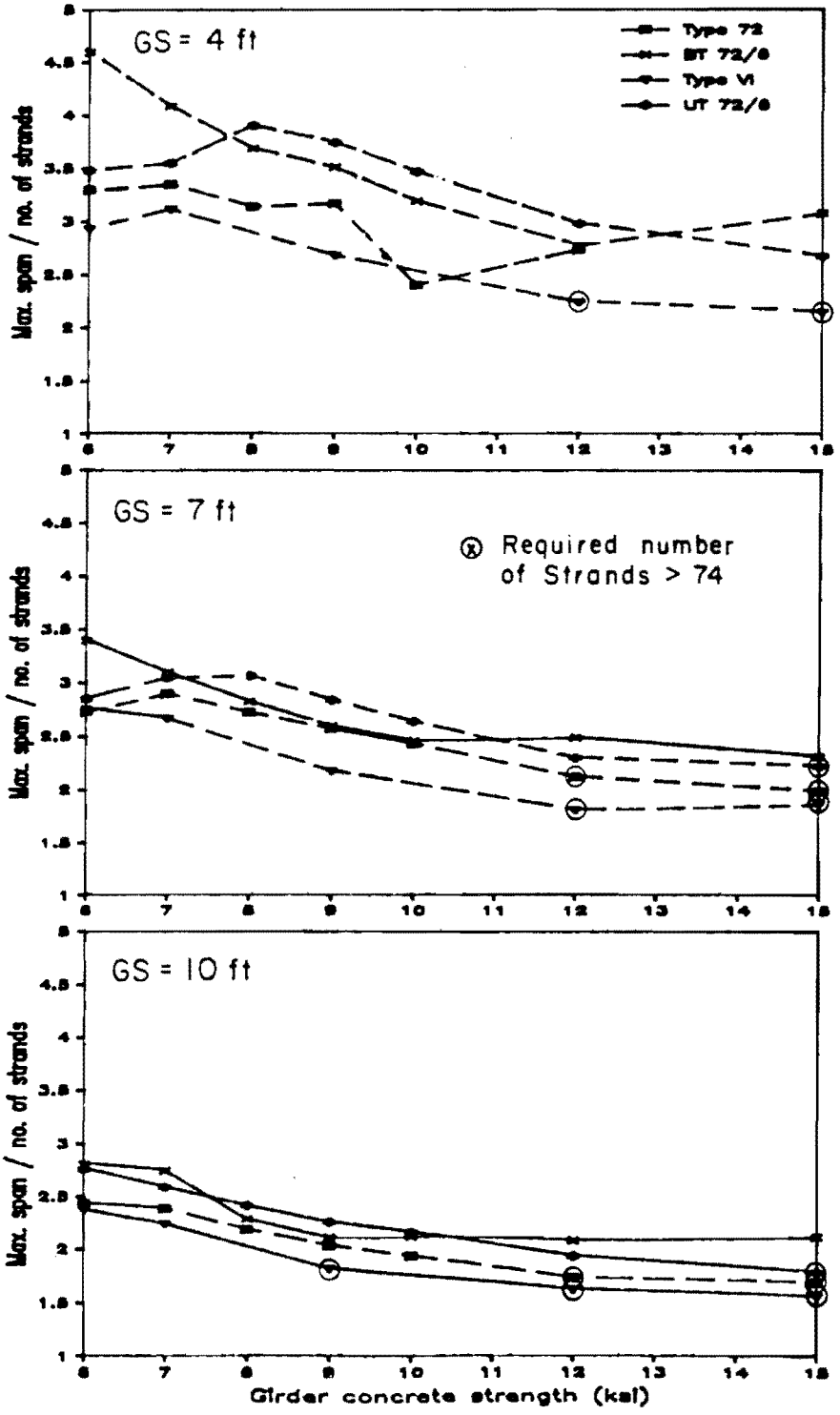

Fig. 3.29 Ratio of maximum span to number of strands versus concrete strength - 72" sections.

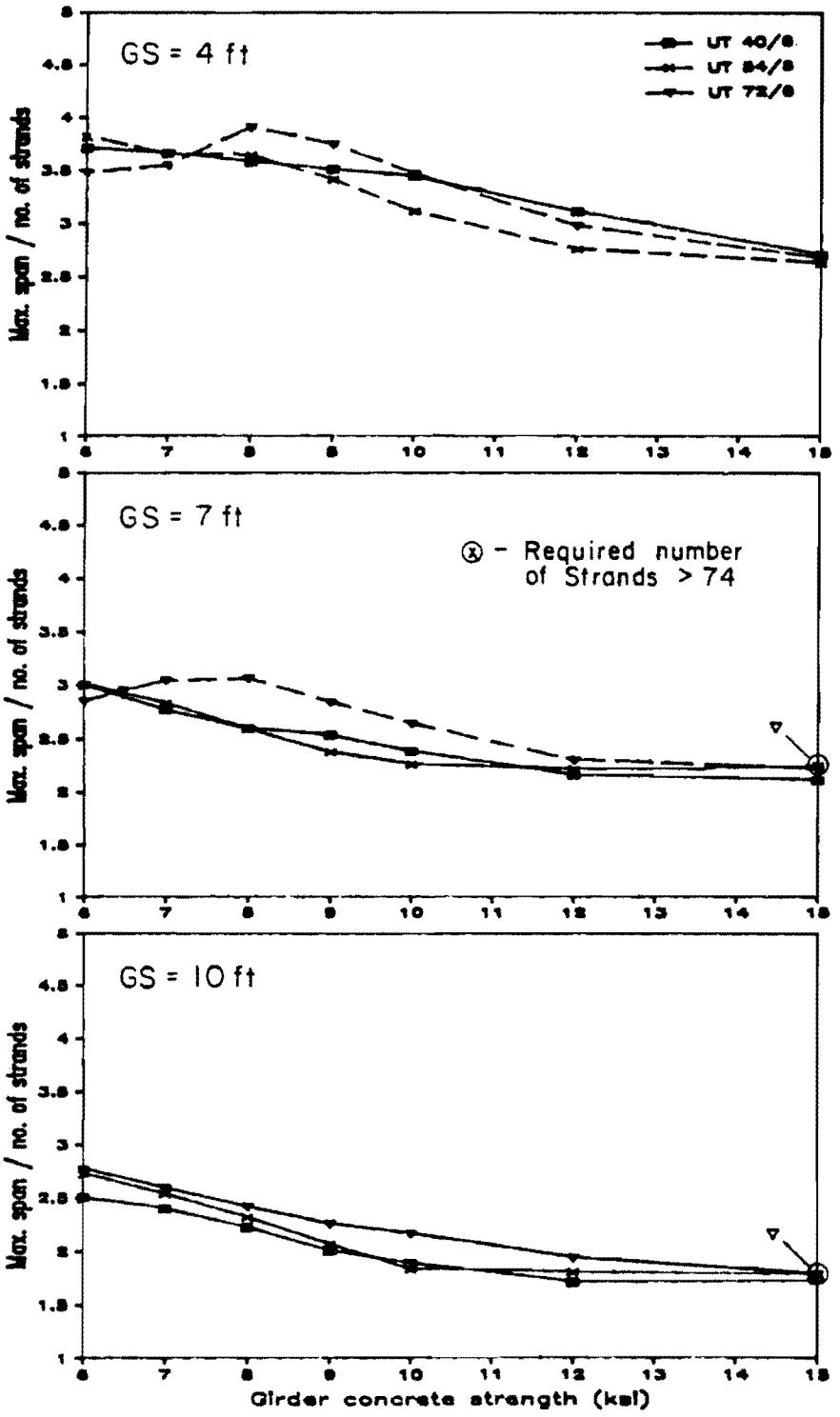

Fig. 3.30 Ratio of maximum span to number of strands versus concrete strength - proposed sections.

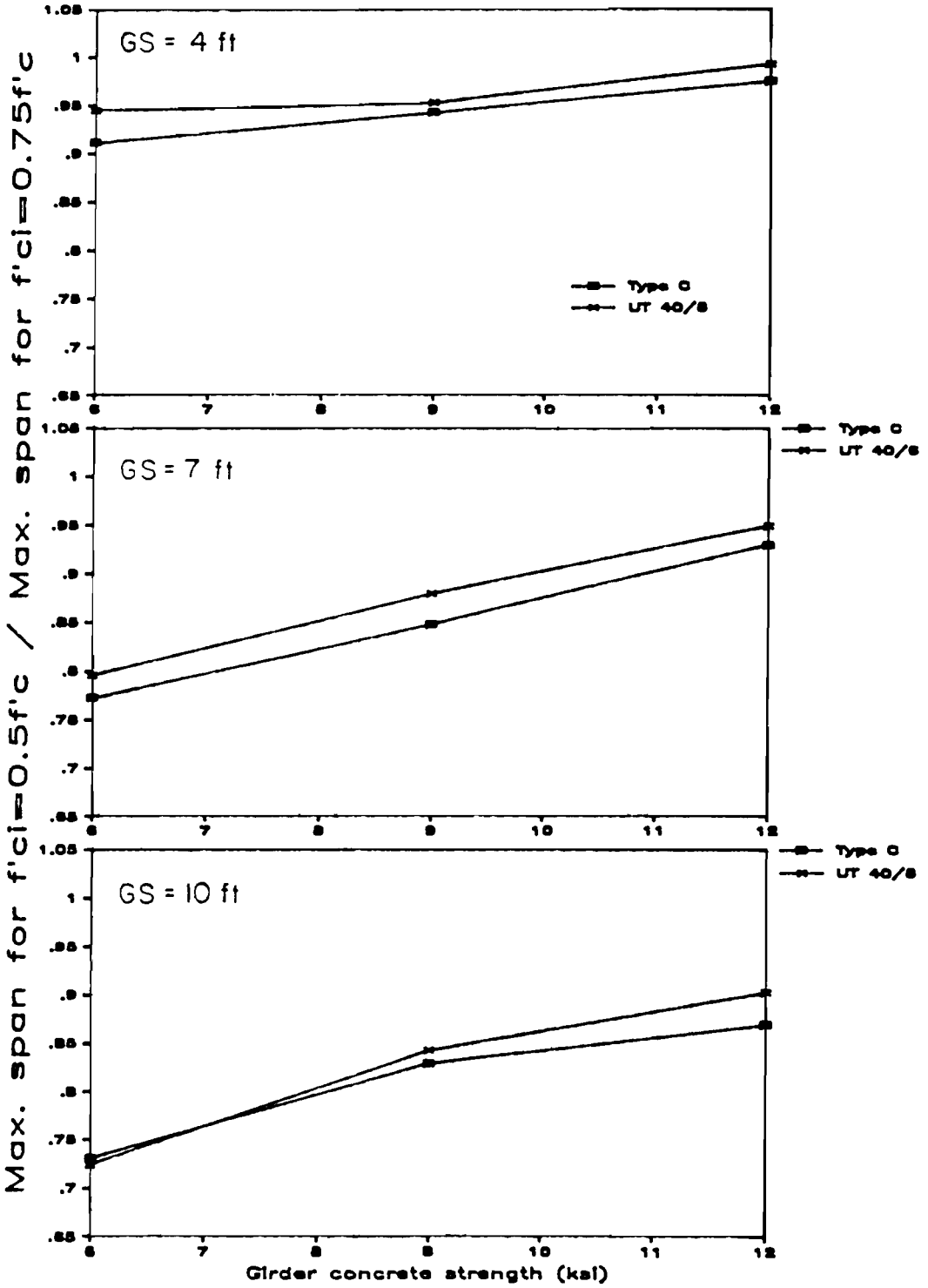

Fig. 3.31 Reduction in maximum spans due to lower concrete strength at release - 40" sections.

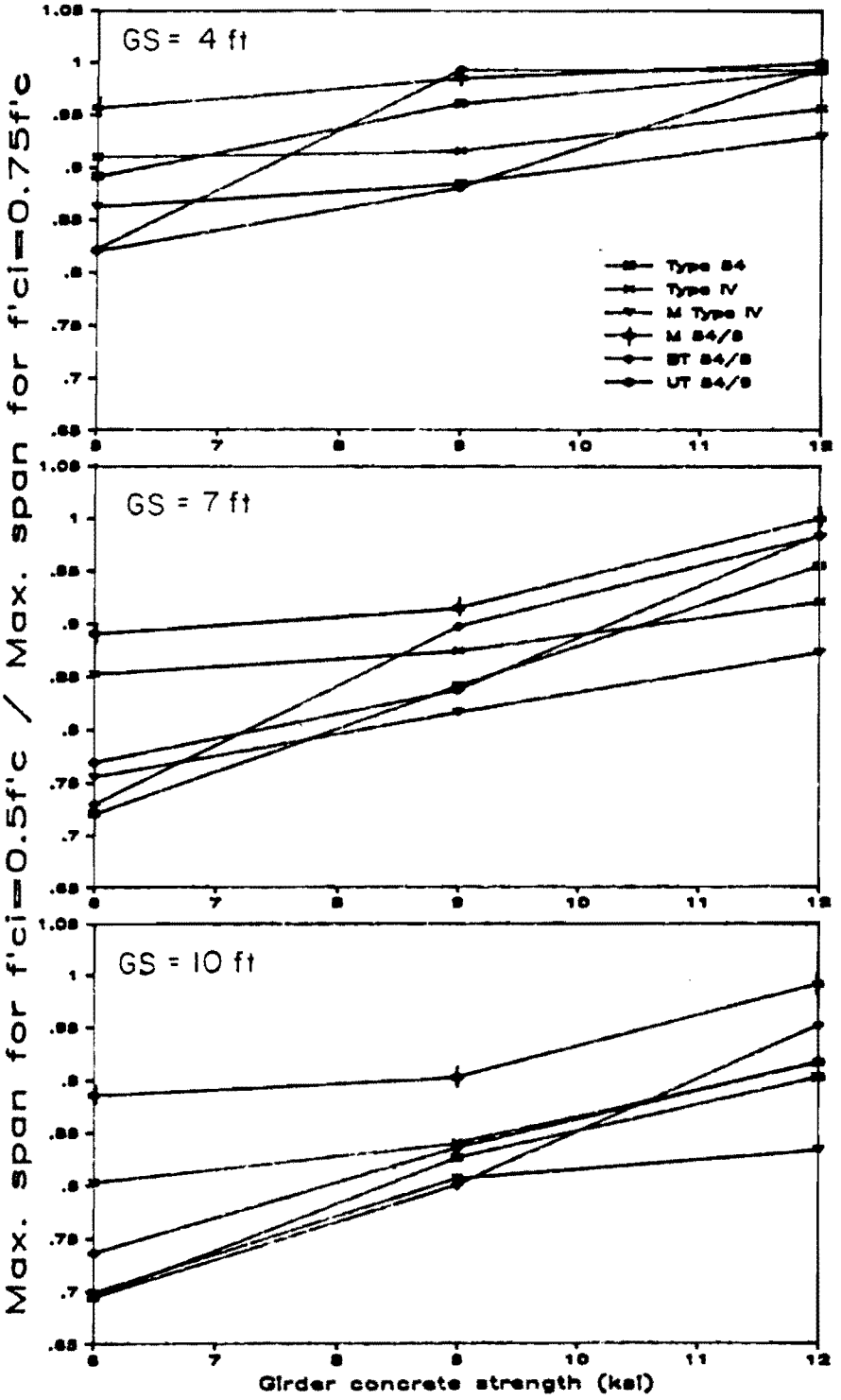

Fig. 3.32 Reduction in maximum spans due to lower concrete strength at release - 54" sections.

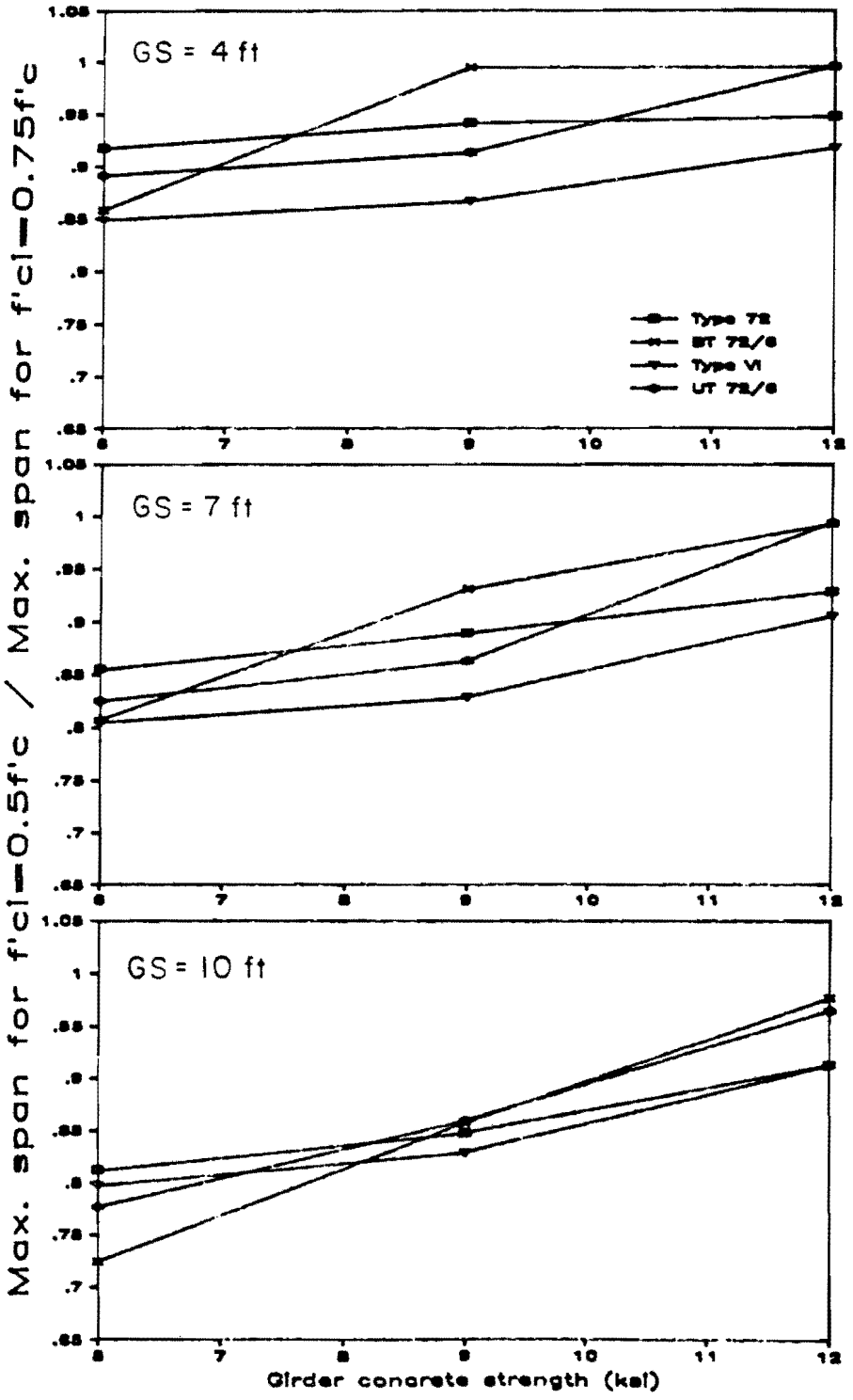

Fig. 3.33 Reduction in maximum spans due to lower concrete strength at release - 72" sections.

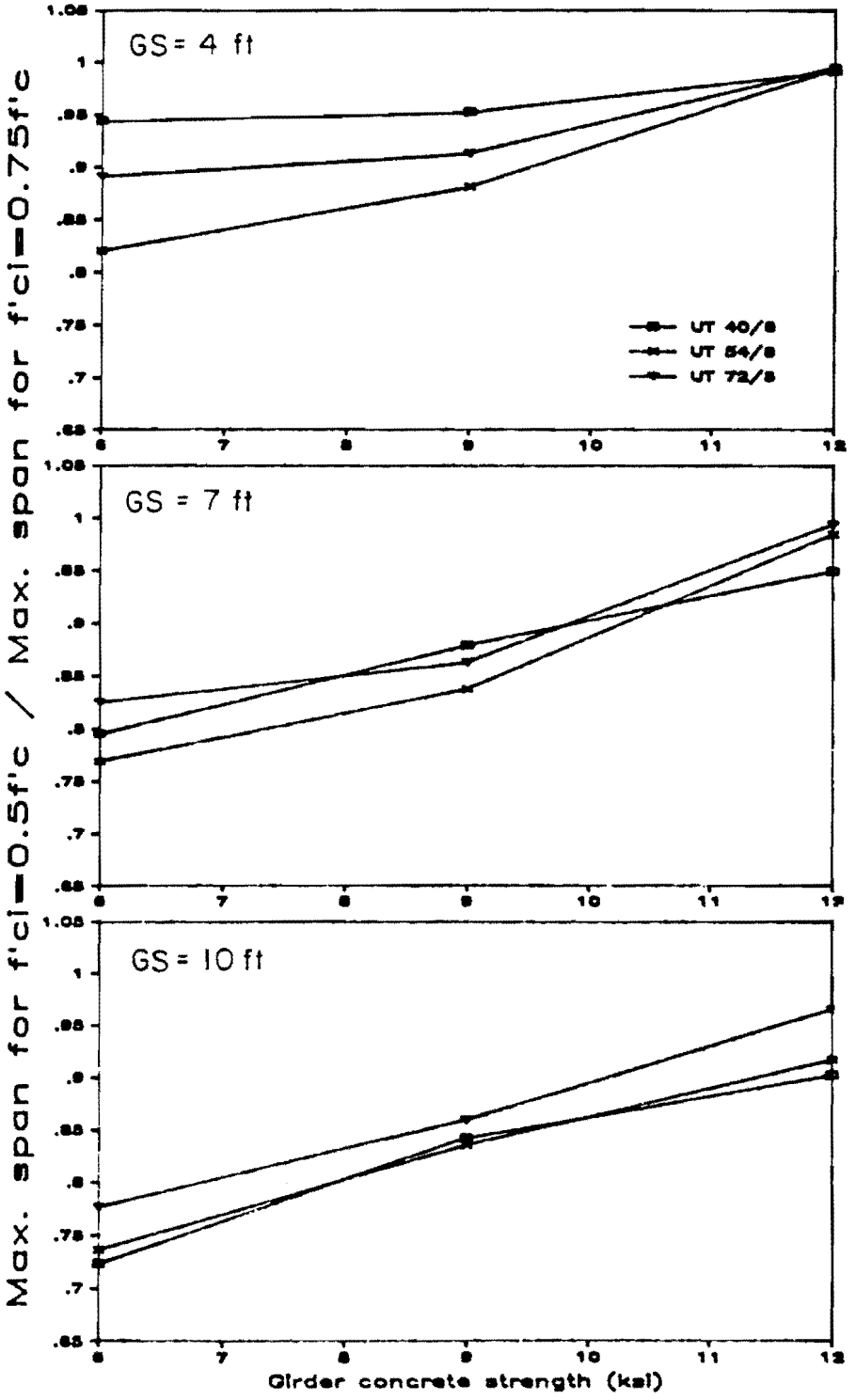

Fig. 3.34 Reduction in maximum spans due to lower concrete strength at release - proposed sections.

average in sensitivity when compared with other sections. Of the proposed sections, the 54-in. section was the most sensitive to reduction of the concrete strength at release. The proposed sections with the largest bottom flange area showed the least sensitivity for all concrete strengths and girder spacings. Therefore, if the use of lower release strengths is perceived as a major concern or advantage for using high strength concrete, a larger bottom flange could be added to the proposed sections to improve this aspect of behavior without greatly affecting other aspects. The use of closer girder spacings would also reduce the impact of lower release strengths. It should be noted that the reduced concrete strength at release would also result in a 5.8 percent reduction in the maximum lifting span.

3.4.5 Effect of Strand Size. Designs using 0.6-in. diameter strand are compared with those for 0.5-in. diameter strands in Fig. 3.35, 3.36, and 3.37 for the AASHTO-PCI Type IV girder. The maximum spans are shown in Fig. 3.35, the ratio of spans is plotted in Fig. 3.36, and the difference in spans is plotted in Fig. 3.37, with all quantities shown versus concrete strength. Spans in excess of the maximum lifting span are shown as dashed lines in Fig. 3.35. The effect of using the larger strand is minimal for lower concrete strengths but increases as the concrete strength increases. The effect also increases as girder spacing is widened. Because of the increased span lengths possible, especially for GS = 10 ft, stability would be a greater problem when 0.6-in. diameter strands are used.

For this study, the use of larger diameter strand appears beneficial only when high strength concrete is used, and only about a 10 percent (which corresponds to about 10 ft) increase in span results. The use of larger strand may also increase the required prestressing force to a level that exceeds the capacity of many prestressing beds. To illustrate, in order to obtain the 10 percent increase in span at GS = 10 ft and f'c = 12 ksi, 62 strands are needed with a maximum initial prestress force of approximately 2.9 million pounds. This force is greater than the capacity of any prestressing bed in Texas.

2.5 Summary and Conclusions

The following conclusions can be drawn from the study presented in this chapter:

1. The three proposed sections provide good alternatives to currently used sections. The proposed sections have similar span capabilities yet reduced section sizes when

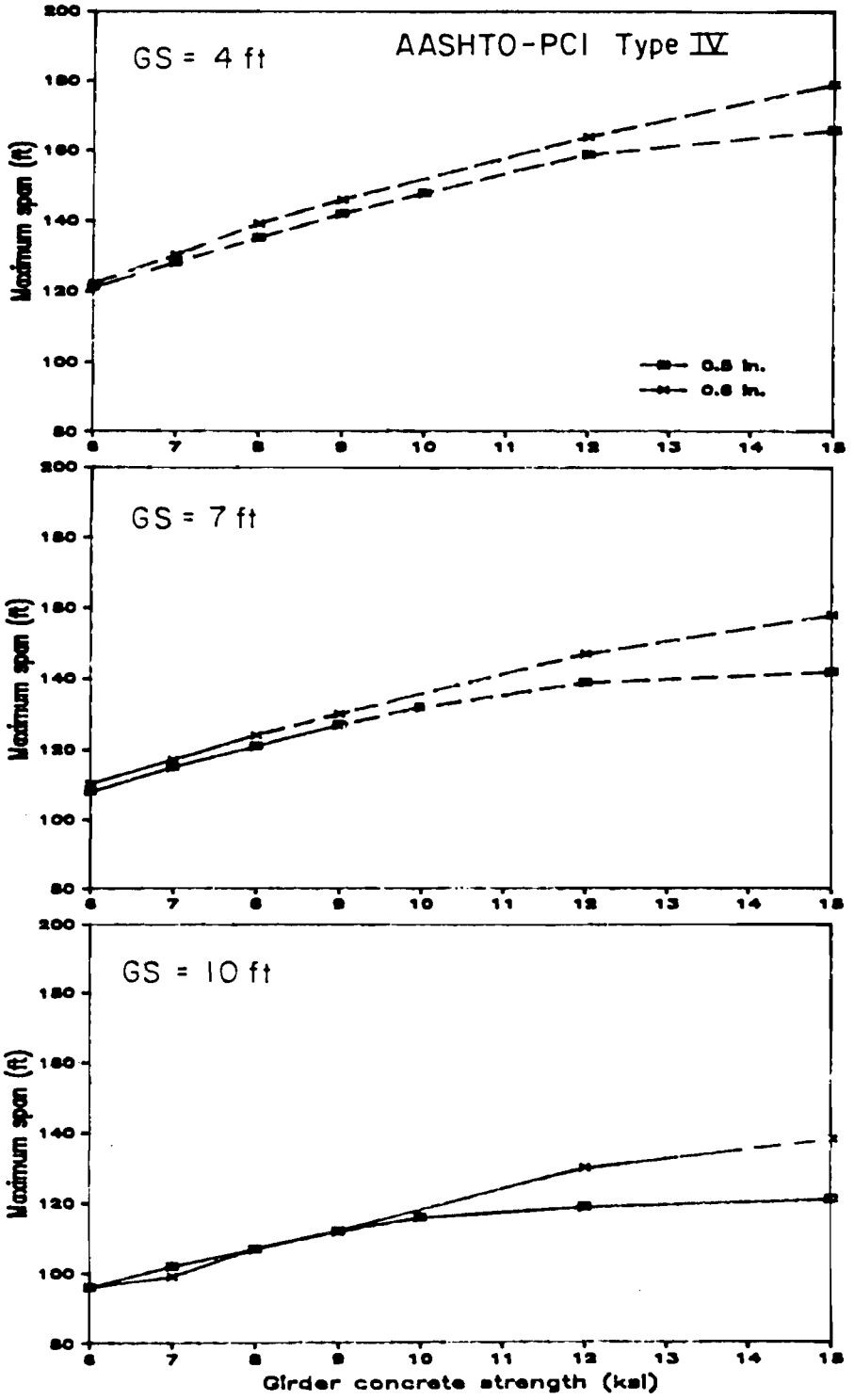

Fig. 3.35 Maximum span versus concrete strength for AASHTO-PCI Type IV with 0.5-in. and 0.6-in. diameter strand.

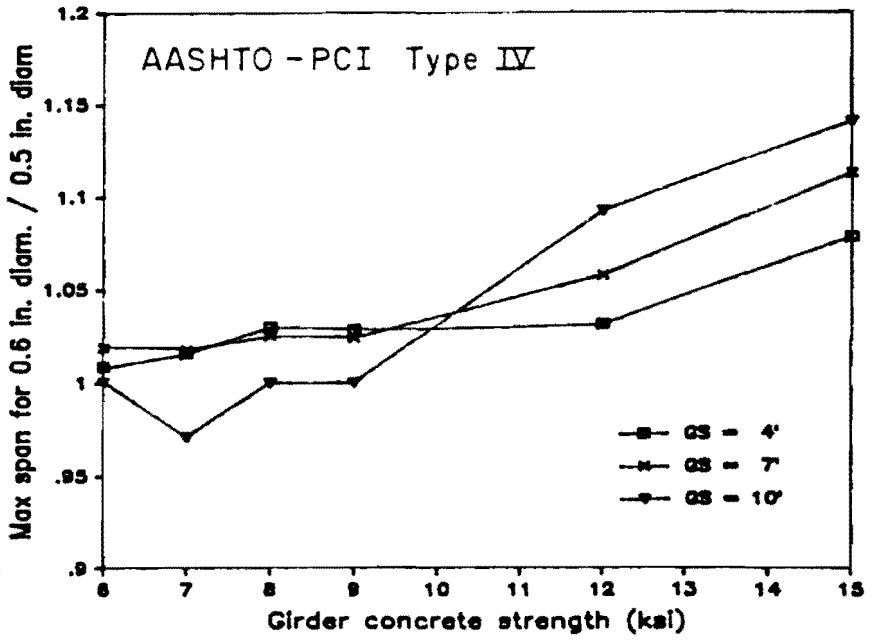

Fig. 3.36 Ratio of increase in maximum span with use of 0.6-in. diameter strand.

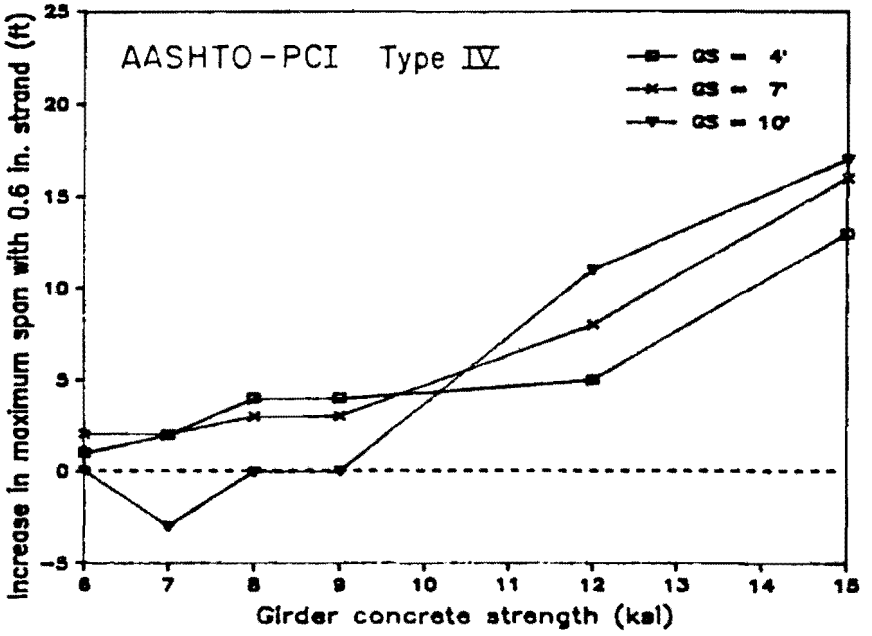

Fig. 3.37 Increase in maximum span with use of 0.6-in. diameter strand.

compared with sections of the same depth that are in current use in Texas. The proposed sections are slightly larger than bulb-tee sections of the same depth and have similar or improved span capabilities.

2. An increase in concrete strength allows an increase of 10 to 40 percent in maximum span for a given section, depending on girder spacing. However, certain practical limits must be considered, such as capacity of the prestressing bed, maximum lifting spans, and transportation of the member.

3. The maximum lifting span, which is intended to prevent lateral buckling of members when they are lifted, may severely limit the maximum span capacity of some sections. This limit is especially restrictive for 54 and 72-in. sections. In general, sections with greater weak axis moments of inertia were affected the least by these stability limitations. (The reader is referred to Sec. 4.7 for a more complete assessment of the lateral stability of these sections. This section indicates that further considerations may be required to determine the safety of a member with respect to lateral stability.)

4. Where increases in maximum spans mentioned above are limited by the maximum lifting span, special considerations may be available in the design or handling of the member to make possible the use of longer spans.

5. An increase in concrete strength can allow a significant increase in girder spacing for a given span, thus requiring fewer girders for a given structure. In some cases, the spacing can be more than doubled when high strength concrete is used.

6. Increasing concrete strength does not significantly reduce the number of strands required for a given span and girder spacing.

7. No simple measure of section efficiency appears to reflect the effect of all significant aspects of design. The comparison of actual designs is the best way to determine relative performance of different sections.

8. Some sections show marked reductions in maximum span capacity when the concrete strength at release is lowered. The section with a large bottom flange, however, showed the least span reduction when a reduced release strength was used.

9. The use of larger strands permits increased maximum spans if high strength concrete is used. Otherwise, no benefit is realized other than a reduction in the number of strands required for a design.

Therefore, high strength concrete can be best used in pretensioned bridge girders to provide a significant increase in span capacity (unless limited by stability considerations) or to reduce the required number of girders for a given span.

CHAPTER 4

EVALUATION OF TEST RESULTS AND CURRENT DESIGN PRACTICE

4.1 Introduction

In this chapter, results of the literature review of Chapter 2 and data gathered during the test programs are compared and evaluated with emphasis on the effect of high strength concrete on design. The organization parallels that of Chapter 3. Major sections conclude with a summary and recommendations where appropriate.

4.2 Flexural Design and Analysis

This section opens with a brief consideration of current allowable stresses for concrete. Two methods of flexural strength analysis of composite bridge members are then considered: the simplified approaches of the AASHTO [10] and ACI [15] Codes, and the strain-compatibility method. Details of the application of each method for use with high strength concrete will be presented. The methods will then be compared with the measured behavior of the long-span girder specimens. Finally, various aspects of flexural design will be investigated using a range of bridge designs. Conclusions will be made at the end of the major subsections.

4.2.1 Allowable Concrete Stresses. Limiting concrete stresses to the levels given in the codes is intended to provide good serviceability in structures by limiting cracking and preventing deterioration of the concrete due to fatigue. It has been reported that current stress limits in tension are appropriate for use with concrete that is cured in field conditions [99] and, although data is very limited, fatigue behavior of high strength concrete is expected to be comparable to that for lower strength concretes [22]. Therefore, current allowable concrete stresses appear appropriate for use with high strength concrete and should be used for design.

4.2.2 Simplified Strength Analysis Methods. This sub-section begins by considering the application of the current equivalent rectangular stress block (ERSB), as found in the ACI Code and AASHTO Specifications, to high strength concrete. Design of composite members with a normal-strength deck and high-strength girders, where the neutral axis is located below the deck, will then be considered.

Finally, AASHTO and ACI equations used to estimate strand stress at ultimate will be evaluated.

4.2.2.1 Stress Block Parameters. From the data presented in Chapter 2 and later in this chapter, the concrete stress block parameters in current use for high strength concrete appear sufficiently accurate and conservative for the prediction of the flexural strength of a section. These parameters include the stress block factor, β_1, the effective compression stress at ultimate, and the maximum usable strain in compression, ϵ_{cu}. The use of these parameters for computations other than the moment capacity may be less accurate, however. This is due to the fact that the ultimate compression strain may be less than the Code specified value of 0.003, as discussed in Ref. [139]. Ductility considerations are especially sensitive to inaccuracies in these parameters and will be discussed in a later section of this chapter.

4.2.2.2 Composite Design. Composite design using the simplified methods is straightforward when the compression zone at ultimate remains in the deck. However, if high strength concrete in the girder is also in compression at ultimate, the application of the analysis becomes dubious because of the different concrete strengths and stress block parameters. A similar situation would exist with light-weight concrete girders because of the different stress block parameters for light-weight and normal-weight concrete.

The analysis of flanged sections in which the neutral axis at ultimate is located below the deck, which will be referred to as "flanged section analysis", deducts the area of steel required to develop the overhanging flange from the total area of tension steel in order to obtain an area of steel for use in strength calculations. This type of analysis is not necessary for flexural strength calculations using the ACI ERSB but is included in the AASHTO equations.

Four possible approaches to representing composite cross-sections for strength analysis are illustrated in Fig. 4.1. Case I assumes that all concrete in the composite member has the strength of the deck. In Case II, the assumptions of the ERSB are applied to both the deck and girder concrete which requires the top of the girder as well as the deck to be at the maximum usable strain. While this condition is very unlikely, it could exist for composite sections in which a large difference in strain exists between the top of girder and bottom of deck, which generally occurs only in pretensioned girders. Therefore, this case is reasonable only for

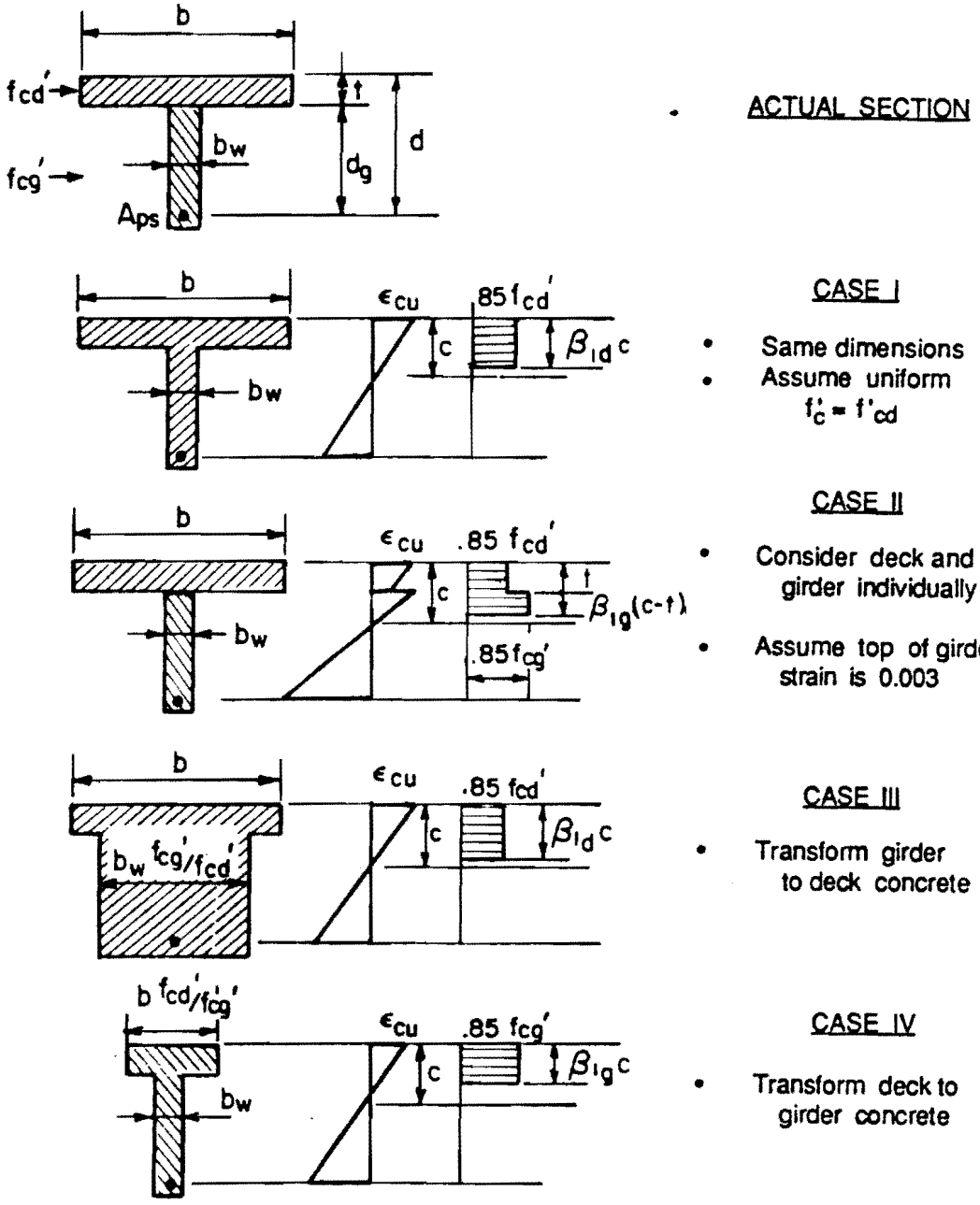

Fig. 4.1 Possible approaches to ultimate analysis of composite sections

composite sections with pretensioned girders. Cases III and IV transform the section by ratios of concrete strengths to obtain an equivalent section with a uniform concrete strength. Case III transforms the section to an equivalent section with concrete strength equal to the deck concrete strength while Case IV transforms the section to the girder concrete strength. All four approaches neglect actual differences in strain and curvature between the girder and deck.

The approaches represented by Cases I, III, and IV can be used with the flexural strength equations given in the AASHTO Specifications while all cases can be used with the ACI ERSB approach. However, the current code flanged section analysis will give different results for Case II. The flanged section analysis approach is used in both codes to compute the reinforcement index to be compared with the maximum reinforcement limit. The major difference between AASHTO and ACI estimates of the flexural strength for a given case results from different estimates of the strand stress at ultimate. Therefore, only Case I will be shown for AASHTO in the following studies, since the ACI strand stress equation is considered to be superior, as discussed in the following section.

Strand stress at ultimate is not affected by the different cases when computed using either the AASHTO or ACI equations. Therefore, for a given section and steel content, the total compression force is the same for all cases. Expressions for the depth of the equivalent stress block and the depth to the neutral axis are derived in Table 4.1 for each case. These can be reduced to a common form by recognizing a common term, designated a_g^*, which represents the depth of the compression block in the girder. This depth of the compression block in the girder is the same for Cases II, III, and IV and is related to the depth for Case I by the ratio of concrete strengths.

The variation in the total depth to the neutral axis, c, versus the term a_g^* for a composite section with the same deck thickness as used for the specimens is shown in Fig. 4.2. Also shown are data points for the specimens, which were determined using strand stresses corresponding to measured strand strains and the location of the neutral axis computed from girder strains. This demonstrates that the neutral axis depth computed using Cases II, III, and IV are similar while those computed using Case I are similar for small depths of compression but diverge from the other cases with increasing depth of compression and increasing difference between deck and girder concrete strengths. Specimen 2 falls among the lines representing

Table 4.1 Derivations of Stress Block Dimensions for Composite Design

CASE I: Nominal dimensions; deck concrete strength

$$C = A_{ps}f_{ps} = 0.85f_{cd}'[b-b_w)t+b_wa]$$

$$a = na^*_g+t = [(A_{ps}f_{ps} - bt0.85f_{cd}')/(b_w0.85f_{cd}')]+t$$

$$c = a/\beta_{id} = (na^*_g+t)/\beta_{id}$$

CASE II: Nominal dimensions; deck and girder concrete strengths

$$C = A_{ps}f/_{ps} = bt0.85f_{cd}'+b_wa0.85f_{cg}'$$

$$a = a^*_g+t = [(A_{ps}f_{ps} - bt0.85f_{cd}')/(b_w0.85f_{cg}')]+t$$

$$c = t+(a-t)/\beta_{1g} = a^*_g/\beta_{1g}+t$$

CASE III: Transformed dimensions; deck concrete strength

$$C = A_{ps}f_{ps} = 0.85f_{cd}[(b-nb_w)t+nb_wa]$$

$$a = a^*_g+t = [(A_{ps}f_{ps} - bt0.85f_{cd}')/(b_w0.85f_{cg}')]+t$$

$$c = a/\beta_{1d} = (a^*_g+t)/\beta_{1d}$$

CASE IV: Transformed dimensions; girder concrete strength

$$C = A_{ps}f_{ps} = 0.85f_{cd}'[(b/n-b_w)t+b_wa]$$

$$a = a^*_g+t = [(A_{ps}f_{ps} - bt0.85f_{cd})/(b_w0.85f_{cg}')]+t$$

$$c = a/\beta_{1g} = (a^*_g+t)/\beta_{1g}$$

Common terms: $a^*_g = [(A_{ps}f_{ps}-bt0.85f_{cd}')/(b_w0.85f_{cg}')]$

$n = f_{cg}'/f_{cd}'$

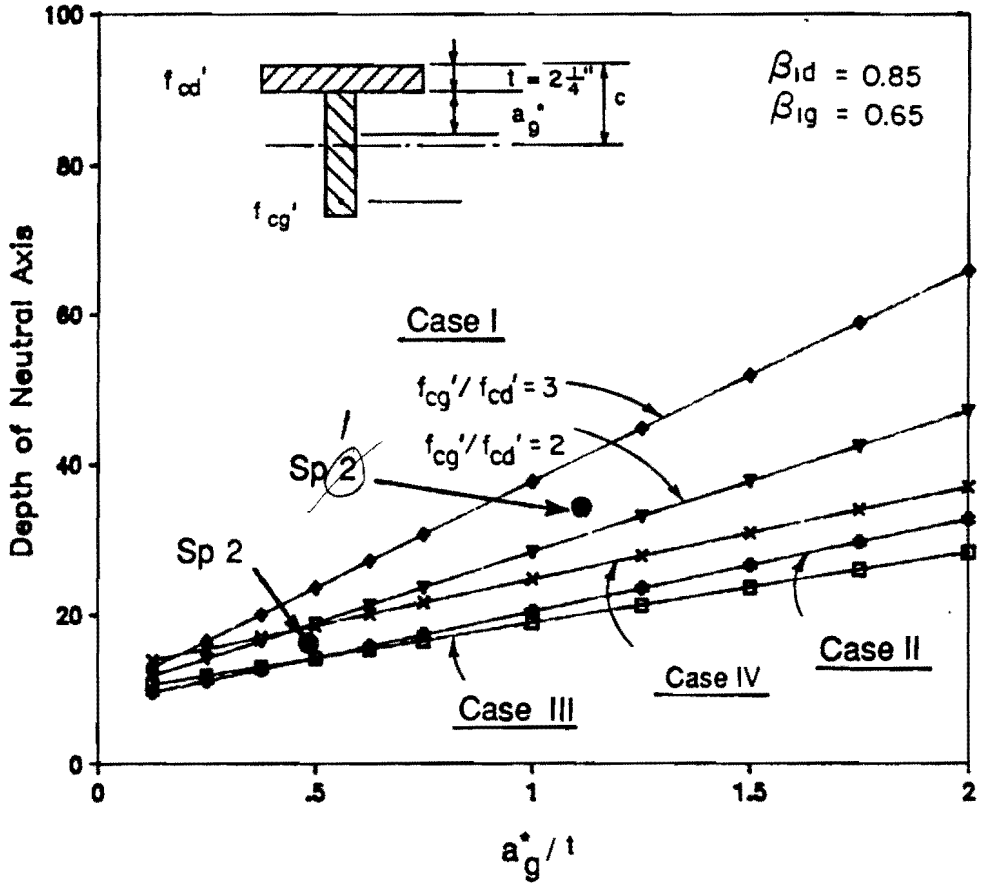

Fig. 4.2 Depth of neutral axis versus depth of compression block for specimens and composite analysis

Cases II, III, and IV, while Specimen 1 falls closest to Case 1. This shows that these Cases II, III, and IV give reasonable estimates for the location of the neutral axis for Specimen 2 while Case I overestimates the depth to the neutral axis for Specimen 1 where the difference between girder and deck concrete strengths is large. It can also be shown that the moment capacity computed using the four cases will be identical if the deck is considered separately for Case II rather than using the flanged section analysis found in the current codes. However, as discussed in the section concerning ductility which follows, the cases provide significantly different measures of ductility.

When some combinations of dimensions and concrete strengths are used with Cases III and IV, the deck width of the transformed section will be less than the width of the top of girder. While use of the current flanged section analysis in this situation results in a negative area of steel required to develop the flange, results are consistent and the situation should not be alarming.

4.2.2.3 Strand Stress at Ultimate. The current equation for estimating stress in bonded prestressing strands at ultimate is based on the observation that stress at ultimate is roughly related to the depth of the neutral axis which is proportional to a term similar to the reinforcement index. No derivation for the form of the equation was found in the literature. The equation was apparently calibrated using test data and was intended for use with rectangular sections. However, as demonstrated by Mattock [84], the original equation and the modified form which now appears in the ACI Code work remarkably well. Mattock also investigated the use of the modified equation for a single series of monolithic T-beams and found that, while the equation becomes unconservative when the neutral axis is located below the bottom of the flange, the maximum reinforcement limit terminates use of the equation before the stress becomes excessively unconservative. However, for the full range of T-beam designs considered, the nominal moment strength computed using the modified equation agreed very well with results of a compatibility analysis. Therefore, he concludes that

> it would be reasonable to use the proposed modified Eq. (18-3) to calculate the stress at nominal moment strength in the prestressed reinforcement of T-beams of normally encountered proportions, providing that the limit of $0.36\beta_1$ on the reinforcement index is observed.

The use of this equation for composite members will be examined further when results of strain compatibility analyses are considered later in this section.

Since the equation includes the concrete strength and, in its modified form, the stress block parameter β_1, its application to a composite section where the compression zone extends below the bottom of the flange is unclear where the concrete strength of the girder and deck differ significantly. Since it appears to be the most reasonable approach, the concrete strength of the deck and its corresponding β_1 value will be used in the equation. This interpretation will be used in the analyses that follow.

4.2.2.4 Summary. The preceding discussion of the use of the simplified methods given in AASHTO and ACI for computing the flexural strength of composite sections can be summarized as follows.

1. Based on available data, the stress block parameters currently used for high strength concrete in the ACI ERSB flexural strength calculations are appropriate. Four possible approaches for determining flexural strength of composite members using the simplified AASHTO and ACI methods are presented.

2. The major difference in estimates of flexural strength using the AASHTO equation and the ACI ERSB is due to different estimates of strand stress at ultimate.

3. Deck concrete strength and effective width should be used for the computation of strand stress at ultimate using either the AASHTO or ACI equations.

4. The computed negative area of steel that results from a flanged section analysis using transformed sections is not in error and provides correct overall results.

4.2.3 Strain Compatibility Method. Analytical representations of concrete and steel stress-strain curves are compared with measured properties from specimen tests. General stress-strain curves are presented for use in the strain compatibility analysis. Details of the analysis are then presented.

4.2.3.1 Concrete Stress-Strain Relationships. In order to develop a successful strain compatibility model for member behavior, stress-strain behavior of the concrete must be accurately modelled.

Figures 4.3 and 4.4 show stress-strain curves from cylinder tests of deck concrete at the time of the flexure test and compare these curves with those predicted by Burns [34] and Carriera and Chu [37] using measured and estimated values for the modulus, and strain at maximum stress. These two analytical stress-strain curves were selected for comparison because they are continuous equations that provide reasonable agreement with the data. Both predictive equations do well when the measured modulus and strain are used (Fig. 4.3a and 4.4a). Agreement is not as good when estimated values are used for the modulus and strain at maximum stress. Burns' equation becomes poor for higher strains but it was not intended to be used in this range. The same type of plots are presented in Fig. 4.5 and 4.6 for the high strength girder concrete. The equation by Carriera and Chu provides very good agreement for both the ascending and descending branches of the curve when both measured and estimated values are used for the modulus and strain at maximum stress. The equation by Carriera and Chu may be used for both normal and high strength concrete when strains beyond ϵ_0 will be considered in analysis. However, the equation should be used with caution because, if the term $f'_c/(E_c\epsilon_0)$ in the definition of the parameter β closely approaches or exceeds 1, the equation produces unsatisfactory results.

For a simplified analysis where strains are not expected to greatly exceed the strain at maximum stress, a bilinear approximation to the curve as shown will give satisfactory results for high strength concrete. This bilinear relationship is the same as the Jensen stress block without the β factor which is used to determine the ultimate strain.

For the strain compatibility analyses that follow, a modified form of Burns' equation is used for the deck concrete because the analysis is simplified by a closed-form solution for the integral of the area and the location of the centroid of the area. The stress-strain curve is modified by using a linear descending branch that begins at maximum stress and closely matches the measured descending branch of the curve. A bilinear stress block will be used to approximate the high strength girder concrete stress-strain curve for the specimens. The measured and analytical stress-strain curves for the concrete in the specimens at the time of the flexure tests are shown in Fig. 4.7 and the parameters defining the curves are given in Table 4.2.

For the general analyses discussed later in this chapter, a deck strength of 4 ksi will be used. The same type of modified

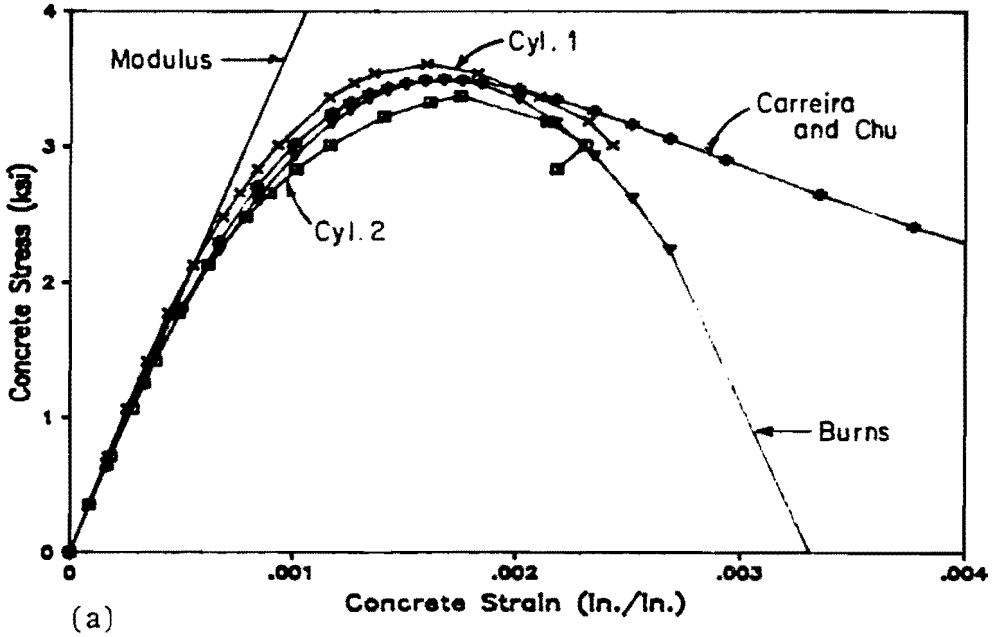

(a)

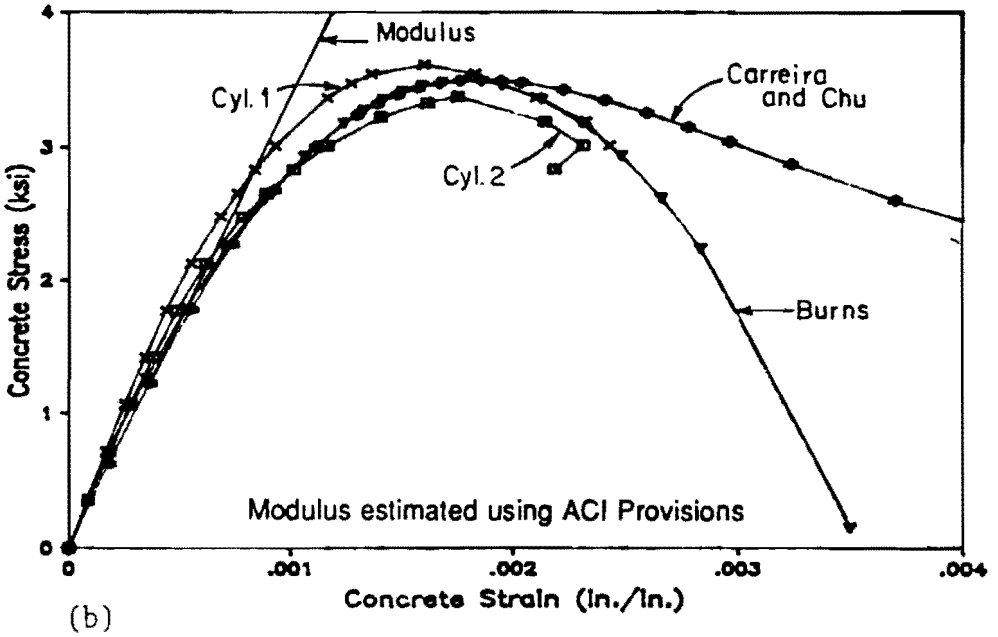

(b)

Fig. 4.3 Measured and analytical stress-strain curves for deck concrete - Specimen 1: a) Using measured E_c and ϵ_0; b) Using estimated E_c and ϵ_0

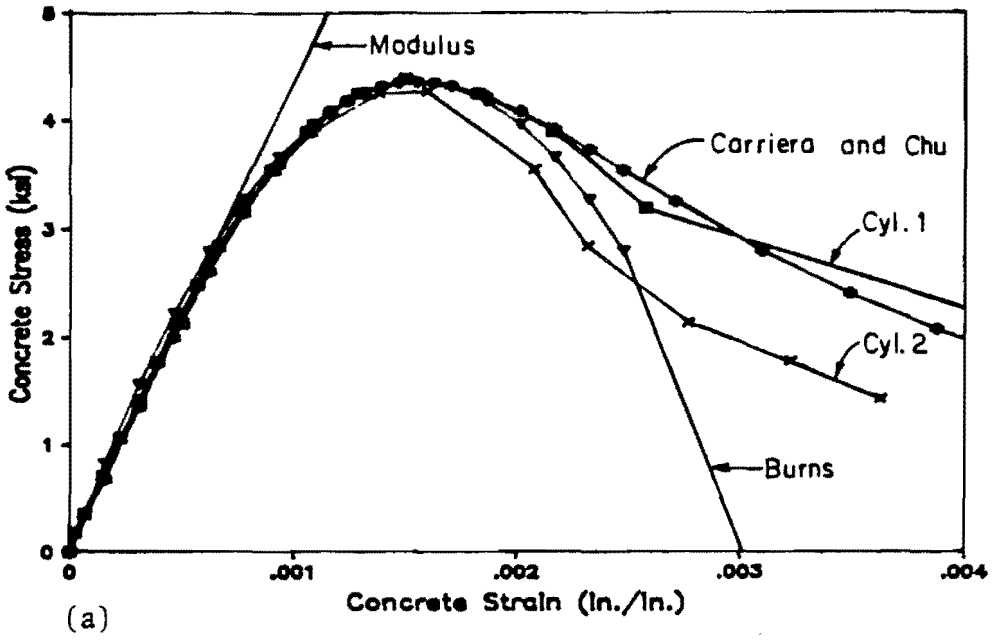

(a)

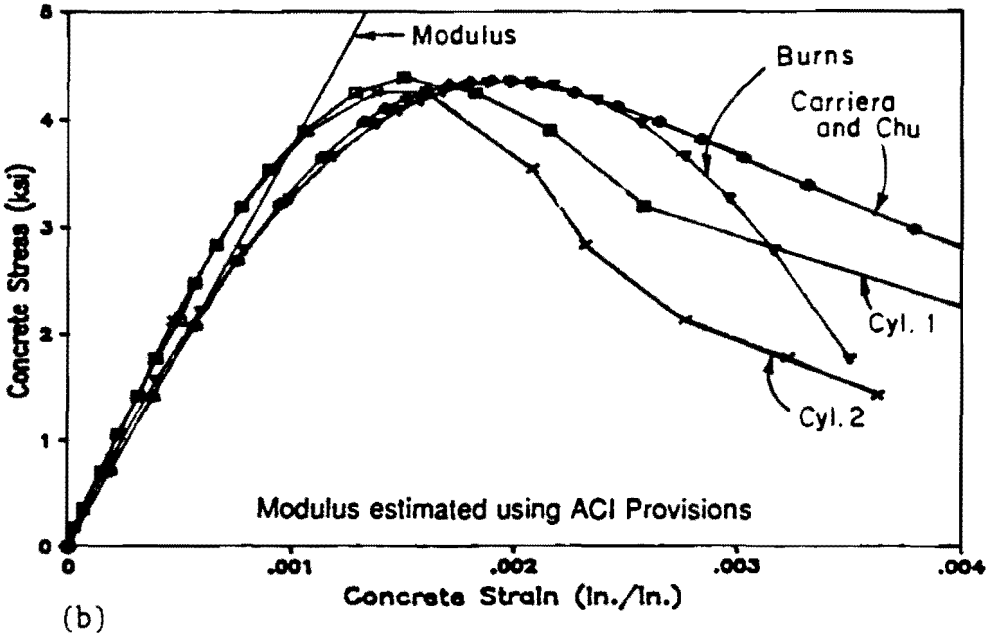

(b)

Fig. 4.4 Measured and analytical stress-strain curves for deck concrete - Specimen 2: a) Using measured E_c and ϵ_c; b) Using estimated E_c and ϵ_c

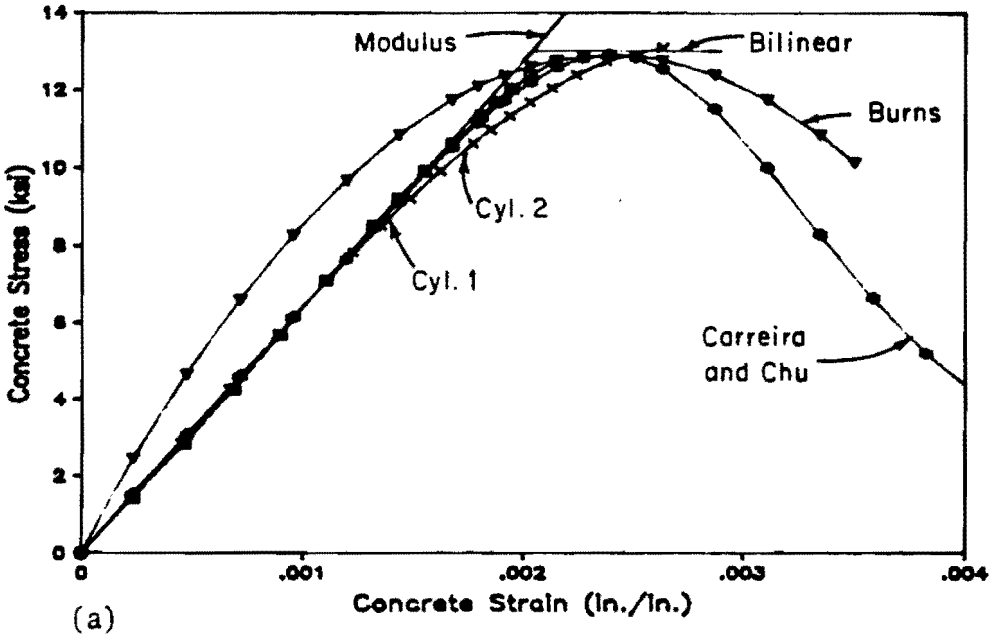

(a)

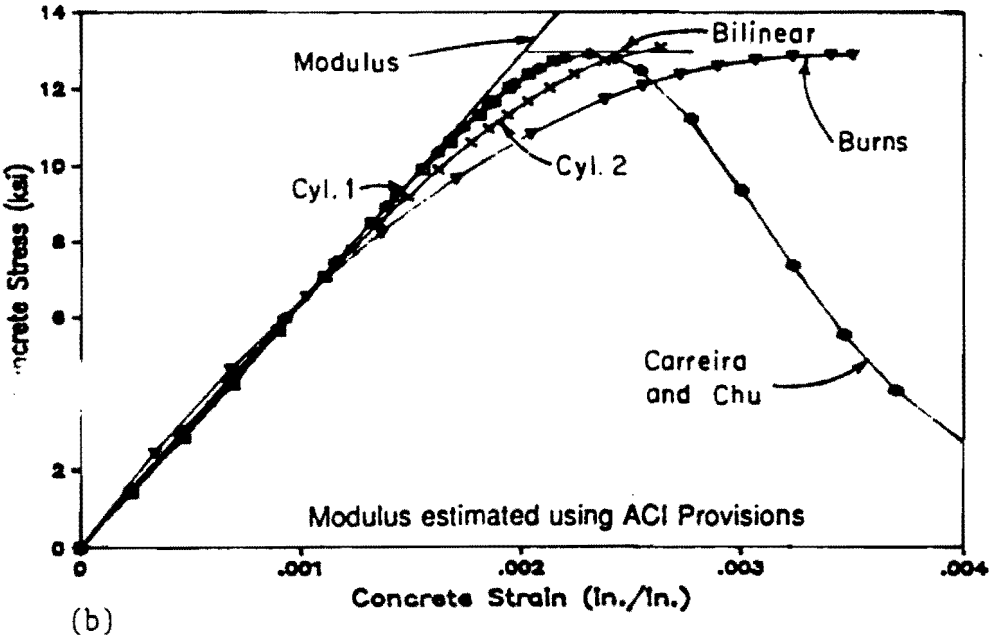

(b)

Fig. 4.5 Measured and analytical stress-strain curves for girder concrete - Specimen 1: a) Using measured E_c and ϵ_c; b) Using estimated E_c and ϵ_c

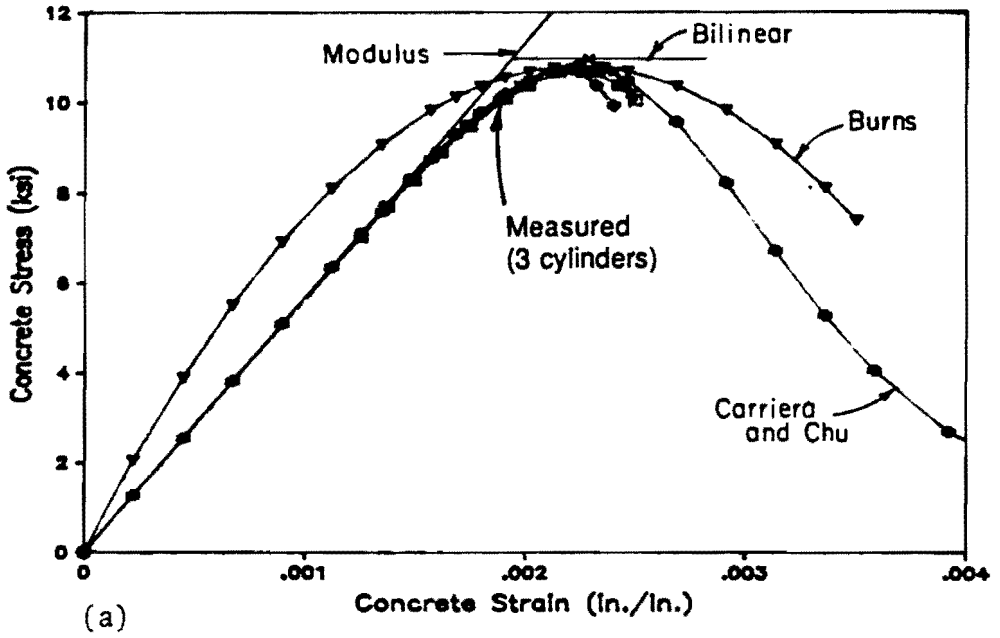

(a)

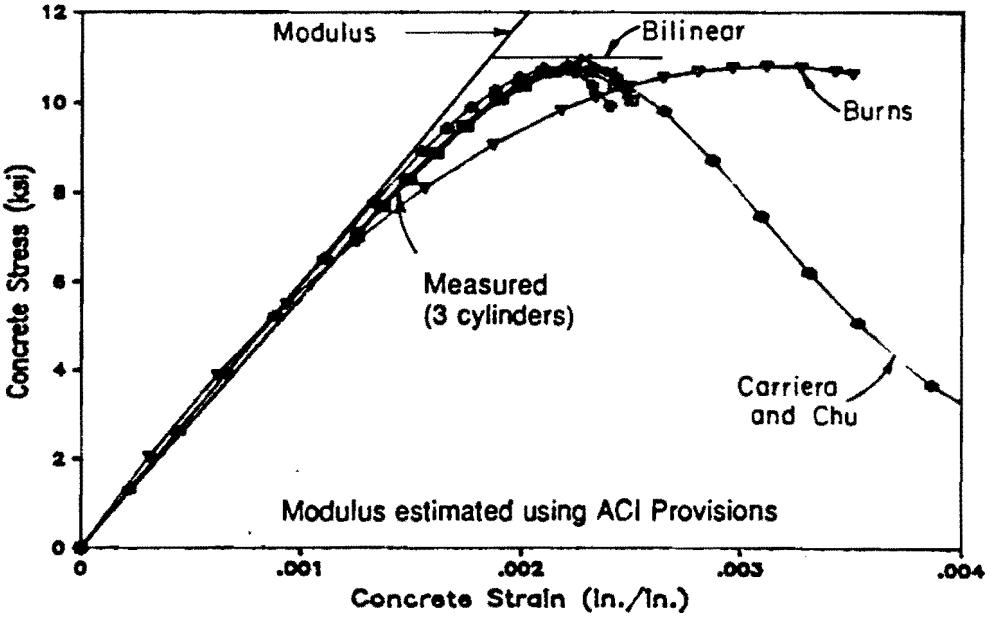

(b)

Fig. 4.6 Measured and analytical stress-strain curves for girder concrete - Specimen 2: a) Using measured E_c and ϵ_c; b) Using estimated E_c and ϵ_c

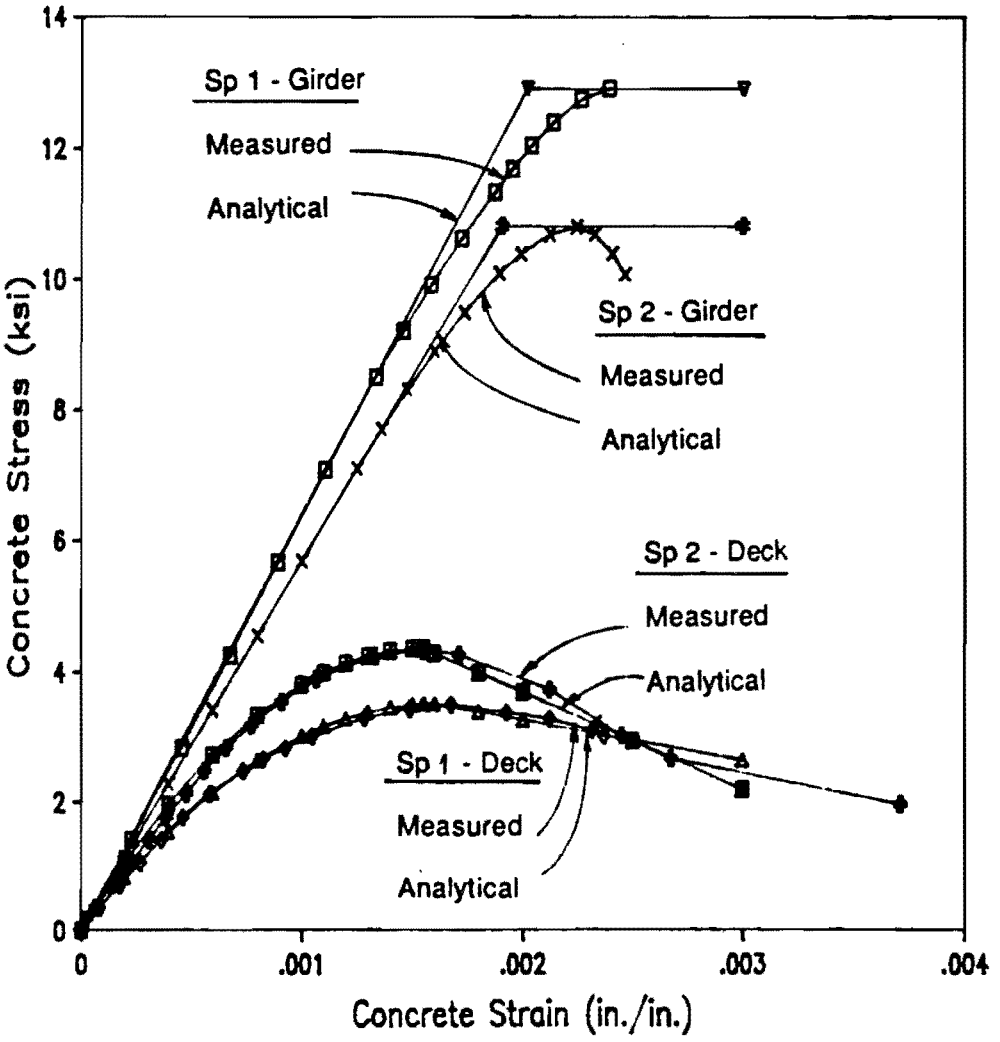

Fig. 4.7 Comparison of average measured and analytical concrete stress-strain curves for Specimens 1 and 2

Table 4.2 Parameters for Analytical Stress-Strain Curves for Concrete

	f_c'	E_c	ϵ_0	Slope
	(ksi)	(ksi)	(in/in)	(ksi)
Specimen 1				
Girder	12.90	6,400		
Deck	3.50	3,800	0.001600	-625
Specimen 2				
Girder	10.80	5,675		
Deck	4.35	4,370	0.001550	-1,500
General Analyses				
Girder	12.00	6,244		
Girder	9.00	5,407		
Girder	6.00	4,415		
Deck	4.00	3,605	0.001600	-1,060

$E_c = 57{,}000\sqrt{f'_c}$ (psi)

Table 4.3 Parameters for Analytical Stress-Strain Curves for Strand

		Specimens	General Analyses	
		LL Strand	LL Strand	SR Strand
E_c	(ksi)	28,400	28,000	28,000
f_{py}	(ksi)	267.10	243.00	229.50
ϵ_y	(in./in.)	0.0100	0.0100	0.0100
f_{pu}	(ksi)	284.00	270.00	270.00
ϵ_{pu}	(in./in.)	0.0547	0.0350	0.0350
N		16.000	6.440	4.510
K		1.0573	1.0800	1.1150
Q		0.001255	0.010536	0.019483

LL = Low relaxation (Low Lax)
SR = Stress-relieved

stress-strain curve will be used for the deck as discussed above with the strain at maximum stress approximately equal to that measured for the specimen concrete, and a descending branch slope equal to the average for the two specimens. For the girder, three concrete strengths will be used and the stress-strain curves will be modelled using the bilinear relationship discussed above. The bilinear approximation will not be as accurate for the lower concrete strengths but will still give a reasonable estimate of section capacity and rotations. Stress-strain curves for the general analyses are shown in Fig. 4.8 with the corresponding parameters given in Table 4.2.

4.2.3.2 Strand Stress-Strain Relationships. Strand stress-strain curves will be defined using the Menegotto and Pinto equation [95] (see Fig. 2.17). Coefficients were developed by trial and error to match the strand used in the specimens and to model strand behavior for stress-relieved and low relaxation strands that satisfy minimum requirements. Figure 4.9 shows the excellent agreement between measured and analytical stress-strain behavior for the strand used in the specimens, and Fig. 4.10 shows stress-strain curves satisfying minimum requirements. The coefficients used to produce the curves are given in Table 4.3.

4.2.3.3 Details of Analysis. A computer program (MOMCURV) was developed to analyze the uncracked, cracked and ultimate behavior of a composite section. The concrete and strand stresses at full dead load conditions serve as the starting point of the analysis. These initial conditions are used to determine differences in strain and curvature between the girder and deck which remain constant throughout the loading of the section. Uncracked behavior is computed using elastic properties and includes the effect of the increase in strand stress that occurs with added load. For cracked section analysis, an iterative technique employing the stress-strain relationships described above is used to establish equilibrium for different levels of strain in the top fiber of the deck. For each value of top fiber strain, the corresponding moment, concrete and strand stresses and strains, curvatures, and location of the neutral axis are determined. The ultimate capacity of the section is defined either by the maximum moment resisted by the section or by the moment reached at a limiting strain in the top of the deck.

A more complete discussion of the program MOMCURV, with sample input and output, is given in Ref. [140].

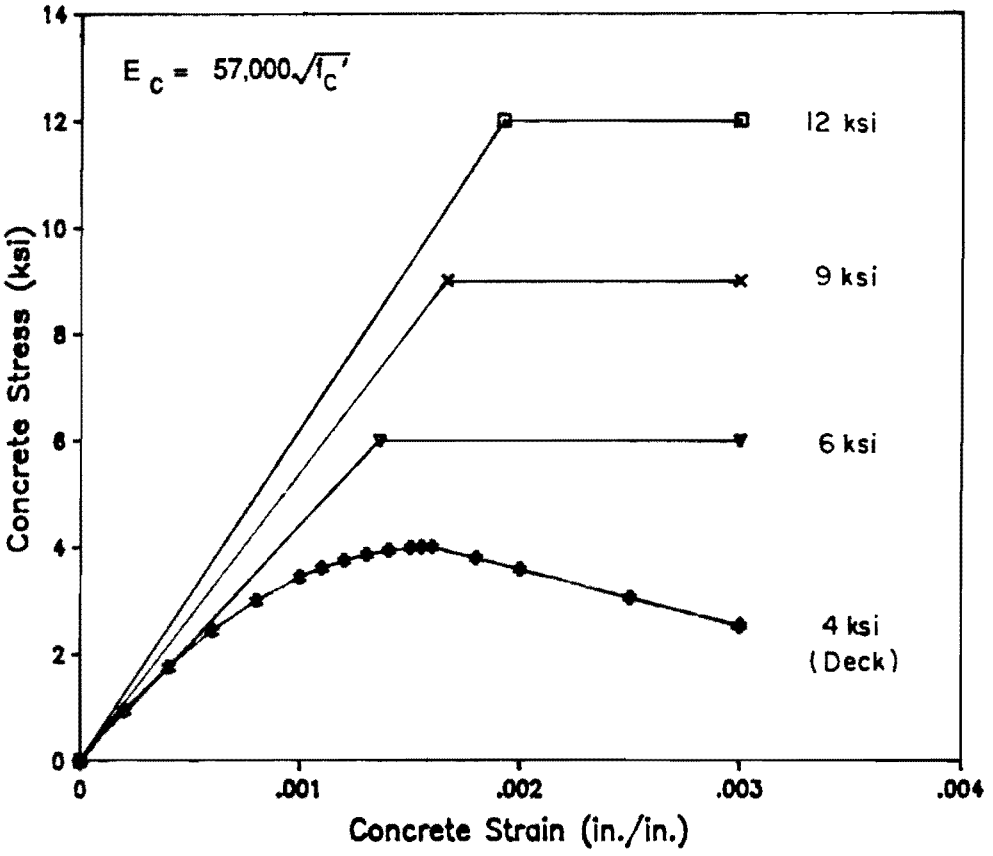

Fig. 4.8 Analytical concrete stress-strain curves for general analyses

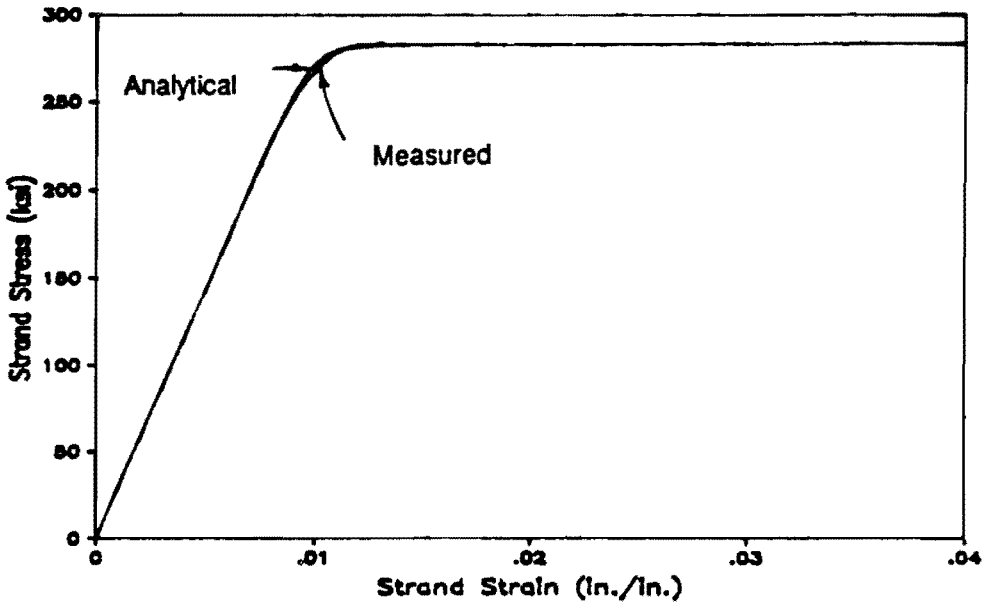

Fig. 4.9 Measured and analytical strand stress-strain curves for Specimens 1 and 2

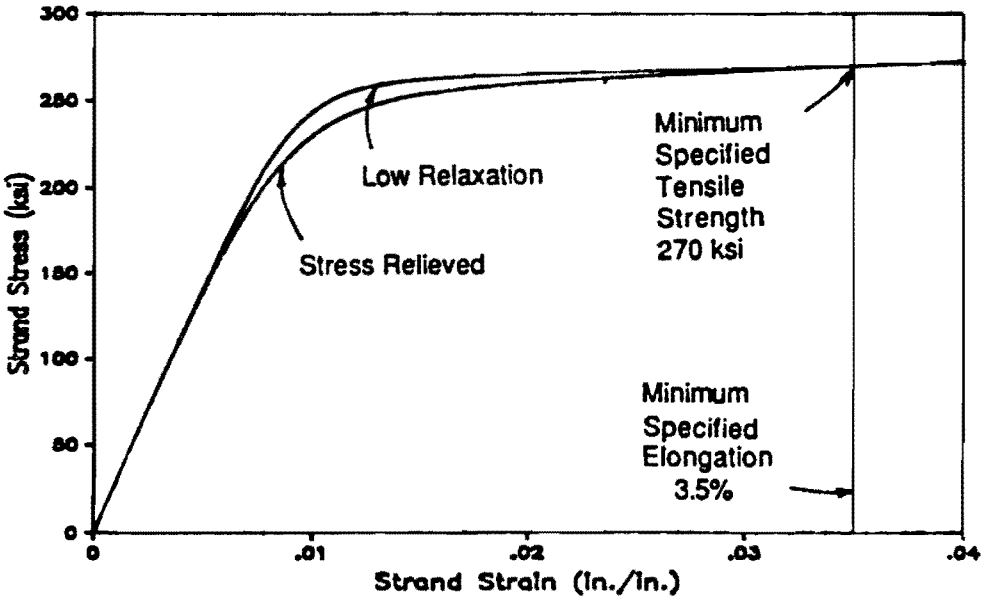

Fig. 4.10 Analytical strand stress-strain curves for general analyses

Load-deflection behavior was obtained using a semi-manual process. The moment-curvature relationship was obtained at 2-ft intervals along half of the specimen using the strain-compatibility program. The effective prestress was assumed to vary linearly from the drape points to the ends with a constant prestress between drape points. A computer spreadsheet program was then used to compute the moments at selected load stages at the intervals along the span, to interpolate between values input from the moment-curvature relationship, and to determine the deflection at midspan using moment-area principles. For Specimen 1, concrete stresses were allowed to reach $7.5\sqrt{f'_c}$. before cracked section analysis results were used at a given location. Since Specimen 2 had well distributed cracks due to shrinkage, cracked section analysis results were used at a given location when tension developed in the bottom fiber. After the maximum moment was reached at midspan, the entire constant moment region was assumed to following the descending portion of the moment-curvature curve. This led to slightly larger curvatures at the load point than at midspan for loads beyond maximum, which would result in a very small increase in midspan deflections. A slightly better estimate might have been to use the curvature computed at midspan for the entire region between load points after maximum moment was reached.

4.2.3.4 Summary. The following is a summary of the preceding discussion regarding aspects of the strain compatibility analysis:

1. The equation by Carriera and Chu appears to be the best mathematical representation of the concrete stress-strain curve for all concrete strengths.

2. The stress-strain curve for high strength concrete can be adequately modelled by a bilinear curve using the modulus and cylinder strength.

3. A modified form of the stress-strain curve used by Burns provides a good approximation of the stress-strain curve for normal strength concrete.

4. Mathematical estimates of stress-strain curves are improved if measured rather than estimated values for the modulus and strain at maximum stress are used.

5. The strand stress-strain curve developed by Menegotto and Pinto provided excellent agreement with the measured strand stress-strain curve. Using a trial and error process, coefficients for the equation were determined for the strand used in the specimens and for strand meeting the minimum requirements of the ASTM specification.

6. The strain compatibility analysis used in this study is presented. A computer program MOMCURV was developed to perform this analysis.

7. Load-deflection behavior can be determined using MOMCURV results and a semi-manual integration process.

4.2.4 Prediction of Test Results. This section first compares measured specimen behavior as load was applied to that predicted by the strain compatibility analysis. The measured or computed conditions at ultimate are then compared with those predicted by the strain compatibility analysis and the simplified methods of the ACI Code [15] and the AASHTO Specifications [10]. Conclusions regarding the accuracy of the predictive methods as compared with this set of test data close the section.

4.2.4.1 Behavior with Increasing Load. Load-deflection curves for both specimens are shown in Fig. 4.11. The predicted curves are close to the measured curves although the analytical curve for Specimen 1 lies below the measured curve. The difference between curves could indicate that the effective prestress at midspan or along the span was actually higher than assumed in the analysis. By a trial and error process, effective stresses of 185 ksi at midspan and 160 ksi at the ends were found to produce very close agreement between measured and computed member behavior. Load-deflection curves for the original analysis and the second analysis using increased effective stresses are compared with the measured curve in Fig. 4.12. Agreement for other aspects of behavior was good as well. However, this level of prestress is roughly equivalent to the initial tension placed on the strands in the prestressing bed which would leave no allowance for losses. Therefore, such a high stress appears unreasonable. An increase in the cracking stress, which was measured to be approximately $9\sqrt{f'_c}$ would also tend to extend the linear portion of the load-deflection behavior of the specimen in the analysis. It is possible that other factors could be modified to produce better results as well.

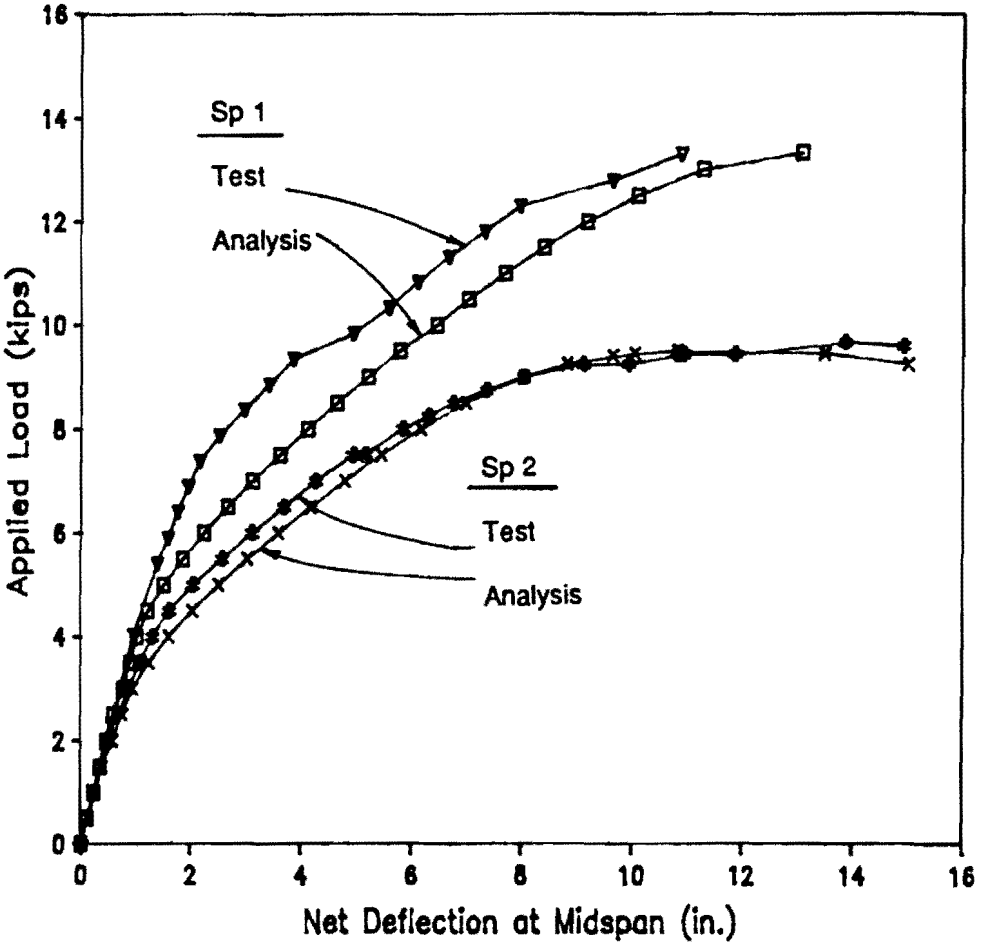

Fig. 4.11 Measured and predicted load-deflection curves during flexure tests.

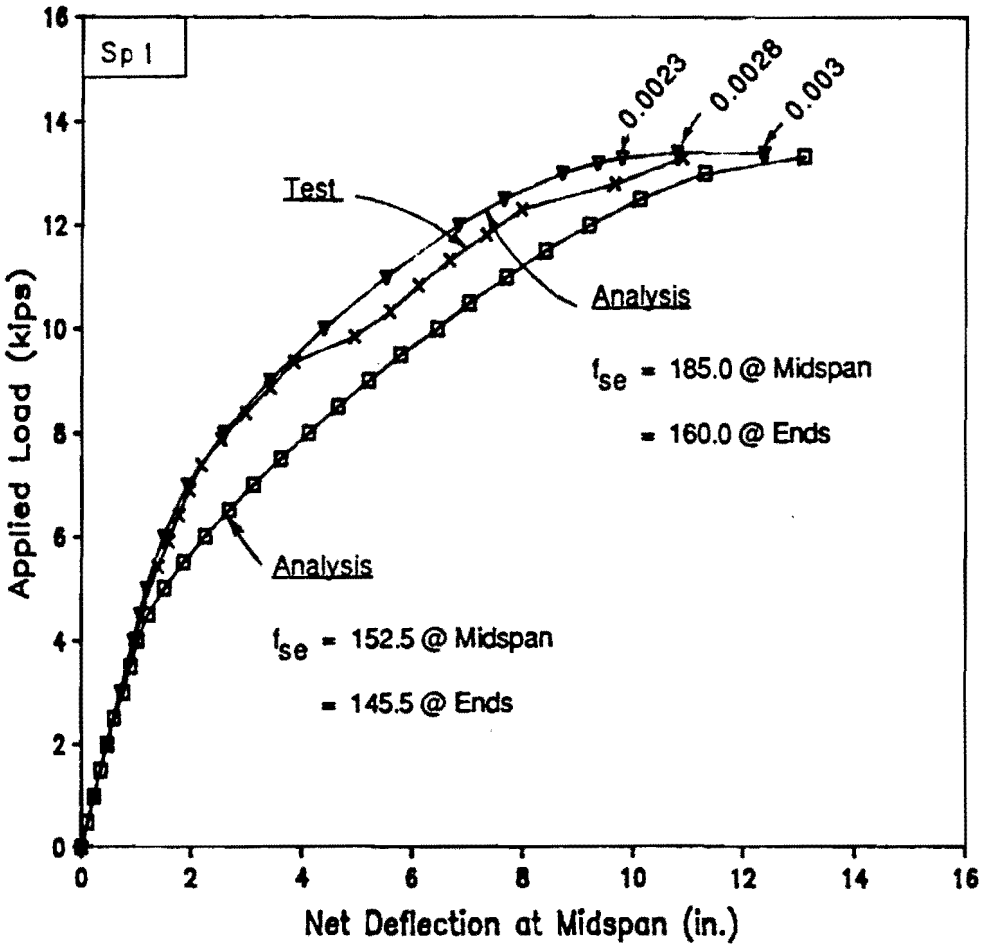

Fig. 4.12 Comparison of measured and predicted load-deflection curves during flexure test for Specimen 1 using revised effective prestress

The shape of the calculated load-deflection curves are very similar to those measured in the tests, differing by an offset after cracking that remained fairly constant for the remainder of the test. Aspects of behavior such as stiffness before and after cracking and the extent of the yield plateau prior to failure are quite similar for the predicted and observed response. As considered below in greater detail, the ultimate capacity of the member is also accurately determined. Discontinuities in the test data were a result of reloading the member after maintaining the deflection for long periods during the test, and should not be considered as part of the short-term deflection curve. The short-term deflection of other members should therefore be reasonably estimated using the method, described above with cracking at $7.5\sqrt{f_c'}$ assumed.

Figures 4.13 and 4.14 show the increase in strand strain and stress, respectively, with load during the flexure tests. Agreement is good, although again, it appears that the prestress or cracking stress may be underestimated for both specimens since the analytical curves depart from their initial tangent earlier than the test data. The similarity between member behavior, as indicated in the load-deflection response, and section behavior, as reflected in this and other load-strain relationships, indicate that assumptions regarding member and section properties and behavior appear consistent. Use of analytical curves, which assume cracking to occur at a stress of $7.5\sqrt{f_c'}$, to determine strand stresses during the tests appears reasonable.

The variation in top-of-girder and top-of-deck strains with increasing load are shown in Fig. 4.15 and 4.16, respectively. The predicted curves in Fig. 4.15 are terminated at a strain of 0.003 at the top of the deck. Curves are again similar to experimental curves which are slightly stiffer than predicted curves. It is interesting that the measured and predicted girder strains for Specimen 2 were similar up to nearly the maximum load where the analytical curve began to "yield" while strains measured in the test failed to increase.

The crack height computed using selected strain gage data compares favorably with that from the analysis, especially at loads near failure, as shown in Fig. 4.17. Curvatures computed using the same strain gage data are compared with those from analysis in Fig. 4.18. Slopes of the curvature curves are similar to the test data, although cracking appears early as in other curves. The curves differ significantly at failure with the analytical curves exhibiting a longer yield plateau than the test data. This indicates that failure occurred prior to reaching a top fiber strain of 0.003 in the

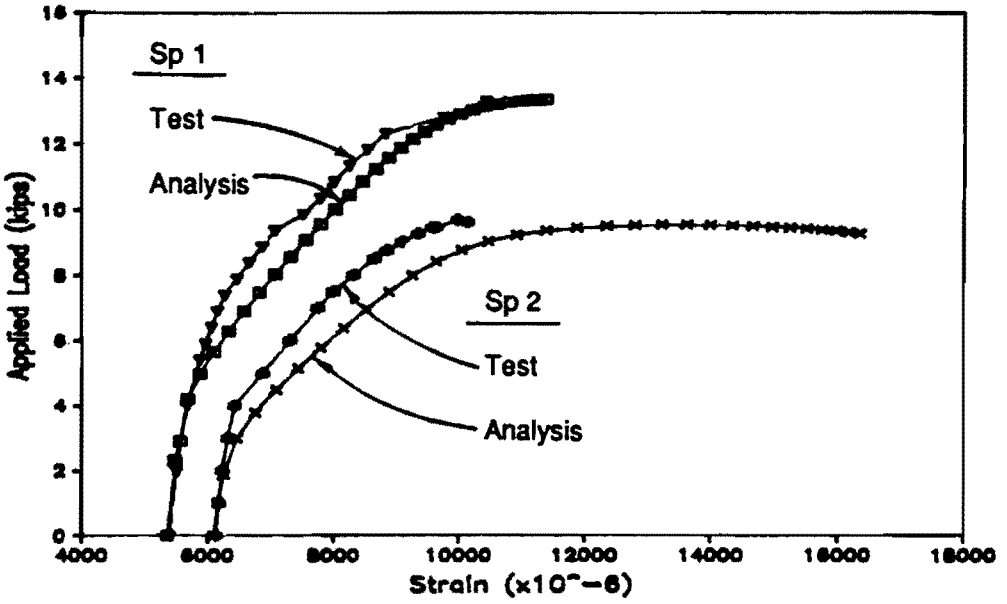

Fig. 4.13 Comparison of measured and predicted strand strains during flexure tests

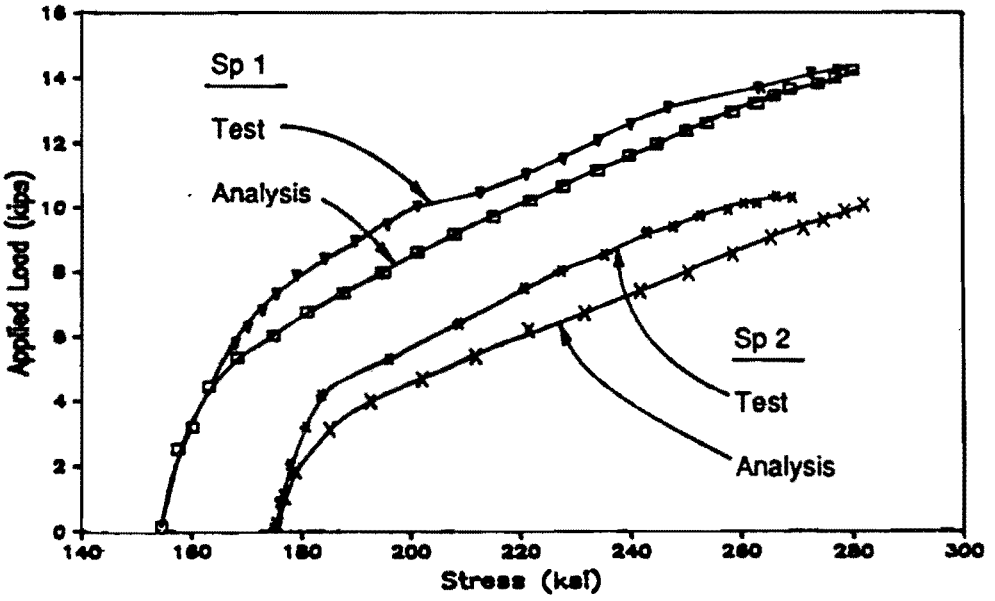

Fig. 4.14 Comparison of measured and predicted strand stress during flexure tests

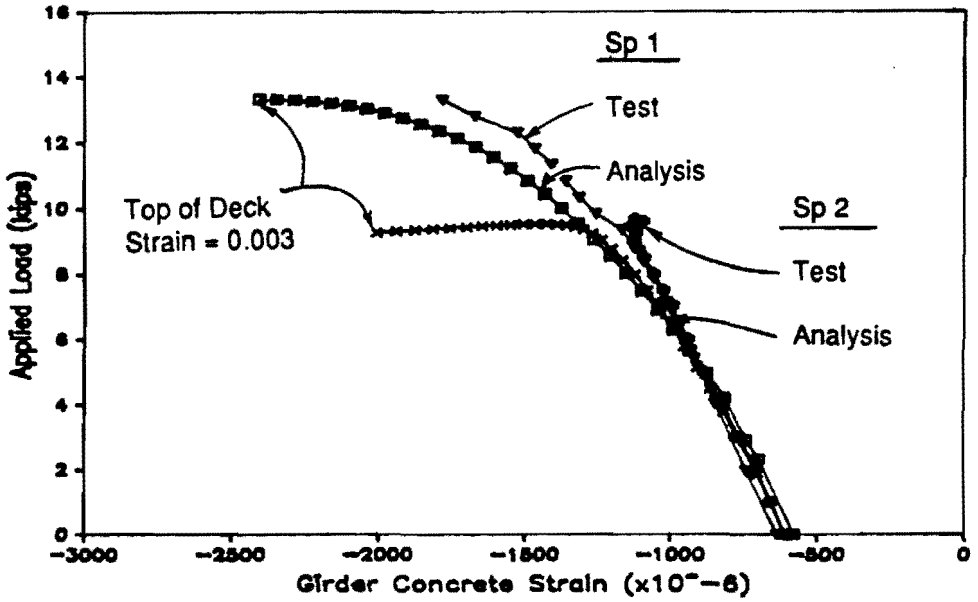

Fig. 4.15 Comparison of measured and predicted top-of-girder concrete strains during flexure tests

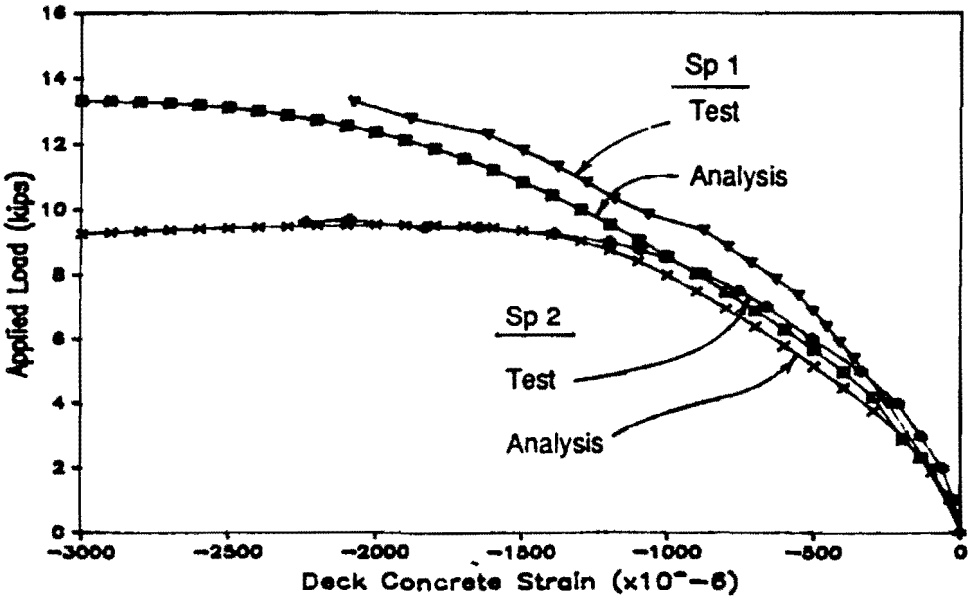

Fig. 4.16 Comparison of measured and predicted top-of-deck concrete strains during flexure tests

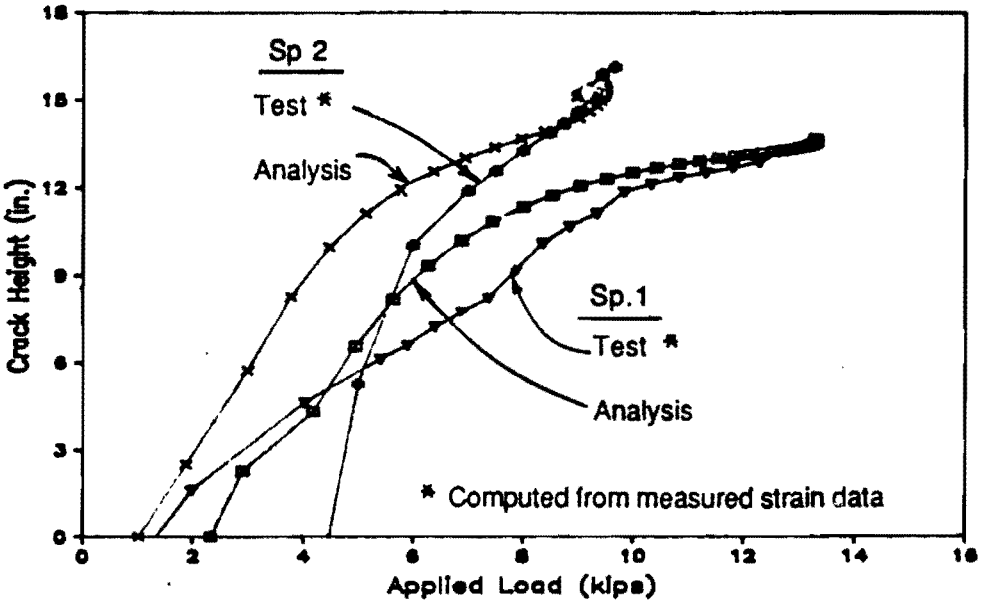

Fig. 4.17 Comparison of computed and predicted crack height during flexure tests

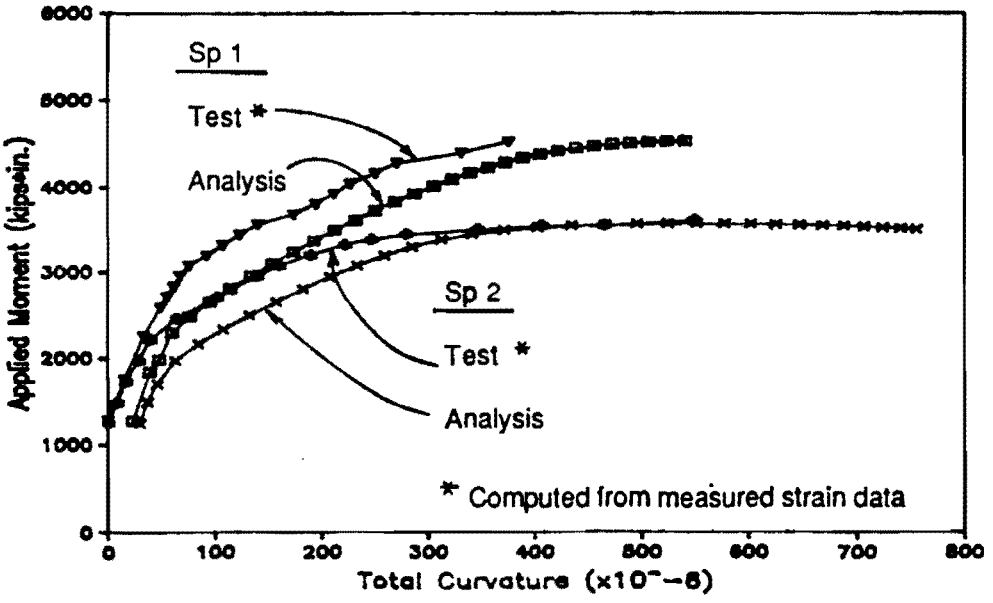

Fig. 4.18 Comparison of computed and predicted total curvature during flexure tests

deck, which determines the final point of the predicted curvature plots.

A final set of curves comparing analytical and test data appear in Fig. 4.19 and 4.20, where the top-of-girder strain and the strand strains, respectively, are plotted versus the top-of-deck strain, which was the independent variable in the analysis. Agreement here is quite good for both quantities for Specimen 1 while divergence is significant for Specimen 2. This indicates that both the strands and the top of girder failed to gain strain as expected as failure approached. For the strands, this could be due to debonding between cracks, but the cause for low strains in the girder is not known. The curves clearly indicate that concrete strains at failure were well below 0.003 and the excellent agreement between the analytical and test curves for Specimen 1 as shown in Fig. 4.19 seems to indicate that the measured strains were reasonable.

The excellent agreement when strains are plotted versus strains is puzzling because of the poor agreement for strains plotted versus load. The good agreement between measured and predicted behavior when strains are plotted versus strains may indicate that the analysis is correct, but that somehow the relationship between load and strain is in error. The good agreement between measured and predicted ultimate loads and the fact that loads involved in the test were known with sufficient precision seem to eliminate the possibility that the loads applied during the test or the dead loads were in error.

4.2.4.2 Capacity and Conditions at Failure. Measured and predicted quantities at failure and defined ultimate conditions will now be compared. The current definition for the stress-block parameter β_1 is used in the following analyses because other investigators have found it to be appropriate for use with high strength concrete as discussed in Sec. 2.4.1.

The moment and load at defined ultimate conditions and failure are shown in Fig. 4.21 and 4.22, respectively. Values from the strain compatibility analysis are given for top-of-deck strains equal to the measured strain at failure, the code specified maximum usable concrete strain (0.003), and the maximum moment. Results were computed for the simplified analysis methods by using the appropriate strand stress equation with the ultimate moment equations in the AASHTO Specifications or the ACI ERSB with the approaches discussed in Section 4.4.2.2. Because the reinforcement index exceeded code specified limits for Specimen 1, computed member capacities were

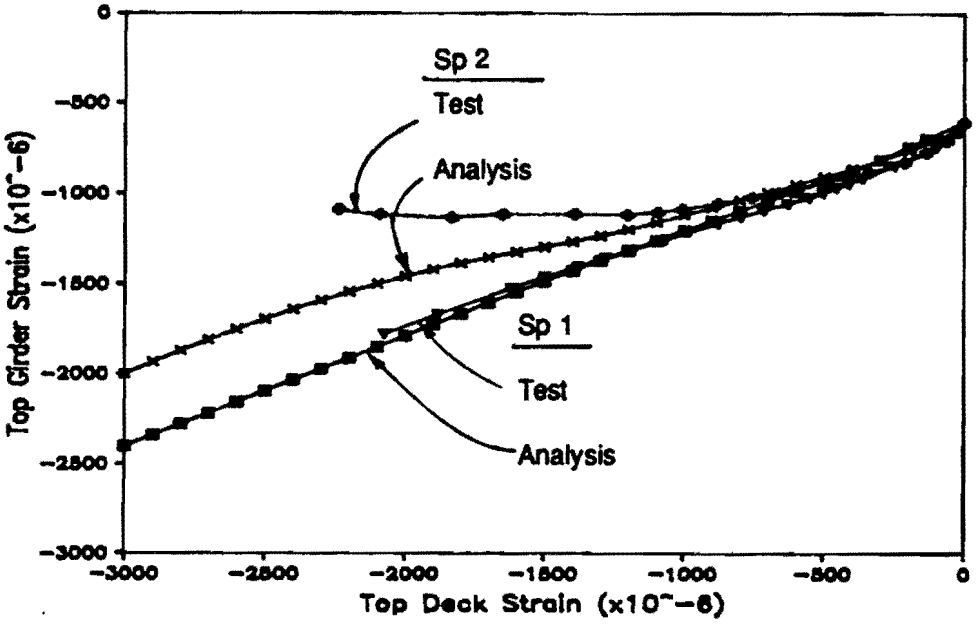

Fig. 4.19 Comparison of measured and predicted concrete strains at top of girder and top of deck during flexure tests

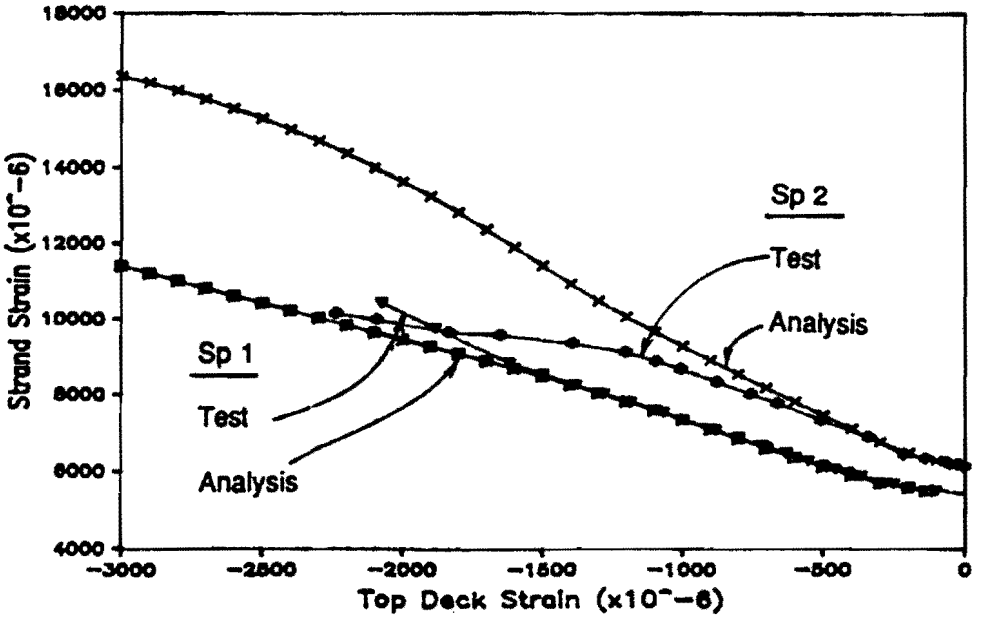

Fig. 4.20 Comparison of measured and predicted strand strains and concrete strains at top of deck during flexure tests

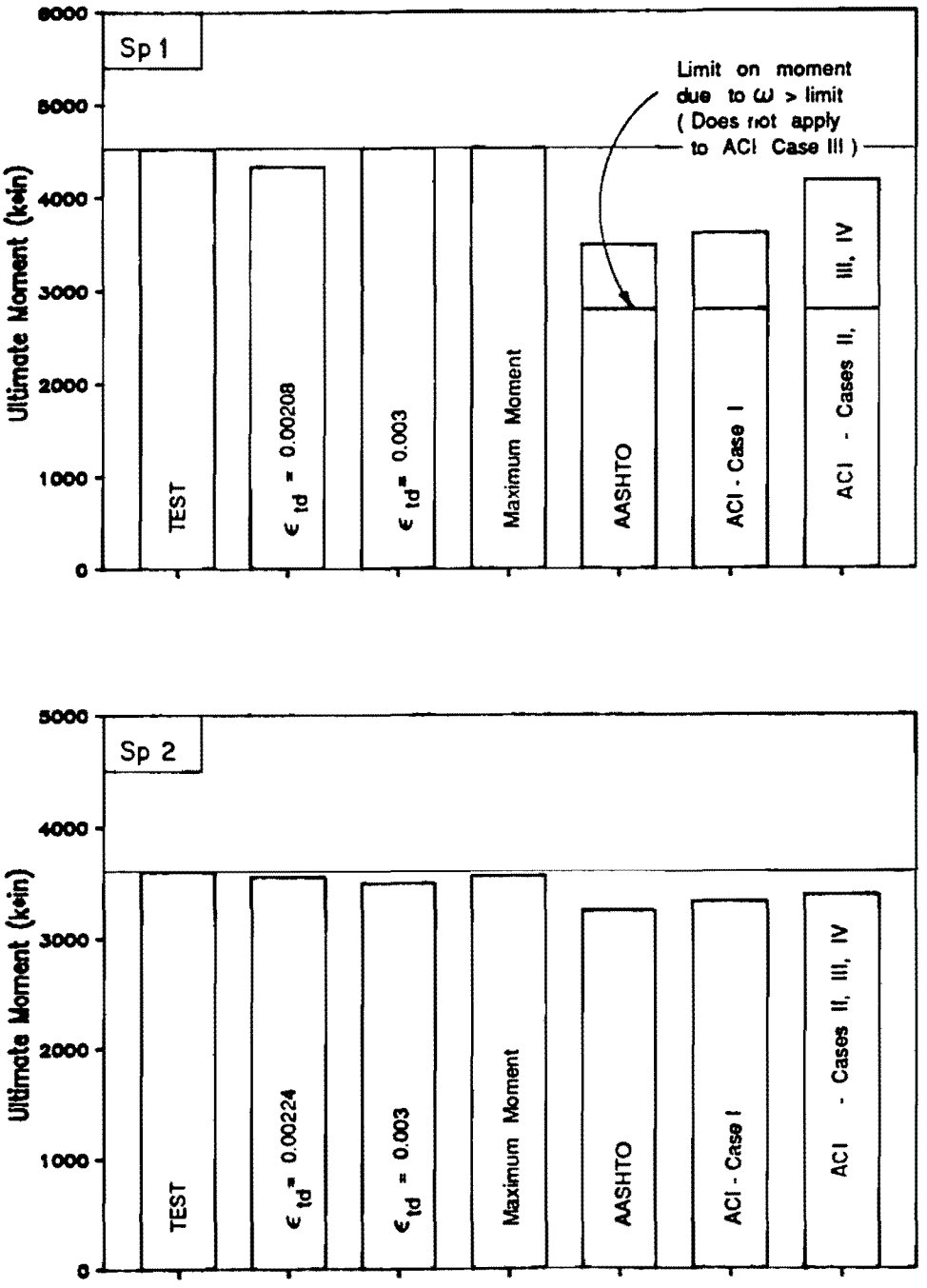

Fig. 4.21 Comparison of measured and predicted ultimate moment capacity for flexure tests

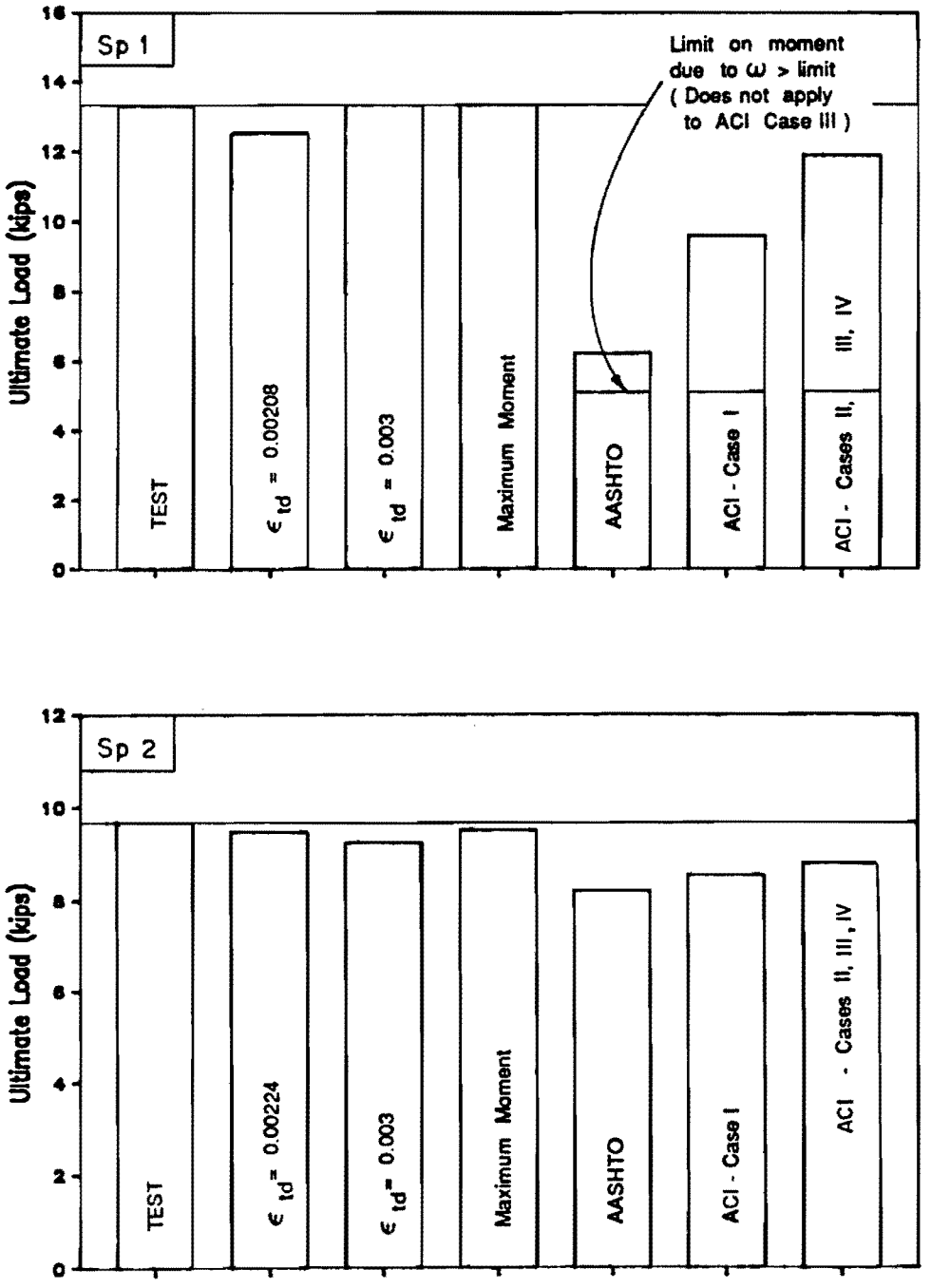

Fig. 4.22 Comparison of measured and predicted ultimate loads for flexure tests

reduced using the equations provided by the AASHTO Specifications and the ACI Code Commentary. Moments and loads predicted by the strain compatibility analysis show very good agreement with test data while the reduced capacities computed using the simplified code methods are significantly below measured values. It is interesting that capacities computed using the simplified methods without the required reduction were conservative for this test data. Agreement is slightly worse for loads because of the conversion from total moment to applied load, which subtracts the dead load moment from the total ultimate moment before the applied load is computed.

Strand stresses at ultimate are compared in Fig. 4.23. Stresses computed by the strain compatibility analysis agree well with measured values, although agreement is better for Specimen 1 where strains increased steadily until failure. Stresses computed using the simplified methods were consistently lower than the values obtained from analysis. No modifications were made in the calculation of ultimate strand stress due to the excessive reinforcement index of Specimen 1 because no such guidance is given in the codes.

Measured deck and girder strains at failure are compared with strains corresponding to the defined ultimate conditions in Fig. 4.24 and 4.25, respectively. For the deck, the measured strain at failure was well below both analytical definitions of ultimate for Specimen 1 while for Specimen 2, failure occurred at a strain near the top-of-deck strain corresponding to maximum moment from the analysis, but was well short of the 0.003 that is assumed to correspond to failure. The results are similar for the top-of-girder strain, although the comparison for Specimen 2 is hampered by the previously noted low girder strain at failure. For Specimen 1, the strain in the deck and girder at failure agrees well for the analysis. That is, the measured strain in the top of the girder at failure agrees well with the predicted strain when the top of the deck is at the strain measured at that location at failure.

4.2.4.3 Summary. This section summarizes the preceding examination of test data, analytical results, and estimates based on the simplified methods given in the codes.

1. Use of the current definition for β_1 is appropriate for use with high strength concrete.

2. The strain compatibility analysis used here provided a conservative yet realistic estimate of all aspects of

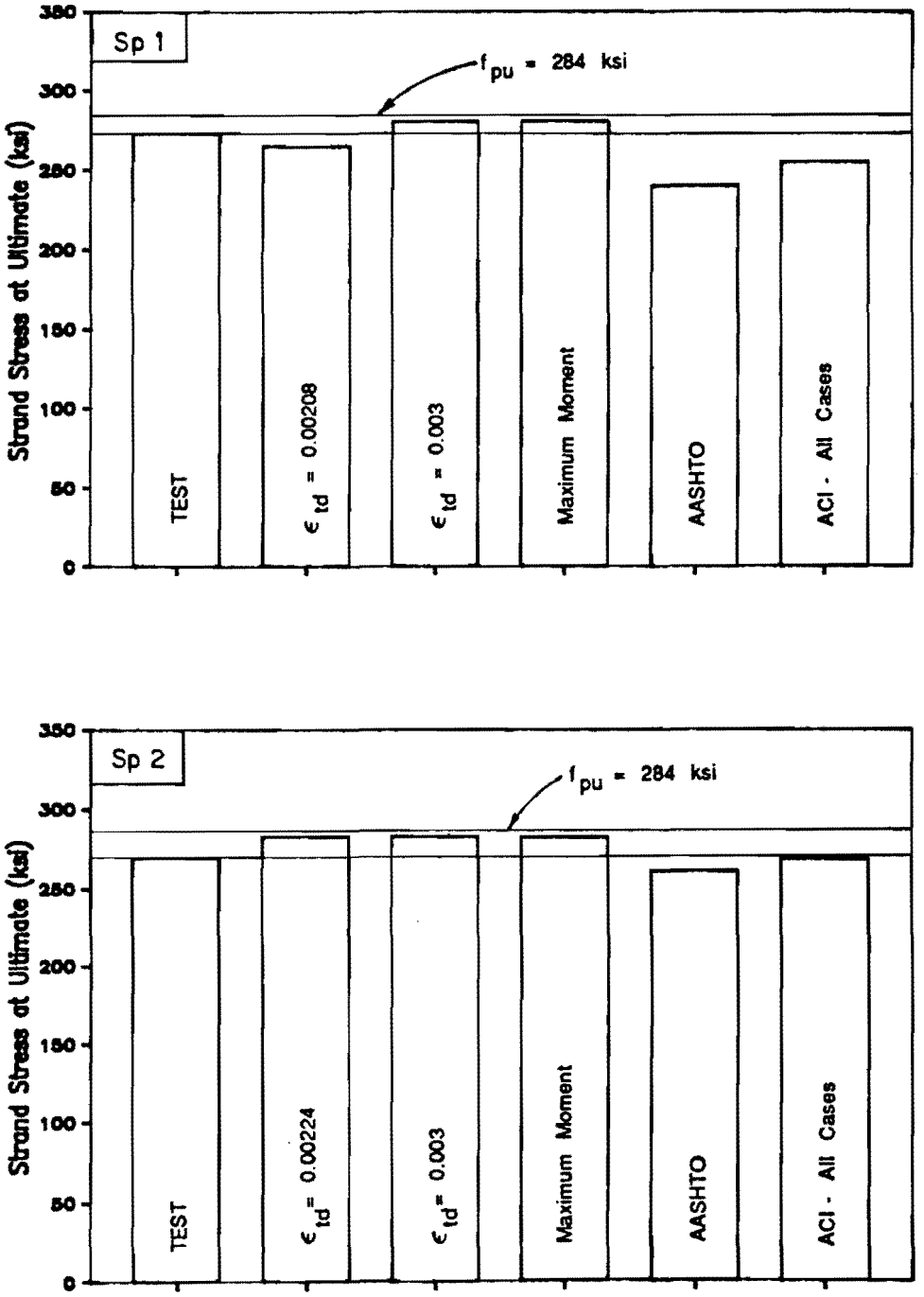

Fig. 4.23 Comparison of measured and predicted strand stress at ultimate for flexure tests

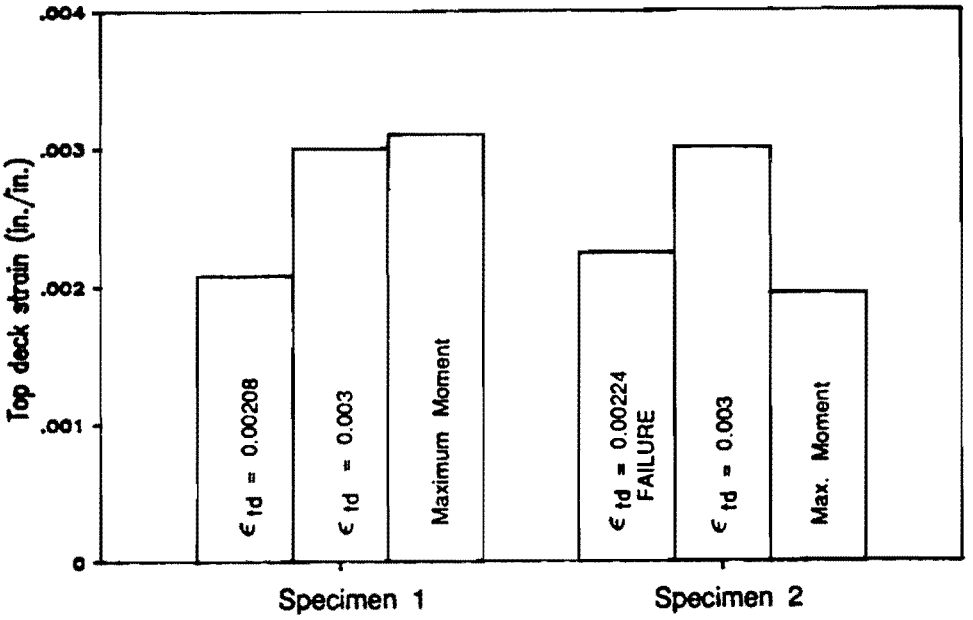

Fig. 4.24 Comparison of top-of-deck concrete strains measured at failure and predicted by analysis at ultimate conditions

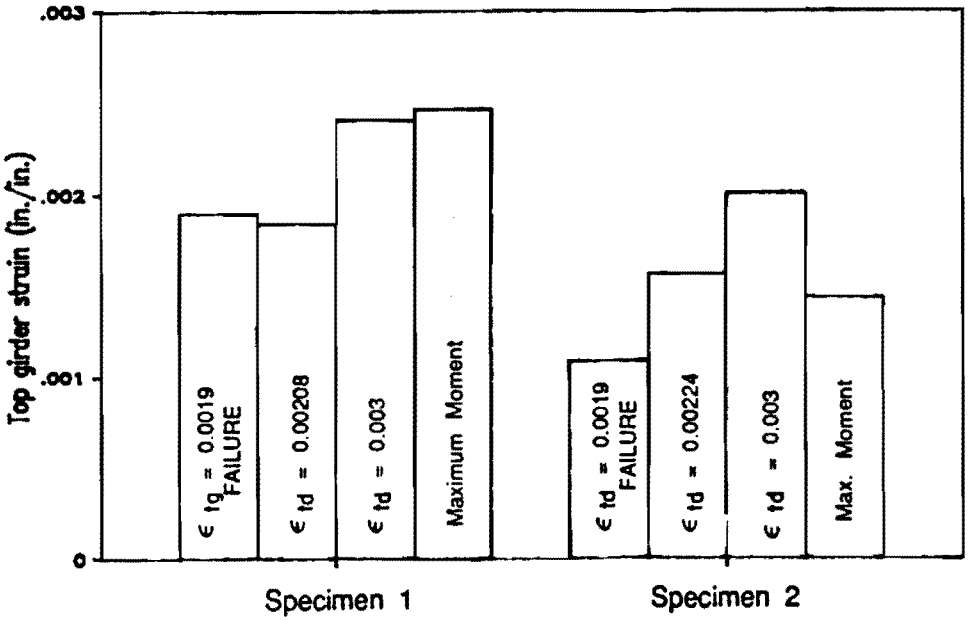

Fig. 4.25 Comparison of top-of-girder strains measured at failure and predicted by analysis at failure and ultimate conditions

flexural behavior, including ultimate capacity, deflections, and strand stresses.

3. The maximum usable concrete strain for sections of this type may be less than the 0.003 specified in the ACI Code, as reflected by strain readings from test specimens. For this data, an average value for the strain at failure for the deck concrete was approximately 0.0022, which was corroborated by results of the strain compatibility analysis. While it is not possible to be dogmatic about an exact value for the ultimate concrete strains measured in the tests because of various limitations in the data, it appears certain that the strains at failure were less than the specified maximum usable strain.

4. The simplified analysis methods provided conservative estimates of the ultimate capacity of the specimens tested.

5. The strain compatibility analysis gave a better estimate of flexural strength than the simplified methods.

6. For Specimen 1, the calculated capacity was reduced because the reinforcement index exceeded specified limits. The reduced capacity greatly underestimated the failure load while the uncorrected capacity provided a reasonable, conservative estimate of the failure load.

7. The strain compatibility analysis provided a good, although slightly high, estimate of the measured strand strains and stresses at failure.

8. Strand stress at ultimate was conservatively and reasonably estimated using the equations from the codes. The recently revised ACI equation provided the better estimate.

9. Agreement between test data and the strain compatibility analysis was better when the information was plotted versus top-of-deck strains than when plotted versus load.

4.2.5 Predicted Behavior for Typical Designs. In this section, designs for a range of span and girder spacings will be compared. An AASHTO-PCI Type IV girder (see Fig. 3.1) is used with three concrete strengths: 6, 9, and 12 ksi. Two girder spacings (GS) will be used, 4 and 10 ft, which represent practical extremes in the range of girder spacings. The deck was assumed to be applied to an unshored girder and had a concrete strength of 4 ksi. Two categories of designs are considered: (1) a design for a given span of 75 ft (GS = 10 ft) or 120 ft (GS = 4 ft), which are extremes for the design using this girder section with 6 ksi concrete, and (2) a design for the maximum span possible for a given girder spacing and concrete strength. The maximum span designs represent extremes of behavior and could be used for actual designs. The typical span designs using the higher strength concrete would not likely be used since the same design could be achieved using normal strength concrete. These typical designs were included to give a direct comparison between behavior of normal and high strength concrete members. Concrete strengths at release are 75 percent of the 28 day strength, except for a series of designs in which the release strength was varied to determine the minimum release strength required for a given span and girder spacing. Low relaxation strands with a 0.5 in. diameter are used for all designs. The recommendations by Zia et al. [137] are used for computing prestress losses.

Actual, practical designs were used for this study to ensure that combinations of variables were reasonable, rather than performing a sensitivity analysis on a few parameters without restraining their relationship by the constraints of practical design. Therefore, the conclusions of this study can be construed as being representative of a range of designs that could be encountered in actual design situations.

Designs were executed using the computer program BRIDGE (see Appendix C of Ref. [140]..2) which was written for this study. Results of the design were used as input for the strain compatibility analysis program (MOMCURV) to determine the behavior of the designs at ultimate conditions.

The "ultimate condition" is defined as the state of the member or section when the maximum capacity is attained. Other definitions, however, are provided to permit estimation of this maximum capacity. In the following study, three definitions for the ultimate condition will be considered in all cases: (1) the strain at the top of the deck equal to the maximum usable strain of 0.003, (2) the maximum moment

resisted by the section, and (3) the top of the deck reaching a strain of 0.0022, which is an approximate average of top fiber strains at failure for the specimens tested. An additional case will be considered where the strand strain reaches the minimum specified elongation of 0.035 prior to the top of the deck reaching a strain of 0.003.

The spans used and number of strands required for the 12 designs considered in this and following sections are summarized in Fig. 4.26 and 4.27, respectively. Figure 4.26 indicates the increase in span with increasing concrete strength for the maximum span designs. The maximum span designs for 9 and 12 ksi concrete with GS = 4 ft exceed the maximum lifting spans corresponding to the girder concrete strength at release, and would therefore require special consideration in design and handling (see Sec. 4.5). Figure 4.27 shows that the use of high strength concrete provides only a slight, if any, decrease in the required number of strands for the typical span designs. A large number of strands is required for the maximum span designs, especially where high strength concrete is used. For the case where f'_c = 12 ksi and GS = 10 ft, the strand limit of 74 was exceeded. This leads to the need for suitable ductility limits in order to control over-reinforcement.

Results from these designs will be considered in this section as they relate to ultimate capacity, strand stress at ultimate, the effect of the girder concrete modulus on the design and ultimate capacity, and the required strength at release. Other results from these designs will be considered in the sections that follow.

The data from the designs are generally presented in bar-chart form with bars grouped for the concrete strengths and separate plots given for the two girder spacings used. Plots for the typical span designs and the maximum span designs will generally appear on separate pages. The bars are labelled for the first group of bars only, with unlabelled bars appearing in the same order as those that are labelled.

4.2.5.1 Ultimate Design Moment. The ultimate capacity of a highway bridge designed by the AASHTO Specification must exceed both the ultimate moment, M_u, which is a combination of factored service loads, and 1.2 times the cracking moment, M_{cr}, computed using a modulus of rupture of $7.5\sqrt{f'_c}$. The ultimate moment is determined using the following equation for the typical load combination of dead and live loads:

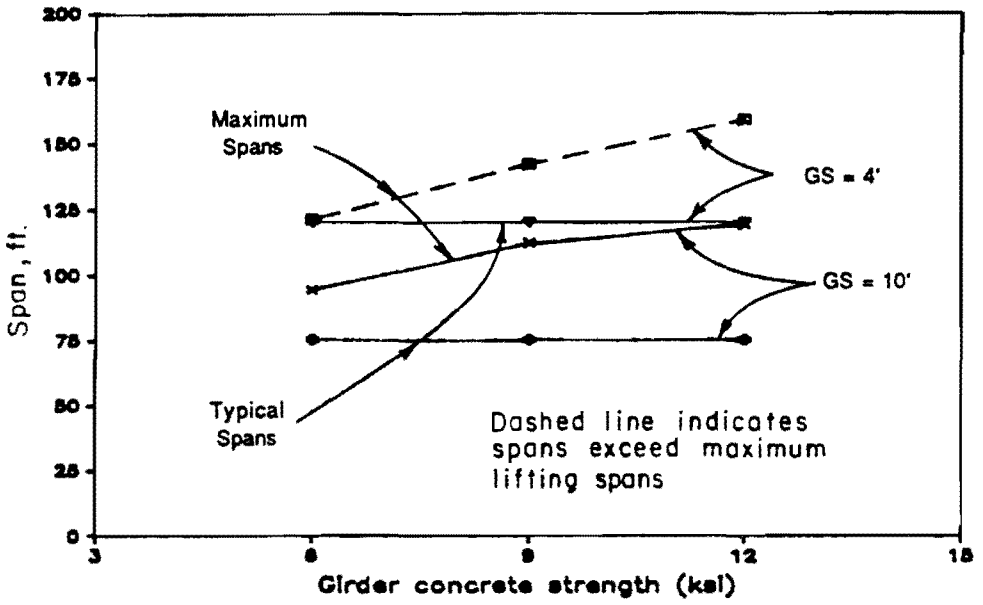

Fig. 4.26 Span length versus girder concrete strength for maximum and typical span designs

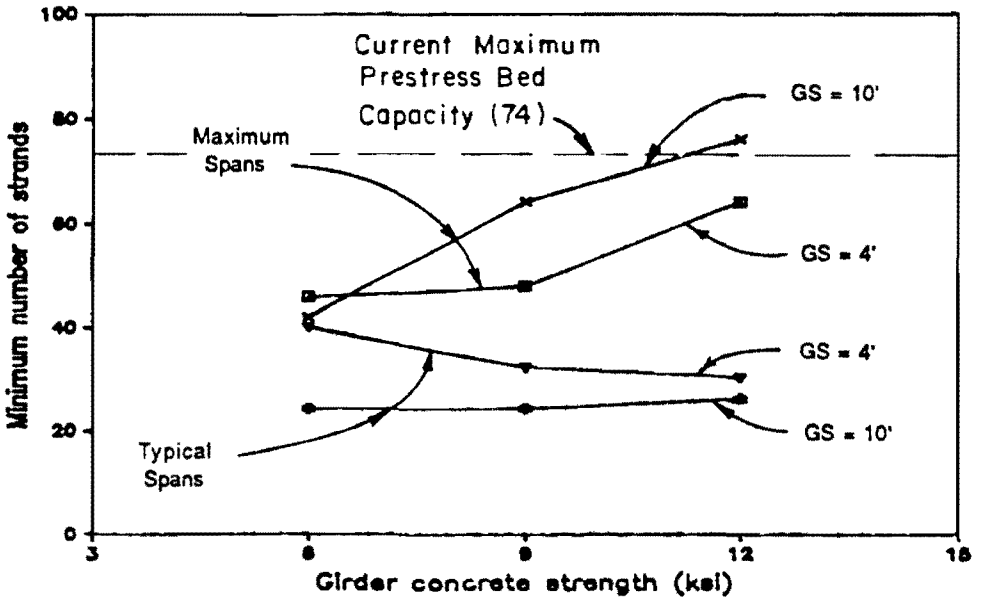

Fig. 4.27 Minimum number of strands versus girder concrete strength for maximum and typical span designs

$$M_u = 1.3*(M_{DL} + 1.67*M_{L+I}) \quad (4.1)$$

where I = impact fraction (maximum 30 percent)

$$= 50/(L+125) \quad (4.2)$$

L = span in feet

M_{DL} = dead load moment

M_{LL} = live load moment

$M_L+I = M_{LL}(1+I)$

The variation of the impact factor with span length is shown in Fig. 4.28 along with tabulated values for selected spans. For spans greater than 125 ft, the impact factor is less than 20 percent.

Ultimate strength design includes the use of a strength reduction factor, ϕ. The AASHTO Specifications use ϕ = 1.0 for flexural analysis of factory produced precast prestressed concrete members. This factor is usually used for composite bridges with pretensioned girders, although deck concrete placed in the field would generally require use of a lower factor. The use of a ϕ factor of 1 for flexural analysis of the entire structure appears appropriate since the use of the precast element provides good control over the quantities of greatest importance in the flexural analysis. Errors in dimensions or strength of the deck will have only a small effect on the capacity of the member. The analysis has also been shown to be conservative and realistic, as was demonstrated earlier in this chapter.

The second limit on ultimate capacity is intended to prevent failure shortly after initial cracking due to a lack of reinforcement, and is actually considered a minimum reinforcement requirement. The cracking moment, M_{cr}, which is the total moment producing cracking, can be expressed as a sum of the dead load moment and some fraction greater than 1 times the live load moment including impact factor, i.e.,

$$M_{cr} = X*M_{M+I} + M_{DL} \quad (4.3)$$

With the cracking moment defined in this way, the 1.2 times M_{cr} limit can be compared with the ultimate moment limit by expressing both limits in terms of the ratio M_{SL}/M_{DL} (where M_{SL} = service load moment = $M_{L+I} + M_{DL}$) or M_{L+I}/M_{DL} as shown in Fig. 4.29. This plot demonstrates that the ultimate load criteria will control for most situations, since X is usually less than 2. Values for the live load plus impact-to-dead load ratio for some of the span/girder spacing

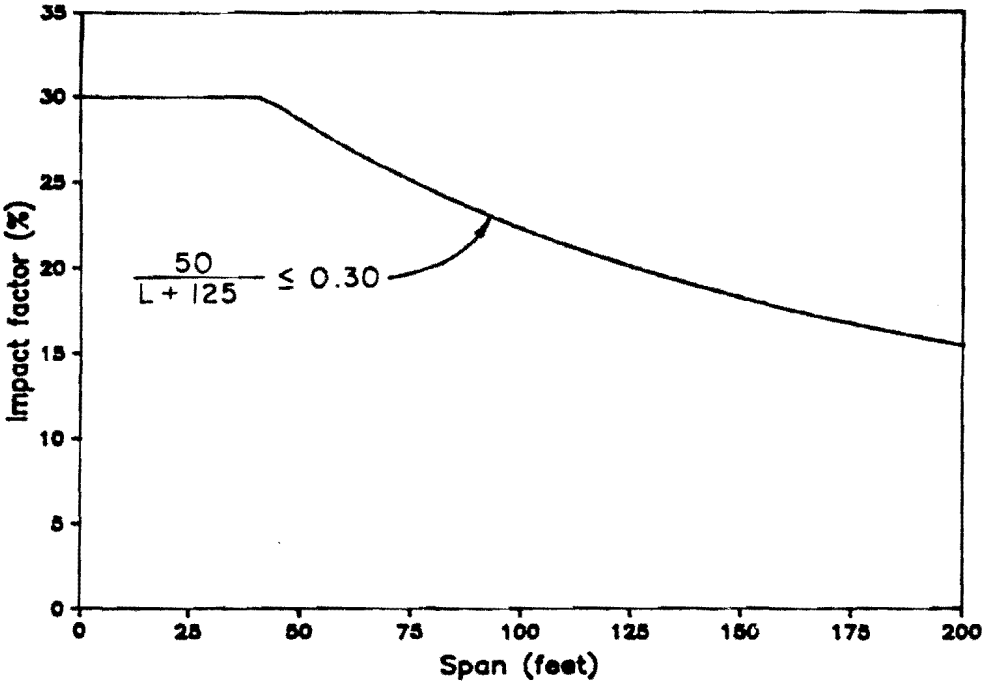

Fig. 4.28 AASHTO live load impact factor

Span	Impact Factor	Span	Impact Factor
0	30.00	120	20.41
40	30.00	125	20.00
45	29.41	130	19.61
50	28.57	135	19.23
55	27.78	140	18.87
60	27.03	145	18.52
65	26.32	150	18.18
70	25.64	155	17.86
75	25.00	160	17.54
80	24.39	165	17.24
85	23.81	170	16.95
90	23.26	175	16.67
95	22.73	180	16.39
100	22.22	185	16.13
105	21.74	190	15.87
110	21.28	195	15.63
115	20.83	200	15.38

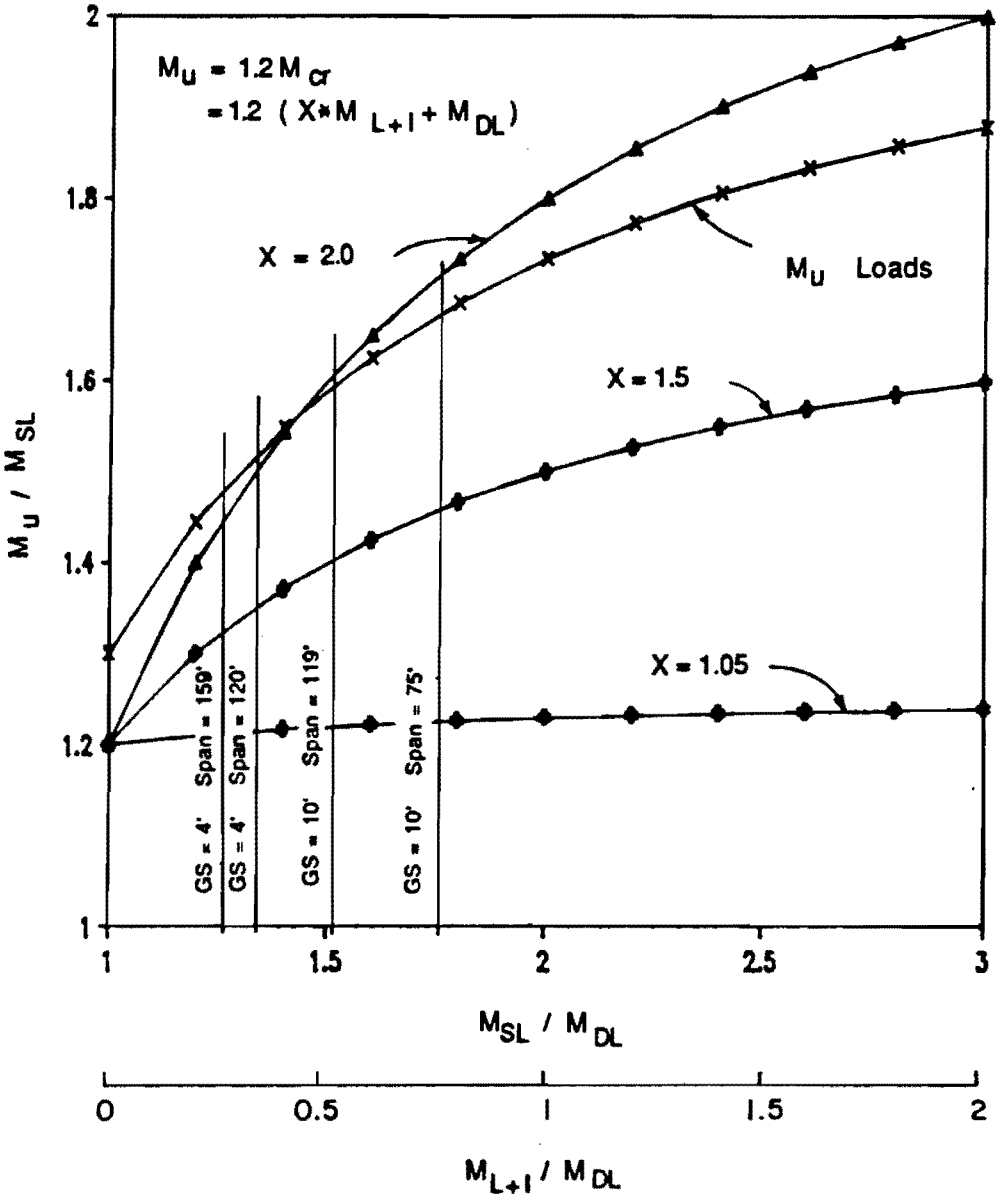

Fig. 4.29 Relative magnitude of ultimate moment limits

combinations are shown on the figure, indicating that most designs will be at values of M_{SL}/M_{DL} near or less than 1.5. A further manipulation of the equations gives the multiple of the live load including impact required to reach the ultimate moment or 1.2 M_{cr} as shown in Fig. 4.30. This figure indicates that an overload of 2.5 to 3 times the live load including impact factor must be applied to bridge members considered in this section in order to reach the ultimate load. While it appears unlikely that such an overload could occur, a comparison of actual and potential highway loadings with AASHTO specified loadings would provide a basis for evaluating the significance of the magnitude of overload required.

This analysis indicates that for most designs, M_u should control. This will not be the case if the cracking moment M_{cr} is computed using a simplified equation in which the effects of dead load are neglected. This simplification is appropriate for shear analysis of noncomposite uniformly loaded beams but has apparently been used for flexural analysis of composite members as well. Using a concrete tensile strength of $7.5\sqrt{f'_c}$, cracking moments computed using the simplified approach overestimated the actual cracking moment by as much as 25 percent. Therefore, full consideration should be given to all loads applied on the appropriate section in the computation of the cracking moment.

4.2.5.2 Ultimate Moment Capacity. Moment capacities computed using the strain compatibility analysis and the simplified approaches are shown in Fig. 4.31 and 4.32 for maximum and typical span designs, respectively. Spans, girder spacings, and girder concrete strengths are shown on the figures.

Agreement is very good between capacities computed using the strain compatibility analysis for the different ultimate conditions. This indicates that the capacity is very close to the maximum when the top-of-deck strain reaches 0.0022 and that it remains near the maximum up to a strain of 0.003. For the maximum span case of GS = 10 ft and f'_{cg} = 6 ksi, the strand reached the minimum elongation at the ultimate capacity. However, for all typical span designs with GS = 10 ft, the strand reached the minimum elongation at the required ultimate capacity, which was slightly below the capacity predicted using the other measures of the ultimate condition and very close to the capacities computed using the simplified methods. This is a cause for concern and will be considered further in the section that follows.

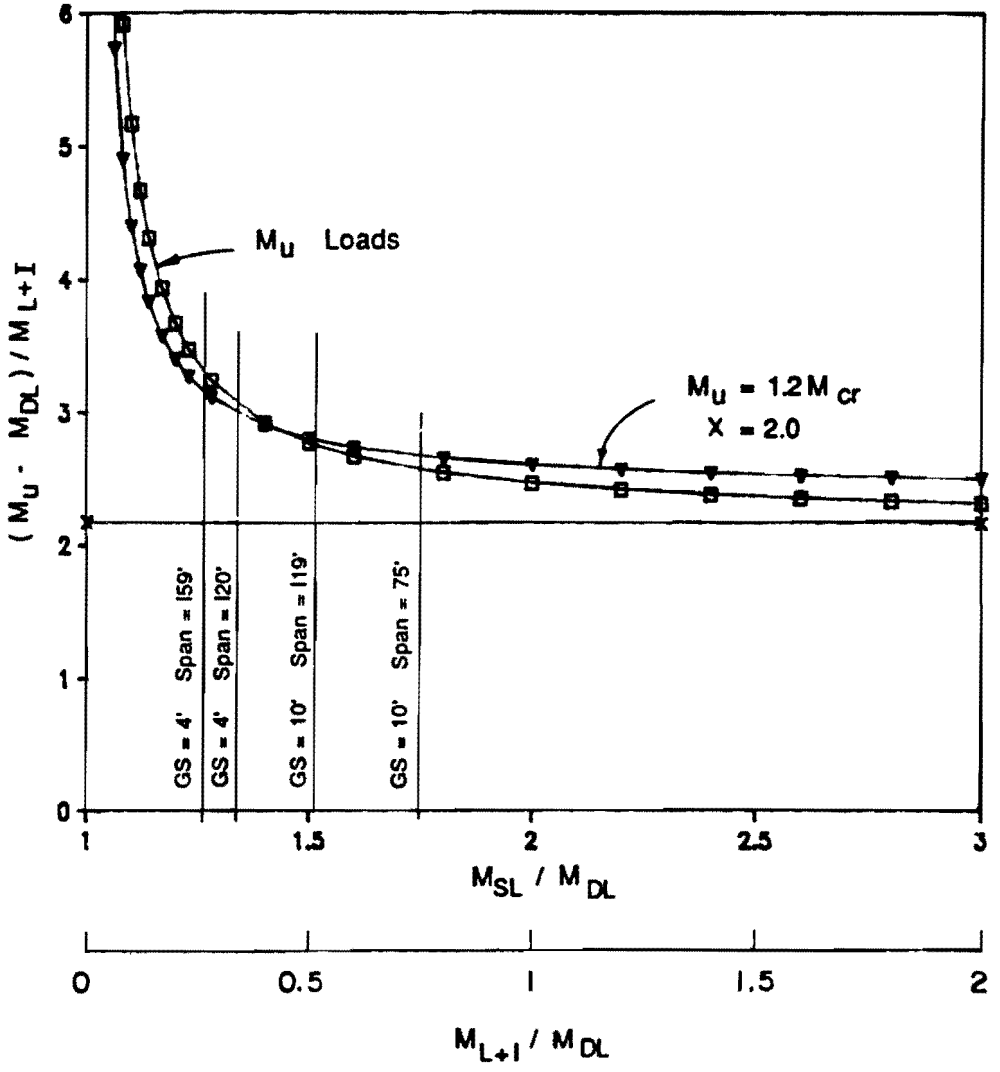

Fig. 4.30 Relative overload required to reach ultimate load

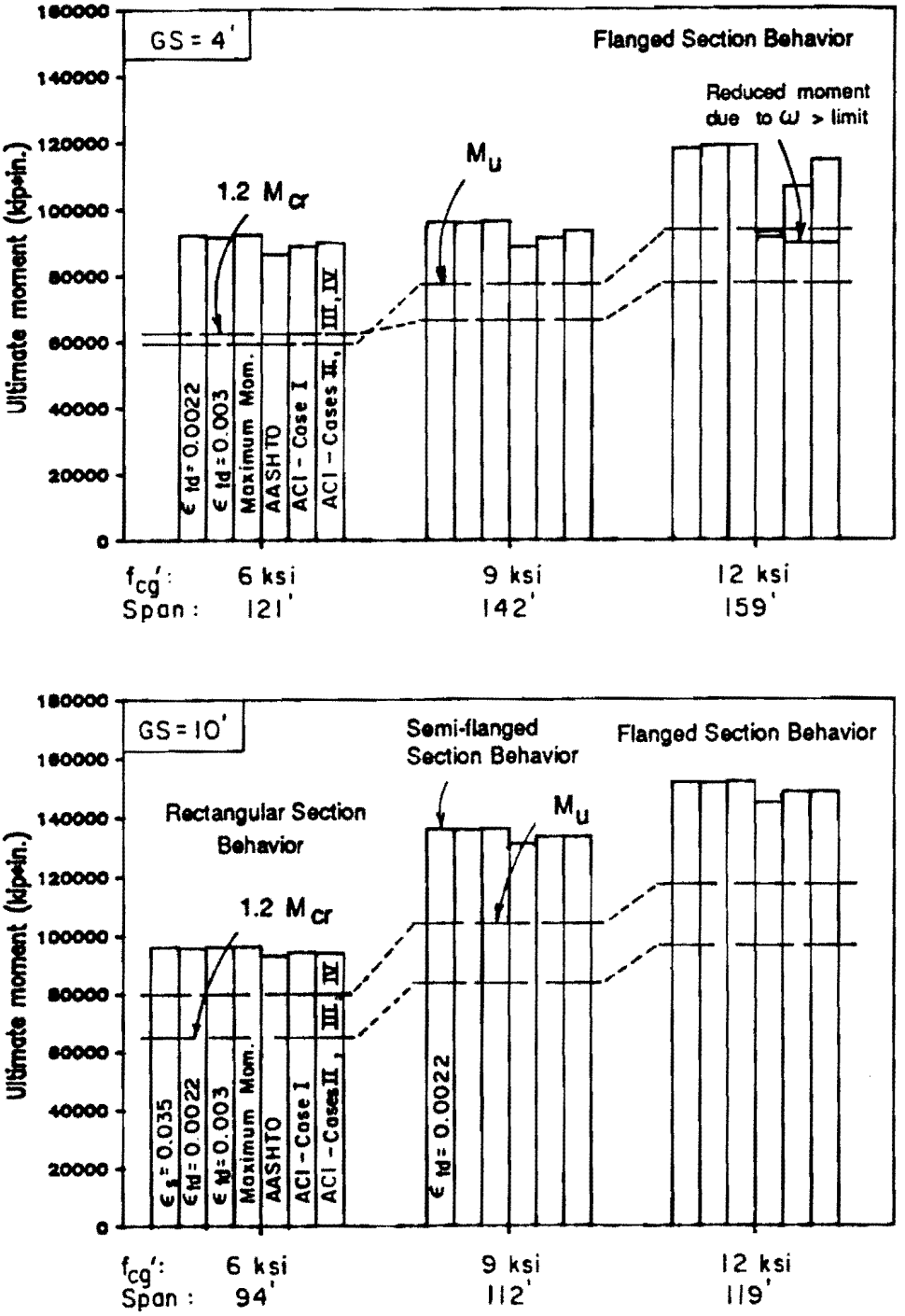

Fig. 4.31 Ultimate moment capacity for maximum span designs

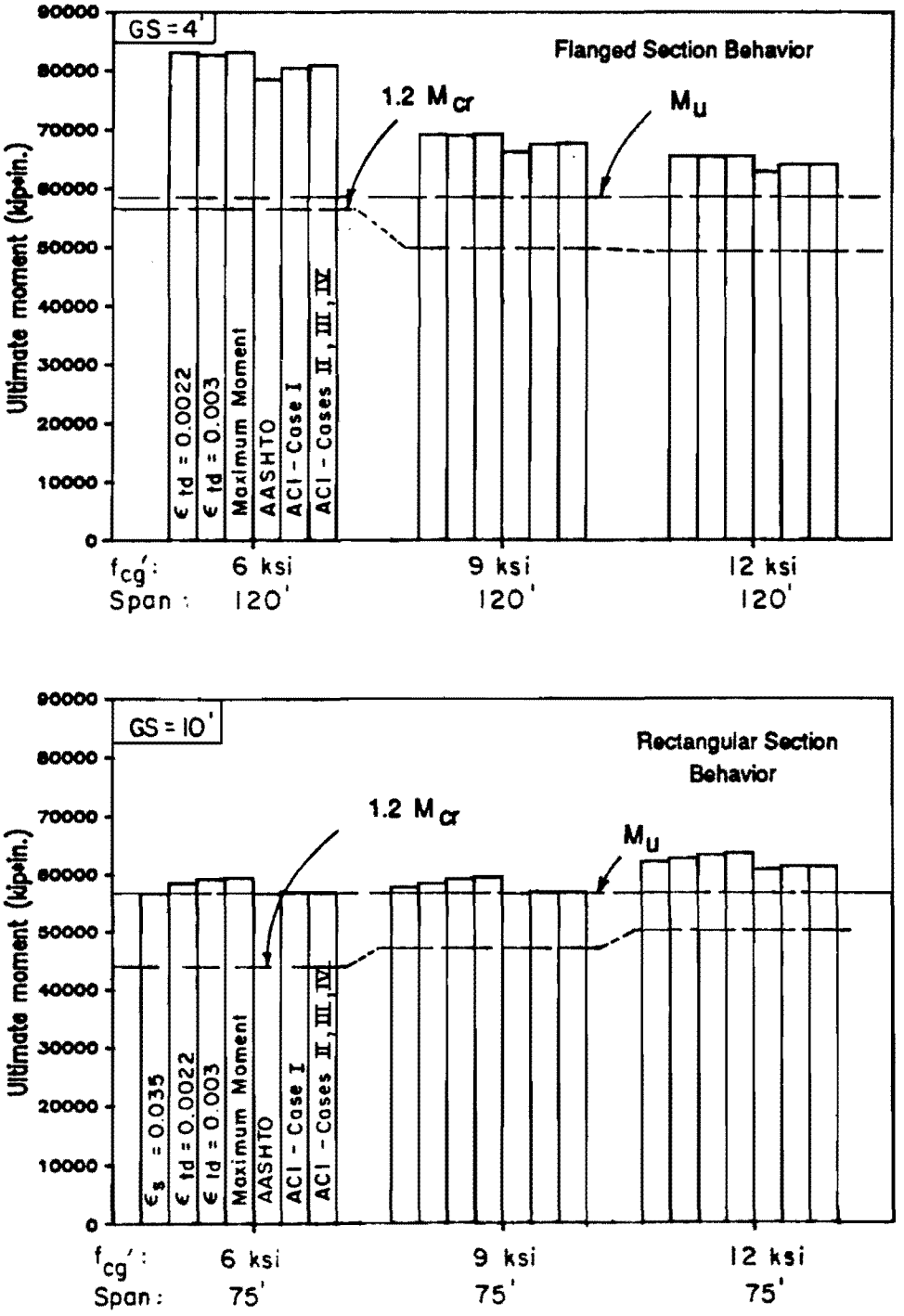

Fig. 4.32 Ultimate moment capacity for typical span designs

The simplified methods showed good agreement with the strain compatibility analysis. Only in the case where the reinforcement index exceeded the specified limits and the capacities were reduced (max. spans, GS = 4 ft, f'_{cg} = 12 ksi) were the simplified methods overly conservative.

The factored ultimate load and the 1.2 M_{cr} limit are also shown on these figures. The 1.2 M_{cr} value plotted is based on a full cracking analysis including dead loads. However, the design program used the approximate relationship to check ultimate capacities during the design process. The larger value obtained using this incomplete analysis controlled the typical span design for GS = 10 ft and f'_{cg} = 12 ksi. If the correct cracking moment had been used, the 12 ksi design would have been essentially the same as for the other concrete strengths considered.

For all but one design, the factored load was larger than the cracking criteria. There was generally a large margin between the controlling ultimate load and the ultimate capacity. This was not the case for the short typical span with a wide girder spacing where ultimate capacity controlled design or came very close to controlling the design. Only in the single case where the reinforcement index exceeded the specified limit and the capacity was reduced did the capacity predicted by the simplified methods fall below the required ultimate capacity. This would have necessitated the addition of more reinforcement in a final design for the member, or a slight reduction in the span.

Flanged section analysis was required for designs where GS = 4 ft. For Cases III and IV, where section dimensions were transformed by the ratio of concrete strengths, a negative value was obtained for the area of steel required to develop the flange as shown in Fig. 4.33. This occurred because the deck of the transformed section was narrower than the top of the girder. While this appears to indicate a flaw in the analysis, the results are reasonable and results of analyses of these sections with transformed dimensions are consistent with other designs.

The maximum span design with GS = 10 ft and f'_{cg} = 9 ksi exhibited "semi-flanged" behavior as noted on Fig. 4.31. This meant that the strain compatibility analysis revealed that the top of the girder remained in compression after the deck cracked. This condition was stable and persisted throughout the range of top-of-deck strains corresponding with all three conditions of ultimate considered for

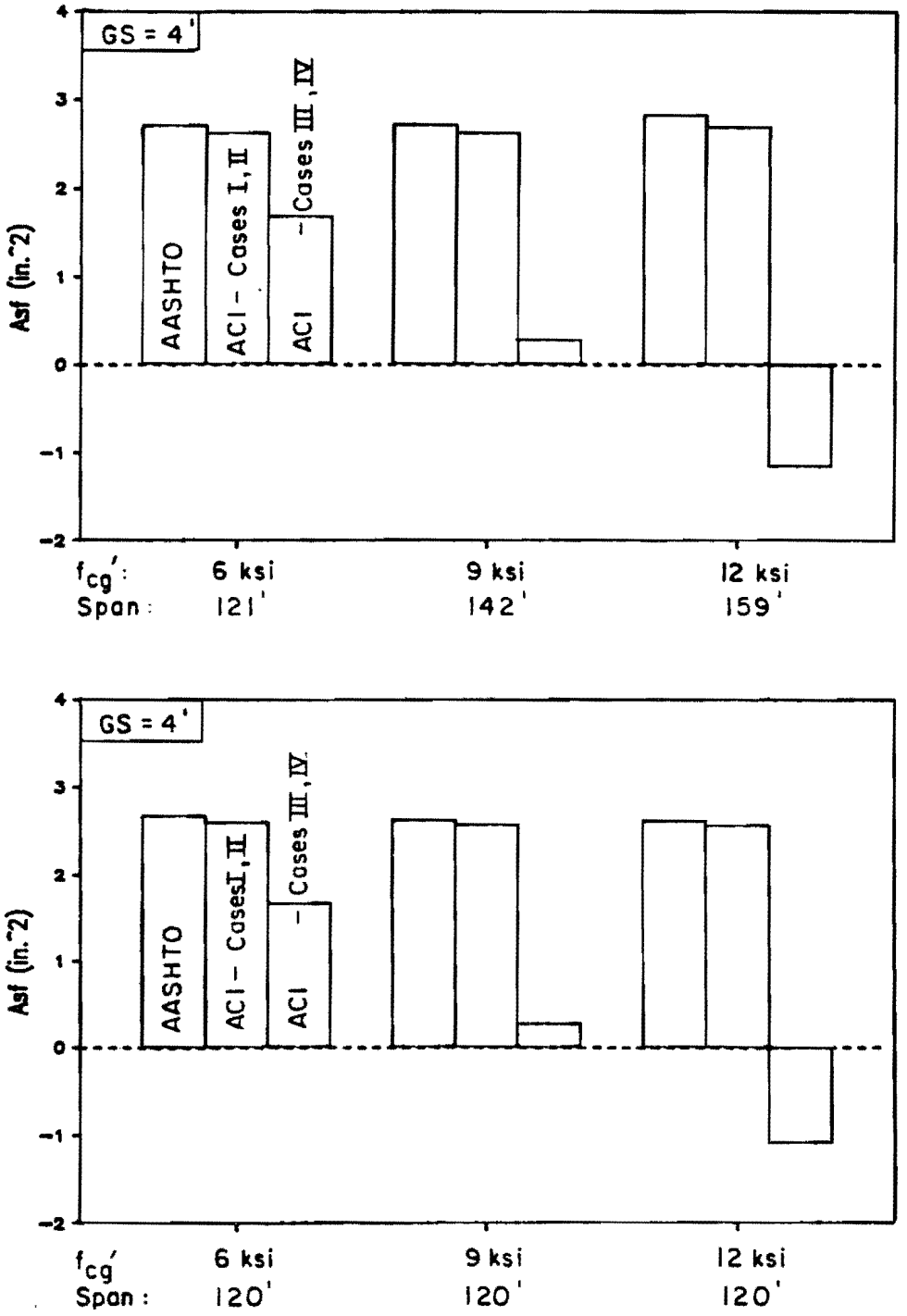

Fig. 4.33 Area of steel required to develop flange for maximum and typical span designs with GS = 4 ft

this design. While this condition is not of great importance for strength design, it would be significant if ductility limits were expressed in terms of the depth of compression at ultimate, as has been proposed by some.

Figure 4.34 indicates the levels of reinforcement present in the designs. The reinforcement ratios are computed using the full girder width (for GS = 10 ft, the effective width was 110 in.) and full area of prestressing steel. It is clear from this figure that the minimum specified elongation of the strand was exceeded for typical span designs with GS = 10 ft because of very low reinforcement ratios in these designs.

The top-of-deck strains corresponding to the four conditions of ultimate for the strain compatibility analyses are shown in Fig. 4.35 and 4.36 for maximum and typical span designs, respectively.

These figures show that the maximum moment frequently occurs at top-of-deck strains below the maximum usable strain of 0.003 but always greater than the estimated failure strain of 0.0022. For the typical span designs with GS = 10 ft, the moment was still increasing, although only slightly, when the analysis was terminated at a top-of-deck strain of 0.0035. For the same design situation, the strand strain exceeded the minimum elongation well before the top-of-deck strain reached 0.0022, and the strand strains were approximately 6 percent when the top-of-deck strain reached 0.003.

Earlier, Fig. 4.31 and 4.32 indicated that the moment corresponding to a top fiber strain of 0.003 was very close to the maximum capacity of the section and therefore provided a good estimate of the ultimate capacity. However, Fig. 4.35 and 4.36 show that a large difference may exist between the top-of-deck strain at the maximum moment and the maximum usable strain. This difference is an indication that other quantities at ultimate, such as curvature, deflection, depth of compression, and strand strain, may be overestimated when the maximum usable strain of 0.003 is used to determine these other conditions at ultimate.

Figures 4.37 and 4.38 show the top-of-girder strains when the top-of-deck strains reach 0.003 for maximum and typical span designs, respectively. The girder strains are shown to be less than or just over 0.002 when the top-of-deck strain reaches 0.003. This indicates that failure in the girder is unlikely, especially since failure of the deck could occur at a strain less than 0.003, which would also result in a lower girder strain.

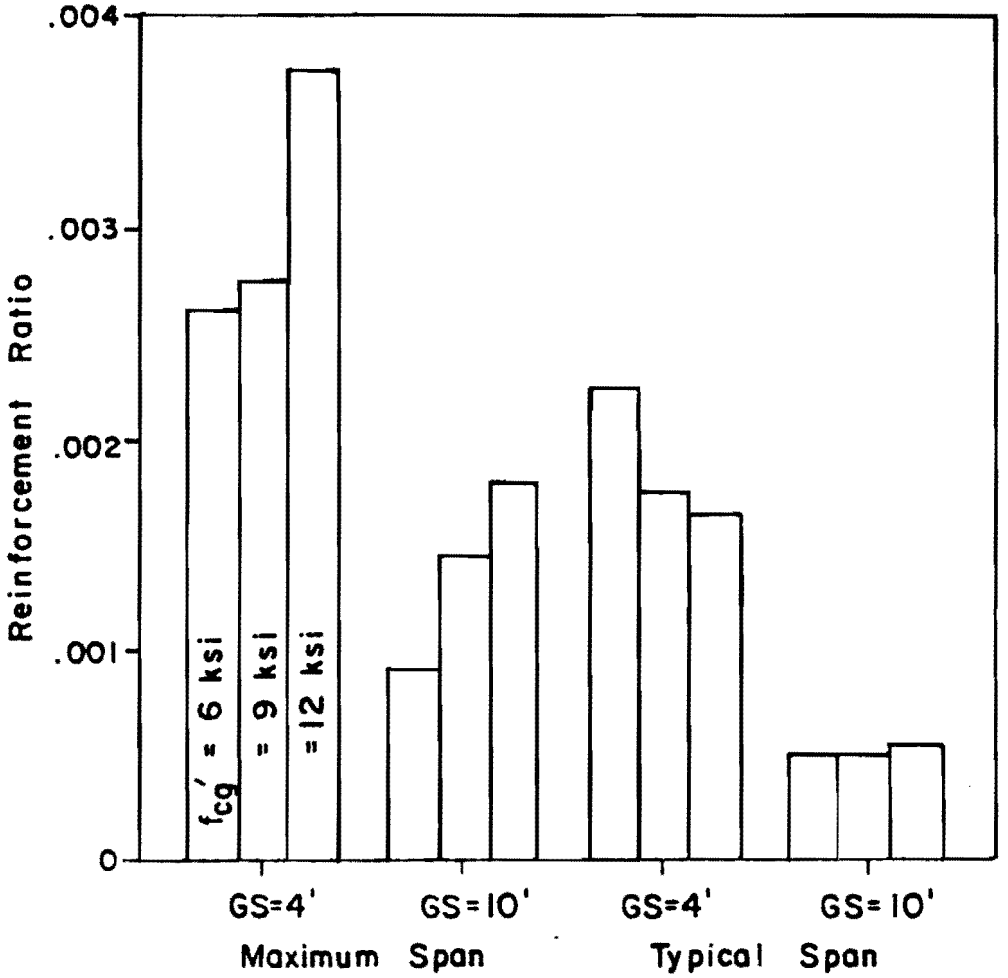

Fig. 4.34 Reinforcement ratio for maximum and typical span designs

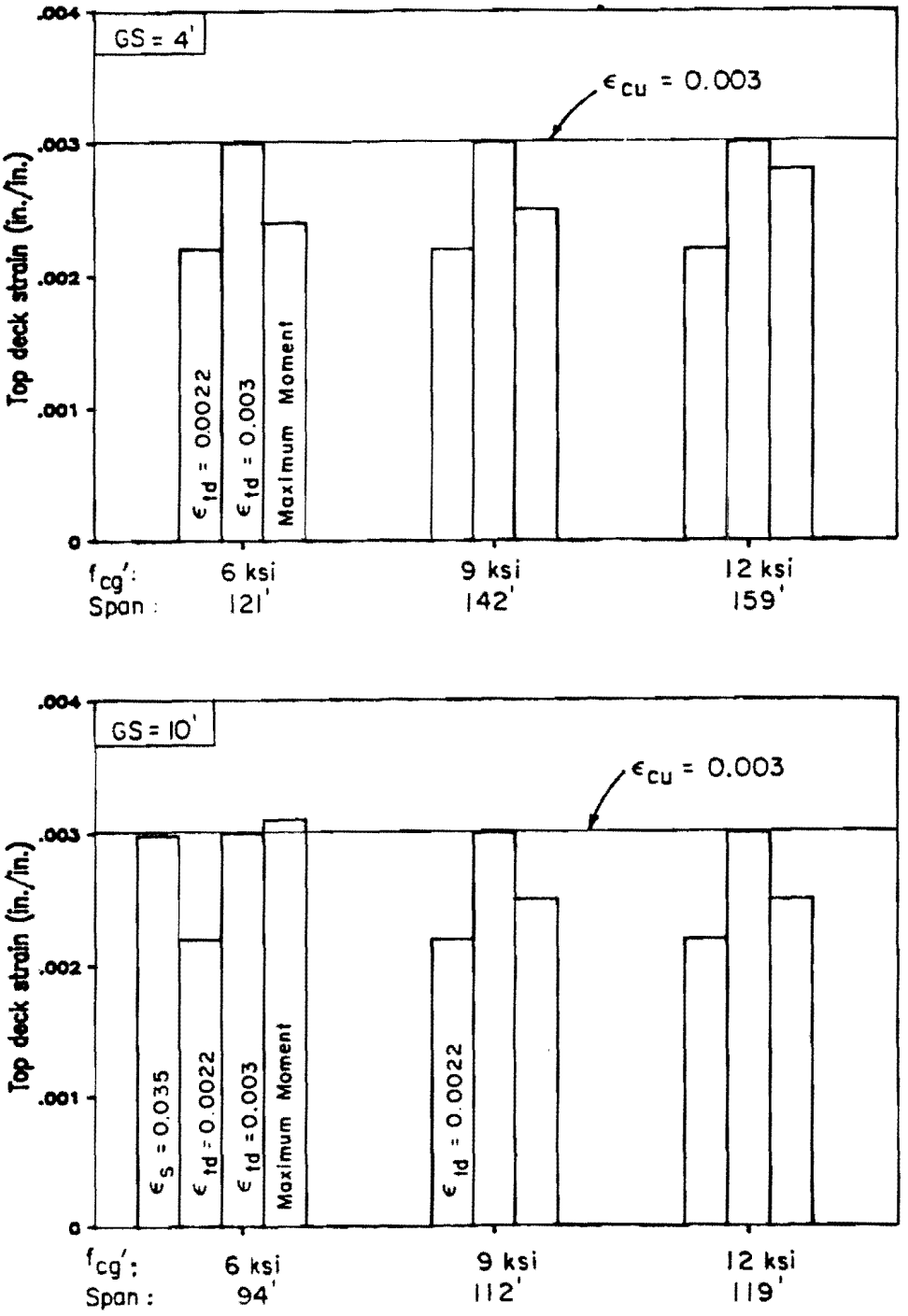

Fig. 4.35 Concrete strains at top of deck for maximum span designs

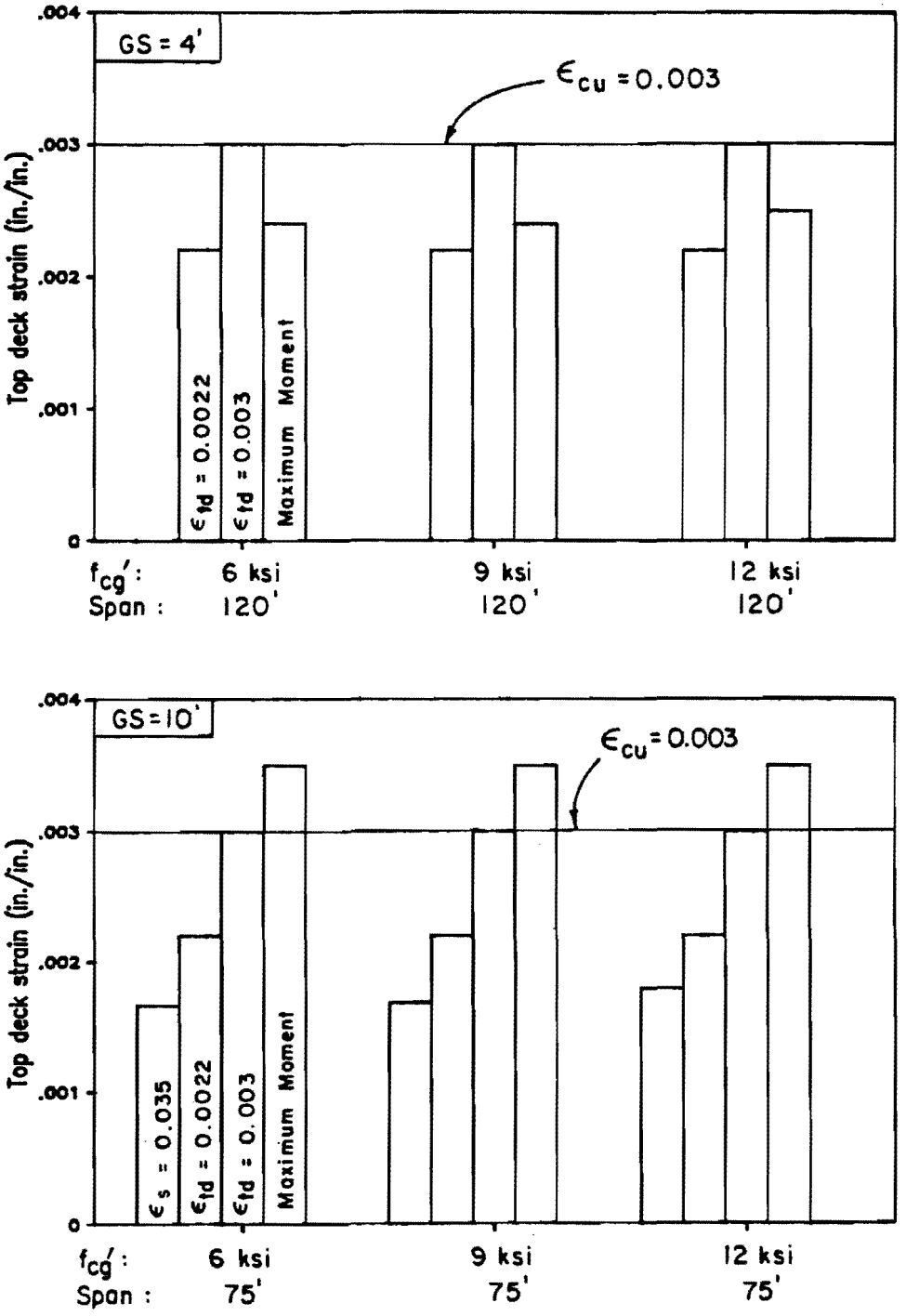

Fig. 4.36 Concrete strains at top of deck for typical span designs

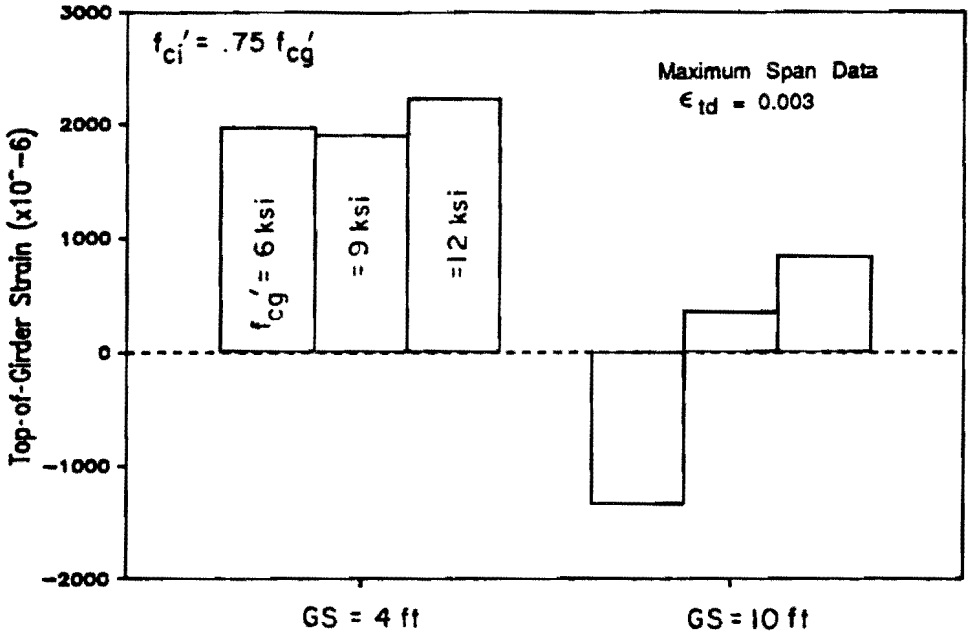

Fig. 4.37 Concrete strains at top of girder for maximum span designs

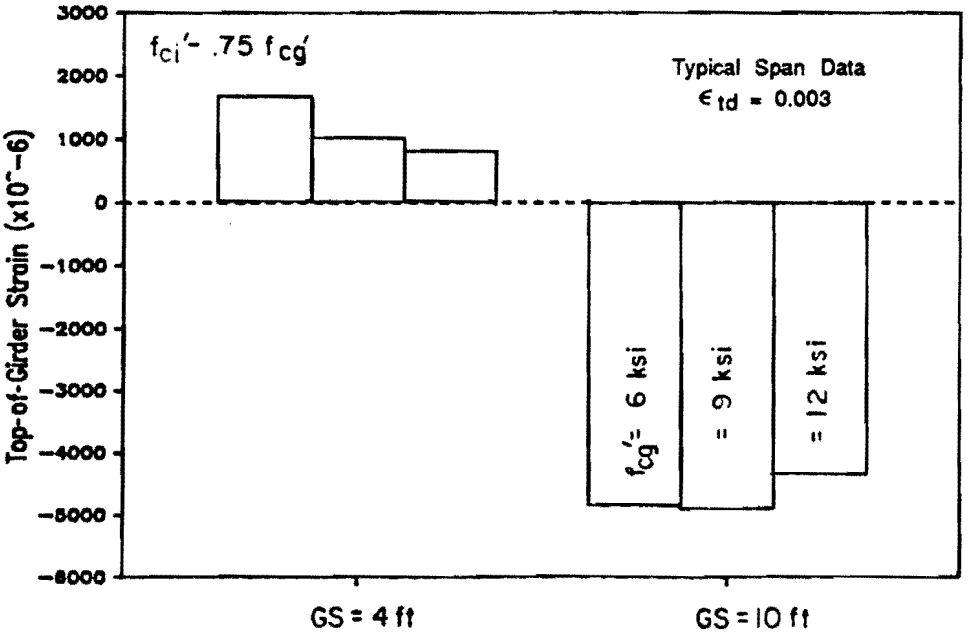

Fig. 4.38 Concrete strains at top of girder for typical span designs

4.2.5.3 Strand Stresses and Strains at Ultimate. Strand stresses at ultimate computed using the strain compatibility analysis and the simplified approaches are shown in Fig. 4.39 and 4.40 for maximum and typical span designs, respectively. The four conditions at ultimate used in the strain compatibility analyses given in the preceding section are also used here. The ultimate strand stress, f_{pu}, which occurs at a strain of 0.035, and the yield stress, f_{py}, which occurs at a strain of 0.01, are indicated on the figures. These stresses and corresponding strains are minimum values specified in ASTM A416 [25] and are typically exceeded by a significant margin for actual strands. The strain 0.035 is specified as the minimum permitted elongation at the ultimate strength of the strand. This strain therefore serves as a maximum strain limit for strands and will be referred to as the "limiting strain" in the following discussion.

For both maximum and typical span designs, the strand stresses at ultimate are very similar at the different ultimate limits used in the strain compatibility analysis. All values exceed the yield stress, which is considered desirable and indicates that the sections are under-reinforced. Where the strand strain exceeds the limiting strain early in the load history of the member (typical spans, GS = 10 ft), the strand stress exceeds the ultimate value. This occurs because the strand stress-strain curve equation does not terminate at the specified ultimate stress, but simply passes through the point and continues to higher stresses.

The simplified analysis methods showed reasonable agreement with the stresses obtained from the strain compatibility analysis. The AASHTO equation gave the lowest estimate for strand stresses, especially for high reinforcement ratios where the modifications that appear in the ACI equation for low relaxation strand have the greatest effect. The modification for concrete strength had no effect on the ACI ultimate stress values in these designs because the deck concrete strength was used in the equation and it remained constant. The simplified methods can give no indication that the strand stresses are excessive at ultimate because the equations are constructed so that the computed ultimate strand stress will approach but never exceed the ultimate strand stress.

While the moment capacity of the maximum span design for GS = 4 ft and f'_{cg} = 12 ksi was reduced for both AASHTO and ACI designs because reinforcement index limits were exceeded, this appears to be overly conservative considering the results of the strain compatibility analysis in which strand stresses were well above yield

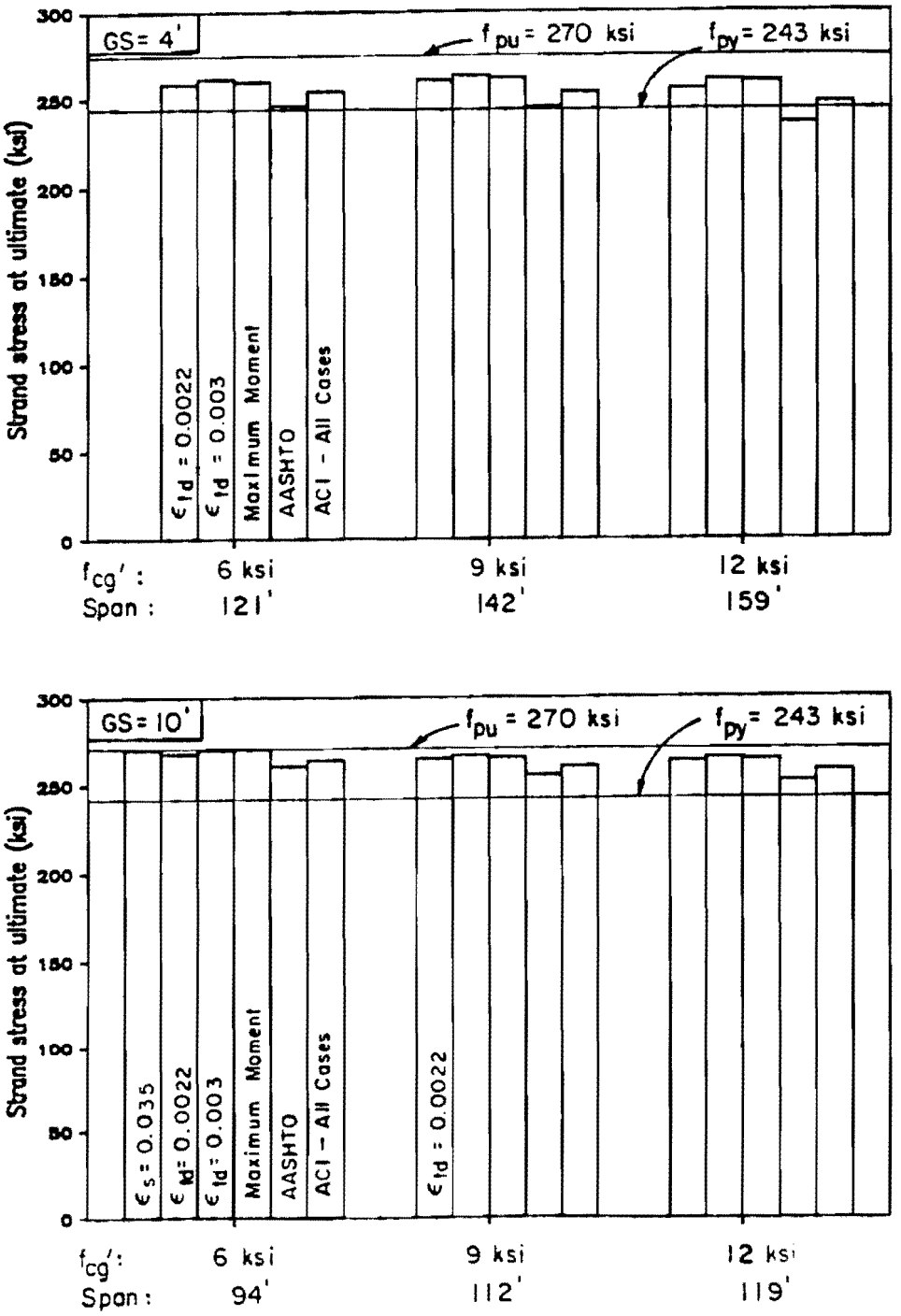

Fig. 4.39 Strand stress at ultimate for maximum span designs

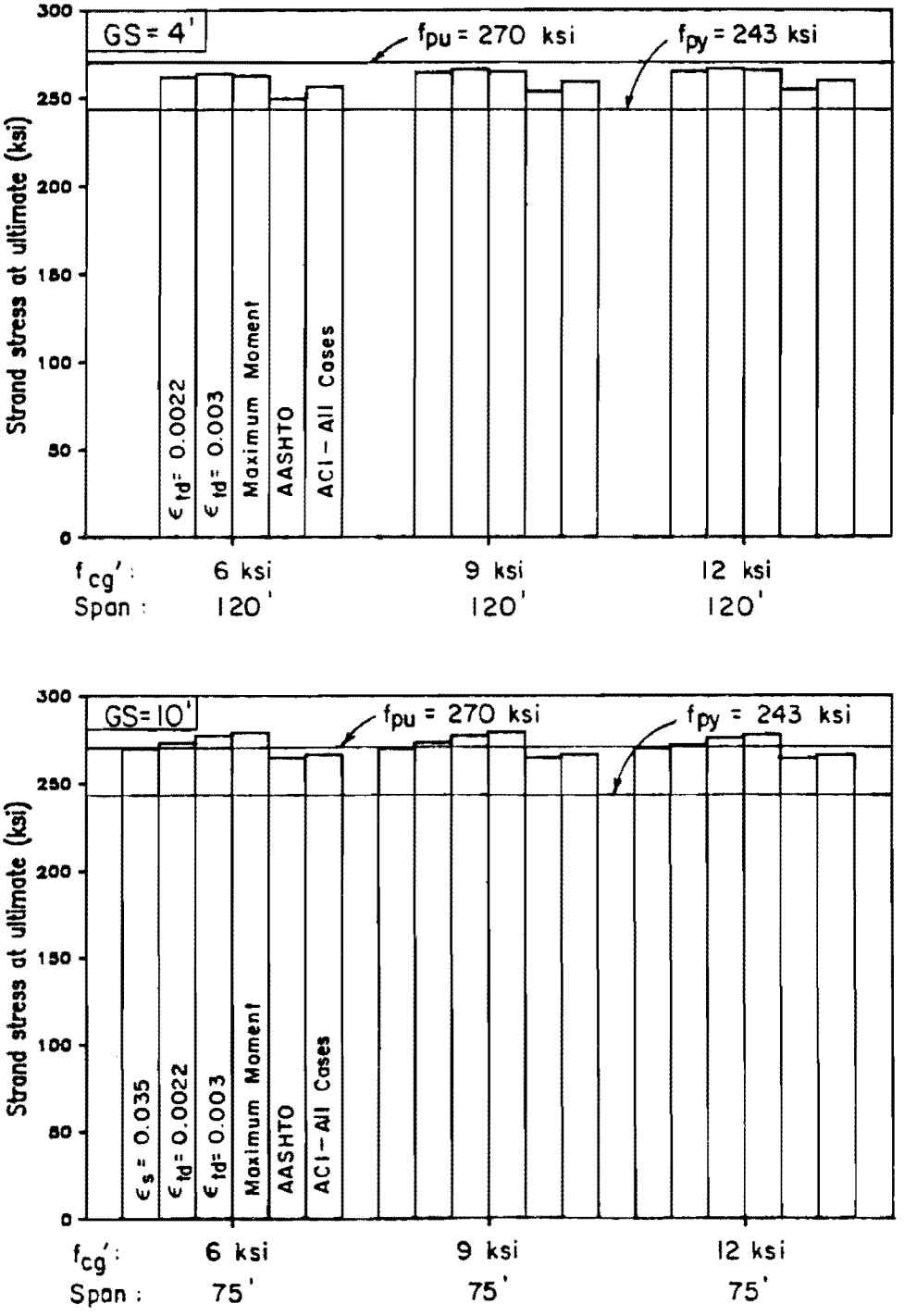

Fig. 4.40 Strand stress at ultimate for typical span designs

for this design. This question will be addressed further in a later section on ductility.

From this discussion and that in preceding sections regarding excessive strand stresses at ultimate, it appears that a minimum reinforcement limit needs to be developed. The current limit of 1.2 M_{cr} which is intended as a minimum limit was not effective in the case considered here, because it was not the controlling ultimate load criteria (see Fig. 4.32). While the actual design considered here may not be frequently encountered in practice, the design of brittle structures must be prevented.

The limiting strain of 0.035 was obtained from ASTM A416 [25] and applies to both stress-relieved and low relaxation strands. Preston [107], however, states that strand can generally sustain an elongation of 0.045 or more before failure. However, even this elongation is well below the 0.060 strain indicated by analysis to occur at a deck strain of 0.003 for the typical span designs with GS = 10 ft. The top-of-deck strains could be expected to reach 0.003 in these cases because a large strain gradient would be present in the deck near ultimate since the neutral axis is located within the deck. It is helpful to put the limiting strain for strands in perspective by noting that the minimum elongation (limiting strain) for new billet Grade 60 deformed bars varies from 0.07 to 0.09 (ASTM A615, [25]) and that deformed bars made of rail steel need an elongation of only 0.045 to 0.06 to meet the specification (ASTM A616, [25]). While these values are minimums, the high strength steel in strands is generally accepted to be more brittle than mild steel reinforcement.

Further consideration of the problem of an effective minimum reinforcement ratio in the context of overall member behavior will be given later in the section on ductility.

4.2.5.4 Effect of Concrete Modulus. In this section, the effect of the concrete modulus on the design and ultimate capacity of selected girder designs will be considered. The equation for estimating the modulus currently found in the codes [10,15]

$$E_c = 33 w_c^{1.5} \sqrt{f'_c} \qquad (4.4a)$$

$$= 57{,}000 \sqrt{f'_c} \text{ (for normal wt. conc.)} \qquad (4.4b)$$

where w_c = unit weight of concrete, lb per cu ft

will be compared with the equation for normal weight concrete proposed by investigators at Cornell [82]

$$E_c = 40{,}000 \sqrt{f'_c} + 1{,}000{,}000 \text{ psi} \quad (4.5)$$

The effect of the modulus on the design of a composite member is related to the ratio of deck to girder moduli since this is the ratio used to transform the deck concrete. This ratio is plotted versus the girder concrete strength for the two modulus equations in Fig. 4.41 using a constant deck concrete strength of 4 ksi. The percentage difference between these ratios, and the percentage difference between moduli for the two equations for a given concrete strength are shown in Fig. 4.42. These quantities vary less than 15 percent for concrete strengths considered in this study. The effect of using the different moduli on transformed section properties for different girder spacings and for different concrete strengths is shown in Fig. 4.43 and 4.44, respectively. These figures show that the moment of inertia is affected by less than 5 percent in both comparisons and that the section modulus for the bottom of the girder changes less than 2 percent. The top-of-girder section modulus, which is the most affected of all section properties, changes by as much as 12 percent.

When a design was performed using the two modulus equations, it was found that the difference was negligible. Using girder spacings of 4 and 10 ft with f'_{cg} = 12 ksi, the maximum spans differed by only one foot. The ultimate behavior was also compared using the strain compatibility analysis and the results were nearly indistinguishable, with ultimate moment capacities varying by at most 0.5 percent and the strand stress at ultimate differing by at most 0.25 percent. The depth to the neutral axis varied most with a 10.8 percent difference between the designs using the different modulus equations. The modulus does not affect ultimate capacities computed using the simplified methods.

A comparison of deflections was made for the same designs. For a beam constructed only of high strength concrete, the computed deflections would be 16 percent greater using the Cornell equation. However, for a composite, pretensioned bridge, the comparison is not as straightforward because the modulus affects losses and the effect of the deck in the composite structure differs according to the modulus of the girder. For the 120 ft spans with GS = 10 ft, the initial camber was 12.3 percent greater and the live load deflection was 9.8 percent greater for the Cornell equation. The comparison for the 159 ft span, which was not as clear because two fewer strands

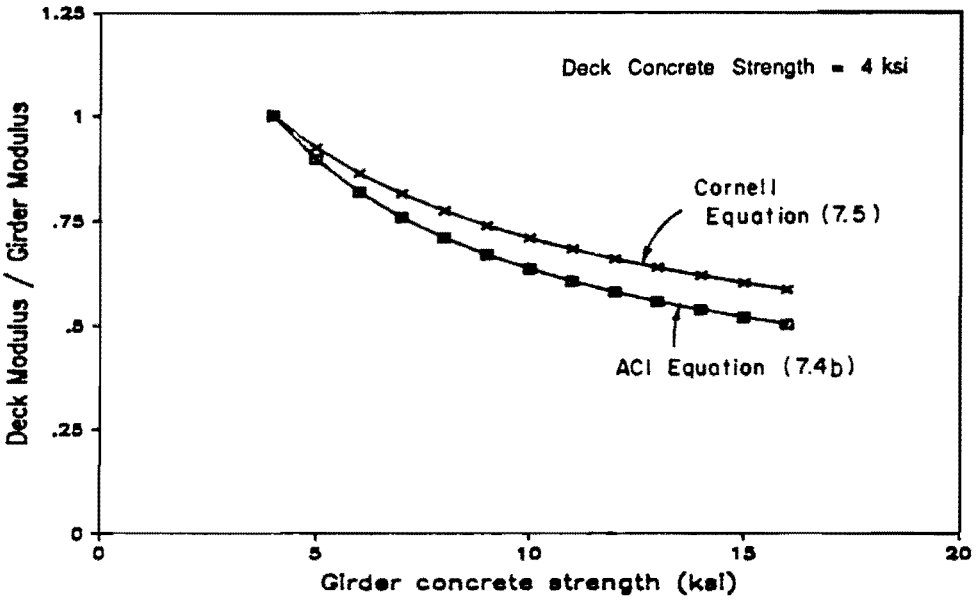

Fig. 4.41 Ratio of deck modulus to girder modulus for increasing concrete strength

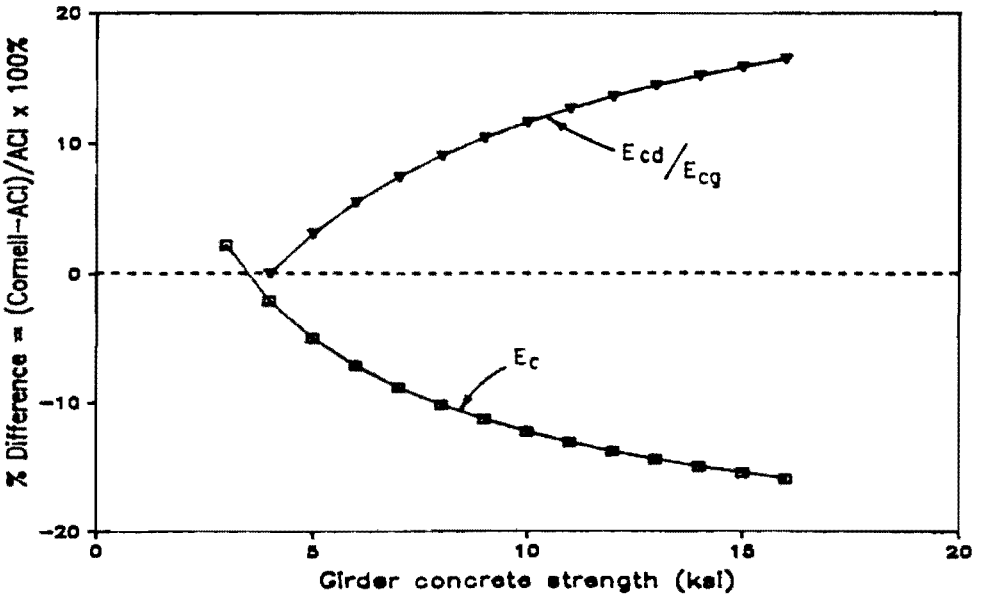

Fig. 4.42 Percentage difference between modulus equations for modulus and ratio of deck to girder moduli

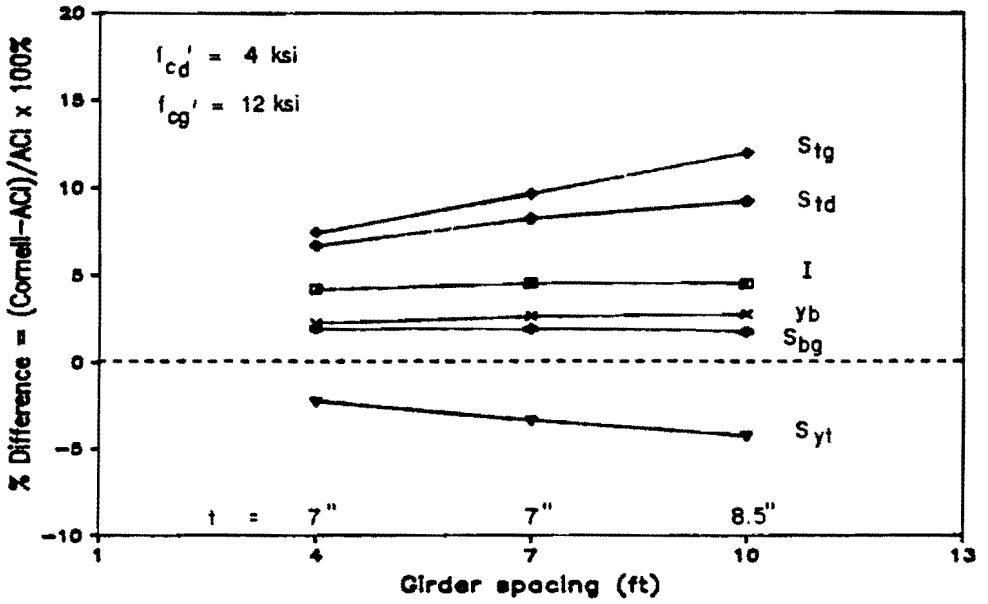

Fig. 4.43 Effect of modulus equations on section properties for different girder spacings

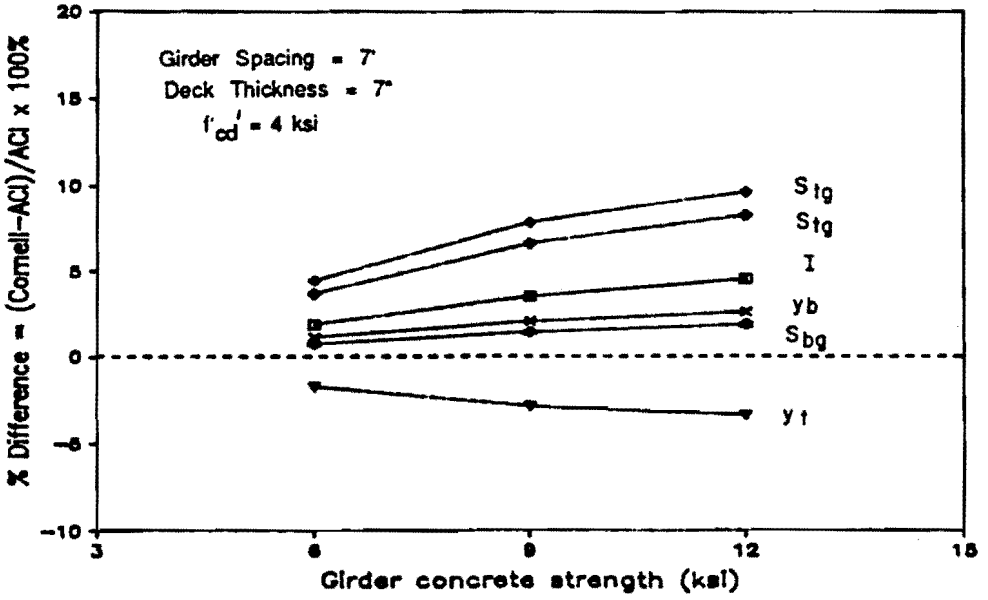

Fig. 4.44 Effect of modulus equations on section properties for different girder concrete strengths

could be used for the design using the Cornell equation, indicated a 4.2 percent increase in the live load deflection but the initial camber decreased by 1.1 percent when the Cornell equation was used. These comparisons indicate deflections are more sensitive to changes in the modulus than the allowable stress design and ultimate capacity, and the effect of the modulus on deflections decreases as the span increases.

This analysis shows that the differences between designs using the two equations for concrete modulus of elasticity are minor. Therefore, a decision on which equation should be used is not critical and should be postponed until more data becomes available to determine whether the Cornell equation or some other expression will provide a better estimate of the modulus than the formula in current use.

4.2.5.5 Concrete Strength Required at Release. A study of the minimum release strength required to satisfy design criteria was conducted for both maximum and typical span designs. The results are presented in Fig. 4.45. The first part of the figure shows the minimum concrete strengths required at release for the 12 designs considered. In all cases, the span length and number of strands used for the initial design, which used $f'_{ci}=0.75\ f'_{cg}$ were maintained, except where this was inadequate for some of the 6 ksi designs. In the case of the maximum span design with GS=4 ft and $f'_{cg}=12$ ksi, two designs were considered when it was found that the release strength could be reduced further by the addition of strands beyond the number required for the initial design. For the typical span designs, the minimum release strength actually decreased or remained constant as the design strength was increased, while the required minimum release strength for maximum span designs was found to increase with increases in the design strength.

The second portion of Fig. 4.45 shows the minimum release strengths as a fraction of the design strength. The higher design strength concrete generally requires a smaller portion of its strength to be available at release, although the reduction is small for the maximum span designs which are more typical of actual practice. For the typical span designs, the release strength could be as low as 25 percent of the 28 day strength. This would be of great benefit to the precast producers.

4.2.5.6 Summary. The following observations are made to summarize the discussion in the preceding sections.

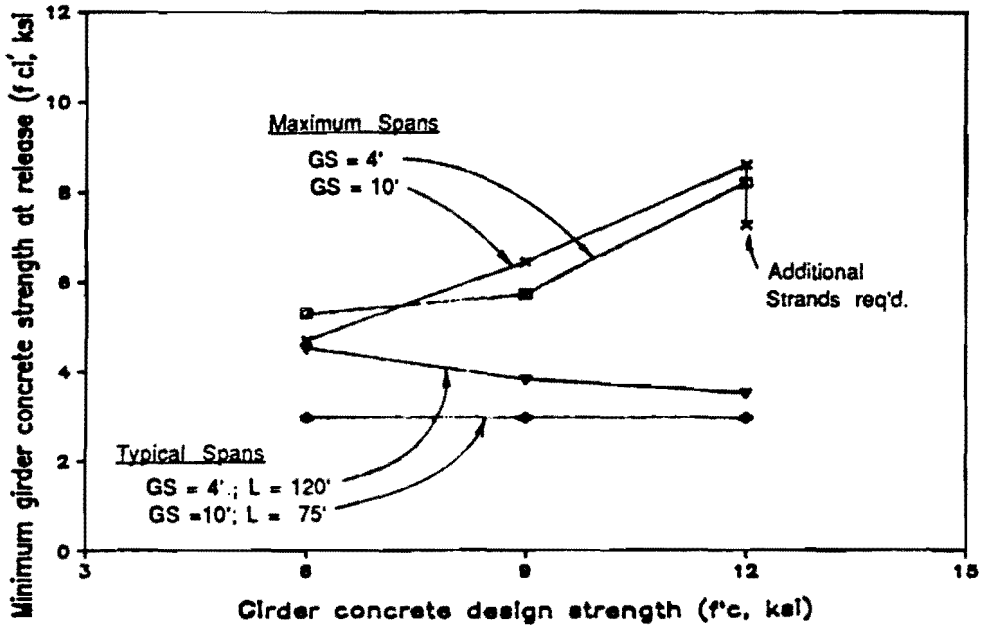

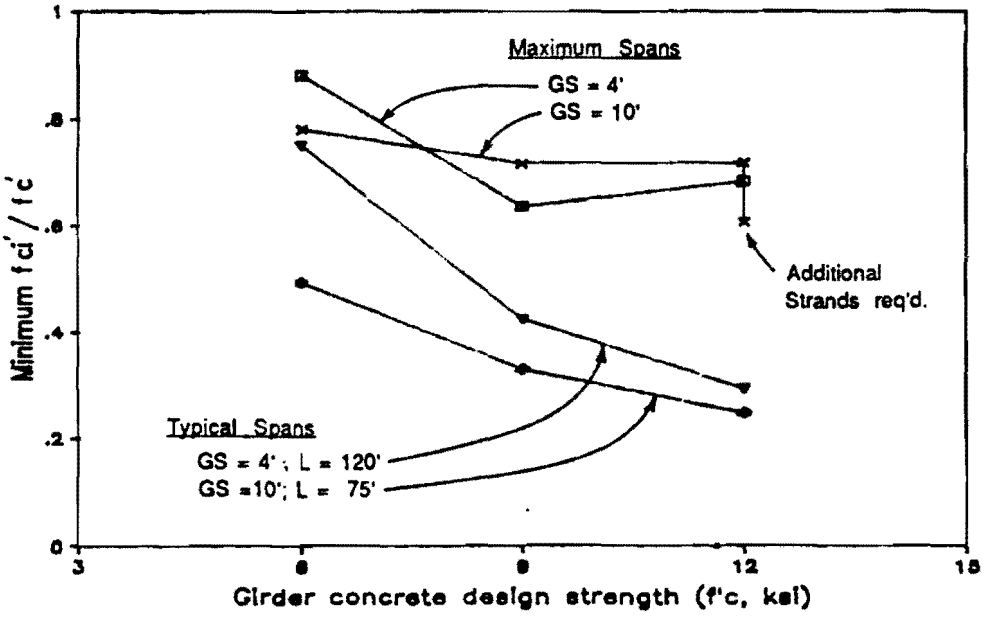

Fig. 4.45 Relationship between minimum concrete strength at release and design concrete strength for maximum and typical span designs: a) Minimum required concrete strength at release; b) Minimum release strength as fraction of design strength

1. Ultimate load criteria will govern most designs rather than the 1.2 M_{cr} limit.

2. An overload of 2.5 to 3 times the live load including impact is required to reach the factored load capacity for the range of designs considered if the dead load is held constant.

3. The cracking moment should be calculated considering all dead load effects rather than using an approximate form which neglects dead load.

4. The capacity for the range of designs considered remains nearly constant for a wide range of top-of-deck strains including 0.0022 to 0.003.

5. Analysis shows that strand may reach the minimum ASTM specified elongation (limiting strain) prior to the top of deck reaching the maximum usable concrete strain.

6. The simplified analysis methods using current assumptions for the ERSB agreed well with ultimate capacities computed using the strain compatibility analysis for a range of concrete strengths including high strength concrete.

7. The computed nominal capacity for the range of designs considered was generally significantly larger than the controlling ultimate load. In cases of short spans, however, the ultimate load controlled design.

8. Analysis indicates that it is possible to obtain a stable "semi-flanged" behavior condition in which, for a wide range of top-of-deck strains, the top of the girder remains in compression after the bottom of the deck has cracked.

9. The maximum moment frequently occurs at a top-of-deck strain less than the maximum usable concrete strain (0.003), but always greater than 0.0022 for the designs studied here.

10. The use of a maximum usable strain of 0.003, while sufficiently accurate for flexural capacity computations,

may lead to unconservative estimates for quantities such as curvature, depth of compression, and strand strain.

11. It is unlikely that the girder concrete would crush prior to the deck concrete in the designs considered here.

12. The strand stress remained fairly constant for the range of top-of-deck strains considered (0.0022 to 0.003).

13. In all designs, the strand stress computed using the strain compatibility analysis exceeded the specified yield stress at ultimate.

14. The simplified methods provided conservative, yet reasonable estimates of the strand stress at ultimate when compared with the strain compatibility analysis results. The current ACI ultimate strand stress equation provided a better estimate of strand stress at ultimate than the AASHTO equation, especially for high reinforcement ratios.

15. The reduction of the ultimate capacity when the reinforcement index exceeds specified limits appears to be over-conservative.

16. The current minimum reinforcement limit involving the cracking moment is not sufficient to prevent rupture of strands before the top of the deck has reached the maximum usable concrete strain. This situation occurred in very lightly reinforced girders which may not be considered typical designs.

17. The effect of using the concrete modulus equation given in the codes or proposed by investigators at Cornell is small for both allowable stress design and strength analysis using the strain compatibility method. Deflections were affected more strongly, but the difference became small at the maximum span length. Therefore, a change in equation does not appear warranted until further study can be made.

18. The minimum concrete strength required at release may be as low as 25 percent of the design strength for high strength concrete and is typically less than that required using normal strength concrete. However, the

minimum release strength remains a fairly constant fraction of the design strength for designs at or near the maximum span for a given concrete strength, which are more typical of current design practice. Any reduction in the release strength relative to the design strength would be an advantage in the manufacture of pretensioned members.

While not directly studied in this section, it is recommended that a maximum usable concrete strain of 0.003 be used for composite sections where the neutral axis is within the deck at ultimate, and a maximum usable concrete strain of 0.0022 to 0.0025 be used where the neutral axis is located within the girder at ultimate. The difference is a result of the strain gradient present at failure, which would be great for the first situation in which concrete near the extreme fiber, which is not as highly stressed, would offer confinement to concrete at the extreme fiber. However, when the girder is in compression at failure, the compression in the deck is more uniform and the confining effect would not be as great. Further study of this problem is needed.

4.3 Ductility

While ductility can be defined in many ways, the historic approach taken for prestressed and reinforced concrete members to ensure a ductile failure is the limitation of the quantity of reinforcement. Limits based on the reinforcement ratio have apparently worked well and they avoid the difficulties encountered when curvatures or deflections are used as a measure of ductility for a prestressed section or member.

This section opens by investigating the accuracy of the reinforcement index computed using the simplified methods when compared with results of strain compatibility analyses. Proposals are then made for both maximum and minimum reinforcement limits that are based on the same reasoning as the original maximum reinforcement limits. The limits will be compared with test and analytical data to determine the adequacy of the limits.

4.3.1 Accuracy of Reinforcement Index for Simplified Methods.

Since reinforcement limits for prestressed members are based on the reinforcement index, the accuracy of this quantity was investigated. Because values of the reinforcement index computed using the AASHTO and ACI simplified methods differ only by the estimate for the

ultimate strand stress, the ACI equation will be used since it is more accurate. Flanged section analysis is used in both codes to compute the reinforcement index when the neutral axis is located below the deck at ultimate.

The reinforcement index, w_p, computed using the equation

$$w_p = \rho_p f_{ps} / f_c'$$

was determined for each maximum and typical span design using the ACI simplified method and results of the strain compatibility analysis. The two values are compared graphically in Fig. 4.46 for both gross section (Cases I and II) and transformed section (Cases III and IV) approaches. The plots include data from Naaman et al. [97] for monolithic rectangular and T-beam sections for a range of concrete strengths. The data are closely clustered about the line of equality for data from both the current study and Naaman et al. [97]. Agreement is similar for the different cases of gross and transformed section dimensions. This demonstrates that the simplified methods give good estimates of the actual reinforcement ratio and will therefore provide reasonable estimates for use with limits. Useof the AASHTO equation will, however, give unconservative estimates since the AASHTO estimate of ultimate strand stress is low. The comparison with Naaman's data indicates that agreement between the simplified method and strain compatibility analysis is consistent for monolithic and composite members.

The effect of nonprestressed tension reinforcement and compression reinforcement can be included in the reinforcement index. The expression proposed by Naaman et al. [97]

$$\omega = \left[A_{ps} f_{ps} + A_s f_s - A_s' f_s' - 0.85 \beta_{1_c}' h_f (b - b_w) \right] / (b_w d f_c') \qquad (4.6)$$

appears to be suitable, although it was derived using a slightly different definition of the effective depth.

4.3.2 Maximum Reinforcement Limit. Current and proposed limits on the reinforcement index are discussed and are then compared with test and analytical data to determine the adequacy of the limits.

4.3.2.1 Current and Proposed Limits. For reinforced concrete sections, a maximum allowable reinforcement ratio is set by limiting the percentage of steel to three-quarters of that required to produce a balanced failure, i.e.,

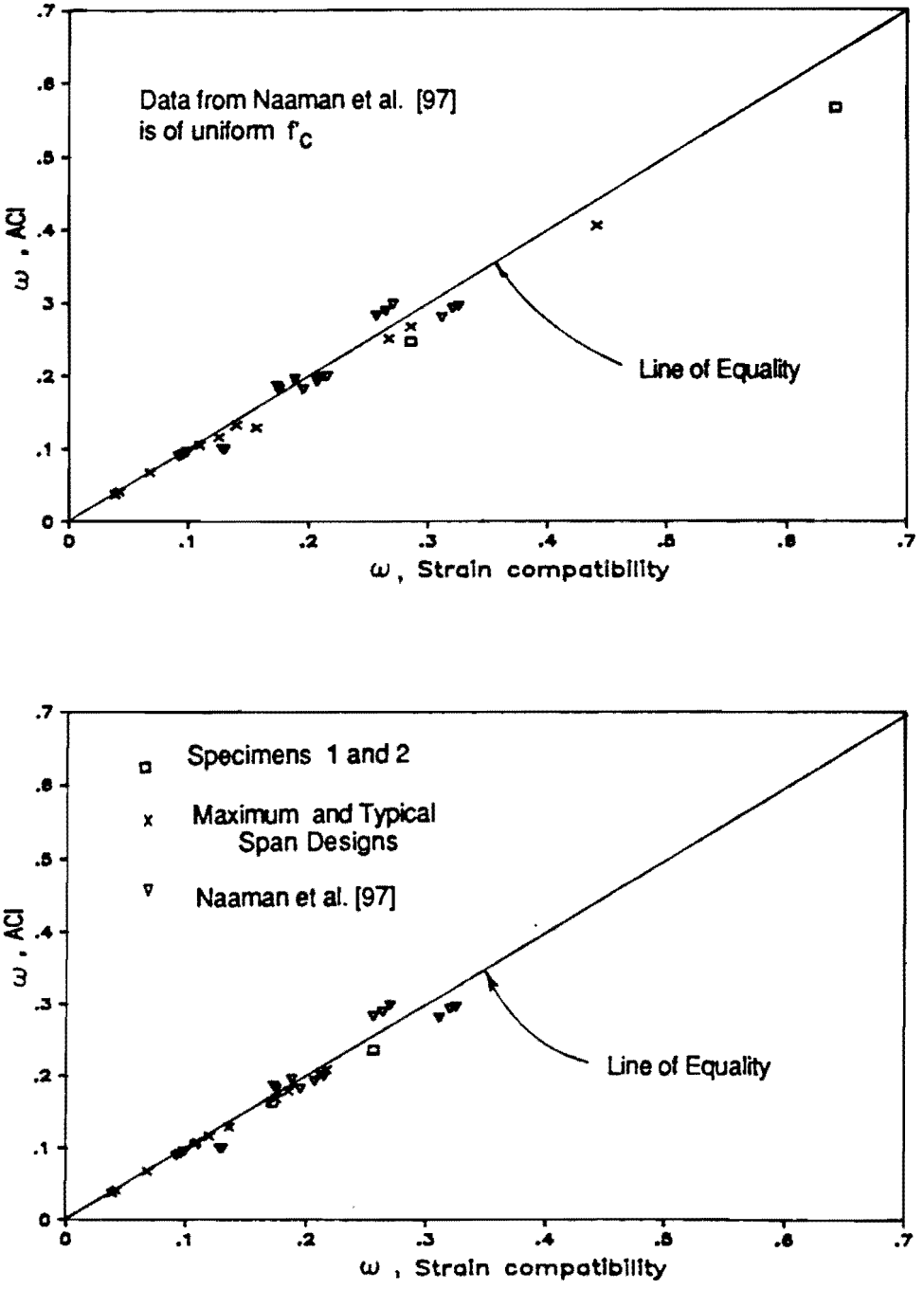

Fig. 4.46 Comparison of w computed using simplified ACI approach and strain compatibility analysis: a) Gross section dimensions - Cases I and II; b) Transformed section dimensions - Cases III and IV

$$\rho = A_s/bd \leq 0.75\ \rho_b$$

where ρ_b = reinforcement ratio corresponding to a balanced failure.

By definition, a balanced failure occurs when the strain in the extreme compression fiber reaches the maximum usable concrete strain as first yielding of the steel occurs. The reinforcement ratio corresponding to balanced failure can be computed for rectangular sections using the following equation

$$\rho_b = \beta_1 0.85 f'_c/f_y[87/(87+f_y)] \qquad (4.7)$$

where stresses are expressed in ksi units, which is given in the Commentary of the ACI Code [17].

For prestressed concrete members, a slightly different approach is taken in which the reinforcement index,

$$\omega_p = \rho_p f_{ps}/f'_c$$

where ρ_p = ratio of prestressed reinforcement
$= A_{ps}/bd_p$

must be less than a limiting value which is intended to correspond to the balanced failure condition. For prestressed members, the definition of a balanced failure is not as clear as for reinforced members because the yield point for prestressing steel is not as well defined as that for reinforcing bars. The motivation for the different approach for prestressed sections was discussed in Sec. 2.5.1 and appears to be reasonable.

The assumptions used to derive the current maximum reinforcement limits are summarized in Fig. 4.47, which also includes an early proposal by Warwaruk et al. [133] which never appeared in the codes. As shown in the figure, the maximum reinforcement limits for both AASHTO and ACI are based on an approximate strain compatibility analysis of a section at ultimate. The top fiber strain was assumed to be 0.004 which is inconsistent with the maximum usable strain specified elsewhere in the codes and significantly exceeds the strains measured in the scale-model tests. The limits also assume a yield strain of 0.01 and an average of typical values for the effective prestress which were based on the use of Grade 250 strand.

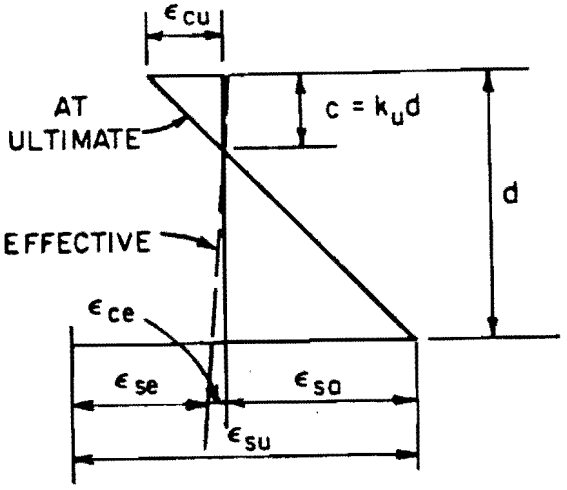

$$k_u = \frac{F\epsilon_{cu}}{F\epsilon_{cu} + \epsilon_{sa}}$$

$$= \frac{F\epsilon_{cu}}{F\epsilon_{cu} + \epsilon_{su} - \epsilon_{se} - \epsilon_{ce}}$$

$$= \rho \frac{f_{su}}{f_{cu}}$$

$$= c/d$$

	Warwaruk et al. 1962	ACI Comm 323 (current AASHTO) 1958	ACI 318-83 1983	Proposal
Reference	[133]	[10, 19]	[15]	Appendix A
F	1	1	1	1
ϵ_{cu}	0.003	0.004	0.004	0.003
ϵ_{su}min.	0.01*	0.01*	0.01*	$0.01+(f_{pu}-250)/28000$
ϵ_{se}	0.0045**	0.0045**	0.0045**	$f_{se}/28000$
ϵ_{ce}	0	0	0	0
$k_u$limit	≤ 0.353	≤ 0.421	≤ 0.421	$\leq 84/[114+f_{pu}-f_{se}]$
f_{cu}	$0.7f'_c$	$0.7f'_c$	$0.85\beta_1 f'_c$	$0.85\beta_1 f'_c$
ω	0.25	0.30	$0.36\beta_1$	$0.85\beta_1[84/(114+f_{pu}-f_{se})]$

* - Based on Grade 250 material.

**- An average of the expected range from 0.004 to 0.005.

Modulus of strand is assumed to be 28000 ksi. Stress units in ksi.

Fig. 7.52 Summary of maximum reinforcement limit assumptions

The new proposal, which follows the same reasoning as the current limits, is also shown in Fig. 4.47. A more complete development of the limit is given in Appendix D.1. The equation expressing the new limit is

$$w_p \leq 0.85\beta_1[84/(114 + f_{pu} - f_{se})] \quad (4.8)$$

where f_{pu} and f_{se} are expressed in ksi. This equation, while more complex than current limits, considers important parameters that are neglected in the current limits and corrects assumptions that are inconsistent with the remainder of the current codes. The maximum usable concrete strain of 0.003 used in the derivation of the proposed limit agrees with the requirements of the ERSB. While this strain may be larger than the actual strain in some cases as mentioned in preceding sections, use of 0.003 is an improvement over the current limit and this value can be modified as needed by the designer or code writers if the derivation of the limit is made available in code documents. Since Grade 270 strand is now in general use and further increases in strength are possible, the yield strain was expressed as a function of the ultimate strength of the strand in order to reflect the changing shape of the stress-strain curve. Although current limits assume a fixed value for the effective prestress, variation in the effective prestress was found to have a significant effect on the limit and is therefore included in the expression. Since the effective prestress is known in design, its inclusion in the equation is not a large complication. The proposed equation appears in a form that is very similar to the equation used to determine the limiting reinforcement ratio for reinforced concrete sections (Eq. 4.7) and should therefore be easily understood and accepted by the profession. The derivation of the limit is based on a monolithic section and is therefore an estimate of the behavior for a composite section, since the difference in curvature between the girder and deck is not included in the analysis. However, this error is small.

It was found that the current limits can be unconservative when compared with the more accurate and consistent proposed limit. This is because existing limits use a high limiting concrete strain and neglect variation in the effective prestress. The existing AASHTO and ACI limits are compared with the proposed limit for low and high strength concrete and three grades of strand in Fig. 4.48. The unconservatism of the current limits for some values of effective prestress and the substantial effect of variation in the effective prestress and grade of strand is evident. The effect of the concrete

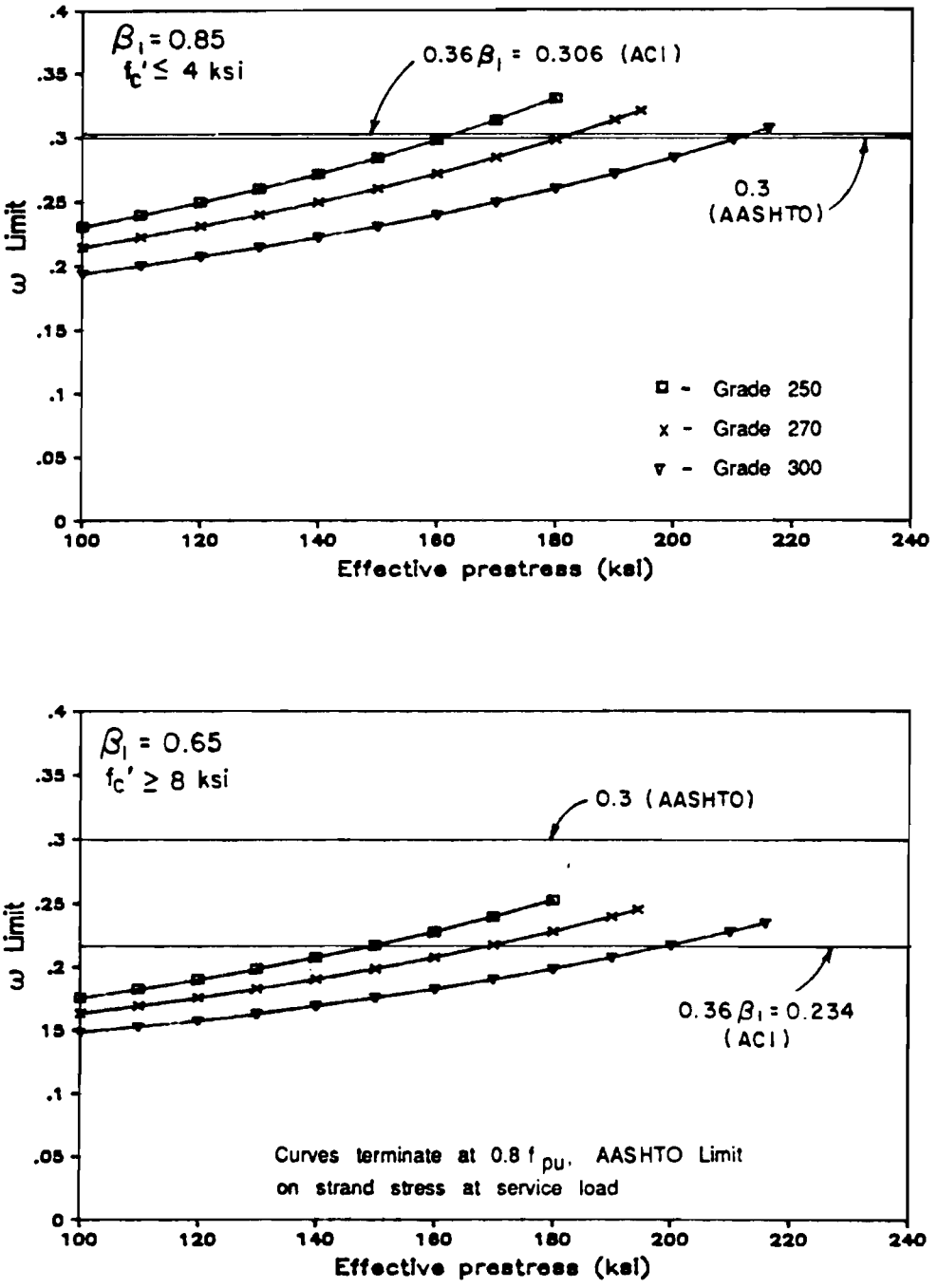

Fig. 4.48 Maximum reinforcement limits versus effective prestress: a) Low strength concrete - $f'_c \leq 4$ ksi; b) High strength concrete - $f'_c \geq 8$ ksi

strength on the limits is removed to facilitate comparison with the ACI limit in Fig. 4.49, and the ratio of the proposed limit to the ACI limit is shown in Fig. 4.50. In Fig. 4.50, it can be seen that for lower effective prestress levels and for increasing strand strength current limits become more unconservative. For the effective prestress encountered in the designs considered in this chapter, which varied from 156 ksi to 182 ksi, the proposed limit for Grade 270 strand is from 87 to 98 percent of the current ACI limit. Therefore, the unconservatism of the current limit is not great and conversely, the proposed limit does not vary greatly from the current limit.

4.3.2.2 Accuracy of Maximum Reinforcement Limit. Two factors are of interest in exploring the accuracy of the maximum reinforcement limit: determination of the best method to use for computing the reinforcement index, ω, and whether the limit accurately or conservatively predicts yielding of the strand.

The need for the determination of appropriate assumptions to be used to compute ω is clear from the variety of values and their relationship to the limits displayed in Fig. 4.51 for the test specimens and maximum span designs with GS = 4 ft. The designs shown in the figure were the only designs where ductility limits were of concern. The confusion is greatest for Specimen 1 and for the 12 ksi maximum span design. In these cases, the limits were exceeded by a large margin for the untransformed cases (AASHTO and ACI Cases I and II) which indicated that failure would be expected well before yielding of the strand.

Examination of Fig. 4.52, which gives the increase in strand strain for the specimens during flexure tests, indicates that failure occurred just after reaching the yield strain. Similar curves for the 12 ksi maximum span designs, which include the case with GS = 4 ft mentioned above, appear in Fig. 4.53 and indicate definite straining of the strand past yield prior to failure. Therefore, the untransformed values of ω are over-conservative. The transformed cases (ACI Cases III and IV) appear to be more reasonable representations of behavior, indicating that yield was still reached or was very close to being attained. Of the two transformed cases, Case III appears to be the more accurate because it correctly predicts that yielding, although limited, would occur in both Specimen 1 and the 12 ksi maximum span design. It is also clear from this comparison that the proposed limit is a better approximation of behavior for Case III, since, for Specimen 1, ω is very close to the limit as is the case based on the test and analytical data.

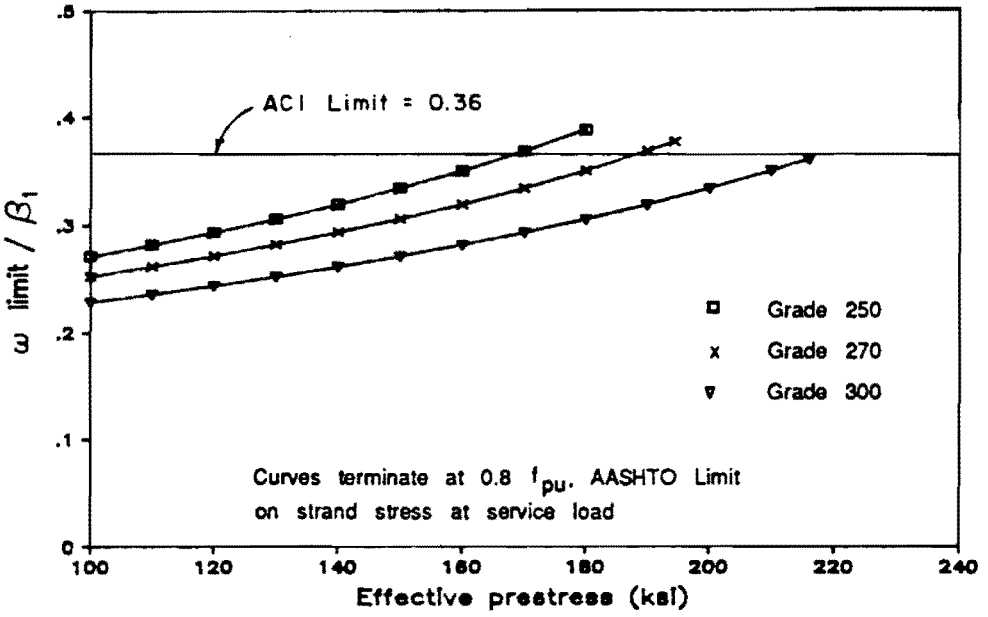

Fig. 4.49 Ratio of maximum reinforcement limit to β_1 versus effective prestress

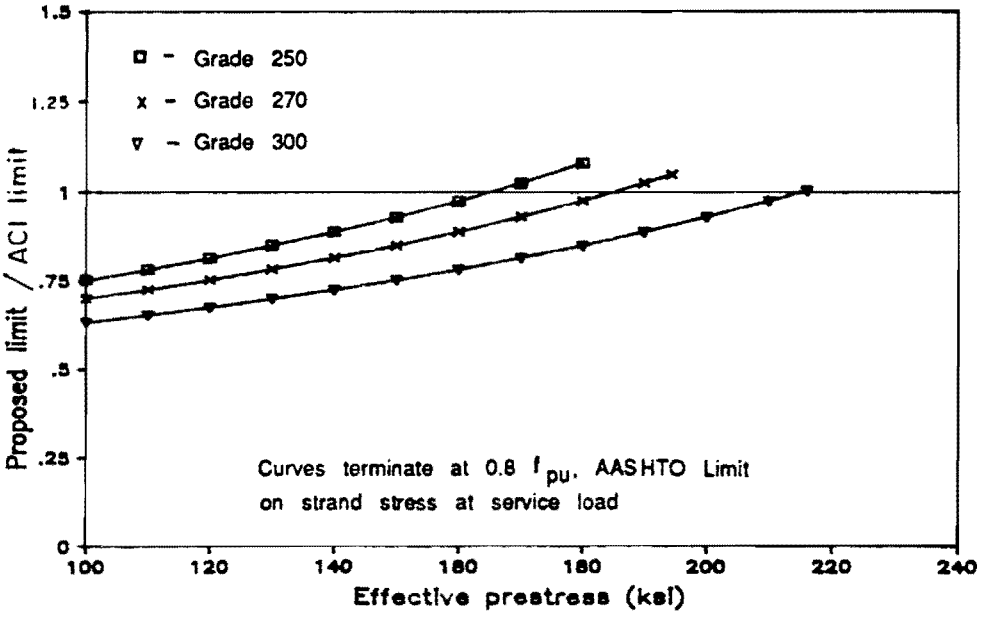

Fig. 4.50 Ratio of proposed maximum reinforcement limit to ACI limit versus effective prestress

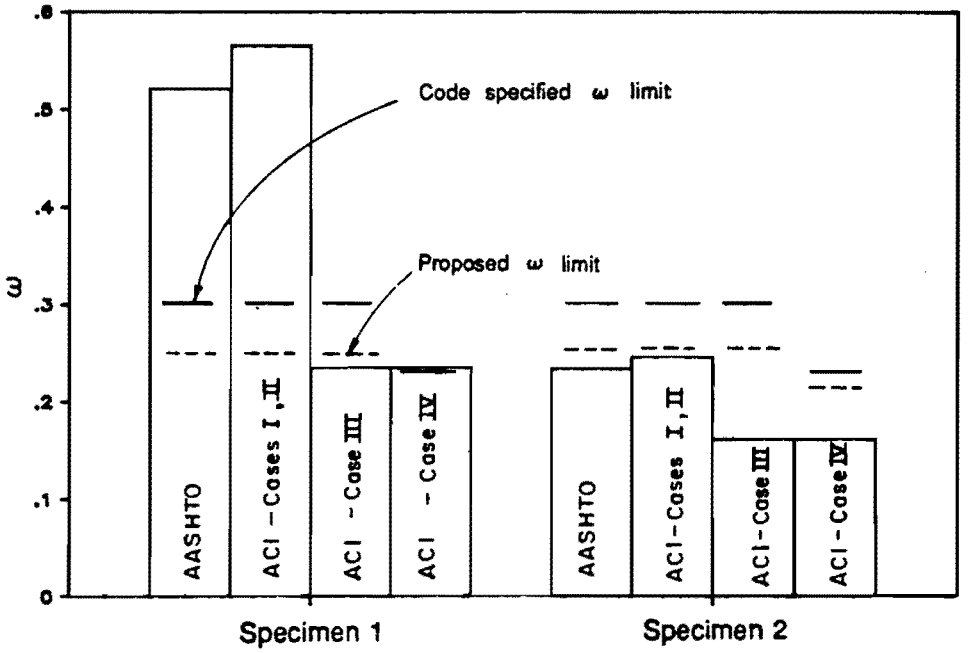

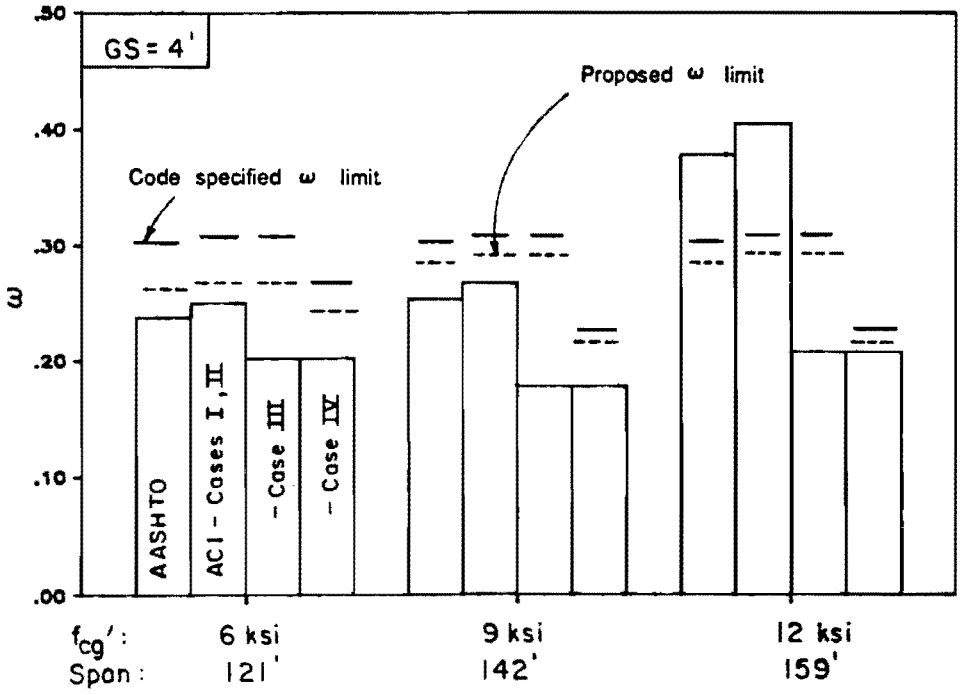

Fig. 4.51 Comparison of values and maximum limits for w for specimens and maximum span designs with GS = 4 ft

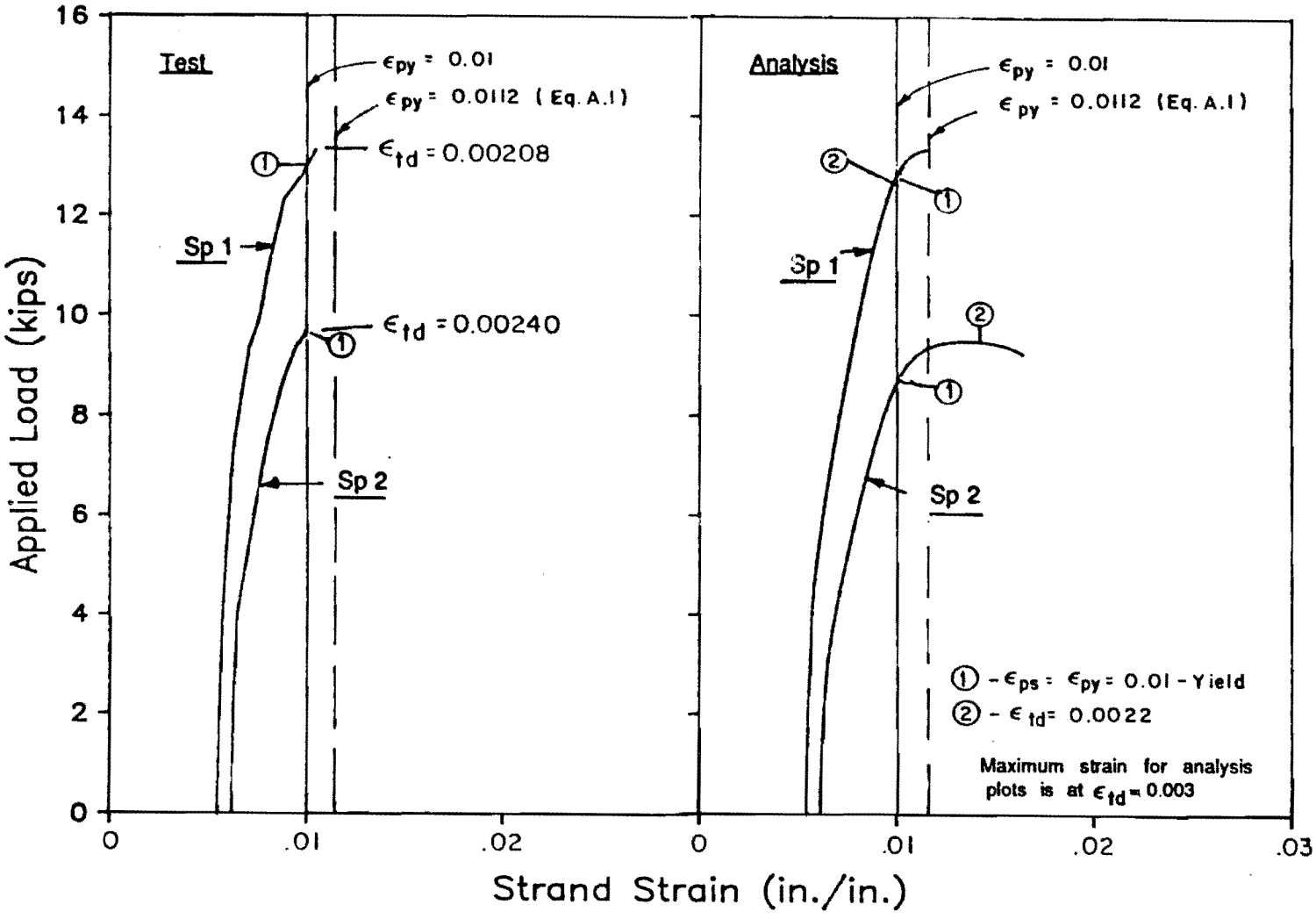

Fig. 4.52 Strand strain versus applied load for specimens

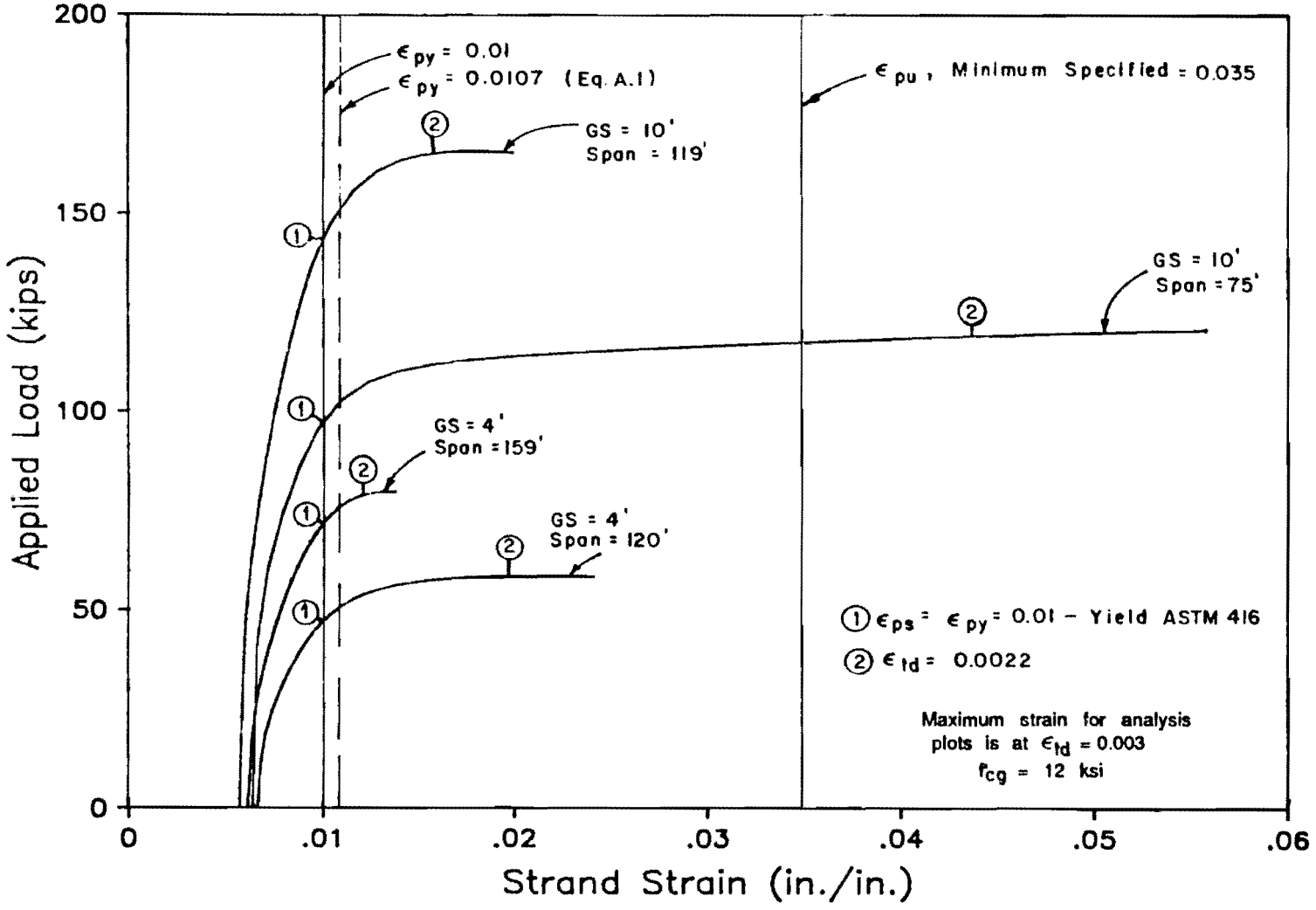

Fig. 4.53 Strand strain versus applied load for maximum and typical span designs with f'_c = 12 ksi

Another comparison which demonstrates that the transformed methods are more accurate is shown in Fig. 4.54. This comparison is based on findings by Naaman et al. [96,97] that, for a wide variety of monolithic rectangular and T-beam sections with a range of concrete strengths and prestressed and nonprestressed reinforcement, the ratio of the depth of the compression zone at ultimate to the effective depth is linearly related to the reinforcement index. The regression equation they developed is shown in the figure. When values for the specimens and designs used in this chapter are added to these plots, it can be seen that data points with ω computed using gross section dimensions do not conform to the trend observed by Naaman, while points using transformed dimensions conform very well. Therefore, it is recommended that ω be computed using section dimensions transformed by the ratio of the concrete strengths of the deck and girder so that predicted behavior for composite sections will conform to behavior of monolithic sections.

A final series of comparisons is made using Fig. 4.55, 4.56 and 4.57, which show the ratio of the ultimate strand strain to the yield strain versus the corresponding ratio of ω to the ω limit for Cases I and II, Case III, and Case IV, respectively. The yield strain is defined by the function of the ultimate strength of the strand as used in the proposed limit (Eq. 4.8) and discussed in Appendix A.1. Points plotted in the figures represent the test specimens and all maximum and typical span designs. Data for the maximum and typical span designs are connected with a curve to indicate the trend of the data. The strain ratio should approach unity as the ω ratio approaches unity if the limit is accurate. The ω limit is conservative if the strain ratio is greater than unity when the ω ratio is one, because this indicates that the strand is actually yielding even though the ω limit has been reached. Data for Cases I and II (Fig. 4.55) demonstrate the conservatism of the use of gross section dimensions. Data for Case IV in Fig. 4.57 is also conservative. The data shown in Fig. 4.56 for Case III appear to best fit the desired behavior.

The maximum reinforcement ratio for prestressed members appears to represent the balanced failure condition ($\rho/\rho_{bal} = 1$) because the strand strain that forms the basis for the limit is the yield strain. This yield strain, however, does not have the same meaning as the yield strain for conventionally reinforced concrete members where the stress-strain behavior of the reinforcement is essentially bilinear. For conventional reinforcement, the yield strain represents the strain at which inelastic behavior begins.

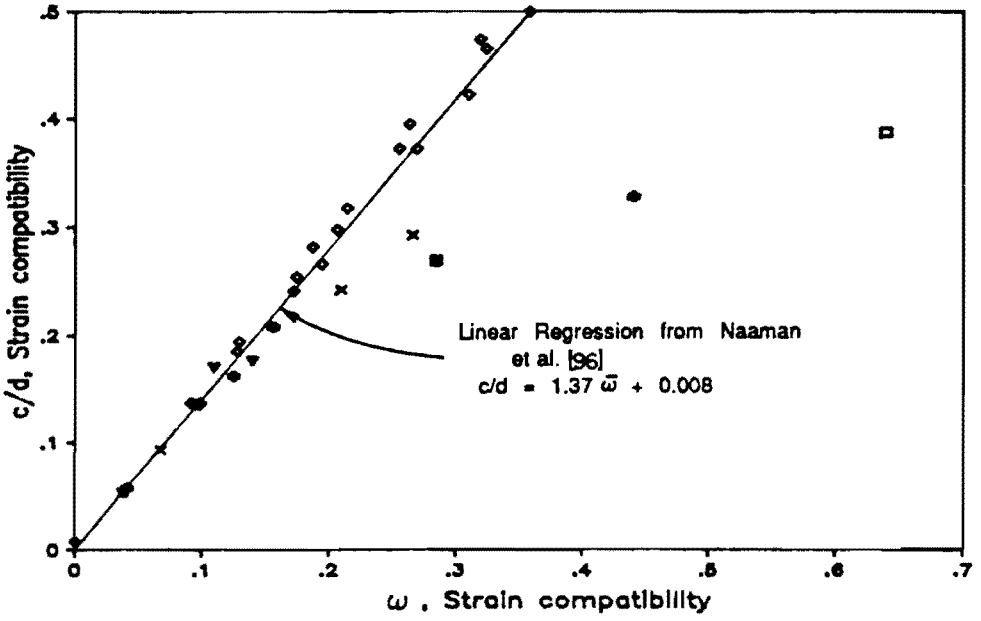

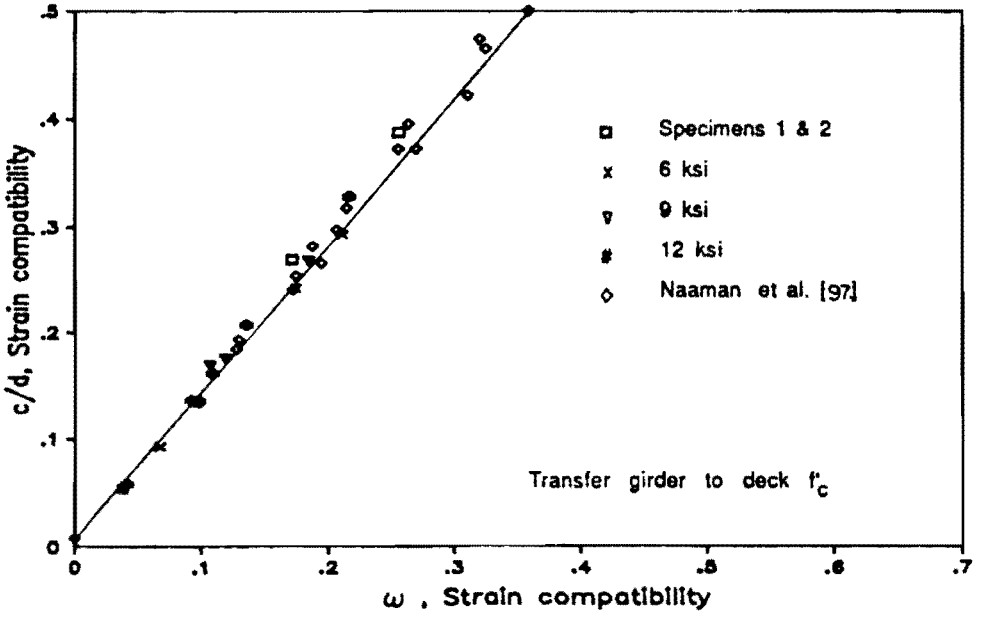

Fig. 4.54 Variation of c/d with w from strain compatibility analysis: a) ω computed using gross section dimensions; b) ω computed using transformed section dimensions

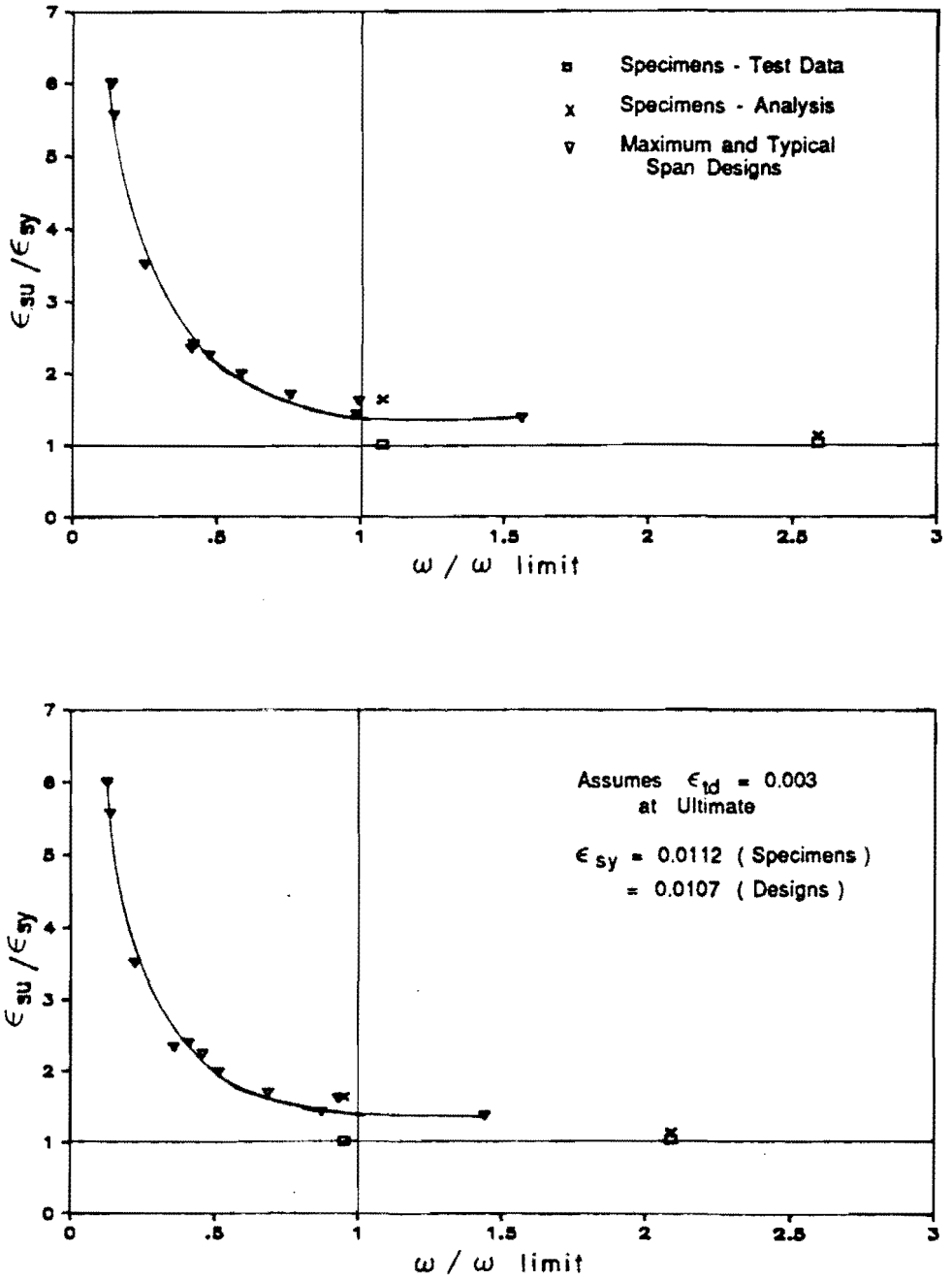

Fig. 4.55 Strand strain ratio at ultimate (/w maximum limit) - Cases I and II: a) Proposed limit; b) Current ACI limit

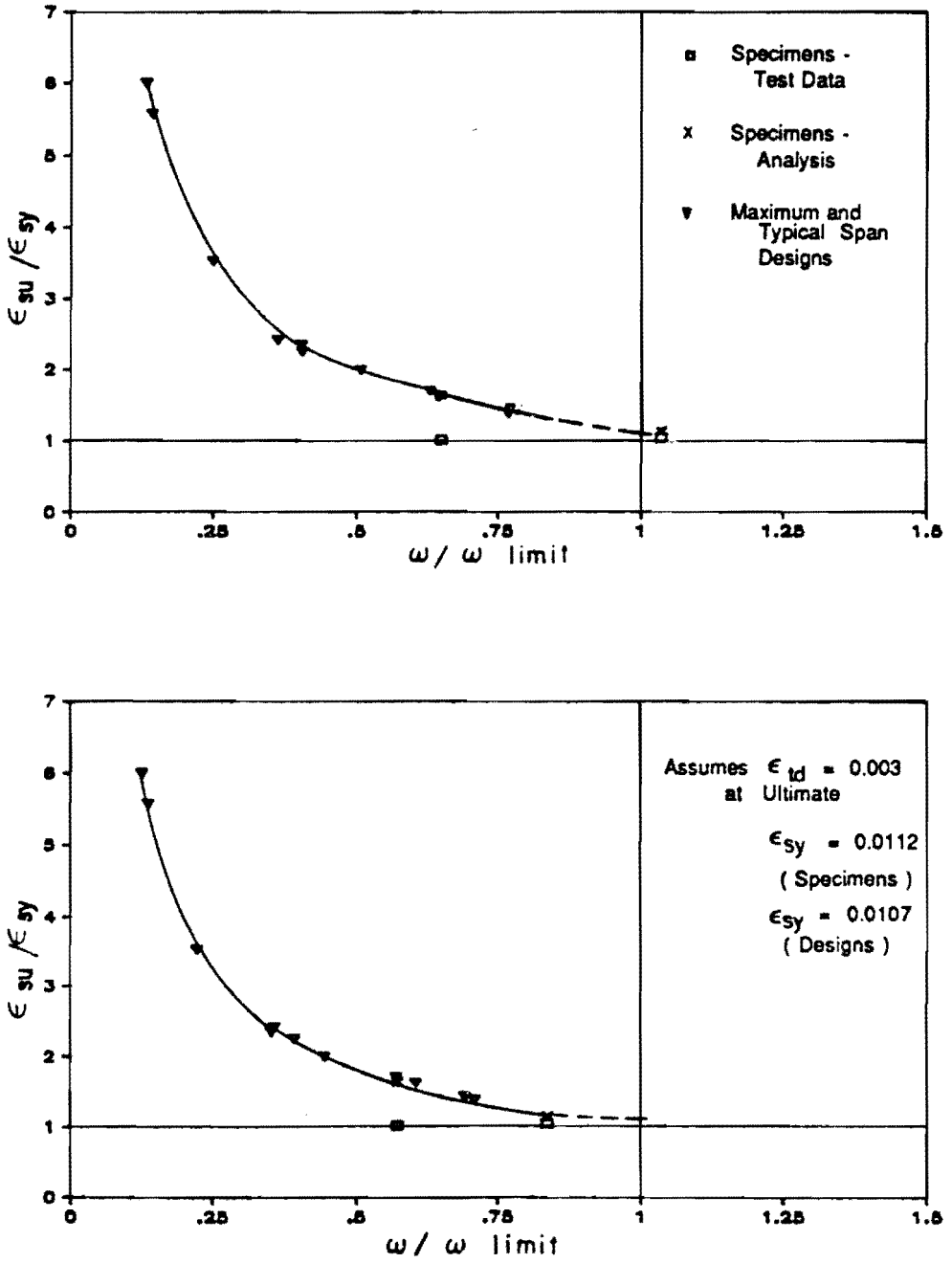

Fig. 4.56 Strand strain ratio at ultimate (/w maximum limit) - Case III: a) Proposed limit; b) Current ACI limit

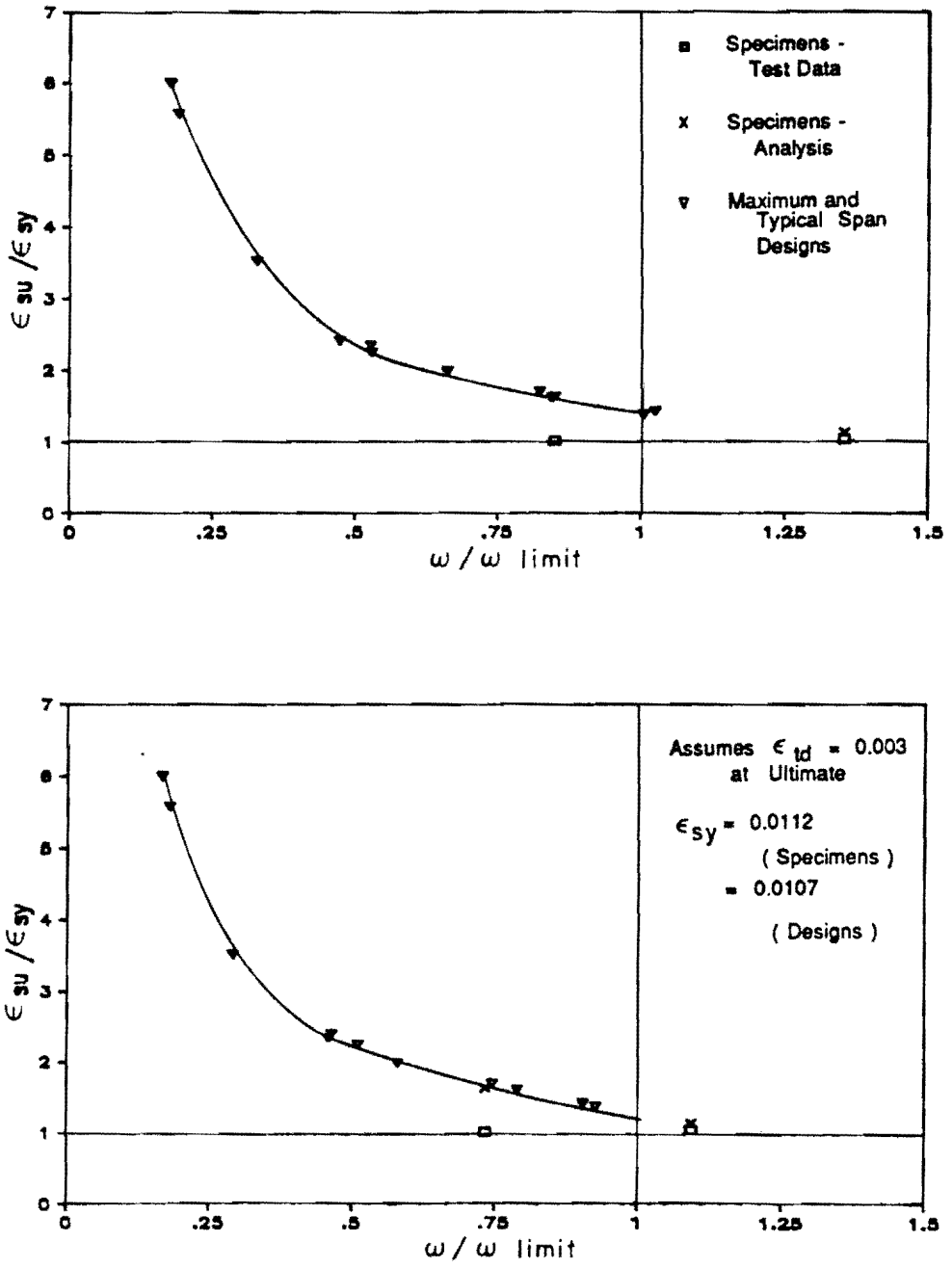

Fig. 4.57 Strand strain ratio at ultimate (/w maximum limit) - Case IV: a) Proposed limit; b) Current ACI limit

Strands, however, experience significant inelastic deformation before reaching the defined yield strain. This aspect of strand behavior is demonstrated dramatically by Specimen 1 in which the strand strain just reached the yield strain prior to crushing of the concrete, yet the deflection was large, providing sufficient warning of impending collapse.

4.3.3 Minimum Reinforcement Limit. The current minimum reinforcement limit insists that the ultimate capacity of the member must exceed the cracking load by a 20 percent margin. However, this limit is not sufficient to prevent designs in which strands rupture before the extreme concrete fiber reaches the maximum usable strain, which has been indicated to be a possibility by the 75 ft span designs studied in this chapter. The load-strain plot for this span in Fig. 4.53 shows that strands could rupture (exceed the limiting strain equal to the ASTM minimum elongation of 0.035) prior to developing even a strain of 0.0022 in the top fiber of the deck.

To address this deficiency in the Codes, a minimum reinforcement limit was developed using the same reasoning as used for the maximum limit. Appendix A.2 contains the derivation of this limit which is based on the limiting strain of 0.035. The complete form of the limit is

$$w \geq 0.85\beta_1[84/(1064 - f_{se})] \tag{4.9}$$

with a simplified form being

$$w \geq 0.08\beta_1 \tag{4.10}$$

where f_{se} is expressed in ksi. The simplified form is acceptable for the minimum limit because it is less sensitive to variation in the effective prestress than the maximum limit. This limit is also quite accurate for composite members because the large strand strain involved minimizes the effect of the strain and curvature differences between the deck and girder.

Accuracy of this limit is demonstrated for maximum and typical span designs in Fig. 4.58 where the ratio of strand strain at ultimate to the limiting strain is plotted versus the ratio of ω to both forms of the minimum reinforcement limit. The data are connected with a curve to indicate the trend of the data. The strain ratio should be unity when the ω ratio is unity to satisfy the intent of the limit. This plot indicates excellent agreement between both forms of the limit and data, which is demonstrated by the trend of the data

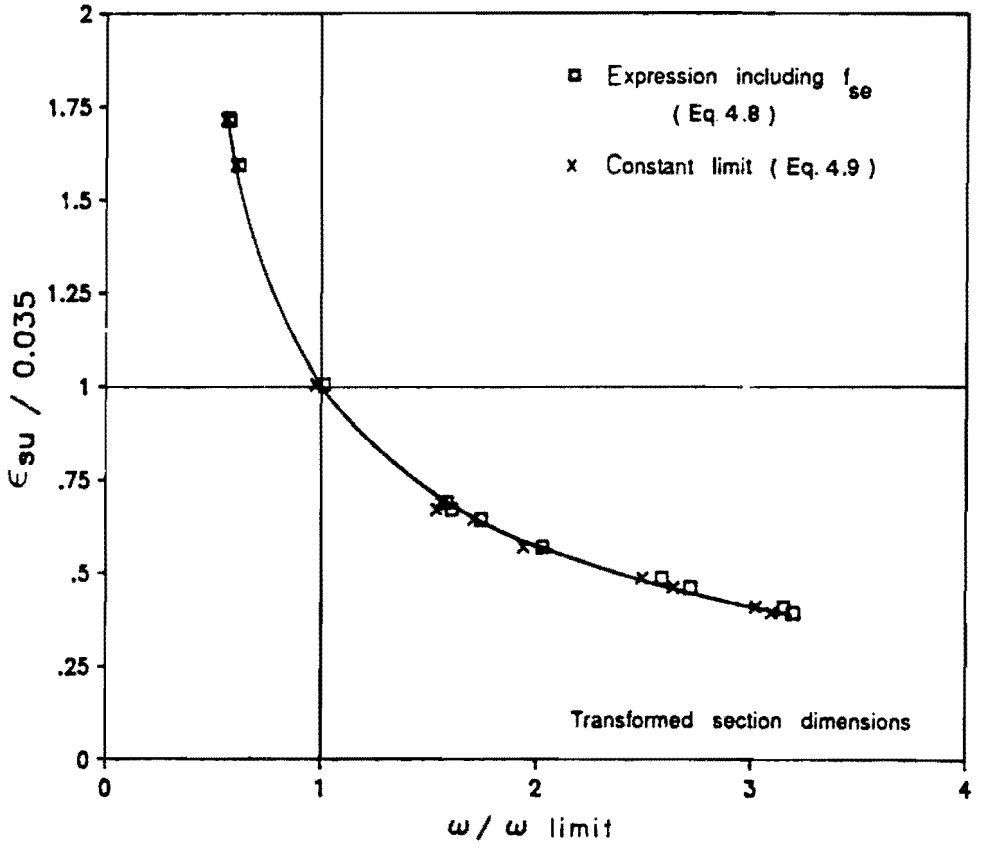

Fig. 4.58 Strand strain ratio at ultimate ($\epsilon_{su}/0.035$) versus ω ratio (ω/ω minimum limit)

passing through the intersection of the lines representing unity on the two axes.

4.3.4 Summary. The following observations can be made regarding ductility and reinforcement limits for composite prestressed members:

1. The reinforcement index, ω correlates well with aspects of behavior related to ductility.

2. Proper use of ω for comparison with certain limits can ensure adequate ductility. It also avoids problems of definition and computation that are associated with use of other quantities, such as the depth of the compression zone at ultimate and ductility ratios based on yield and ultimate curvatures or deflections.

3. Reinforcement indices computed using the simplified design assumptions of the AASHTO and ACI codes are accurate estimates of reinforcement indices computed using a strain compatibility analysis.

4. The effect of nonprestressed tension reinforcement and compression reinforcement can be included in the reinforcement index by using an expression such as proposed by Naaman et al. [97].

5. Use of a proposed maximum reinforcement limit, which is derived using assumptions consistent with current codes and practice, is recommended.

6. To obtain the same behavior for different grades of strand, the limiting strand strain for use in the maximum reinforcement limit should be a function of the ultimate strength of the strand. A function is proposed and included in the proposed limit.

7. The proposed maximum reinforcement limit is more restrictive in most cases than current limits.

8. The effective prestress was shown to be a significant factor in determining the maximum reinforcement limit, although it is neglected in the current limit. It is, however, included in the proposed limit.

9. In computing the reinforcement index, section dimensions for composite sections should be transformed by the ratio of the deck and girder concrete strengths to provide the most accurate comparison with reinforcement limits and to be consistent with results from analysis of monolithic construction. A transformation to a section using the deck concrete strength is recommended.

10. A proposed minimum reinforcement limit, which would be used in addition to the current minimum requirement, is intended to prevent rupture of strands prior to the strain at the top fiber reaching the maximum usable strain. The proposed minimum reinforcement limit is based on a limiting strand strain of 0.035.

11. The simplified form of the proposed limit is as effective as the more complete form in establishing an accurate minimum reinforcement limit.

Furthermore, it is recommended that strand strain limits equivalent to both the maximum and minimum reinforcement limits be provided in the code or commentary. These equivalent limits could be used with more detailed analyses that compute strand strains and stresses and therefore do not require an indirect approach. This would be appropriate since the intent of the current and proposed limits is to ensure a specified level of strain in the strand at ultimate.

Derivations for the reinforcement limits should also be provided in the commentary to the codes so that they may be understood and properly applied by designers. Such an explanation is currently included in the ACI Code Commentary for the maximum reinforcement limit for reinforced concrete sections, but no information is given on the limit for prestressed members.

4.4 Deflections

This section contains discussions regarding the evaluation of both long and short-term deflections. Limits for these deflections are also considered.

4.4.1 Long-Term Deflections. Long-term deflections were computed using the computer program CAMBER [72] for the maximum and typical span designs using 12 ksi concrete. The construction

schedule, creep factors, and humidity assumed by Kelly [72] for his examples, and actual, rather than estimated, quantities for section properties were used as input. Elastic deflections computed by the girder design program BRIDGE were also input.

The results of the analysis are shown in Fig. 4.59. While the typical span designs (GS = 4 ft, span = 120 ft; GS = 10 ft, span = 75 ft) produced deflections that were very stable with time, the maximum span designs exhibited large cambers and significant continuing sag with time. The longest span design experienced a sag of aproximately 3.5 in. after the deck was added. This could be an unacceptably large value. The long-term behavior indicated in the figure generally agrees with PBEAM [119] analyses performed during the preliminary design of the specimens.

As part of a related study, Kelly [72] performed a sensitivity analysis of the girders he was considering to determine the effect of variations in significant parameters on the time-dependent deflections of girders. Such a study should be performed for high strength girders to determine the possible range in camber due to different age at release, curing conditions, age at erection, and other effects. The use of very long spans with high strength concrete may result in greater sensitivity to variations in parameters which would result in unacceptably large differential camber between girders. When significant parameters are known to be different for girders within the same span, steps can be taken, as suggested by Kelly, while girders are in storage to reduce the final differences in camber.

The program CAMBER could also be used to study the effect of release strength and strand profile on the long-term deformation of the member. Since designs using high strength concrete can be achieved with different combinations of strengths at release and strand profiles, the designer could select a combination which would provide the best performance considering both initial and final conditions.

As observed in the instrumented girders reported by Kelly [72] and from discussions with Texas SDHPT field personnel, there is generally no long-term deflection problem after the deck has been placed. This was also confirmed by the early PBEAM analyses. This is reasonable because the deck will resist any time-dependent movement of the girder, causing a small amount of load redistribution. However, long-term deflections for very long members should be investigated due to the lack of field experience with such members.

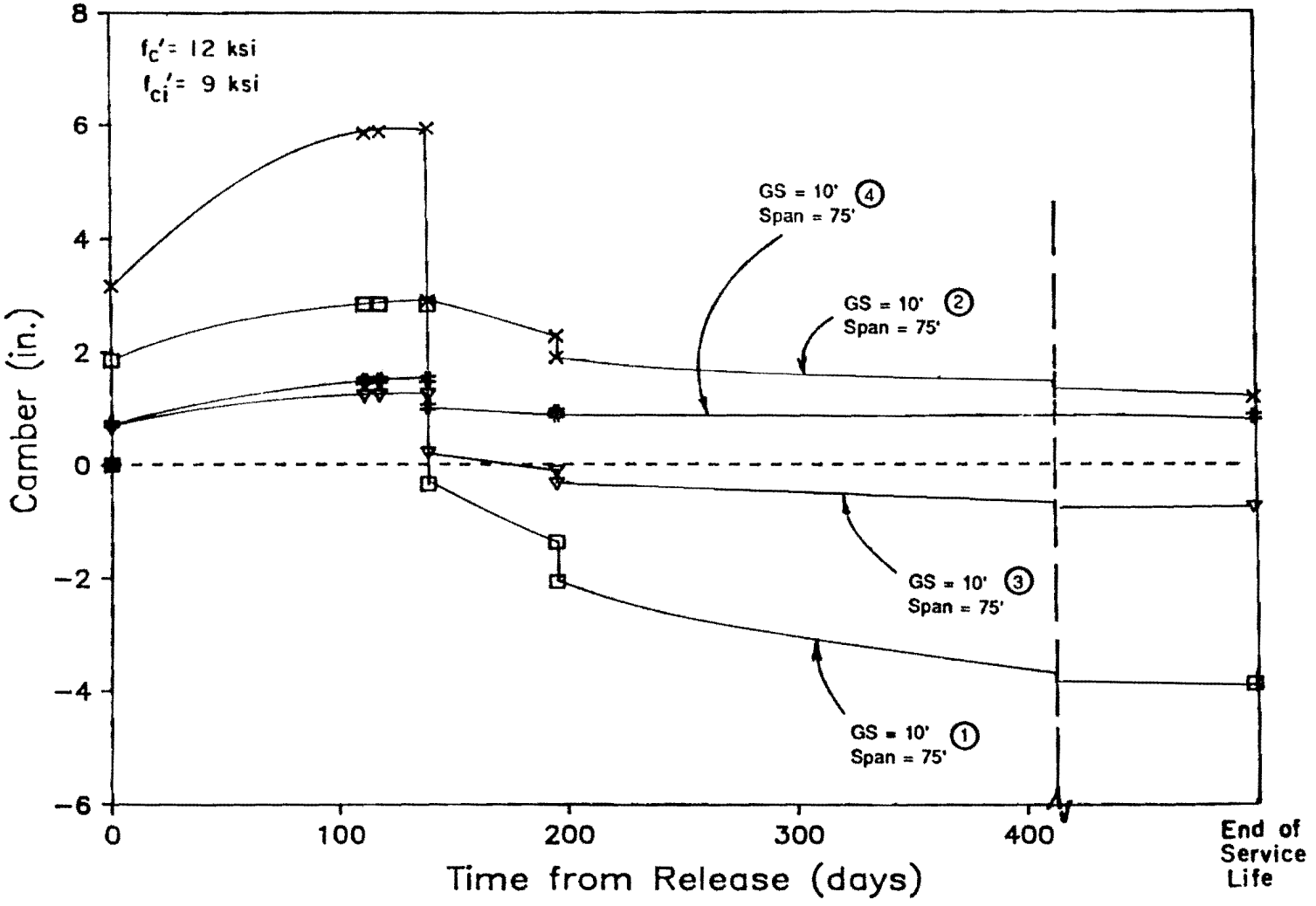

Fig. 4.59 Time dependent deflections for maximum and typical span designs

An attempt was made to relate the curvature at release and the curvature under full dead load to the long-term deflections experienced under these conditions as shown in Fig. 4.60. This approach seemed reasonable because a large curvature would generally indicate a tendency for camber or sag with time. However, the data in the figure do not indicate a close correlation. This is probably due to the fact that deflection depends on the strain conditions all along the member and therefore, span length and other considerations are also significant factors in determining the final deflection of a member.

In the absence of a correlation between curvature and long-term deflections, it is recommended that any designs which approach the maximum span for a given girder spacing should be investigated for possibly excessive long-term deflections. An indication of a possible problem may be a large curvature, but this needs to be investigated further. Use of the program CAMBER is recommended for estimation of long-term deflections.

4.4.2 Deflections Due to Applied Loads. Deflections with applied load have been discussed in preceding sections. Calculation of deflections for uncracked members is straightforward and can be performed using elastic analysis techniques. For loadings beyond cracking, computation of deflections is a lengthy and tedious process unless a computer program is used. Programs such as PBEAM [119] are available to perform the calculations, or the partially automated approach used in this study can be employed. These methods, which employ some form of strain compatibility analysis, provide sufficient accuracy in the prediction of deflections all the way to failure. Since the criteria used to define failure will affect the computed deflection, it is recommended that a careful assessment of the conditions at ultimate be made to determine the level of concrete strain that may correspond to failure or maximum capacity. It appears that a value of 0.003 will be appropriate if the compression region is confined to the deck, resulting in a significant strain gradient across the deck. If the girder remains in compression at failure, a value of 0.0022 to 0.0025 may be more appropriate, since the deck is in more uniform compression and lacks the confining effect associated with a strain gradient.

4.4.3 Deflection Limits. As mentioned in Chapter 2, there are no limits on deflection for prestressed members in the current AASHTO Specifications. However, the live load deflection limit of the span divided by 800, which applies to steel members in the AASHTO Specifications [10], is often used for prestressed bridge members.

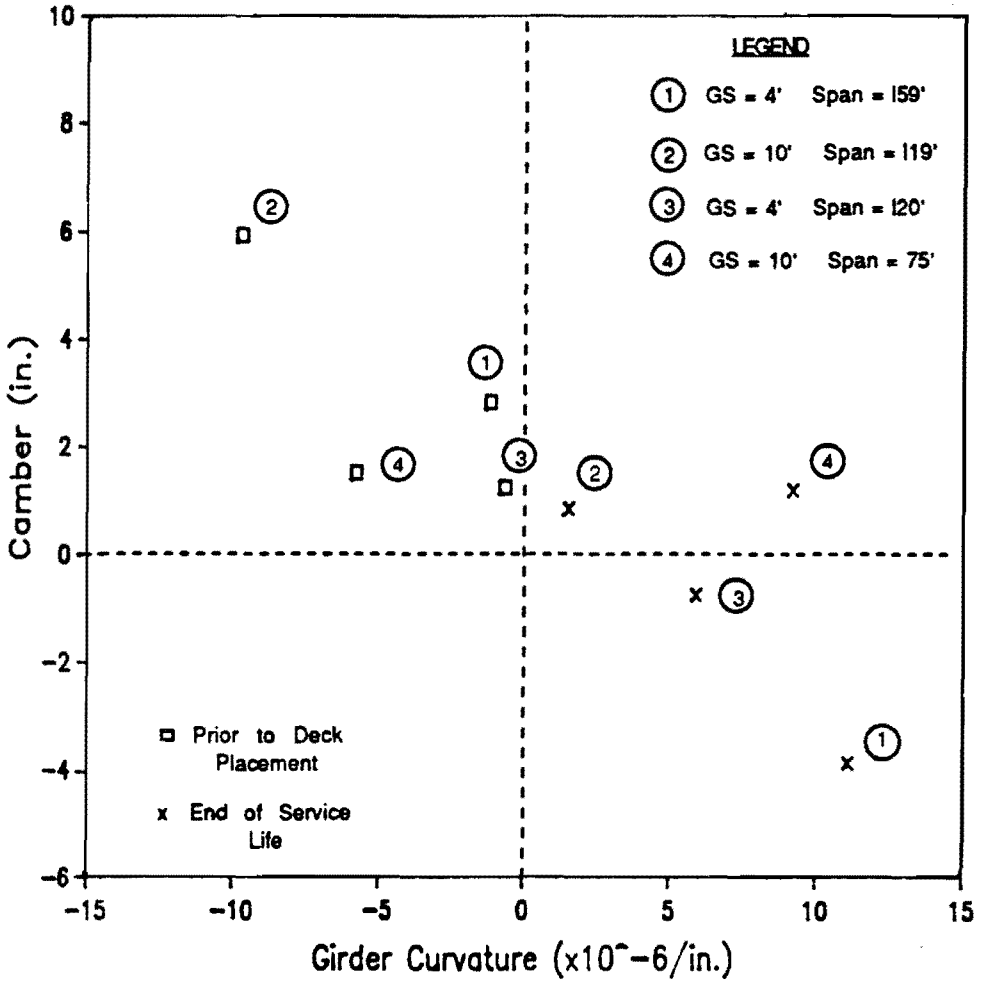

Fig. 4.60 Camber versus girder curvature prior to deck placement and at end of service life for maximum and typical span designs with f'_c = 12 ksi

This limit is compared to deflection-to-span ratios in Fig. 4.61 for the sample designs used in this chapter. An additional limit of the span divided by 1000, which is specified for steel bridges with pedestrian traffic, is also shown on the figure. The deflections are well below the span/800 limit for all cases and only for the longest span is the more strict limit encountered. The data also shows the expected decrease in deflection with use of high strength concrete for a given span. The decrease is not sizable and would not be sufficient motivation to use high strength concrete in most cases. However, where member depths are restricted, the use of high strength concrete may be warranted in order to control deflections.

No limits for final long-term deflections are known to exist. As means to compute long-term deflections become more practical, it appears prudent that such limits be developed, especially where very long spans are used. These limits should be correlated to the level of deformation in a bridge that creates an unacceptable ride or results in maintenance or other problems.

4.5 Girder Stability

In this section, the methods of stability analysis discussed in Chapters 2 and 3 will be developed further. The analysis will then be used to study the lateral stability of the girder cross-sections considered in Chapter 3. Methods for improving the lateral stability of girders are also discussed. Experience related to lateral stability during the fabrication and testing of the long-span scale-model specimens described in Ref. [139]. is then discussed.

4.5.1 Analysis. The approach and associated equations presented in Chapter 2 for determining the factor of safety against lateral buckling can be solved for the maximum span. Where lifting points are located at a distance, a, from the ends of the girder, the weak axis deflection at midspan can be written as

$$\Delta_y = \frac{w_g}{16 E_c I_y} (l\text{-}2a)^2 \, (5/24) \, (l\text{-}2a)^2 - a^2) \qquad (4.11)$$

Using this equation with the definition for the factor of safety against lateral buckling, FS,

$$FS = y_T/(0.64 \, \Delta_y) \qquad (4.12)$$

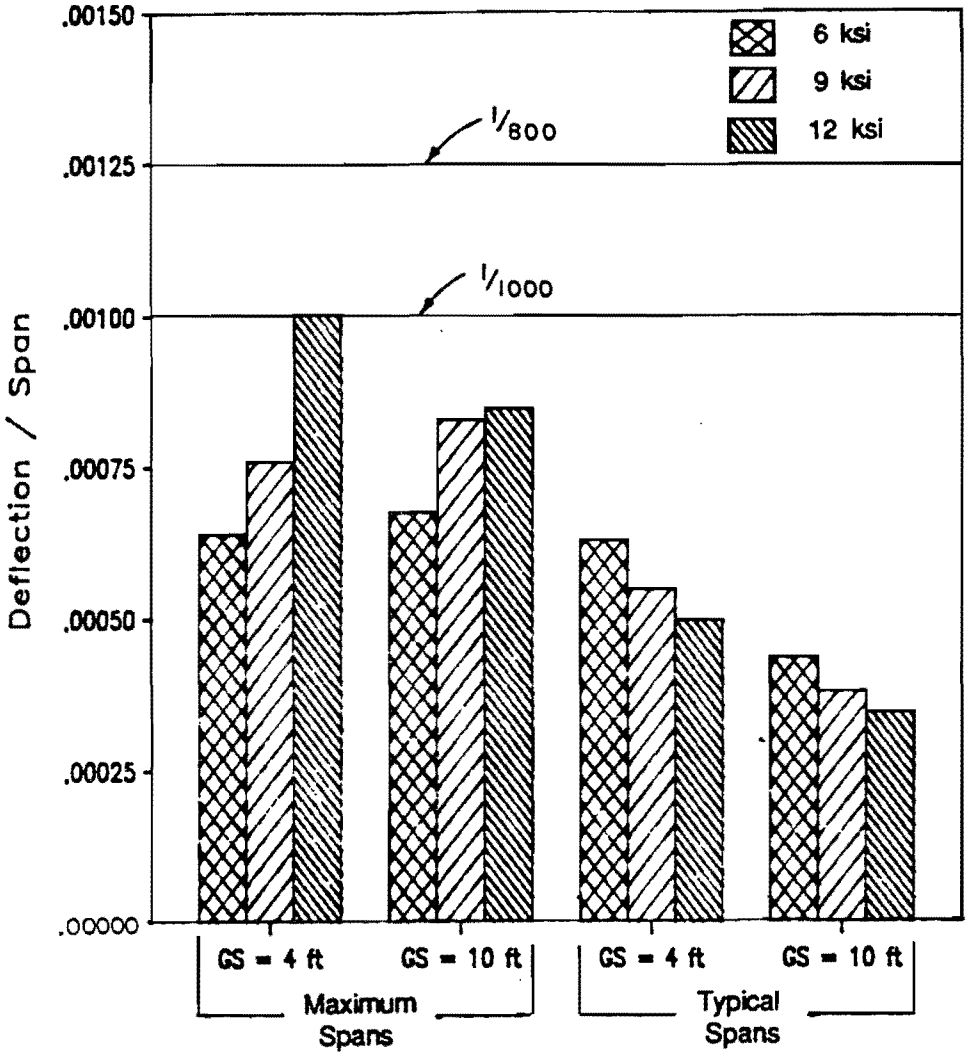

Fig. 4.61 Comparison of live load deflections to limits for maximum and typical span designs

the maximum lifting span for a girder, l_{max}, can be computed using the following equation:

$$l_{max} = \sqrt{\frac{(y_T/.64FS)(16E_cI_y/w_g}{(1-2(a/l))^2(5/24)(1-2(a/l))^2-(a/l)^2)}} \qquad (4.13)$$

The quantity (a/l), which is the ratio of the distance from the lifting point to end of the girder to the full span length, is assumed to be a constant. The equation assumes all quantities to have consistent units. This equation was used to compute spans given in Table 3.4.

As indicated by Swann [122], y_T is the vertical distance between a line through the two lifting points and the center of gravity of the whole beam, and represents the distance from the center of mass of the girder to its center of rotation. This definition can therefore be expressed as

$$y_T = y_t + y_L - y_C \qquad (4.14)$$

where y_t = distance from centroid of section to top of girder

y_L = vertical distance from top of girder to lifting eye

y_C = vertical distance from centroid of section at lifting points to centroid of whole member due to camber of girder

$$= (0.67 - 4\,(a/l)^2)\,\Delta_c \qquad (4.15)$$

Δ_c = camber of member at midspan.

Because most lifting loops are not rigid enough to prevent rotation about a point lower than their full height, use of a reduced height or zero is recommended. However, the full height may be used for rigid lifting yokes that are rigidly attached to the girder. The definition for y_C (Eq. 4.15) assumes that a girder with camber has a parabolic shape.

The equation by Swann [122] can be used to determine the lateral bending moment, M_y, caused by imperfections in the member. The lateral bending moment, which is the potential cause of failure, is related to the moment due to member self-weight about the x-axis, M_x, the tilt due to imperfections, ϕ_o, and the factor of safety against lateral buckling, FS. The equation is:

$$M_y = M_x\phi_o(FS/(FS-1)) \qquad (4.16)$$

where FS is defined using Eq. 4.12 and the correction for lifting point location that is applied to Δ_c in Eq. 4.15 is also applied to ϕ_o, resulting in the expression

$$\phi_o = (d_o + (.67 - 4\ (a/l)^2)b_o)/y_T \qquad (4.17)$$

where d_o = transverse distance from the minor axis of the section to where the lifting points have been inadvertently fixed

b_o = lateral bow or sweep of the beam at midspan.

The proposed definition for y_T (Eq. 4.14) should be used in these equations. When using Eq. 4.17 to examine the condition of an actual member, the direction of sweep and lifting point eccentricity should be considered because they may act in opposite directions. For design purposes, realistic maximum values for d_o and b_o acting in the same direction should be used.

If cracking occurs due to the lateral moment, transverse section properties are reduced which can lead to increasing instability (Δ_y increases, resulting in a decrease in FS, which leads to a further increase in M_y and the cycle repeats) and sudden collapse [122]. Therefore, to avoid cracking and failure, the total stress at the extreme fiber due to lateral moment, prestress, and self-weight should be limited to a value less than the cracking stress. It is recommended that an allowable stress of $6\sqrt{f_c'}$ be used. The extreme fiber stress can be computed using the equation

$$\begin{aligned} f_{ytop} &= \text{total stress in top fiber of the girder including effect of lateral moment } M_y \\ &= f_{top} - M_y/S_{ytop} \qquad (4.18) \\ &\geq -6\sqrt{f_c'} \end{aligned}$$

where f_{top} = stress in the top fiber of the girder due to prestress and self-weight, with compression positive.

S_{ytop} = section modulus about the weak axis for the top flange of the section
$= I_y/(bl/2)\ bl$

bl = width of top flange.

This equation assumes that cracking due to the lateral moment occurs in the top flange, which is generally the case because the greater precompression of the bottom flange delays cracking. However,

stresses in the bottom flange should also be checked because in some cases (see data for the Specimen 2 prototype in Table 4.5), cracking may initiate at this location. The critical stress for the bottom flange will typically occur at the top corner of the bottom flange.

These equations can be used to determine the factor of safety against lateral buckling for perfect girders, and to estimate the extreme fiber stress due to the lateral moment caused by initial imperfections (sweep, b_o, and eccentricity of lifting points, d_o) Using these equations, the factor of safety (FS) and the top fiber stress (in terms of $\sqrt{f'_c}$ were determined over a range of span lengths for the sections considered in Chapter 3. The results are shown in Fig. 4.62 for the 54-in. sections and in Fig. 4.63 for both the 40-in. and 72-in. sections. A sweep of 2 in. and a lifting point eccentricity of 0.5 in. were used in the calculations as reasonable estimates of the quantities, although larger values couldoccur. The net stress at the top fiber prior to consideration of lateral effects was assumed to be zero in order to simplify the comparison. However, if f_{top} were a tensile stress, the spans shown would be reduced, while presence of a compressive stress would lengthen the spans. Camber was neglected and the height of lifting points above the top of the girder was assumed to be zero. Other assumptions are indicated on the figures. Spans greater than maximum lifting span lengths computed using Eq. 4.13, which are repeated in Table 4.4, are shown on the figure as dashed lines.

The comparisons shown in Fig. 4.62 and 4.63 indicate that the factor of safety against buckling gradually approaches 2 as the span approaches l_{max}. The maximum lifting span, l_{max}, occurs at the intersection of the curves and the line representing FS = 2. An additional increase in span of approximately 20 ft is required to obtain FS = 1. The second half of the figures shows that the total top fiber stress, f_{ytop}, caused by the lateral moment resulting from the specified imperfections, increases rapidly as the span is increased. Stresses approach infinity as FS approaches one. These plots indicate that, at the maximum lifting span (the span at which the dashed line begins), f_{ytop} exceeds the allowable stress ($6\sqrt{f'_c}$) and even the cracking stress ($7.5\sqrt{f'_c}$) for all sections except the MOT/C&CA inverted-tee section (M 54/6). Values for $f_{ytop}/\sqrt{f'_c}$ at the maximum lifting spans are tabulated in Table 4.4. The fact that stresses at l_{max} exceed the cracking stress for most sections indicates that the presence of initial imperfections of moderate size could lead to a lateral stability failure at spans less than l_{max}.

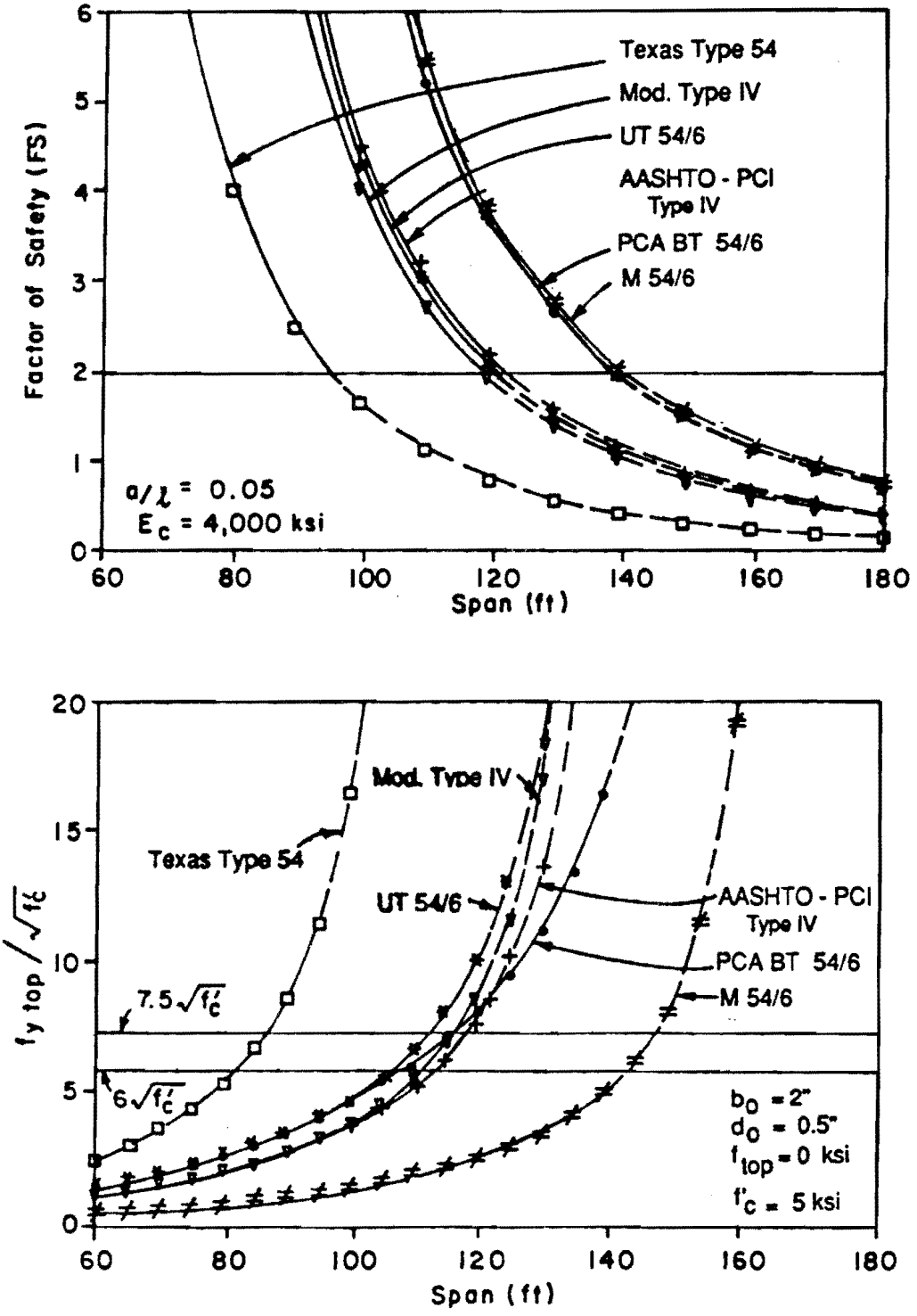

Fig. 4.62 Factor of safety and top fiber stress versus span length for 54-in. sections: a) Factor of safety (FS); b) Top fiber stress

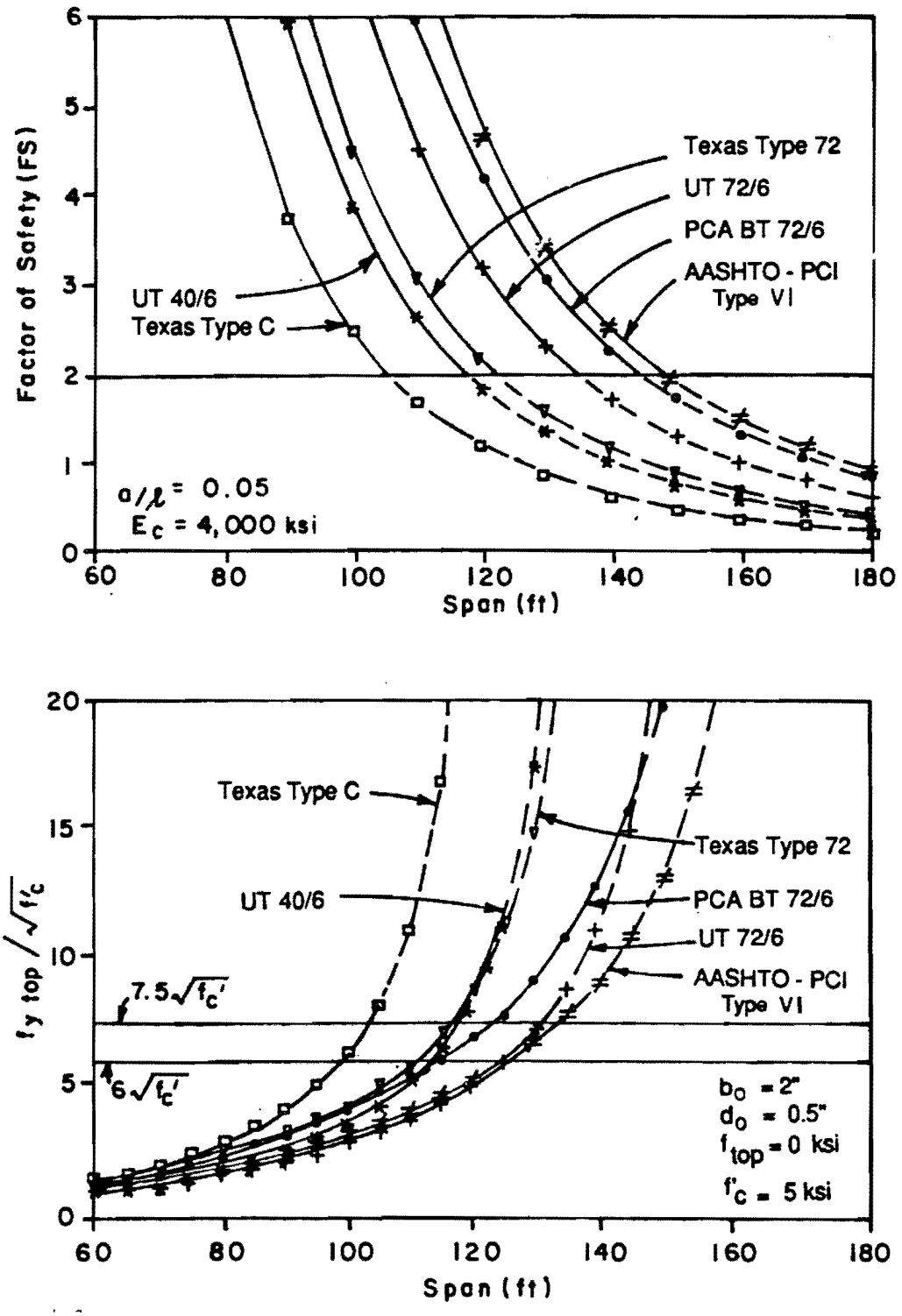

Fig. 4.63 Factor of safety and top fiber stress versus span length for 40- and 72-in. sections: a) Factor of safety (FS) b) Top fiber stress

Table 4.8 Additional Section Properties Influencing Girder Stability

	y_T * (in.)	I_y ($in.^4$)	g (plf)	$\frac{y_T I_y^4}{g}$ ($in.^{1.5}/lb^{0.25}$)	l_{max} ** (ft)	S_{ytop} ($in.^3$)	$\frac{f_{ytop}}{f'_c}$ ***
40-in. sections							
Texas Type C	22.91	13,020	516	51.3	106	1,860	-8.34
UT 40/6	23.40	18,486	477	57.4	118	2,311	-7.61
54-in. sections							
Texas Type 54	28.47	6,927	514	46.3	95	866	-11.69
AASHTO-PCI Type IV	29.27	29,513	822	59.6	123	2,951	-8.83
Modified Type IV	29.63	22,550	709	58.0	119	2,506	-8.39
MOT/C&CA M 54/6	32.45	37,410	654	68.7	141	4,676	-5.32
PCA BT 54/6	26.56	41,310	617	68.0	140	1,721	-16.30
UT 54/6	27.72	23,578	649	59.0	121	1,965	-10.83
72-in. sections							
Texas Type 72	38.27	24,707	899	59.6	123	2,246	-9.71
AASHTO-PCI Type VI	35.62	72,776	1,130	72.4	149	3,466	-12.55
PCA BT 72/6	35.64	41,634	730	70.3	145	1,735	-15.24
UT 72/6	38.55	32,560	808	65.7	135	2,713	-8.72

* - $y_T = y_t$

** - Maximum lifting spans, l_{max}, computed using Eq. 4.13, assuming lifting point located at 0.051 from ends of girder, factor of safety against buckling (FS) = 2.0, and E_c = 4,000 ksi.

*** - $f_{ytop} = M_y/S_{ytop}$ for l_{max} using Eqs. 4.16 and 4.18, and assuming d_o = 0.5 in., b_o = 2 in., f_{top} = 0 kis, and f'_c = 5 ksi.

For most sections, the span at which f_{ytop} equals the allowable stress is approximately 15 ft less than the maximum lifting span (for the specified values of b_o and d_o). For the PCA bulb-tee sections and the AASHTO-PCI Type VI, the difference is from 25 to 30 ft. Therefore, Eq. 4.16, 4.17, and 4.18 should be used even when spans are less than l_{max} to estimate expected behavior for anticipated or actual imperfections in members, and to determine whether special steps need to be taken to ensure safe handling of girders.

Plots similar to those in Fig. 4.62 are shown in Fig. 4.64 for 54-in. sections with high strength concrete. Maximum lifting spans increase only 8 percent for an 80 percent increase in f'_c and a corresponding 35 percent increase in the modulus. Top fiber stresses were reduced only slightly at l_{max} and the M 54/6 remained the only 54-in. section for which f_{ytop} at l_{max} was less than the allowable stress. However, for a given span (especially those approaching lmax), increasing the concrete strength leads to a significant reduction in the stress at the extreme fiber. For example, the extreme fiber stress for an AASHTO-PCI Type IV with a 120 ft span is $7.8\sqrt{f'_c}$ with normal strength concrete (Fig. 4.62) while for high strength concrete at the same span (Fig. 4.64), the stress is $4.8\sqrt{f'_c}$, which is below the allowable limit. Therefore, high strength concrete can be more effectively used to reduce stresses due to lateral moments for a given span rather than to increase the maximum lifting span.

These figures also reveal that the maximum lifting spans are similar for sections of different depths. To illustrate, maximum lifting spans for the UT 40/6, the modified Type IV (54 in. deep) and the Texas Type 72 are 118, 119, and 123 ft, respectively. This occurs because transverse section dimensions for deeper sections are the same or only slightly larger than those for shallower sections. Therefore, the change in weak axis properties is small for sections of different depths. This leads to an increasing disparity between the strong and weak axis moments of inertia which means that maximum span designs, which are based on strong axis properties, will increase more than the maximum lifting span, which is strongly influenced by weak axis properties. Therefore, if both the span length and lateral stability are to be improved, the weak axis section properties must be increased significantly for deeper members.

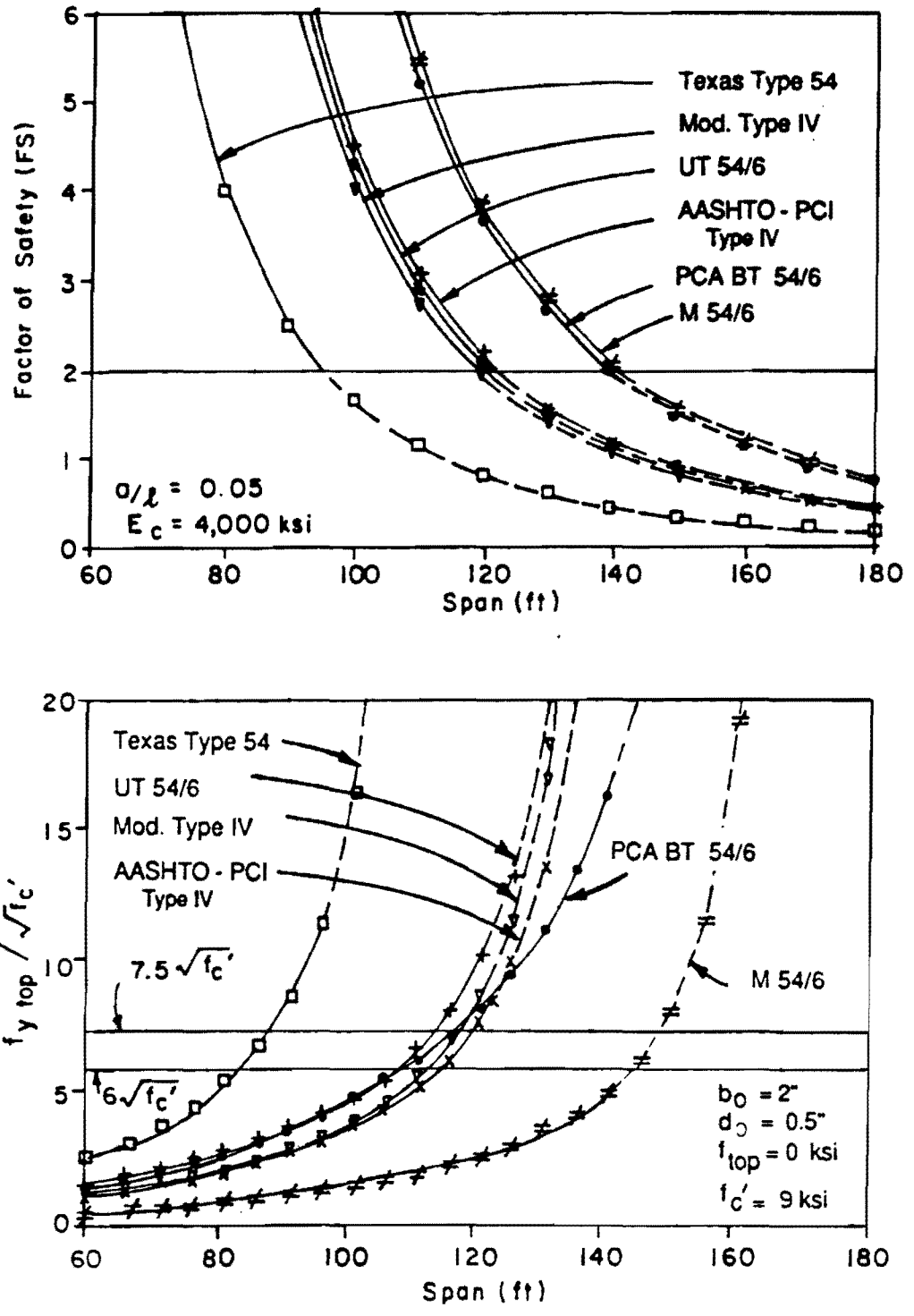

Fig. 4.64 Factor of safety and top fiber stress versus span length for 54-in. sections using high strength concrete: a) factor of safety (FS); b) Top fiber stress

A lateral stability factor was developed relating section properties to the maximum lifting span for a given a/l ratio. The factor is taken from Eq. 4.13 and appears in the fourth column of Table 4.4, which contains the quantities that are used in the factor. This factor is linearly related to l_{max} as demonstrated in Fig. 4.65 for different values of a/l. The figure demonstrates that the AASHTO-PCI Type IV and the Texas Type 72, which have the same value for the lateral stability factor, will have the same maximum lifting span when lifting points are located at a given distance from the ends of the girder. This factor is therefore an indicator of the lateral stability of a section, with larger values indicating that a longer maximum lifting span would be possible. However, stresses caused by lateral moments must also be investigated for a complete understanding of the stability of a member, as illustrated by the fact that the bulb-tee sections have among the highest (best) values for the lateral stability factor, yet have the highest (worst) stresses due to lateral moment at the maximum lifting span.

A simple relationship was also sought for stress at the top fiber (last column in Table 4.4), but the relationship was too complex. The weak axis section modulus for the top flange is included in the table for use in computing the stress. Because the inverted-tee M 54/6 had the smallest stress and was the only section for which the stress was below the allowable value ($6\sqrt{f'_c}$), this section could be used at l_{max} without cracking for the values of b_o and d_o considered. Stresses at l_{max} for the bulb-tee sections were the highest and exceeded twice the cracking stress. Increased initial imperfections and large cambers would increase stresses further, thus increasing the potential for failure. Because stresses at l_{max} for the bulb-tees and AASHTO-PCI Type VI exceed the stress for the Texas Type 54, which was reported as having stability problems in use, it is possible that problems may also occur with these sections when spans near the maximum lifting span are used.

Considering the lateral stability factor and the above findings with respect to stresses caused by lateral moments resulting from sweep and lifting point eccentricity, the MOT/C&CA M 54/6 inverted-tee section, or one like it, appears to provide the best combination of potential maximum span lengths with increasing concrete strength (Chapter 3) and satisfaction of stability criteria. This occurs because the section has a large weak axis moment of inertia, a fairly low weight per foot, and the largest value of y_t for any 54-in. section considered.

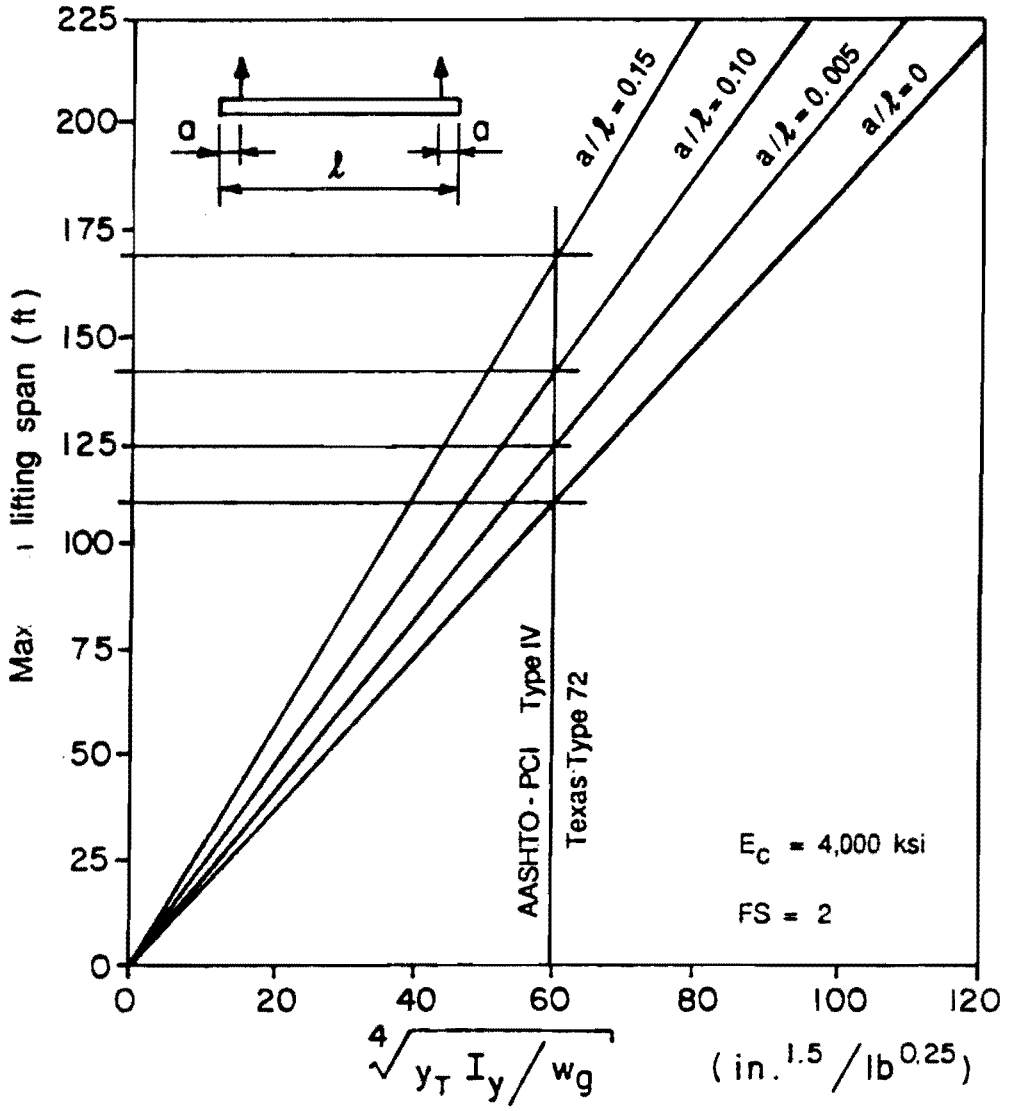

Fig. 4.65 Maximum lifting span versus lateral stability factor

The complete stability analysis presented here should be used to compare sections in order to obtain the most complete understanding of the stability of a section instead of relying on the partial perspective given by the lateral stability factor and the maximum lifting span. Girder designs should also be checked to determine whether initial cracking due to the lateral moment could occur at the bottom flange rather than the top flange as assumed for the analyses in this section.

As mentioned in Sec. 2.7, a number of means are available to improve the lateral stability of members with spans greater than the maximum lifting span or where extreme fiber stresses due to lateral moment caused by imperfections exceeds the allowable stress. A very effective method for increasing the maximum lifting span is to locate lifting points farther from the ends of the girder. The plots shown in Fig. 4.65 indicate that, by locating lifting points at 15 percent of the span from the ends of the girder rather than 5 percent, the maximum lifting span is increased by approximately 35 percent. This improvement in l_{max} is related to the ratio a/l and is independent of section shape or span. The member must be capable of resisting the stresses produced by lifting the member at these locations.

The use of external bracing or "hog rods" can also be used to stiffen members during handling and transportation. The Texas State Department of Highways and Public Transportation specifies their use when span lengths exceed limits given in Chapter 2. Another externally applied means for increasing the stability of members during lifting, which is relatively simple and effective, is the use of a rigidly attached lifting yoke. This increases y_T by introducing a value for y_L which results in a significant improvement in stability, especially for members where y_t is small, such as for the bulb-tee sections. If a yoke is provided with a height sufficient to double y_T, the maximum lifting span is increased 19 percent. A rigid lifting yoke is any device which maintains the lifting eye, to which the hook of the crane is attached, in the plane of the y-axis of the member.

The effect of using higher strength concrete was discussed earlier (see Fig. 4.64). Since the stability of a section improves only slightly when high strength concrete is used, it is recommended that other means be used as primary methods for improving stability.

More study of the lateral stability of long, slender pretensioned girders during fabrication and erection is needed. A survey of the experience of state and federal highway departments,

fabricators, and erectors with long, slender members should be taken, since such data certainly exists but has not been collected and published. A range of expected values for sweep and lifting point eccentricity should also be obtained. The analysis presented and discussed above should then be compared to actual experience to determine whether it is appropriate and whether the limiting factor of safety and allowable stresses are sufficient.

4.5.2 Experience with Scale-Model Specimens. The specimens described in Ref. [139] were lifted using nearly vertical cables. No difficulties were encountered during handling although sweep was present in both girders. The cause of the observed increase in sweep of both specimens following placement of the deck is uncertain. It is possible that irregularities in the deck forms could have forced the girder out of alignment or the added load above the girder could have aggravated the stability problem. The deck forms, however, were sufficiently rigid to stiffen the top flange and prevent buckling. The fact that an increase in sweep following release of approximately 0.6 in. for Specimen 1 and 0.4 in. for Specimen 2 indicates the lateral behavior of these members is sensitive to added load and manipulation during the construction process.

Table 4.5 gives information concerning the lateral stability of the specimens and corresponding prototypes. The specimen data reflects conditions at the time at which the girder was lifted from the prestressing bed, which was immediately following release for Specimen 1 but was approximately 6 weeks after release for Specimen 2. Specimen 1 had no added dead load when moved while Specimen 2 had full dead load compensation present when moved. The added dead load for Specimen 2 was hung from spreader beams which crossed over the top of the girder. Because the height of the centroids of the hanging masses were located close to the height of the centroid of the girder, the height of the centroid of the girder was used for the centroid of the combined masses of the girder and added dead load. Data for prototypes is assumed to be at release which occurs within one or two days after casting.

The data in Table 4.5 indicate that Specimen 2 was close to the maximum lifting span and had a low value for factor of safety against buckling, but because of the small initial imperfections and the presence of compression in the top flange due to prestress and self-weight, both the top and bottom of the girder were in compression after lateral bending had been considered. The maximum lifting span and factor of safety for Specimen 1 were greater than for Specimen 2 because no dead load compensation was used. The total

Table 4.5 Lateral Stability Data for Specimens and Prototypes

Quantity	Units	Test Specimens		Prototypes	
		Sp 1	Sp 2	Sp 1	Sp 2
I_y	in.4	276	276	22,550	22,550
ω_g	plf	78.4	235.2	709	709
S_{ytop}	in.3	92	92	2,506	2,506
S_{ybot}	in.3	69	69	1,880	1,880
f'_c	ksi	10.2	10.75	10.2	10.75
E_c	ksi	5,750	5,700	5,750	5,700
l	ft	49	49	147	147
a	ft	5	5.5	15	15
Net camber	in.	1.6	0.1	2.95	1.63
d_o	in.	0	0	0.5	0.5
b_o	in.	0.5	0.03	2.0	2.0
l_{max}	ft	64.1	51.4	147.8	148.6
y_T	in.	8.87	9.81	27.8	28.6
Δ_y	in.	2.37	6.31	21.2	21.4
FS		5.85	2.43	2.04	2.09
θ_o	rad.	0.0354	0.0019	0.0632	0.0614
M_x	k in.	167	467	13,601	13,601
M_y	k in.	7.14	1.50	1,684	1,604
f_{top}	ksi	-0.279	0.534	1.840	1.690
f_{bot} f_{lng}	ksi	3.781	2.495	3.110	2.022
f_{ytop}	ksi	-0.357	0.518	1.168	1.050
f_{ybot}	ksi	3.677	2.473	2.213	1.169
$f_{lim}=6$ f'_c	ksi	-0.606	-0.622	-0.606	-0.622
$f_{ymin}/$ f'_c	**	-3.53	4.99	11.6	10.1

* - At top corner of bottom flange.
** - Minimum of total stress at top or bottom.
$y_L = 0$ for all analyses.

stress at the top of Specimen 1 was slightly greater than half the allowable stress due to the effect of larger initial imperfections and tension in the top flange.

Prototype designs corresponding to the specimens are included in Table 4.5 to obtain an indication of whether the behavior of scale-model girders could be expected to be indicative of the stability of the prototype girders and to illustrate the application of the preceding equations to actual designs. Specimen 1 does not compare well to the prototype designs because the full dead load compensation was not in place when the girder was lifted. The same values for concrete strength and modulus are used for companion specimens and prototypes to assist in comparisons regarding the scale effect. Stresses at the top and bottom of the prototype girders after release were taken from the design calculations in which losses were computed. The length of the prototype girders was very slightly less than l_{max} for both designs while the difference between girder length and l_{max} was greater for both specimens. Therefore, the factor of safety for each of the prototype girders was approximately 2, which was less than the FS values for the specimens. The smaller values of FS and the larger values of ϕ_o (due to larger assumed sweep and lifting point eccentricities) resulted in moderately large lateral moments. However, since the stresses at the top of girder were larger, total stresses were larger than in the specimens. It was determined that if the lateral moment had been sufficiently large, the prototype corresponding to Specimen 2 would crack in the bottom flange prior to the top flange.

4.6 Fatigue

While little data is available on the fatigue characteristics of high strength concrete, it is expected that the fatigue strength of high strength concrete is the same as that for concretes of lower strengths [22]. However, it appears that the fatigue characteristics of strands actually control the fatigue behavior of composite pretensioned girder bridges. Therefore, the fatigue of strands will be the focus of this section.

This section includes a discussion of the recommended approach for considering fatigue in the design of pretensioned members. Methods for computing strand stress ranges are then compared. Finally, strand stress ranges for various designs are considered.

While not considered in this section, it has been found that the fatigue behavior of pretensioned girder bridges is extremely sensitive to the actual prestress. This fact should be taken into consideration when the following analysis approach is used to evaluate the fatigue performance of pretensioned girders.

4.6.1 Design Approach. Recommendations made by Overman et al. [101] provide a direct approach to the consideration of fatigue in the design of pretensioned girders. The approach recognizes strand fatigue as the limiting factor in the fatigue of pretensioned girders. While they conclude that use of a nominal bottom fiber concrete stress of $3\sqrt{f'_c}$ may be adequate to provide acceptable fatigue behavior, the limiting of strand stress ranges to ensure good fatigue resistance is recommended. Where strand stress ranges are used, the fatigue life of the girder would be determined using either the strand fatigue model

$$\text{Log } N = 11.0 - 3.5 \text{ Log } S_r \qquad (4.19)$$

where N = the fatigue life in number of cycles
Sr = the strand stress range
= maximum stress - minimum stress (ksi)

or the more conservative AASHTO Category B fatigue model for redundant structural steel members [10]. Where service life criteria are not satisfied, the design would have to be altered by reducing girder spacing or by increasing bottom flange reinforcement as recommended in the report.

An effective endurance limit of 16 ksi, which corresponds to a fatigue life of 6 million cycles, is recommended for use with either fatigue model. However, no fatigue endurance limit greater than 10 ksi was found in the tests he reported and some of the tests were loaded to 10 million cycles.

For bridge members, the strand stress range is the difference between strand stresses computed at full dead load and service load conditions. The effect of an overload equal to 10 percent of the live load will also be considered.

4.6.2 Estimation of Strand Stress Range. Overman et al. [101] proposed a simplified approach for estimating the strand stress range in a cracked section that can be performed by hand. The method requires the strand stress and moment for three conditions: (1) at full dead load (effective prestress), (2) when a crack extends

to the bottom of the web, and (3) at flexural capacity. A bilinear relationship between applied moment and strand stress is defined by these three points from which the strand stress range may be computed.

The strand stress at full dead load and at flexural capacity will normally be computed as part of the design process. The strand stress and moment corresponding to the remaining conditions are determined by developing expressions for the steel tension and concrete compression forces in terms of the curvature across the section and elastic material properties. The curvature is then determined by equating the two expressions. The deck is transformed by the ratio of moduli of elasticity as in standard uncracked analyses. A stress offset between the girder and deck is used and the curvature is assumed to be the same for girder and deck. The shape of the section is approximated by rectangles by neglecting the triangular transition from web to top flange.

A computerized method for computing the strand stress range in a cracked section was developed for use in the program BRIDGE. This method uses an iterative strain compatibility analysis with elastic material properties to determine the stress directly for a given moment. Full section properties are used. This routine differs from the strain compatibility analysis used elsewhere in this chapter only in the use of elastic material properties and its capability to solve for conditions at a given moment rather than at a given top-of-deck strain.

The two methods are similar, since both are based on strain compatibility, but the BRIDGE analysis is more accurate than Overman's method because it directly computes the strand stress for a given moment and considers the full girder cross-section. It provides, however, a slightly less accurate estimate than would be obtained from the other strain compatibility analysis since elastic properties are used. The error, however, is very small due to the low stress levels involved in service load analysis. Overman's analysis is also dependent on the accuracy of the estimate of ultimate conditions made by the AASHTO equations. Since the simplified code approaches underestimate the flexural capacity, the resulting estimate of stress range is greater than the value predicted by strain compatibility analysis.

Stress ranges computed by the two methods for live load and a 10 percent overload are compared in Fig. 4.66 for maximum and typical span designs using 12 ksi concrete. A third value was computed using a modification of Overman's method in which the initial difference

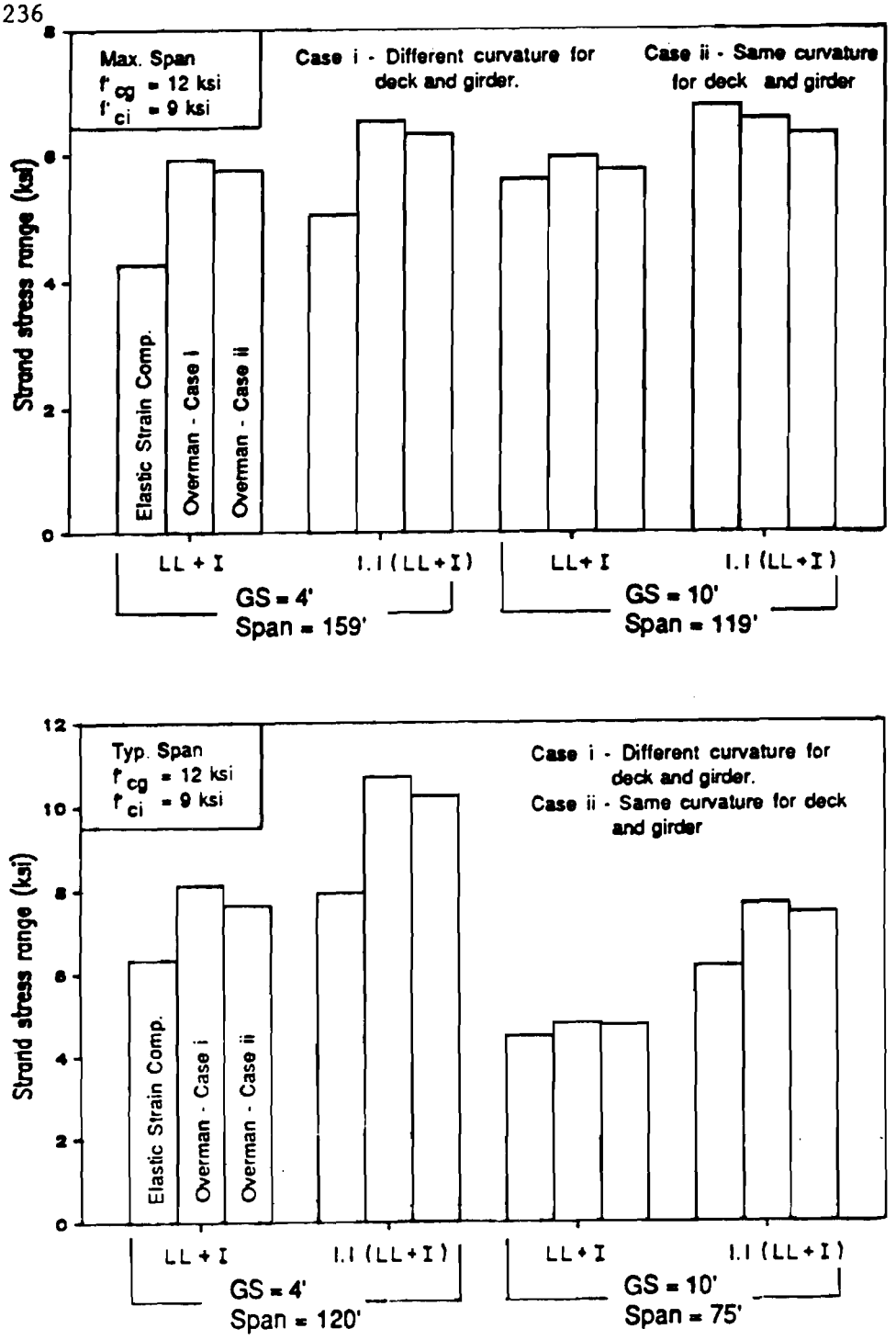

Fig. 4.66 Comparison of methods for computing strand stress range

between deck and girder curvatures is preserved in the analysis. Both forms of Overman's method used AASHTO equations for ultimate strand stress and moment. A computer spreadsheet program was used to perform calculations for both forms of Overman's analysis. In all but one case, both types of Overman's analysis gave slightly larger values of the stress range compared with values from the BRIDGE analysis. No specific reason could be found for the one exception for which the difference was small. The difference between the two forms of Overman's analysis is negligible which demonstrates that, for the accuracy intended for the original analysis, the complication added by considering the difference in deck and girder curvatures outweighs the increase in accuracy gained.

The accuracy of the strain compatibility analysis using inelastic section properties (MOMCURV) is compared with strand stresses determined from the tests of Specimens 1 and 2 in Fig. 4.67. Computed design loads are indicated on the curves. Agreement between the analysis and test data was excellent for Specimen 1 to loads exceeding a 10 percent overload. Behavior of Specimen 2 was accurately modelled to a load equal to the live load, at which point the curves began to diverge. While the approximation became worse with increasing load, the error, which was conservative, remained small for loads up to a 10 percent overload. It can therefore be expected, on the basis of this limited data, that strand stress ranges computed using strain compatibility methods should be reasonable estimates of actual stress ranges.

4.6.3 Investigation of Strand Stress Ranges. Strand stress ranges were computed for all maximum and typical span designs considered in this chapter using the routine included in BRIDGE. Data for the initial analysis using a concrete strength at release of 0.75 times the design strength and the subsequent analysis in which the minimum release strength was determined are shown in Fig. 4.68 and 4.69 for maximum and typical span designs, respectively. Where data is not given for designs with normal strength concrete, either a design using a release strength of 0.75 times the design strength was not possible or the girder was not in tension at service load or overload. The maximum stress range for a cracked section with live load was about 11 ksi, and the overload condition produced a maximum stress range of just over 14 ksi. The stress ranges at service load differed by as much as 6 ksi for uncracked and cracked sections, and the overload caused stress ranges up to 4 ksi greater than those at the service load level with a cracked section. The change in concrete strength at release had little effect on the stress range. It is interesting that for the typical span design with GS = 4 ft,

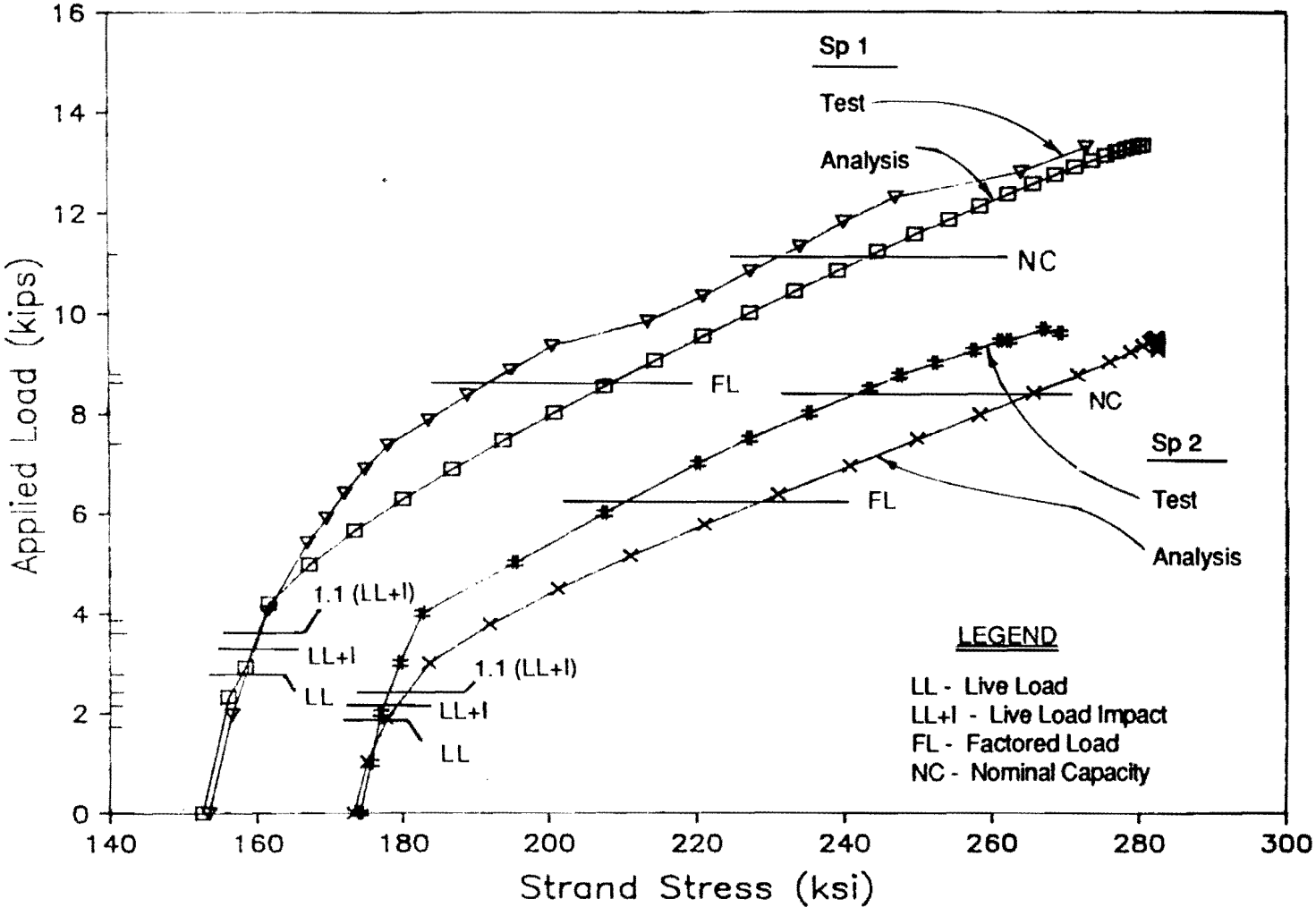

Fig. 4.67 Measured and predicted load-strand stress curves for Specimens 1 and 2

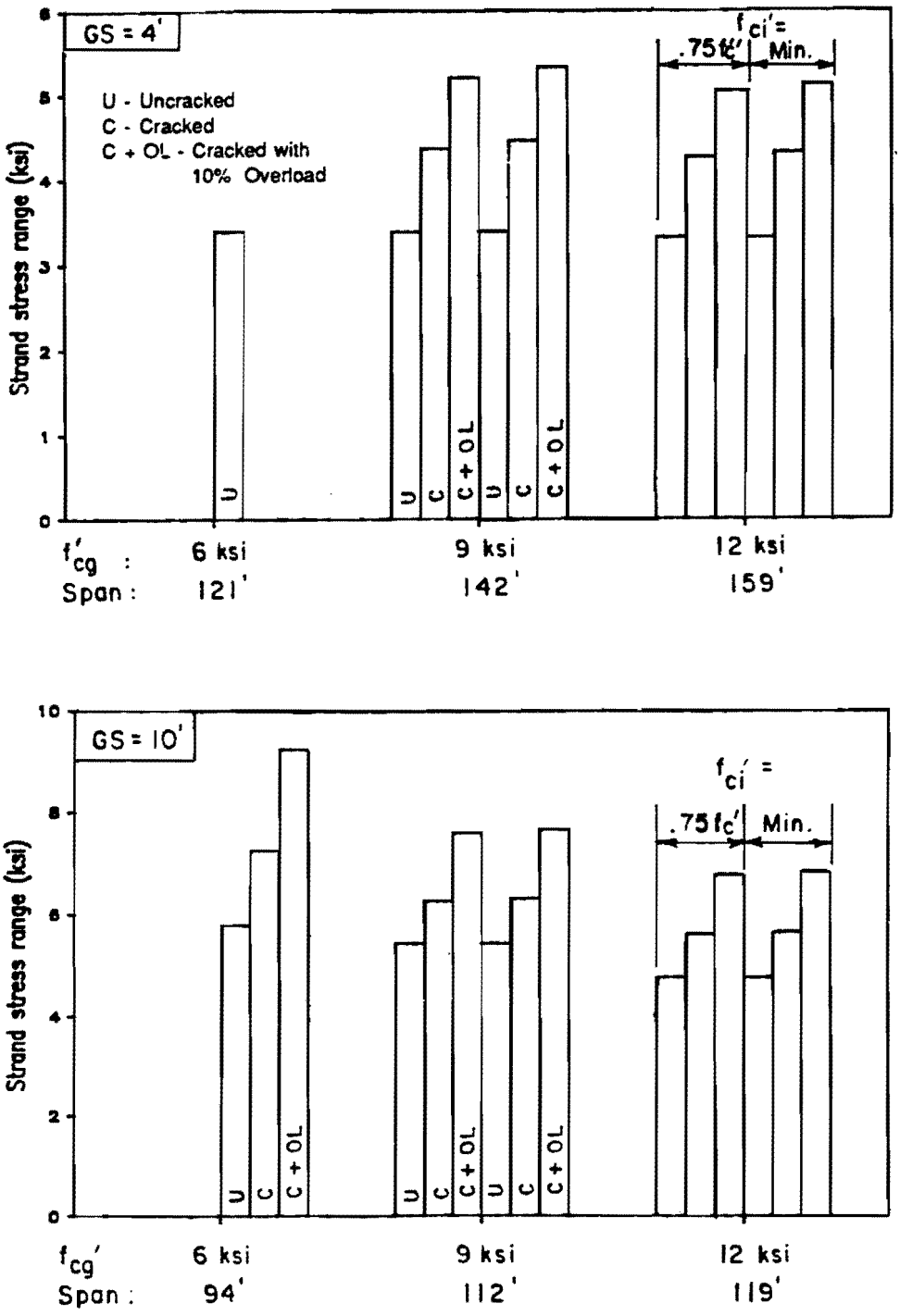

Fig. 4.68 Strand stress ranges for maximum span designs

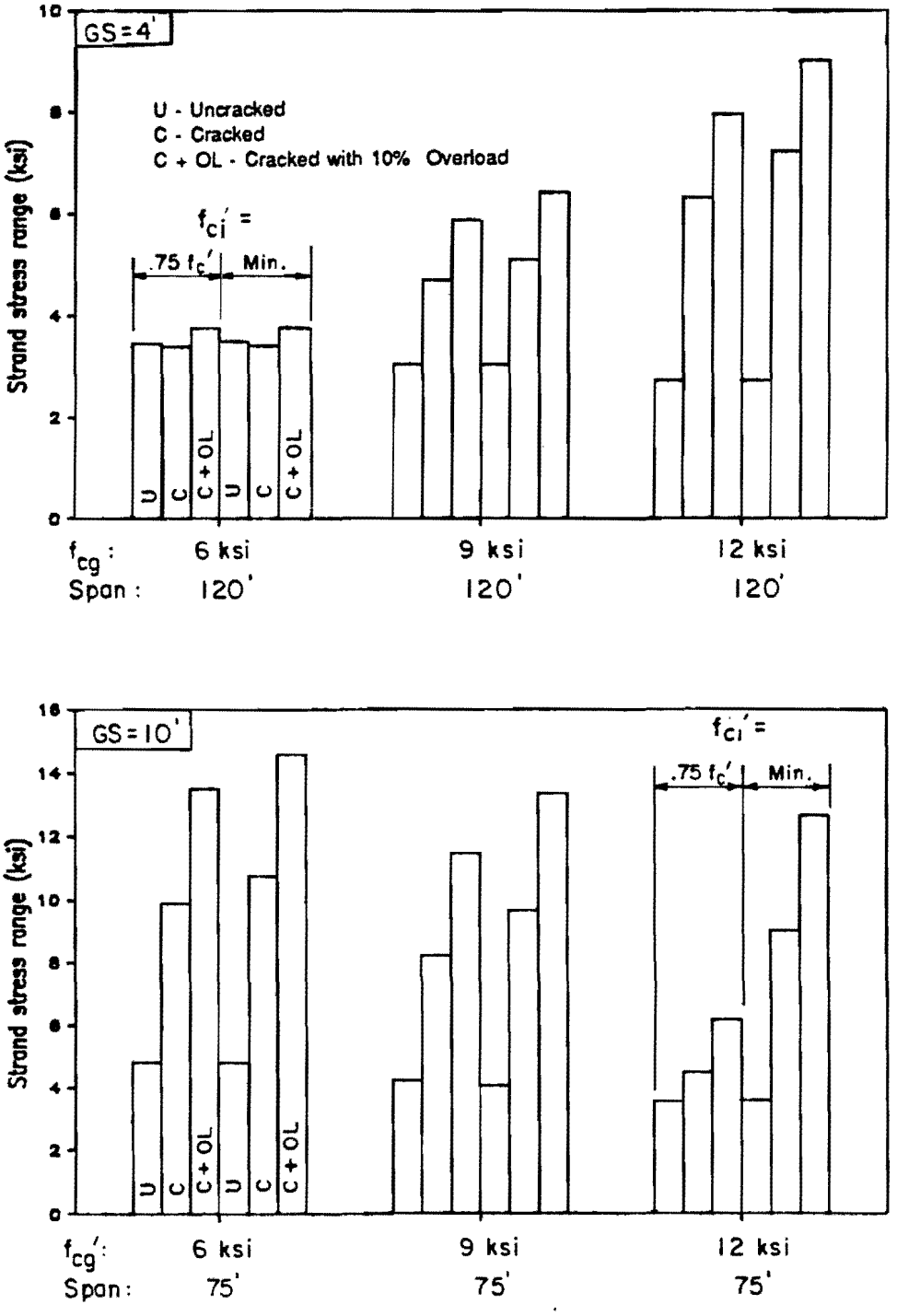

Fig. 4.69 Strand stress ranges for typical span designs

increasing the concrete strength caused a significant increase in the strand stress range. This was due to the fact that the girders were lightly reinforced and that cracking extended higher in the stronger concrete since less area of the cross section was required to provide the compression force. The marked decrease in the cracked section stress ranges for the 12 ksi design with a 75 ft span was due to the addition of 2 strands (from 24 to 26) to the lower strength designs. This dramatically demonstrates the sensitivity of stress range to quantity of reinforcement.

Due to the sensitivity of the stress range to the cracked or uncracked condition of the section, the ratio of the applied load that causes cracking to the live load (including impact) was computed for the maximum and typical span designs. The results are summarized in Fig. 4.70. This data reveals that some designs are very susceptible to cracking with only a small overload. The maximum span designs are especially sensitive with some cracking at overloads as low as 12 percent. Use of a lower release strength lowered these values only a very small amount.

The difference between strand stress ranges at the centroid of the strands and for the bottom row of strands was considered. It was found that the difference was negligible because where the stress range was large, the girder was lightly reinforced and the distance from the centroid of the strands to the bottom strand was small. However, if strand patterns are used that distribute strands in the bottom flange rather than filling each row from the bottom, the difference could be significant and should be investigated.

Due to the sensitivity of strand stress ranges to cracking and the potential for some girders to crack with small overloads, it is recommended that cracked section analysis be used to determine strand stress ranges. This is not a prohibitive limit on design since the likelihood that the endurance limit will be exceeded is small. However, an accurate assessment of the actual loads experienced by bridge girders should be made and the elevated stress ranges caused by overloads should be considered in design. Overman's method of computing stress ranges should be sufficient to provide conservative estimates of strand stress ranges. However, a more sophisticated strain compatibility analysis should be used if more accurate results are desired.

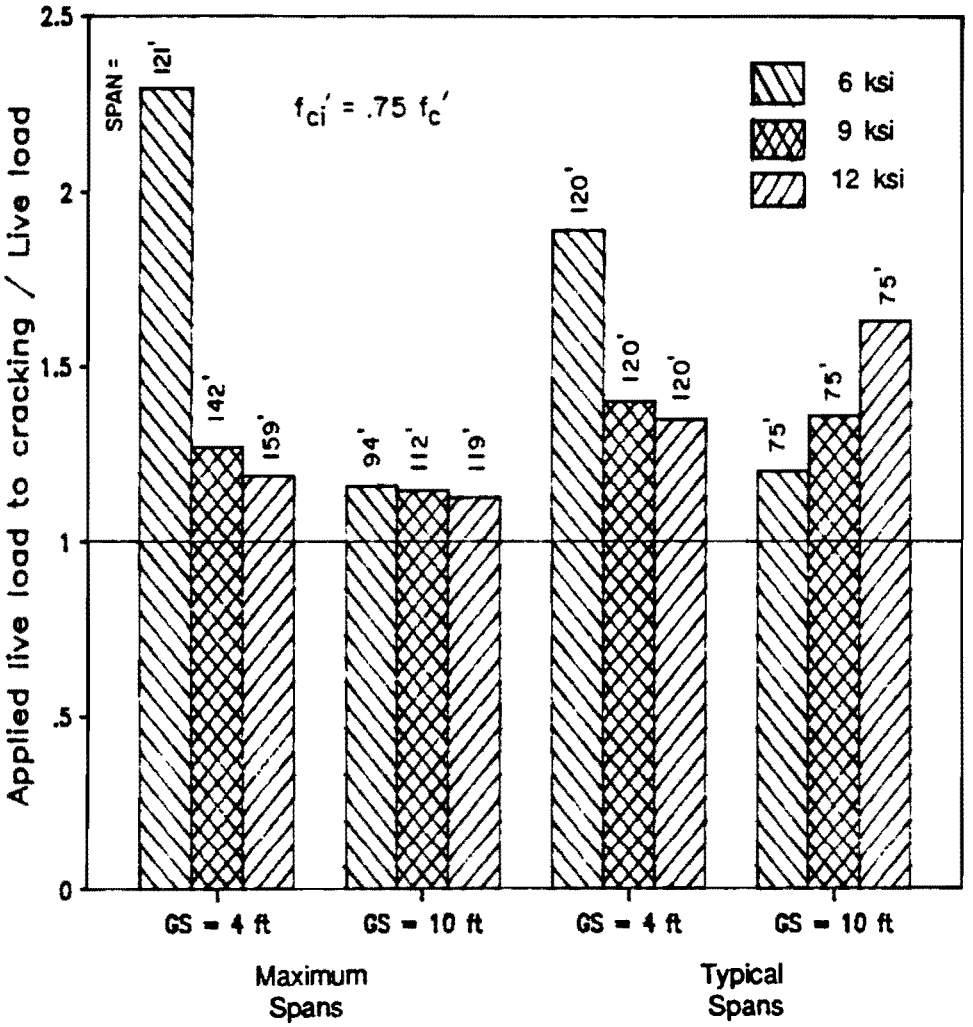

Fig. 4.70 Applied load to cracking as a fraction of live load for maximum and typical span designs

4.7 Prestress Losses

The method for computing prestress losses proposed by Zia et al. [137] was used for the design of the beams used in the comparisons in this chapter. However, Kelly [72] recommends that the method provided in the AASHTO Specifications [10] or a slight modification of that method be used. He points out that the current AASHTO procedure gives losses that are probably a few percent greater than the actual losses, but closer to reality than the method by Zia et al. [137] which underestimates losses.

The losses computed for maximum and typical span designs used in this chapter are presented in Fig. 4.71 and 4.72, respectively. The AASHTO losses shown are computed using the procedure currently appearing in the AASHTO Specifications. While a direct comparison is difficult for the maximum span data because the span length affects the losses, the losses do appear to be of similar magnitude. For the typical span designs with GS = 4 ft, losses decreased markedly as the concrete strength increased. However, the trend reversed slightly for the typical span designs with GS = 10 ft. Therefore, it appears that no definitive statement can be made with respect to prestress losses and high strength concrete, although losses are generally of the same magnitude as computed for normal strength girders.

4.8 Bond of Prestressing Steel

Data from the transfer tests reported in Ref. [139] are shown graphically in Fig. 4.73. It is clear from the tests that high strength concrete had shorter transfer lengths than normal strength concrete. The AASHTO equation for transfer length is quite conservative for the high strength concrete data shown. This behavior is comparable to the data reported by Mayfield et al. [89]. It should be noted that the strand was cut using a torch between only two of the specimens for each strength, giving a "cut end" condition for only those specimens. The specimens with the longest transfer lengths (for normal strength concrete) were released by detensioning the ram. Figure 4.74 shows data from Kaar et al. [70], Hanson [53], Mayfield et al. [89] and data from this test. No distinction is made between cut end or dead end conditions. The AASHTO transfer equation is also plotted on the figure. It appears that transfer lengths tend to decrease with increasing concrete strength and the AASHTO equation becomes more conservative with higher concrete strength. Therefore, the current equation should be used with confidence for high strength

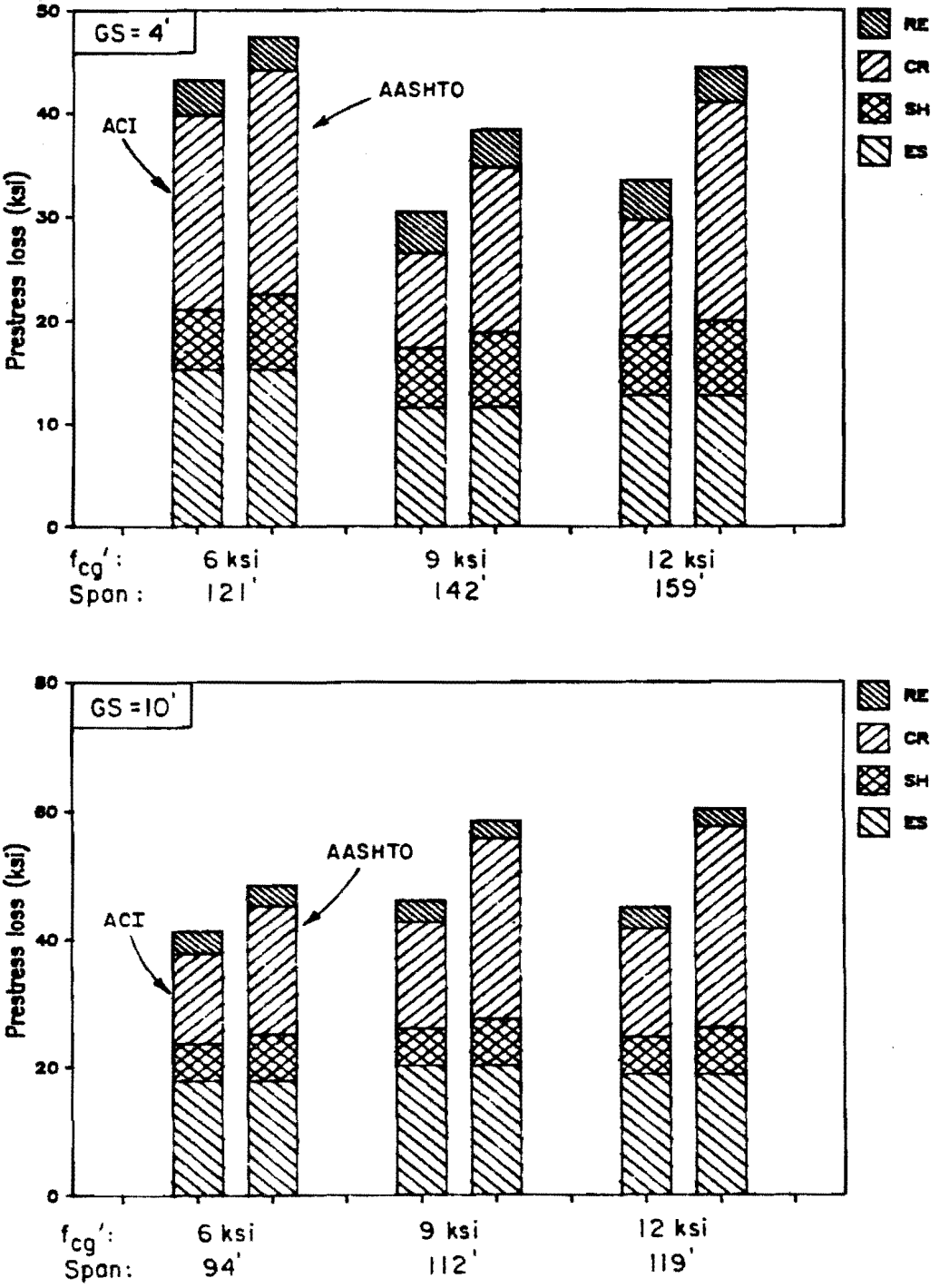

Fig. 4.71 Prestress losses for maximum span designs

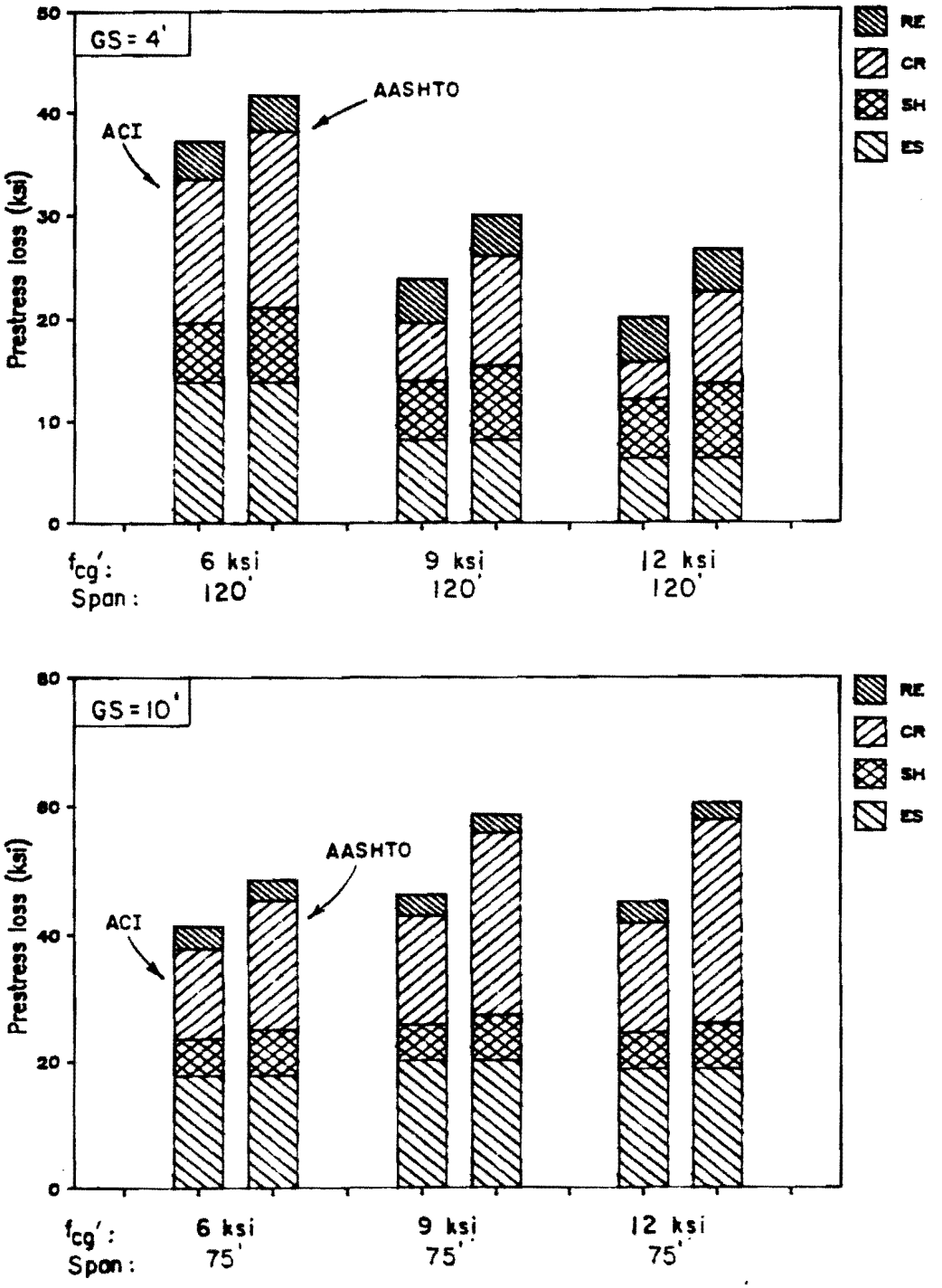

Fig. 4.72 Prestress losses for typical span designs

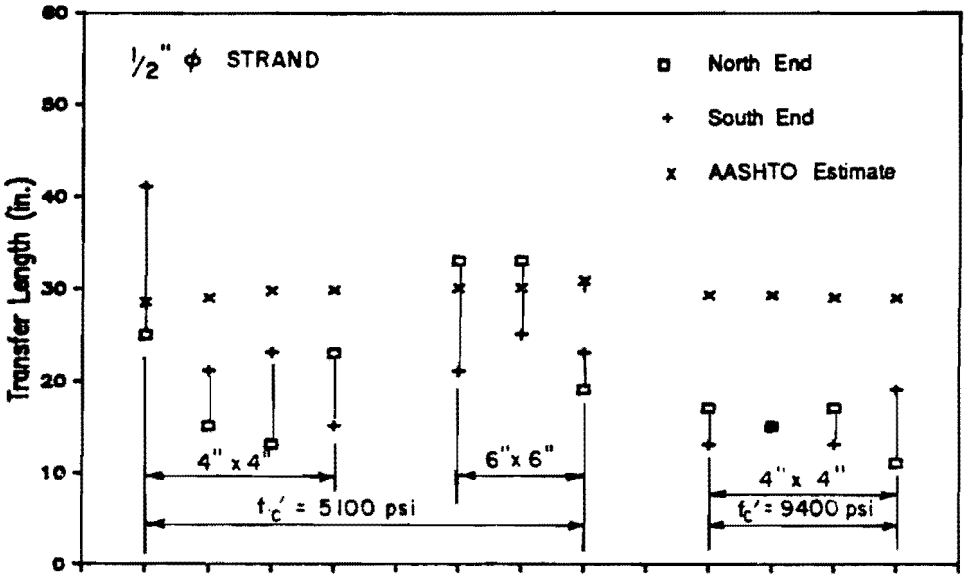

Fig. 4.73 Transfer length data from this study

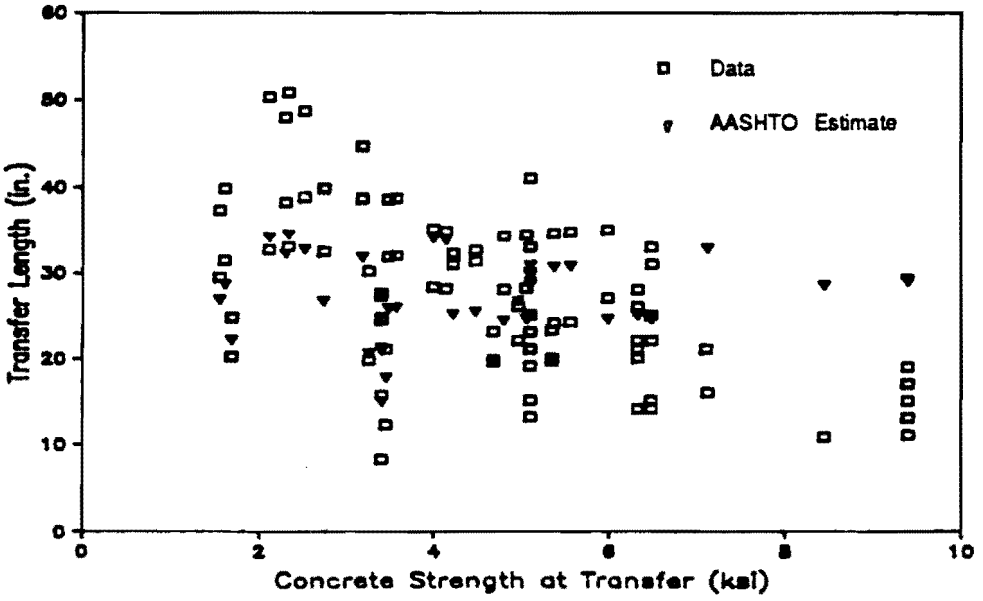

Fig. 4.74 Comparison of measured and computed transfer lengths

concrete because it works at least as well if not better for high strength concrete than for normal strength concrete.

More work needs to be done on the development length of strand in high strength concrete.

4.9 Notation

The differences in notation between AASHTO and ACI codes are confusing and unnecessary. Notation found in both codes gives the impression of being assembled in a piecemeal, haphazard manner rather than in a way to provide order and meaning.

The simple proposal made here is that the first letter subscript to any quantity be indicative of the material to which the quantity applies. Specifically, these letters when appearing as a first subscript would have the following meaning:

p: prestressing steel
s: nonprestressed steel
c: concrete.

A single quotation mark used as a superscript would differentiate between the quantity in the compression zone, where the same quantity without the mark would apply to the tension zone. For example, d_p applies to tension zone prestressed reinforcement and d_p' refers to compression zone prestressed reinforcement. These subscripts would be applied to stresses, strains, areas of steel, and effective depths to the centroid of the area of steel.

A set of letters used as the second subscript would also have unique meanings:

0: initial value, at tensioning
i: initial value, after release
e: effective value, at full dead load
y: value at yield
n: value at computed nominal capacity
u: specified ultimate value for material.

Other letters may also appear as second subscripts with unique meanings.

The letter w may be used as either the only or the second subscript to indicate the web dimension or a quantity determined using web dimensions for flanged analysis, such as the reinforcement ratio.

This system of notation would permit use of variables without subscripts to represent a total or resultant value. Examples of this would be the use ω to indicate the total reinforcement index or the use of d to represent the distance from the extreme fiber to the resultant tension force of all reinforcement.

Table 4.6 presents a sample of the proposed notation system and compares it with the current equivalent notation used in the AASHTO and ACI codes. Definitions are given only as an indication of the meaning of the entries in the table and are not intended to be new or proposed definitions. Notation for both codes would be changed in some instances to conform with the proposed notation. Changes in other notation would be necessary to create complete uniformity among the codes.

While the proposed change in notation to provide uniformity among codes is desirable, it is recognized that there may be considerable resistance to such a change. It would also be a change of convenience and is not necessary to improve the safety or accuracy of designs using the codes.

Table 4.6 Proposed and Current Notation

Proposed	AASHTO	ACI	Brief definition
f_{p0}	-	-	stress in prestressed reinforcement immediately after tensioning
f_{pi}	-	-	stress in prestressed reinforcement immediately after release
f_{pe}	f_{se}	f_{se}	effective stress in prestressed reinforcement after losses
f_{py}	f^*_y	f_{py}	specified yield stress of prestressed reinforcement
f_{pu}	f'_s	f_{pu}	specified ultimate tensile stress of prestressed reinforcement
f_{pn}	f^*_{su}	f_{ps}	stress in prestressed reinforcement at nominal strength
f_{sy}	f_{sy}	f_y	specified yield stress of non-prestressed reinforcement in tension
f_{sn}	-	-	stress in nonprestressed reinforcement in tension at nominal strength
f'_{sy}	f'_y	f_y	specified yield stress of non-prestressed reinforcement in compression
f'_{sn}	-	-	stress in nonprestressed reinforcement in compression at nominal strength
A_p	A^*_s	A_{ps}	area of prestressed reinforcement
A_{pf}	A_{sf}	-	area of prestressed reinforcement required to develop overhanging portion of flange
A_{pw}	A_{sr}	-	area of prestressed reinforcement required to develop web of a flanged section
A_s	A_s	A_s	area of nonprestressed tension reinforcement
A'_s	A'_s	A'_s	area of nonprestressed compression reinforcement

Table 4.6 Proposed and current notation (continued)

Proposed	AASHTO	ACI	Brief definition
ρ_p	p*	ρ_p	ratio of prestressed reinforcement
ρ_s	p	ρ	ratio of nonprestressed tension reinforcement
$\rho p'_s$	p'	ρ	ratio of nonprestressed compression reinforcement
ω_p	-	ω_p	reinforcement index for prestressed reinforcement
ω_{pw}	-	ω_{pw}	reinforcement index for prestressed reinforcement for flanged section
ω_s	-	ω	reinforcement index for prestressed tension reinforcement
ω_{ws}	-	ω_w	reinforcement index for nonprestressed tension reinforcement for flanged sections
d_p	d	d_p	distance from extreme fiber to centroid of prestressed reinforcement
d_s	-	d	distance from extreme fiber to centroid of nonprestressed tension reinforcement
d'_s	-	d'	distance from extreme fiber to centroid of nonprestressed compression reinforcement
E_p	E_s	E_s	modulus of elasticity for prestressed reinforcement
E_s	E_s	E_s	modulus of elasticity for nonprestressed reinforcement
E_c	E_c	E_c	modulus of elasticity for concrete at 28 days
E_{ci}	E_{ci}	-	modulus of elasticity for concrete at release

CHAPTER 5

SUMMARY AND CONCLUSIONS

5.1 Summary

Recently, it has been demonstrated that high strength concrete can be produced using conventional materials and appropriate admixtures. For purposes of this study, high strength concrete is defined as concrete with a design compressive strength from 6,000 psi to 12,000 psi, which is the current range of strengths for readily attained field-produced concrete. For some analytical investigations in this study, concrete with strengths up to 15,000 psi was considered in order to identify trends.

Use of high strength concrete is expected to produce more economical bridge designs by allowing fewer girders for a given span, or increased span lengths. However, there are uncertainties about use of current design codes for high strength concrete because of differences in behavior between high and normal strength concrete and the lack of test data for structures constructed with high strength concrete. Current codes are also largely empirical and are based on tests utilizing concrete with compressive strengths rarely greater than 6 ksi. Realization of the full potential of high strength concrete may also be limited by outdated design and construction practices.

Therefore, this study was conceived for the purpose of investigating the use of high strength concrete in design of pretensioned girders with a normal strength composite deck. The scope of the study was limited to the consideration of simple span, non-skew pretensioned girder highway bridges where a composite deck is placed with the girder unshored.

A selection of pretensioned girder sections was compared to determine how well given sections utilize high strength concrete. It was demonstrated that a significant increase in span or girder spacing was possible with use of high strength concrete. The lateral stability of girders during handling was found to restrict the span capability of many sections although some means are available to improve girder stability. Three new girder cross-sections were developed and shown to have span capabilities similar to or better than sections of the same depth that are currently used in Texas.

A review of the literature was conducted to determine the state-of-the-art in design using high strength concrete, and to determine the intent of pertinent code provisions. A wide range of topics were considered because the observed brittle behavior of high strength concrete and the potential of extending sections and materials to their limits necessitated the examination of nearly all aspects of design.

Due to the lack of data for composite bridge construction with high strength concrete pretensioned girders, three test programs were developed and completed.

The first set of tests, which are described in Ref. [139] compared transfer characteristics of 0.5-in. diameter seven-wire strand in normal and high strength concrete. Two strengths of concrete were used to cast two sizes of specimens with square cross section which were pretensioned with a single concentric strand. The strands were pretensioned to levels common in practice. Concrete strains measured mechanically before and after release were used to determine transfer lengths. The data collected allowed evaluation of current code transfer length provisions with respect to use with high strength concrete.

Two scale-model high strength concrete pretensioned girders with normal strength composite decks, which were representative of possible long-span bridge designs, were tested in the second phase of the project. The specimens were one-third scale models of prototype modified Type IV girders spanning 146 ft and spaced 4 ft apart. The span-to-total depth ratio was 28.8. Specimen 2 contained close to the minimum number of strands permitted using current allowable stress and ultimate strength design criteria. Specimen 1 contained additional strands and still satisfied the allowable stress criteria but exceeded the maximum reinforcement limit.

High strength concrete was easily placed in the girders even where reinforcement was very congested. No problems in consolidation were encountered. Widespread shrinkage cracking occurred prior to release of Specimen 2. Although sweep was measured in both specimens at release, no difficulties were encountered handling the girders. Prior to testing, however, both specimens were found to have significant sweep that necessitated lateral restraint of the specimens during testing to prevent further lateral movement.

The specimens were tested in flexure by applying equal loads at equal distances from midspan. Data were collected throughout the tests for strand strains, concrete strains, and deflections. A sudden

and violent compression failure occurred for both specimens. At failure, the top portion of the girder was still in compression. It was not possible to determine conclusively whether crushing of the girder or deck concrete initiated failure.

The third phase of the test program involved shear tests on the end details of the two flexural test specimens and a series of six girders. Details of the shear tests and evaluation of the test results are presented in Ref. [138].

The literature review and test data were used as the basis for evaluation of current design practice. The flexural test data were used to verify a basic strain compatibility analysis program as a simple yet effective and accurate tool for analysis of composite pretensioned girder bridges. Representative bridge designs were used to determine the accuracy and appropriateness of current design procedures, and to study the sensitivity of design aspects to different parameters. Recommendations were made where changes to current code provisions and practice appeared necessary.

5.2 Conclusions

In this section, major conclusions from the study are presented. Each conclusion or group of related conclusions is numbered and followed by a reference to the section from which the conclusion is taken. More complete and detailed conclusions were given as specific topics were considered in the body of the text.

1. The use of high strength concrete in pretensioned bridge girders results in significant increases in span length or girder spacing. (3.4.1)

2. Increasing the concrete strength for a given span and spacing will not generally affect the minimum number of strands required to satisfy design criteria. (3.4.2)

3. The lateral stability requirements for handling severely limit the above mentioned increase in maximum span capacity for some sections, especially 54- and 72- in. sections. (3.3.3, 3.4.1)

4. Sweep and eccentricity of lifting points have a significant effect on the lateral stability of girders and must be considered in design. (4.5.1)

5. The use of high strength concrete to improve the stability of a girder is most effective when used for a given span rather than to increase the maximum lifting span. (4.5.1)

6. The lateral stability of a girder may also be improved by moving lifting points in from the ends of a girder, using external bracing ("hog-rods"), or using rigidly attached lifting yokes. (4.5.1)

7. Sections with greater weak-axis moments of inertia generally have the greatest lateral stability when lifted. The MOT/C&CA M 54/6 section, which has a large bottom flange, had the best overall performance with respect to stability. (3.3.3, 3.4.1, 4.5.1)

8. In some cases, use of high strength concrete will permit a reduction in the fraction of design strength required at release as compared to that required for normal strength designs. (4.2.5.5)

9. Three proposed sections provide good alternatives to currently used sections considering span capabilities, section size, and lateral stability. (3.4.1)

10. A comparison of actual designs provides the best indication of relative performance of different sections. (3.3.1, 3.4.3)

11. On the basis of limited test data, the transfer length of strand in high strength concrete is slightly shorter than for normal strength concrete. (2.6 of Ref. [139])

12. The AASHTO expression for estimating transfer length is conservative for high strength concrete. (2.6 of Ref. [139])

13. Because the modulus of elasticity can vary widely due to a number of factors, it is recommended that the modulus be determined experimentally when an accurate value is needed. (5.3.2 of Ref. [139])

14. Current code expressions for the modulus of elasticity are sufficiently accurate if data for a specific mix is not available. (5.3.2 of Ref. [139])

15. The effect of using the modulus equation proposed by investigators at Cornell rather than current modulus equations is small. (4.2.5.4)

16. In this study, the maximum usable concrete strain was found to be lower for high strength concrete than for normal strength concrete, which agrees with the trend of data reported by other investigators. (5.3.2 of Ref. [139], 4.2.3.2)

17. In composite members, the normal strength deck concrete will generally reach the maximum usable strain before the girder concrete reaches its limiting strain. (4.2.4.2, 4.2.5.2)

18. In this study, compression failures occurred while measured compressive strains in both the deck and girder concrete were below the current code specified value of 0.003. (5.3.2 of Ref. [139])

19. The use of a reduced maximum usable concrete strain in design and analysis does not generally affect the capacity but would result in reduced deflections, section ductility, and other strain related quantities at failure. (4.2.5.2)

20. Placement of high strength concrete in narrow, congested sections is possible through the use of high range water reducers (superplasticizers). (5.3.7 of Ref. [139])

21. The AASHTO and ACI simplified ultimate flexural design approaches provide good, conservative estimates of the capacity of composite sections when compared with test data and results of strain compatibility analyses. (4.2.4.2, 4.2.5.2)

22. Horizontal girder dimensions should be transformed by the ratio of girder-to-deck concrete strengths when using the simplified flexural strength analysis methods in order to obtain the best agreement with results of strain compatibility analyses. (4.2.2.2, 4.3.2.2)

23. Current expressions for determining strand stress at ultimate are adequate. The revised equation in the ACI Code gives better estimates than the AASHTO expression

when compared to test data and results of strain compatibility analyses. (4.2.4.2)

24. The strain compatibility analysis program MOMCURV gave conservative yet realistic estimates of measured flexural behavior for specimens. The capacity of the section was very closely predicted and provided a better estimate of capacity than the simplified methods. (4.2.3)

25. Suitably accurate analytical relationships for defining concrete and steel stress-strain curves are available and should be used to obtain the best estimate for all aspects of section behavior when using a strain compatibility analysis. (4.2.3.1, 4.2.3.2)

26. The current practice of limiting the reinforcement index ω to ensure a section has sufficient ductility is appropriate and accurate. (4.3.1, 4.3.2.2)

27. The current maximum reinforcement limit is based on assumptions that are inconsistent with other code provisions and current practice. (4.3.2.1)

28. A maximum reinforcement limit that is consistent with code provisions and current practice, and similar to the current limit is proposed. This limit includes the effect of strand strength and effective prestress. The limit is slightly more restrictive than the current limit in most cases. Because the proposed limit appears in a form similar to the maximum reinforcement limit for reinforced concrete members, it should be readily understood and accepted for use by designers. (4.3.2.1)

29. A minimum reinforcement limit is proposed which would prevent rupture of strands prior to the extreme concrete compression fiber reaching the maximum usable strain. The proposed limit has the same form as the maximum reinforcement limit but can also be expressed in a simplified form without significant loss of accuracy. (4.3.3).

30. Deflections due to applied loads can be accurately estimated using a strain compatibility analysis. (4.4.2)

31. Live load deflections should be limited to the levels currently specified for steel bridges in the AASHTO Specification. (4.4.3)

32. Long-term deflections should be estimated for girders to ensure good serviceability, especially for long-span members. Limits for long-term deflections of pretensioned concrete highway bridges should be developed. The possibility for differential camber should be investigated where significant differences in age or curing conditions exist between girders within a span. (4.4.1)

33. Strand stress ranges should be used for determining the fatigue resistance of pretensioned girder bridges. Suitably accurate estimates of strand stress ranges in cracked sections can be made using a strain compatibility analysis. (4.6)

5.3 Recommendations

The following recommendations are made for further study or for changes in current codes of practice. The same format will be used as for the conclusions.

1. Further study should be performed to determine the strain in the top fiber that leads to crushing in a member, especially for T - shaped members. The development of a correlation between maximum usable concrete strain and depth of the neutral axis at failure should be explored.

2. Derivations and intent of the proposed maximum and minimum reinforcement limits should be published as part of the codes or in associated commentaries in order to help designers understand the reinforcement limits.

3. Further study should be conducted on the lateral stability of girders during lifting and transportation operations. A survey of state and federal highway departments, fabricators, and erectors is recommended to determine their experience with different sections and to obtain data which can be used to verify stability analyses. A range of typical imperfections should also be obtained for use in the design process. (4.5.1)

4. Further study should be conducted on typical bridge designs for various sections. In these studies, the effect of various parameters, including concrete strength, should be studied to determine how they affect

all aspects of design, including lateral stability, fatigue, cracking, and deflections.

5. Use of an approximate equation to compute the cracking moment for the current minimum reinforcement limit should be discontinued since it leads to excessively high ultimate strength requirements in some cases.

6. AASHTO and ACI notation should be revised to be consistent in order to minimize confusion. The notation proposed in Chapter 4 is consistent and could serve as a starting point for the standardization process.

A P P E N D I X A

DEVELOPMENT OF REINFORCEMENT LIMITS

A.1 Maximum Reinforcement Limit

The development of this limit will be presented in outline form, explaining the assumptions made for each quantity listed in Fig. 4.47 which is repeated her as Fig. A.1.

F — This is a factor which indicates the efficiency or effectiveness of the bond between concrete and steel. The value of 1 used indicates that the bond is full and that strains computed in the concrete at the level of the steel will also apply to the steel. This is a reasonable assumption for bonded prestressed construction.

ϵ_{cu} — This is the maximum usable concrete strain at ultimate. As the summary in Fig. A.1 indicates, the early and current forms of the limit used a value of 0.004 for the limiting concrete strain in the derivation of the maximum reinforcement limit. This is inconsistent with other provisions in current codes. Therefore, to correct this inconsistency, a value of 0.003 is used for the proposed limit.

ϵ_{su} — This strain is the limit which represents yield in the strand. The intent of the limit is for this strain to be reached or exceeded at ultimate conditions. The full development of the reason for this limit is given in Chapter 3 but can be summarized as follows:

> The capacity of the section is very sensitive to material or dimensional variations when the strand strain at ultimate is in the linear portion or initial part of the knee of the stress-strain curve. Therefore, it is desirable for the strain at ultimate to be greater than that corresponding to the latter part of the knee in the stress-strain curve.

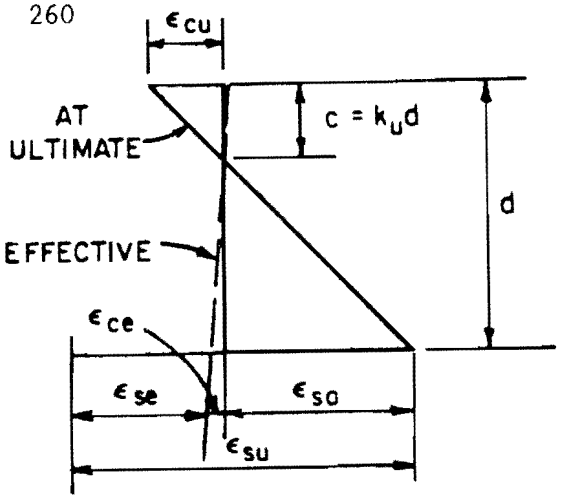

$$k_u = \frac{F\epsilon_{cu}}{F\epsilon_{cu} + \epsilon_{sa}}$$

$$= \frac{F\epsilon_{cu}}{F\epsilon_{cu} + \epsilon_{su} - \epsilon_{se} - \epsilon_{ce}}$$

$$= \rho \frac{f_{su}}{f_{cu}}$$

$$= c/d$$

	Warwaruk et al. 1962	ACI Comm 323 (current AASHTO) 1958	ACI 318-83 1983	Proposal
Reference	[133]	[10, 19]	[15]	Appendix A
F	1	1	1	1
ϵ_{cu}	0.003	0.004	0.004	0.003
ϵ_{su}min.	0.01*	0.01*	0.01*	$0.01+(f_{pu}-250)/28000$
ϵ_{se}	0.0045**	0.0045**	0.0045**	$f_{se}/28000$
ϵ_{ce}	0	0	0	0
$k_u$limit	≤ 0.353	≤ 0.421	≤ 0.421	$\leq 84/[114+f_{pu}-f_{se}]$
f_{cu}	$0.7f'_c$	$0.7f'_c$	$0.85\beta_1 f'_c$	$0.85\beta_1 f'_c$
ω	0.25	0.30	$0.36\beta_1$	$0.85\beta_1[84/(114+f_{pu}-f_{se})]$

* - Based on Grade 250 material.

**- An average of the expected range from 0.004 to 0.005.

Modulus of strand is assumed to be 28000 ksi. Stress units in ksi.

Fig. A.1 Assumptions for maximum reinforcement limits

The value of 0.01 which was used for the derivation of prior limits was based on the use of Grade 250 material. However, Grade 270 material is now the standard and higher grades of material are being developed. Therefore, it appears appropriate to increase this limit to provide the same behavior as was intended with the original limit. This can be accomplished by assuming stress-strain curves for different grades of steel differ only in the extent of the initial linear portion of the curve. The limiting strain could then be determined for other grades of steel by adding an increment of strain to the original limit (0.01) which is assumed equal to the difference in ultimate strand stresses divided by the modulus of the strand. This is illustrated in Fig. A.2. The following expression is then used to compute the limiting strain:

$$\epsilon_{su} = 0.01 + \left(f_{pu} - 250 \right) / E_p \qquad (A.1)$$

where E%p = modulus of prestressed reinforcement
= 28,000 ksi (from AASHTO)

and f_{pu} is expressed in ksi. As the strains shown in Fig. A.2 indicate, the difference between the proposed expression for ϵ_{su} and the current limit of 0.01 is only 7 percent for Grade 270 strand. The difference would become greater for either higher or lower grades of steel. For lower grade prestressing reinforcement, the current limit would be overly conservative.

It should also be noted that this approach to limiting the strain in the prestressing steel is based on balanced failure as the limit. While this is consistent with the practice of allowing over-reinforced prestressed after an appropriate reduction in ultimate capacity, it does not agree with the concept employed for reinforced concrete sections where the strain in the reinforcement is forced to be nearly twice the yield strain at ultimate. Therefore, this limit could not be extended for use with reinforced members without modification.

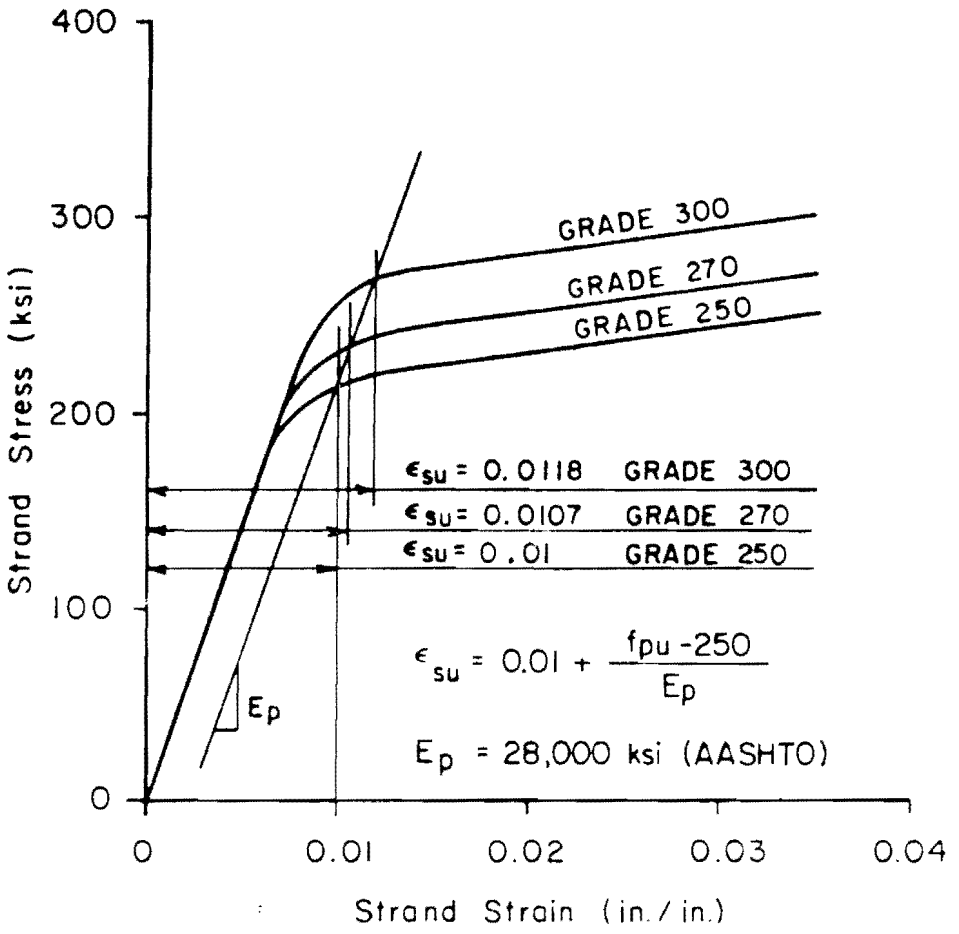

Fig. A.2 Limiting prestressed reinforcement strain for maximum reinforcement limit

ϵ_{se}

This is the effective strain in the steel after losses which corresponds to the stress f_{se}. In the current limits, a value of 0.0045 is assumed which represents and average of the expected range of strains (0.004 to 0.005). However, as was demonstrated in Sec. 4.3.2.1, the limit is sensitive to the value of ϵ_{se} used. These strains, however, also represent the practice for Grade 250 steel and correspond to stresses of 112 to 140 ksi, which are very low for current practice. The use of such low strains would result in excess conservatism in the limit. It is therefore proposed that the effective prestress be used in the limiting equation. This would not be an undue hardship on the designer since this value must be computed for use in the allowable stress design of the member.

The sensitivity of the new limit to variation in effective strand stress is demonstrated for Grade 270 steel in Table A.1. The limit varies approximately ± 8 percent for stresses ranging 20 ksi below and 15 ksi above the 170 ksi value which is a rough estimate for current practice using Grade 270 steel.

The use of higher grades of steel would lead to higher effective stresses, resulting in a conservative error if an average value for Grade 270 steel were used. However, where lower grades of prestressed reinforcement are used, use of the average effective prestress for Grade 270 strand would lead to unconservative results.

It appears that this error introduced by using grades of steel other than the one with which the limit was derived would tend to offset the error introduced by using a constant value for the limiting strain as mentioned above. However, even though this may be the case, a direct approach where all variables are considered individually is preferred over an approximate method that remains reasonable by the chance interaction of variables. Such limits cannot be applied to unusual situations. The inclusion of both the ultimate stress of the strand and the effective stress is therefore strongly recommended to maintain validity and clarity for future situations which are not reflected in current practice.

Table A.1 Variation of proposed maximum reinforcement limit with effective prestress

f_{se} (ksi)	Eq. A.2. $\beta_1 = 0.85$	Eq. A.2. $\beta_1 = 0.65$	% diff. *
150	0.2594	0.1983	9.33
170	0.2836	0.2169	0
185	0.3050	0.2332	-7.02

* The percentage different (% diff.) is between the 170 kis and the other values of f_{se} (150 or 185 ksi) and is computed using the other values as the basis of the comparison. The percentages apply to both values of β_1.

ϵ_{ce} The effective strain in the concrete at the level of the prestressed reinforcement is small compared with the other stress involved in the analysis. Neglecting this component of total strand strain unconservative, but the magnitude of the error is very small.

ϵ_{sa} This strain (the notation is taken from Warwaruk et al. [133]) is the product of the curvature across the section at ultimate and the distance from the neutral axis to the centroid of the prestressed reinforcement. This quantity appears in the derivation and is replaced by the difference between the limiting strain, ϵ_{su}, and the effective strain, ϵ_{se}.

f_{cu} This is the average stress in the compression zone. It was used in the Warwaruk et al. report [133] to describe the stress block rather than the equivalent rectangular stress block. However, this quantity can be expressed in terms of the stress block parameter β_1 as shown in Fig. A.1. This was the basis for the change in the limit that appeared in ACI 318-83. The inclusion of the β_1 factor is appropriate and will be used in the proposed limit.

The derivation of the limit is shown in Fig. A.1. It is based on the determination of the factor k_u which represents the ratio of the depth of compression at ultimate, c, to the effective depth, d. This limit has been shown to be related to the reinforcement ratio and in this way, using the relationship between f_{cu} and f'_c, the following limit for the reinforcement index can be developed:

$$\omega \leq 0.85\beta_1\left[84/(114 + f_{pu} - f_{se})\right] \qquad (A.2)$$

where f_{pu} and f_{se} are expressed in ksi.

This approach is identical to that used for developing the reinforcement ratio corresponding to balanced failure, with the addition of the effective prestress term. The resulting equation appears very similar to that used for rectangular reinforced concrete sections. There, it is anticipated that such an expression would gain rapid acceptance among designers since it is not an unfamiliar concept and because it adds reason to a limit which at the present time is

misunderstood as a result of the total lack of information on its intent and derivation.

A.2 Minimum Reinforcement Limit

The derivation of the minimum reinforcement limit follows the same approach as discussed for the maximum limit. The only difference is that the limiting strain ϵ_{su} is changed to 0.035, which is the ASTM minimum specified elongation for seven wire stress-relieved and low-relaxation prestressing strand. This limit will be assumed to be constant for all grades of strained, although it could be different for prestressing materials other than seven wire strands. Therefore, the only variable related to strand stress that appears in the expression for the limit is the effective prestress. The minimum reinforcement limit is

$$\omega \geq 0.85\beta_1 \left[84/(1064 - f_{se}) \right] \tag{A.3}$$

where f_{se} is expressed in ksi. However, since the constant in the denominator is fairly large compared with the effective prestress, the use of a constant value for f_{se} is appropriate for Grade 270 strand. The resulting limit, where f_{se} is approximately 170 ksi, is

$$\omega \geq 0.08\beta_1 \tag{A.4}$$

A comparison of the limits from Eq. A.3 and A.4 is made in Table A.2 for Grade 270 strand and $\beta_1 = 0.85$. A single value is considered for β_1 because the ratios between limits computed with the two equations will be identical for any value of the constant. The data in the table indicates that the error in using the constant limit would be no more than 2.5 percent for Grade 270 steel, which is an acceptable level of error for this limit.

While a constant limit may be used, it is essential that the derivation and intent of the limit be made available to engineers at large so that modifications to the limit can be made where necessary for other grades of steel or where it can be shown that the elongation of the strand is greater than the 0.035 value assumed in this limit.

Table A.2 Variation of proposed minimum reinforcement limit with effective prestress

f_{se} (ksi)	Eq. A.3. $\beta_1 = 0.85$	% diff. *	Eq. A.4. $\beta_1 = 0.85$	% diff. **
150	0.0664	2.24	0.0680	2.41
170	0.0679	0	0.0680	0.16
185	0.0690	-1.67	0.0680	-1.51

* The percentage difference (% diff.) is between the 170 ksi and the other values of f_{se} (150 or 185 ksi) and is computed using the other values as the basis of the comparison. The percentages apply to all values of β_1.

** The percentage difference is between values of the minimum limit calculated using Eq. A.4. and A.3 and is computed using Eq. A.3 values as the basis for the comparison. these percentages apply to all values of β_1.

R E F E R E N C E S

1. Ahmad, S.H., and Shah, S.P., "Stress-Strain Curves of Concrete Confined by Spiral Reinforcement," ACI Journal, Proceedings Vol. 79, No. 6, Nov.-Dec. 1982, pp. 484-490.

2. Ahmad, S.H., and Shah, S.P., "Structural Properties of High Strength Concrete and Its Implications for Precast Prestressed Concrete" PCI Journal, Vol. 30, No. 6, Nov.-Dec. 1985, pp. 92-119.

3. Ahmad, S.H., Khalo, A.R., and Poveda, A., "Shear Capacity of Reinforced High-Strength Concrete Beams," ACI Journal, Proceedings Vol. 83, No. 2, Mar.-Apr. 1986, pp. 297-305.

4. Aitcin, Pierre-Claude, Laplante, Pierre, and Bedard, Claude, "Development and Experimental Use of a 90 MPa (13,000 psi) Field Concrete", High Strength Concrete, SP-87, American Concrete Institute, Detroit, 1985, pp. 51-70.

5. Ali, I. Discussion of "Researches Toward a General Flexural Theory for Structural Concrete," by Hubert Rusch, ACI Journal, Proceedings Vol. 32, No. 9, Mar. 1961, pp. 1147-1149.

6. Anderson, Arthur R., "Lateral Stability of Long Prestressed Concrete Beams", PCI Journal Vol. 16, No. 3, May-June 1971, pp. 7-9.

7. Anderson, Arthur R., Author's closure to discussion of "Lateral stability of Long Prestressed Concrete Beams," PCI Journal, Vol. 16, No. 6, Nov.-Dec. 1971, pp. 86-87.

8. American Association of State Highway Officials, Standard Specification for Highway Bridges, Seventh Edition, Washington, D.C., 1957.

9. American Association of State Highway Officials, Standard Specification for Highway Bridges, Eighth Edition, Washington, D.C., 1961.

10. American Association of State Highway and Transportation Officials, Standard Specification for Highway Bridges, Thirteenth Edition, Washington, D.C., 1983.

11. American Concrete Institute, "Building Code Requirements for Reinforced Concrete (ACI 318-56)", ACI Journal, Proceedings, Vol. 52, No. 9, May 1956, pp. 913-986.

12. American Concrete Institute, Building Code Requirements for Reinforced Concrete (ACI318-63), Detroit, 144 pp.

13. American Concrete Institute, Building Code Requirements for Reinforced Concrete (ACI 318-71), Detroit, 78 pp.

14. American Concrete Institute, Building Code Requirements for Reinforced Concrete (ACI 318-77), Detroit, 102 pp.

15. American Concrete Institute, Building Code Requirements for Reinforced Concrete (ACI 318-83), Detroit, 111 pp.

16. American Concrete Institute, Commentary on Building Code Requirements for Reinforced Concrete (ACI 318-63), SP-10, American Concrete Institute, Detroit, 1965.

17. American Concrete Institute, Commentary on Building Code Requirements for Reinforced Concrete (ACI 318-83), Detroit, 1983.

18. American Concrete Institute, 318 Change Submittal, No. CE11, "Shear Strength of High Strength Concrete", Nov. 19, 1986.

19. American Concrete Institute - American Society of Civil Engineers, Committee 323, "Tentative Recommendations for Prestressed Concrete," ACI Journal, Proceedings Vol. 54, No. 7, Jan. 1958, pp. 545-578.

20. American Concrete Institute - American Society of Civil Engineers, Committee 327, Ultimate Load Design, "Ultimate Strength Design", ACI Journal, Proceedings Vol. 52, No. 5, Jan. 1956, pp. 505-524. Also, "Report of ASCE-ACI Joint Committee on Ultimate Strength Design," Proceedings, ASCE, Vol. 81, Oct. 1955, 68 pp.

21. American Concrete Institute Committee 343, "Analysis and Design of Reinforced Concrete Bridge Structures," ACI Manual of Concrete Practice, Part 4, American Concrete Institute, Detroit, 1981, 118 pp.

22. American Concrete Institute Committee 363, "State-of-the Art Report on High-Strength Concrete," ACI Journal, Proceedings Vol. 81, No. 4, July-Aug. 1984, pp. 363-411.

23. American Concrete Institute Committee 435, "Deflections of Prestressed Concrete Members," (ACI 435.1R-63)(Reaffirmed 1979), ACI Journal, Proceedings Vol. 60, No. 12, Dec. 1963, pp. 1697-1728. Also, ACI Manual of Concrete Practice, Part 4, American Concrete Institute, Detroit, 1981.

24. American Concrete Institute Committee 435, Subcommittee 5, "Deflections of Prestressed Concrete Members," ACI Journal, Proceedings Vol. 60, No. 12, Dec. 1963, pp. 1697-1728.

25. ASTM Standards in ACI 301, 318 and 349, SP-71, American Concrete Institute, Detroit.

26. Aswad, A. and Hester, W.T. "Impact of High-Strength Concrete on Design and Service Behavior of Prestressed Precast Concrete Members," High Strength concrete, SP-87, American Concrete Institute, Detroit, 1985, pp. 9-20.

27. Base, G.D., "An Investigation of Transmission Length in Pre-Tensioned Concrete," Session III, Paper No. 9, Third Congress of the Federation Internationale de la Preconstrainte, Berlin, 1958, Papers, pp. 603-623.

28. Base, G.D., "An Investigation of Transmission Length in Pretensioned Concrete," Research Report No. 5, Aug., 1958, Cement and Concrete Association, London, 24 pp.

29. Base, G.D., "An Investigation of the Use of Strand in Pretensioned Prestressed Concrete Beams," Research Report No. 11, Jan. 1961, Cement and Concrete Association, London, 12 pp.

30. Billet, D.F., and Appleton, J.H., "Flexural Strength of Prestressed Concrete Beams", ACI Journal, Proceedings, Vol. 50, No. 10, June 1954, pp. 837-854.

31. Blume, J.A., Newmark N.M., and Corning, L.H., "Design of Multistory Reinforced Concrete Buildings for Earthquake Motions," Portland Cement Association, Chicago, 1961, 318 pp.

32. Bradberry, T.E., "Time Dependent Deformation of Long Span Prestressed Concrete Beams Having Low Relaxation Strands," Unpublished M.S. Report, The University of Texas at Austin, May 1986.

33. Bureau of Public Roads, Strength and Serviceability Criteria-Reinforced Concrete Bridge Members - Ultimate Design, U.S. Department of Commerce, U.S. Government Printing Office, Washington, D.C., Aug. 1966, 81 pp.

34. Burns, Ned H., "Moment Curvature Relationships for Partially Prestressed Concrete Beams," PCI Journal, Vol. 9, No. 1, Feb. 1964, pp. 52-63.

35. Carrasquillo, P.M. and Carrasquillo, R.L., "Guidelines for Use of High Strength Concrete in Texas Highways," Research Report 367-1F, Center for Transportation Research, The University of Texas at Austin, Aug. 1986, 227 pp.

36. Carrasquillo, R.L., Nilson, A.H., and Slate, F.O., "Properties of High Strength Concrete Subject to Short-Term Loads", ACI Journal, Proceedings Vol. 78, No. 3, May-June 1981, pp. 171-178.

37. Carreira, Domingo J., and Chu, Kuang-Han, "Stress-Strain Relationship for Plain Concrete in Compression," ACI Journal, Proceedings, Vol. 82, No. 6, Nov.-Dec. 1985, pp. 797-804.

38. Castrodale, R.W., "The Shear Design of Prestressed Concrete Members Using the Truss Model," Unpublished M.S. Thesis, University of Texas at Austin, Dec. 1983, 348 pp.

39. Colaco, J.P., "75-Story Texas Commerce Plaza, Houston - The Use of High-Strength Concrete," High Strength Concrete, SP-87, American Concrete Institute, Detroit, 1985, pp. 1-8.

40. Collins, M.P., and Mitchell, D., "Shear and Torsion Design of Prestressed and Non-Prestressed Concrete Beams," PCI Journal, Vol. 25, No. 5, Sept. - Oct. 1980, pp. 32-100.

41. Comite Euro-International du Beton, Recommendations for an International Code of Practice for Reinforced Concrete, Translation by American Concrete Institute and Cement and Concrete Association, 156 pp.

42. Csagoly, P., "Bridge Girder Test," Engineering News-Record, Mar. 13, 1986, p. 9.

43. Drake, Kingsley D., "High-Strength Concrete in Seattle," High Strength Concrete, SP-87, American Concrete Institute, Detroit, MI, 1985, pp. 21-34.

44. Elzanaty, A.H., Nilson, A.H. and Slate, F.O., "Shear-Critical High-Strength Concrete Beams," Research Report No. 85-1, Department of Structural Engineering, Cornell University, Feb. 1985, 216 pp.

45. Elzanaty, A.H., Nilson, A.H., and Slate, F.O., "Shear Capacity of Reinforced Concrete Beams Using High-Strength Concrete," ACI Journal, Proceedings Vol. 83, No. 2, Mar.-Apr. 1986, pp. 290-296.

46. Elzanaty, A.H., Nilson, A.H., and Slate, F.O., "Shear Capacity of Prestressed Concrete Beams Using High-Strength Concrete," ACI Journal, Proceedings Vol. 83, No. 3, May-June 1986, pp. 359-368.

47. Fafitis, A., and Shah, S.P., "Lateral Reinforcement for High-strength Concrete Columns," High Strength Concrete, SP-87, American Concrete Institute, Detroit, 1985, pp. 213-232.

48. Furlong, R.W., "Design of Concrete Frames by Assigned Limit Moments," ACI Journal, Proceedings Vol. 67, No. 4, Apr. 1970, pp. 341-353.

49. Ghosh, S.K., and Chandrasekhar, C.S., Discussion of "Flexural Behavior of High-Strength Concrete Beams" by Leslie, Rajagopalan and Everard, ACI Journal, Proceedings Vol. 74, No. 3, Mar. 1977, pp. 140-142.

50. Grossfield, B., and Birnstiel C., "Tests of T-Beams with Precast Webs and Cast-in-Place Flanges," ACI Journal, Proceedings Vol. 59, No. 6, June 1962, pp. 843-851.

51. Hansen, T.C., and Mattock, A.H., "Influence of Size and Shape of Member on the Shrinkage and Creep of Concrete," ACI Journal, Proceedings Vol. 63, Feb. 1966, pp. 267-290. Also PCA Bulletin D103 which contains an added appendix.

52. Hanson, Norman W., "Precast-Prestressed Concrete Bridges - 2. Horizontal Shear Connections," Journal of the PCA Research and Development Laboratories, Vol. 2, No. 2, 1960, pp. 38-58.

53. Hanson, Norman W., "Influence of Surface Roughness of Prestressing Strand on Bond Performance," PCI Journal, Vol. 14, No. 1, Feb. 1969, pp. 32-45.

54. Hanson, N.W., and Kaar, P.H., "Flexural Bond Tests of Pre-Tensioned Prestressed Beams," ACI Journal, Proceedings Vol. 55, Jan. 1959, pp. 783-802.

55. Harajli, M.H., and Naaman, A.E., "Deformation and Cracking of Partially Prestressed Concrete Beams under Static and Cyclic Fatigue Loading," Research Report No. UMEE 84R1, Department of Civil Engineering, The University of Michigan, Ann Arbor, Aug. 1984, 179 pp.

56. Harajli, M.H., and Naaman, A.E., "Static and Fatigue Tests on Partially Prestressed Beams," Proceedings, ASCE, Vol. 111, ST7, July 1985, pp. 1602-1618.

57. Harajli, M.H., Naaman, A.E., and Wight, J.K., "Analysis of Ductility in Partially Prestressed Concrete Flexural Members", PCI Journal, V. 32, No. 3, May-June 1986, pp. 64-87.

58. Hognestad, Eivind, "A Study of Combined Bending and Axial Load in Reinforced Concrete Members," Bulletin No. 399, University of Illinois Engineering Experiment Station, Nov. 1951, 128 pp.

59. Hognestad, Eivind, "Confirmation of Inelastic Stress Distribution in Concrete," Proceedings, ASCE, Vol. 83, ST2, Mar. 1957, pp. 1-17. Also PCA Bulletin D31.

60. Hognestad, E., Hanson, N.W., and McHenry, D., "Concrete Stress Distribution in Ultimate Strength Design," ACI Journal, Proceedings Vol. 52, Dec. 1955, pp. 455-479. Also PCA Bulletin D6.

61. Hognestad, E., Hanson, N.W., and McHenry, D., Authors' closure to discuss of "Concrete Stress Distribution in Ultimate Strength Design," ACI Journal, Proceedings Vol. 52, Part 2, Dec. 1956, pp. 1305-1330. Also, PCA Bulletin D6A.

62. Horn, D.G., and Preston, H.K., "Use of Debonded Strands in Pretensioned Bridge Members", PCI Journal, Vol. 26, No. 4, July-Aug. 1981, pp. 42-58.

63. Huang, T., "Loss Estimation for Multistage Prestressed Concrete Members," Advances in Structural Concrete Design, Proceedings of NJIT-ASCE-ACI Structural Concrete Design Conference, Newark, 1983, pp. 187-203.

64. Hunt, F.F., and Preston, H.K., "Performance of a New Corrosion Resistant Prestressing Strand", Presentation at "Advances in Prestressed Concrete" Session at ASCE Fall Convention and Structures Congress, Houston, Texas, Oct. 17-21, 1983.

65. Janney, Jack R., "Nature of Bond in Pretensioned Prestressed Concrete," ACI Journal, Proceedings, Vol. 50, May 1954, pp. 717-736. Also, PCA Bulletin D2.

66. Janney, J.R., Hognestad, E., and McHenry D., "Ultimate Flexural Strength of Prestressed and Conventionally Reinforced Concrete Beams", ACI Journal, Proceedings Vol. 52, Feb. 1956, pp. 602-620. Also, PCA Bulletin D7.

67. Janney, Jack R., "Report of Stress Transfer Length Studies on 270k Prestressing Strand", PCI Journal, Vol. 8, No. 1, Feb. 1963, pp. 41-45.

68. Jensen, V.P., "The Plasticity Ratio of Concrete and Its Effect on the Ultimate Strength of Beams," ACI Journal, Journal Vol. 39, No. 6, June 1943, pp. 565-582.

69. Jobse, H.J., "Applications of High Strength Concrete for Highway Bridges,", Report No. FHWA/RD-82/097, Oct. 1981, Federal Highway Administration, 228 pp.

70. Karr, P.H., LaFraugh, R.W., and Mass, M.A. "Influence of Concrete Strength on Strand Transfer Length," PCI Journal Vol. 8, No. 5, Oct. 1963, pp. 47-67. Also, PCA Bulletin D71.

71. Kaar, P.H., Hanson, N.W., and Capell, H.T., "Stress-Strain Characteristics of High-Strength Concrete," Douglas McHenry International Symposium on Concrete and Concrete Structures, SP-55, American Concrete Institute, Detroit, 1978, pp. 161-185.

72. Kelly, D.J., "Time Dependent Deflections of Pretensioned Beams," Unpublished M.S. Thesis, The University of Texas at Austin, Aug. 1986, 307 pp.

73. Kent, D.C., and Park R., "Flexural Members with Confined Concrete," Proceedings, ASCE, Vol. 97, ST7, July 1971, pp. 1969-1990.

74. Khachaturian, Marbey, and Gurfinkel, German, Prestressed Concrete, McGraw-Hill, New York, 1969, 460 pp.

75. Kriz, L.B. and Lee, S.L., "Ultimate Strength of Over-Reinforced Beams," Proceedings, ASCE, Vol. 86, EM3, June 1960. Also, PCA Bulletin D36.

76. Leslie, Keith E., Rajagopalan, K.S., and Everard, Noel J., "Flexural Behavior of High-Strength Concrete Beams," ACI Journal, Proceedings Vol. 73, No. 9, Sept. 1976, pp. 517-521.

77. MacGregor, J.G., "Ductility of Structural Elements," Handbook of Concrete Engineering, 1st Ed., M. Fintel (Editor), Prentice Hall, 1974, pp. 229-248.

78. Malhotra, V.M., "Are 4 X 8 Inch Concrete Cylinders as Good as 6 X 12 Inch Cylinders for Quality Control of Concrete?", ACI Journal, Proceedings Vol. 73, No. 1, Jan. 1976, pp. 33-36.

79. Martin, L.D. and Scott, N.L., "Development of Prestressing Strand in Pretenioned Members," ACI Journal, Proceedings Vol. 73, No. 8, Aug. 1976, pp. 453-456.

80. Martin, L.D., "A Rational Method for Estimating Camber and Deflection of Precast Prestressed Members," PCI Journal, Vol. 22, No. 1, Jan.-Feb. 1977, pp. 100-108.

81. Martinez, S., Nilson, A.H., and Slate, F.O., "Short-Term Mechanical Properties of High-Strength Light-Weight Concrete," Research Report No. 82-9, Dept. of Structural Engineering, Cornell University, Aug. 1982, 98 pp.

82. Martinez, S., Nilson, A.H., and Slate, F.O., "Spirally Reinforced High-Strength Concrete Columns," ACI Journal, Proceedings Vol. 81, No. 5, Sept.-Oct. 1984, pp. 431-442.

83. Mast, R.F., "Auxiliary Reinforcement in Concrete Connections," Proceedings, ASCE, Vol. 94, ST6, June 1968, pp. 1485-1504.

84. Mattock, Alan, H., "Modification of ACI Code Equation for Stress in Bonded Prestressed Reinforcement at Flexural Ultimate," ACI Journal, Proceedings Vol. 81, No. 4, July-

85. Mattock, A.H., Kaar, P.H., "Precast-Prestressed Concrete Bridges - 4. Shear Tests of Continuous Girders," Journal of the PCA Research and Development Laboratories, Vol. 3, No. 1, Jan. 1961, pp. 19-46.

86. Mattock, Alan, H., and Kriz, Ladislav, B., "Ultimate Strength of Nonrectangular Concrete Members," ACI Journal, Proceedings Vol. 57, No. 7, Jan. 1961, pp. 737-766.

87. Mattock, Alan H., Kriz, Ladislav, B., and Hognestad, Eivind, "Rectangular Concrete Stress Distribution in Ultimate Strength Design", ACI Journal, Proceedings Vol. 57, Feb. 1961, pp. 875-928. Also PCA Bulletin D49.

88. Mattock, A.H., and Hawkins, N.M., "Shear Transfer in Reinforced Concrete - Recent Research," PCI Journal, Vol. 17, No. 2, Mar.-Apr. 1972, pp. 55-75.

89. Mayfield, B., Davies, G., and Kong, F.K., "Some tests on the transmission length and ultimate strength of pretensioned concrete beams incorporating Dyform strand:", Magazine of Concrete Research, Vol. 22, No. 73, Dec. 1970, pp. 219-226.

90. Mphonde, Andrew G., and Frantz, Gregory C., "Shear Tests of High- and Low-Strength Concrete Beams Without Stirrups," ACI Journal, Proceedings Vol. 81, No. 4, July-Aug. 1984, pp. 350-357.

91. Mphonde, A.G., and Frantz, G.C., "Shear Tests of High- and Low-Strength Concrete Beams with Stirrups," High Strength Concrete, SP-87, American Concrete Institute, Detroit, 1985, pp. 179-196.

92. Muller, Jean, "Lateral Stability of Precast Members During Handling and Placing," PCI Journal, Vol. 7, No. 1, Feb. 1962, pp. 20-31.

93. Naaman, A.E., "Ultimate Analysis of Prestressed and Partially Prestressed Sections by Strain Compatibility," PCI Journal, Vol. 22, No. 1, Jan.-Feb. 1977, pp. 32-51.

94. Naaman, A.E., "A Proposal to Extend Some Code Provisions on Reinforcement to Partial Prestressing," PCI Journal, Vol. 26, No. 2, Mar.-Apr. 1981, pp. 74-91.

95. Naaman, A.E., "Partially Prestressed Concrete: Review and Recommendations," PCI Journal, Vol. 30, No. 6, Nov.-Dec. 1985, pp. 30-71.

96. Naaman, A.E., Harajli, M.H., and Wight, J.K., "Analysis of Ductility in Partially Prestressed Flexural Members," PCI Journal, Vol. 31, No. 3, May-June 1986, pp. 64-87.

97. Naaman, A.E., Harajli, M.H., and Wight, J.K., Authors' Closure to discussion of "Analysis of Ductility in Partially Prestressed Flexural Members," PCI Journal, Vol. 32, No. 1, Jan.-Feb., 1987, pp. 142-145.

98. Ngab, Ali S., Nilson, Arthur H., and Slate, Floyd O., "Shrinkage and Creep of High Strength Concrete," ACI Journal, Proceedings Vol. 78, No. 4, July-Aug. 1981, pp. 255-261.

99. Nilson, Arthur H., "Design Implications of Current Research of High-Strength Concrete," High Strength Concrete, SP-87, American Concrete Institute, Detroit, 1985, p. 85-118.

100. Over, R.S., and Au, Tung, "Prestress Transfer Bond of Pretensioned Strands in Concrete," ACI Journal, Proceedings Vol. 62, No. 11, Nov. 1965, pp. 1451-1460.

101. Overman, T.R., Breen, J.E., and Frank, K.H., "Fatigue Behavior of Pretensioned Concrete Girders," Research Report 300-2F, Center for Transportation Research, The University of Texas at Austin, Nov. 1984, 354 pp.

102. Park, R., and Paulay, T. Reinforced Concrete Structures, John Wiley and Sons, New York, 1975, 769 pp.

103. Pastor, J.A., Nilson, A.H., and Slate, F.O., "Behavior of High-Strength Concrete Beams," Research Report No. 84-3, Department of Structural Engineering, Cornell University, Feb. 1984, 311 pp.

104. Peterman, M.B. and Carrasquillo, R.L., "Production of High Strength Concrete," Research Report 315-1F, Center for Transportation Research, The University of Texas at Austin, Oct. 1983, 286 pp.

105. PCI Committee on Allowable Stresses in Prestressed Concrete Design, "Allowable Tensile Stresses for Prestressed Concrete," PCI Journal, Vol. 15, No. 1, Feb. 1970, pp. 37-42.

106. PCI Committee on Prestress Losses, "Recommendations for Estimating Prestress Losses", PCI Journal, Vol. 20, No. 40, July-Aug. 1975, pp. 43-75.

107. Preston, H.K., "Testing 7-Wire Strand for Prestressed Concrete-The State of the Art", PCI Journal, Vol. 30, No. 3, May-June 1985.

108. Rabbat, B.G., and Russell, H.G., "Optimized Sections for Precast, Prestressed bridge Girders," (RD080.01E), Portland Cement Association, 1982.

109. Rabbat, B.G., Takayanagi, T., Russell, H.G., "Optimized Sections for Major Prestressed Concrete Bridge Girders," Report No. FHWA/RD-82/005, Feb. 1982, Federal Highway Administration, 172 pp.

110. Ramirez, J.A., and Breen, J.E., "Proposed Design Procedures for Shear and Torsion in Reinforced and Prestressed Concrete," Research Report 248-4F, Center for Transportation Research, The University of Texas at Austin, Nov. 1983, 254 pp.

111. Ramirez, J.A., and Breen, J.E., "Review of Design Procedures for Shear and Torsion in Reinforced and Prestressed Concrete," Research Report 248-2, Center for Transportation Research, The University of Texas at Austin, Nov. 1983, 186 pp.

112. RILEM, Final REcommendations, Reinforcements for Reinforced and Prestressed Concrete: II. Recommendations for Prestressing Steels. Materials and Structures, Research and Testing (RILEM, Paris), Vol. 12, No. 68, Mar.-Apr. 1979, pp. 75-127.

113. Rowe, R.E., "Trends and Needs in Concrete Bridge Design," Seventh Annual Henry M. Shaw Lecture Series in Civil Engineering, Department of Civil Engineering, North Carolina State University, Raleigh, Mar. 1972, 36 pp.

114. Rusch, Hubert, "Researches Toward a General Flexural Theory for Structural Concrete," ACI Journal, Proceedings Vol. 57, No. 1, July 1960, pp. 1-28.

115. Saemann, J.C., and Washa, G.W., "Horizontal Shear Connections Between Precast Beams and Cast-in-Place Slabs," ACI Journal, Proceedings, Vol. 61, No. 11, Nov. 1964, pp. 1383-1409.

116. Shaikh, A.F., and Branson, D.E., "Non-Tensioned Steel in Prestressed Concrete Beams," PCI Journal, Vol. 15, No. 1, Feb. 1970, p. 14-36.

117. Smadi, M.M., Slate, F.O., and Nilson, A.H., "High-, Medium-, and Low-Strength Concretes Subject to Sustained Overloads - Strains, Strengths, and Failure Mechanisms," ACI Journal, Proceedings Vol. 82, No. 5, Sept.-Oct. 1985, pp. 657-664.

118. Smith, R.G., Discussion of "Researches Toward a General Flexural Theory for Structural Concrete," by Hubert Rusch Reference, ACI Journal, Proceedings Vol. 32, No. 9, Mar. 1961, pp. 1160-1163.

119. Suttikan, C., "A Generalized Solution for Time Dependent Response and Strength of Non-Composite and Composite Prestressed Concrete Beams," Unpublished Ph.D. Dissertation, The University of Texas at Austin, Aug. 1978.

120. Swamy, R.N., "High-Strength Concrete - Material Properties and Structural Behavior," High Strength Concrete, SP-87, American Concrete Institute, Detroit, 1985, pp. 119-146.

121. Swamy, R.N., and Anand, K.L., "Transmission Length and Prestress Losses in High Strength Concrete," Paper presented at the Seventh International Congress of the Federation Internationale de la Preconstrainte, New York, May 26 - June, 1974.

122. Swann, R.A., Discussion of "Lateral Stability of Long Prestressed Concrete Beams," by Arthur R. Anderson, PCI Journal, Vol. 16, No. 6, Nov.-Dec. 1971, p. 85-86.

123. Swann, R.A., and Godden, W.G., "The Lateral Buckling of Concrete Beams Lifted by Calbes," The Structural Engineer, Vol. 44, No. 1, Jan. 1966, London, pp. 21-23.

124. Swartz, S.E., Nikaeen, A., Harayan Babu, H.D., Periyakaruppan, N., and Refai, T.M.E. "Structural Bending Properties of Higher Strength Concrete," High Strength Concrete, SP-87, American Concrete Institute, Detroit, 1985, pp. 147-178.

125. Tadros, M.K., and Peterson, D.N., "Code Consideration of Flexural Design with Partial Prestressing," Vol. 3, Hyperstatic Structures: Nonlinear Design, Codes and Practice, International Symposium - Nonlinearity and Continuity in Prestressed Concrete, University of Waterloo, 1983, pp. 125-156.

126. Thoman, William, H., and Raeder, Warren, "Ultimate Strength and Modulus of Elasticity of High Strength Portland Cement Concrete," ACI Journal, Proceedings Vol. 30, No. 3, Jan. - Feb., 1934, pp. 231-=238.

127. Thompson, K.J., and Park R., "Ductility of Prestressed and Partially Prestressed Concrete Beam Sections," PCI Journal, Vol. 25, No. 2, Mar.-Apr. 1980, pp. 46-70.

128. Tognon, G., Ursella, P., and Copetti, G., "Design and Properties of Concretes with Strength over 1500 kgf/cm^2," ACI Journal, Proceedings Vol. 77, No. 3, May-June 1980, pp. 171-178.

129. Towles, Thomas T., "Advantages in the Use of High Strength Concretes," ACI Journal, Proceedings, Vol. 28, No. 9, May 1932, pp. 607-612.

130. Wang, F., Shah, S.P., and Naaman, A.E., Discussion of "Flexural Behavior of High-Strength Concrete Beams," ACI Journal, Proceedings Vol. 74, No. 3, Mar, 1977, pp. 143, 144.

131. Wang, Pao-Tsan, Shah, Surendra P., and Naaman, Antoine E., "High-Strength Concrete in Ultimate Strength Design", Proceedings, ASCE, Vol. 104, ST11, Nov. 1978, pp. 1761-1773.

132. Wang, P.T., Shah, S.P., and Naaman, A.E., "Stress-Strain Curves of Normal and Lightweight Concrete in Compression," ACI Journal, Proceedings, Vol. 75, No. 11, Nov. 1978, pp. 603-611.

133. Warwaruk, J., Sozen, M.A., and Siess, C.P., "Investigation of Prestressed Reinforced Concrete for Highway Bridges, Part III-Strength and Behavior in Flexure of Prestressed Concrete Beams," Bulletin No. 464, Engineering Experiment Station, University of Illinois, Urbana, 1962, 105 pp.

134. Whitney, Charles S., "Plastic Theory of Reinforced Concrete Design," Proceedings ASCE, Dec. 1940; Transactions ASCE, Vol. 107, 1942, pp. 251-326.

135. Zia, Paul, "Review of ACI Code for Design with High Strength Concrete," Concrete International: Design and Construction, Vol. 5, No. 8, Aug. 1983, pp. 16-20.

136. Zia, P., and Mostafa, T., "Development Length of Prestressing Strands," PCI Journal, Vol. 22, No. 5, Sept. - Oct. 1977, pp. 54-65.

137. Zia, P., Preston, H.K., Scott, N.L., and Workman, E.B., Estimating Prestress Losses," Concrete International: Design and Construction, Vol. 1, No. 6, June 1979, pp. 32-38.

138. Hartmann, D., Breen, J.E., and Kreger, M.E., "Shear Capacity of High-Strength Prestressed Concrete Girders," Research Report 381-2, Center for Transportation Research, The University of Texas at Austin, January 1988, 243 pp.

139. Castrodale, R.W., Burns, N.H., and Kreger, M.E., "A Study of Pretensioned High-Strength Concrete Girders in Composite Highway Bridges - Laboratory Tests," Research Report 381-3, Center for Transportation Research, The University of Texas at Austin, January 1988, 209 pp.

140. Castrodale, R.W., "A Study of Pretensioned High Strength Concrete Girders in Composite Highway Bridges," Unpublished Ph.D. Dissertation, The University of Texas at Austin, May 1988.